

Investigating structural cerebellar differences associated with schizophrenia pathophysiology

Tom William Chambers

2021

Cardiff University



Supervisors:

Prof. Krish D. Singh

Dr Xavier Caseras

Prof. James T. Walters

A thesis submitted in fulfilment of the requirements for the degree of Doctor of Philosophy

Summary

While historically overlooked, there is growing interest in the possible pathophysiological roles played by the cerebellum in various psychiatric and neurodevelopmental disorders, including schizophrenia. While structural cerebellar differences have been noted in individuals with psychiatric diagnoses compared to normative controls, whether these effects reflect true underlying neuropathology, confounding (spurious associations caused by uncontrolled for demographic, medical or imaging factors) or reverse causation (i.e. arising following principal symptom onset) is still to be established. The use of large datasets of homogeneously collected Magnetic Resonance Imaging (MRI), with genetic and health record data will help advance our knowledge in this regard.

Chapter 1 provides an overview of the relevant literature around schizophrenia, its genetic aetiology, pathophysiology, genetic neuroimaging techniques, the cerebellum and its relevance to schizophrenia. In *Chapter 2* I investigate whether psychiatric disorders are associated with reduced cerebellar volume in a large population-based cohort, when taking into account any shared medical comorbidities, sub-clinical comorbidities and other imaging and non-imaging based confounding measures. In *Chapter 3*, to circumvent the problem of reverse causation, in a cohort of non-psychiatric participants, I use genetic imaging analyses to investigate whether an individual's increased common and rare genetic risk burden for schizophrenia is similarly associated with cerebellar reductions. In *Chapter 4*, I identify the common genetic variants important for cerebellar structure volume and use these results to ascertain the genetic correlation between the cerebellum and schizophrenia liability. Finally, in *Chapter 5*, I use these introduced cerebellar-associated variants to explore their significance in a clinical cohort, investigating whether those individuals with treatment-resistant schizophrenia, a feature associated with impairment brain development, showed a lower genetic predisposition for cerebellar growth. *Chapter 6* provides a summary of the findings presented in this thesis, their relevance to the wider scientific literature and avenues for future research.

Acknowledgments

I would firstly like to thank all of my supervisors: Professor Krish Singh, Dr Xavier Caseras and Professor James Walter for their guidance and support throughout this thesis. I have learned so much through their direction and count myself very lucky to have had the experience.

While there is a vast number of people in CUBRIC and HEB to thank and whom I greatly miss, I am particularly indebted for the help provided by Dr Thomas Lancaster, Dr Sophie Legge and Dr Richard Anney. Their incredible knowledge of their respective fields, ability to disseminate this knowledge, and immensely kind and helpful natures meant a great deal to me.

While the project did unfortunately not continue, I would equally like to thank Dr Mohammed Tachrount and Dr Christopher Jenkins for all their help and guidance for the MRS study.

I am extremely grateful to the Wellcome Trust and Cardiff University for the opportunity to undertake this PhD and provide such continued support.

Finally, a huge thank you to all my family and friends for all their encouragement. A special thank you to my brother, for everything.

Statements of others work

Chapters 2-5 use data from the UK Biobank resource data, with explanations of their data collection and analysis provided within each chapter. *Chapters 3, 4 and 5* uses the UK Biobank genetic data which has undergone an initial in-house quality control by Dr Richard Anney (as outlined within each chapter, using https://github.com/ricanney/stata_summaryqc function). Additional quality control for each specific analysis was also conducted by myself. *Chapter 3* uses polygenic schizophrenia risk scores which were produced by Dr Sophie Legge and copy number variant (CNV) calling performed by Professor George Kirov and Dr Kimberley Kendall. *Chapter 4* includes fine-mapping, functional annotation and mapping results (*COJO*, *SMR* and cis-eQTL expression analysis) performed by Dr Richard Anney. For comparison to other traits, I used GWAS summary statistics which had also undergone a standardised in-house quality control check by Dr Richard Anney (using https://github.com/ricanney/stata_summaryqc function). *Chapter 5* CardiffCogs genetic data quality control was performed by Dr Antonio Pardini as outlined in the provided references, with additional quality control steps for the specific analysis also conducted by myself.

Abbreviations

TERM	DEFINITION
B	Unstandardised regression coefficients (outcome in original units)
β	Standardised regression coefficients (outcome in SD)
CNV	Copy number variant
CCTTC	Cortico-cerebellar-thalamic-cortical circuit
COJO	Conditional and joint analysis
DNA	Deoxyribonucleic acid
eQTL	Expression quantitative trait loci
EUR	European (genetic ancestry similarity)
FDR	False discovery rate
FSL	FMRIB software library
FWE	Family-wise error
GBR	Great Britain (genetic ancestry similarity)
GCTA	Genome-wide complex trait analysis
GREML	Genome-based restricted maximum likelihood
GWAS	Genome-wide association study
$h^2_{(SNP)}$	Heritability (SNP-based)

IDP	Image derived phenotype
LD	Linkage Disequilibrium
LDSC	Linkage disequilibrium score
Lob.	Lobule
mRNA	Messenger RNA (ribonucleic acid)
MRI	Magnetic resonance imaging
p	p-value
p_{BONF}	P-values adjusted for Bonferroni correction for multiple comparison
p_{FDR}	P-values adjusted for false discovery rate (FDR) for multiple comparison
PCA	Principal component analysis
PGC	Psychiatric genetics consortium
fMRI	Functional MRI. Including resting-state (rs-fMRI) and task-based (t-fMRI) studies.
R²	Coefficient of determination (i.e. variance in outcome variable explained by predictor variable)
SD	Standard deviation
SE	Standard error
SMR	Summary data-based Mendelian randomisation
SNP	Single nucleotide polymorphism

T1w	T1-weighted MRI scan
TBV	Total brain volume (total brain grey and white matter)
VBM	Voxel-based morphometry

PhD thesis Outline

1	Background	19
1.1	Schizophrenia	19
1.1.1	Prevalence, symptomatology and treatments	19
1.1.2	Aetiology	20
1.1.3	Common genetic variants	21
1.1.4	Rare genetic variants	23
1.1.5	Functional annotation and gene mapping	24
1.1.6	Pleiotropy	25
1.1.7	Neurological pathophysiology	26
1.1.8	Limitations of traditional case-control studies	28
1.2	Genetic neuroimaging	29
1.2.1	Family-based studies	29
1.2.2	Copy number variants	30
1.2.3	Polygenic schizophrenia risk score	31
1.2.4	GWAS of brain-based measures	31
1.2.5	Relevance of neuroimaging genetic results	32
1.3	The cerebellum	33
1.3.1	Structure	33
1.3.2	Modular functionality	34
1.3.3	Non-motor roles	37
1.4	Cerebellum and schizophrenia	39
1.4.1	Cerebellar relevance to schizophrenia symptomatology	39
1.4.2	Cerebellar alterations in case-control studies	40
1.4.3	The neurodevelopmental origin of cerebellar differences	42
1.5	Conclusion	43
1.6	Thesis aims	45
2	Comorbidities and covarying factors to consider for both clinical and non-clinical studies of the UK Biobank	47
2.1	Abstract	47
2.2	Background	48
2.3	Methods	49
2.3.1	Imaging cohort characteristics	49
2.3.2	Medical conditions	50
2.3.3	Statistical analysis	51

2.4	Results.....	54
2.4.1	Tier-1 ICD-10 Clinical variables	56
2.4.2	Multivariate analysis.....	60
2.4.3	BMI and head motion covariates.....	61
2.4.4	Tier 2 ICD-10 medical records.....	64
2.5	Discussion.....	65
2.6	Supplementary Tables.....	71
3	Assessing the association between common and rare allele risk for schizophrenia and cerebellar structure.....	82
3.1	Abstract.....	82
3.2	Background	83
3.3	Methods.....	85
3.3.1	Participants.....	85
3.3.2	Genetic data.....	85
3.3.3	Imaging data	87
3.3.4	Statistical analysis	87
3.4	Results.....	88
3.4.1	Demographic information	88
3.4.2	Polygenic risk score.....	90
3.4.3	CNV carrier-status.....	90
3.4.4	Cerebellar lobules	92
3.5	Discussion.....	95
3.6	Supplementary Tables.....	100
4	Investigating the shared genetic architecture between the cerebellum, schizophrenia and other psychiatric traits	111
4.1	Abstract.....	111
4.2	Introduction	112
4.3	Methods.....	113
4.3.1	Processing genetic data	113
4.3.2	Total cerebellar volume measure generation.....	114
4.3.3	Genome-wide association study (GWAS)	115
4.3.4	SNP-based heritability (h^2_{SNP}).....	115
4.3.5	Identification of independent regions	116
4.3.6	Comparison of phase data	116
4.3.7	Meta-analysis.....	117
4.3.8	Annotation of GWAS Loci	117
4.3.9	Summary-data-based Mendelian randomization (SMR)	118

4.3.10	Genetic correlation analyses with other traits.....	118
4.3.11	SNP sign test	120
4.4	Results	120
4.4.1	Generation of total cerebellar volume GWAS summary statistics	120
4.4.2	Functional consequences and associated genes of identified genome-wide significant loci	123
4.4.3	Analysis of overlap in genetic architecture with schizophrenia	128
4.5	Discussion	130
4.6	Supplementary Figures	137
4.7	Supplementary Tables	138
5	The effect of increased common genetic burden for total brain and cerebellar volume on treatment-resistance in schizophrenia	167
5.1	Abstract	167
5.2	Background.....	168
5.3	Methods	170
5.3.1	CardiffCogs participants	170
5.3.2	Genetic analysis.....	171
5.3.3	Statistical analysis.....	172
5.4	Results	173
5.4.1	PGS Prediction of treatment-resistance.....	175
5.4.2	PGS Prediction of premorbid factors.....	176
5.5	Discussion	180
5.6	Supplementary Notes	186
5.7	Supplementary Tables	188
6	General discussion	192
6.1	Is cerebellar volume reduced in those with schizophrenia?.....	192
6.2	What is the contribution of comorbidities to the cerebellar reductions seen in psychiatric disorders?	193
6.3	Are cerebellar differences in schizophrenia related to schizophrenia’s genetic aetiology?	195
6.4	What is the pathophysiological relevance of genetics for cerebellar volume?	198
6.5	Considerations and future directions	199
6.6	Conclusion	202
7	References	203

List of Figures

Figure 1.1: Genetic variants associated with increased schizophrenia liability across allele frequencies and strength of association.	23
Figure 1.2: Cerebellar lobule and fissure anatomy.	34
Figure 1.3: The internal forward model of the cerebellum.	35
Figure 1.4: Cerebellar functional boundaries following application of a multi-domain task battery in the same subjects.	38
Figure 2.1: The effect of each tier-1 ICD-10 recorded hospital diagnosis on total cerebellar volume.....	59
Figure 2.2: Identifying comorbidities for psychiatric disorders.	60
Figure 2.3: The effect of participant A) body mass index (BMI) and B) mean resting-state functional MRI (rs-fMRI) head motion on total cerebellar volume.....	62
Figure 2.4: The effect of Psychiatric tier-1 ICD-10 recorded hospital diagnosis on total cerebellar volume without and with body mass index (BMI), resting-state fMRI mean head motion and both covariates..	63
Figure 3.1: The effect on total cerebellar volume and total brain volume of increasing polygenic schizophrenia risk score at different SNP inclusion thresholds (p_T -values) and of carrier status for the different schizophrenia-associated copy number variants (CNVs).	92
Figure 3.2: The effect on cerebellar lobules of increasing (A) polygenic schizophrenia risk score and of (B) carrier status for the different schizophrenia-associated copy number variants (SCZ-CNVs) ($n>5$) in a UK Biobank sample.	94
Figure 4.1: Manhattan plots of associations with total cerebellar volume for A) Phase 1 data release ($n= 17,818$), B) Phase 2 data release ($n= 15,447$), and C) Phase 1 + Phase 2 combined METAL meta-GWAS.	122
Figure 5.1: Analysis flow-chart including sample sizes for the whole cohort and the schizophrenia sub-cohort.	174

Figure 5.2: The association between polygenic scores of total cerebellar and total brain volume with treatment resistant psychosis (TRP) status in individuals with any psychosis-related diagnosis (n=868)..... 177

**Figure 5.3: The association between polygenic scores of total cerebellar and total brain volume with outcomes of interest in individuals with any psychosis-related diagnosis (n=868).
..... 178**

List of Tables

Table 2.1: Demographic information for the UK Biobank cohort included in this study.....	55
Table 2.2: The effect of each 19 tier 1 ICD-10 recorded hospital diagnosis on total cerebellar volume.....	57
Table 3.1: Demographic information for the total 15,802 cohort, including carriers of schizophrenia-associated copy number variants (CNVs) carriers.....	89
Table 3.2: The effect on total cerebellar volume of increasing polygenic schizophrenia risk score and schizophrenia-associated copy number variants (SCZ CNVs) carrier status.....	91
Table 4.1: List of 33 conditionally independent index SNPs and corresponding LD ranges following COJO analysis of the genome-wide association results for total cerebellar volumes in UK Biobank, and their association statistics in the latest Schizophrenia GWAS.....	125
Table 4.2: The prioritised 21 unique genes from functional annotation, positional and cis-eQTL mapping and SMR analysis	127
Table 4.3: Genetic correlation of total cerebellar volume with psychiatric previously associated with cerebellar anatomy/function	129
Table 5.1: Demographic information and premorbid risk factors for treatment resistance in the whole cohort, split by treatment resistance status.....	175
Table 5.2: The association between polygenic scores of total cerebellar volume and outcomes of interest in individuals with any psychosis-related diagnosis (n=868).....	179

List of Supplementary Materials

Supplementary Tables are provided at the end of each chapter. To optimise readability, larger Supplementary Tables which are of less direct relevance to the specific research question of this thesis - but which will be of interest to the wider research field – are provided in an additional file and are also viewable in an online Open Science Framework file: https://osf.io/jr8m2/?view_only=29906bc730f64cf58a81d67ff5c5036

Supplementary Table 2.1: The frequency of A) tier 1 and B) tier 2 ICD-10 recorded hospital diagnoses present in our 19,369 UK Biobank sample. Viewable in the provided additional file and https://osf.io/jr8m2/?view_only=29906bc730f64cf58a81d67ff5c50363	71
Supplementary Table 2.2: The effect of our default list of covariates on total cerebellar volume	72
Supplementary Table 2.3: The effect of each tier-1 ICD-10 recorded hospital diagnosis on total cerebellar volume (without total brain volume correction)	73
Supplementary Table 2.4: Sex distribution of tier 1 ICD-10 recorded diagnoses. Viewable in the provided additional file and https://osf.io/jr8m2/?view_only=29906bc730f64cf58a81d67ff5c50363	74
Supplementary Table 2.5: Sex interactional effects with tier 1 ICD-10 recorded diagnoses on total cerebellar volume. Viewable in the provided additional file and https://osf.io/jr8m2/?view_only=29906bc730f64cf58a81d67ff5c50363	74
Supplementary Table 2.6: The presence of ICD-10 recorded hospital comorbidities (Non-Psych) of psychiatric diagnoses (Psych) in our cohort	75
Supplementary Table 2.7: Multivariate analysis of the effect of each tier 1 ICD-10 recorded diagnoses on total cerebellar volume	77
Supplementary Table 2.8 : Body mass index (BMI) and head motion differences in those with/without tier 1 ICD-10 recorded diagnoses. Viewable in the provided additional file and https://osf.io/jr8m2/?view_only=29906bc730f64cf58a81d67ff5c50363	78

Supplementary Table 2.9: Tier 1 ICD-10 recorded diagnoses on total cerebellar volume with additional head motion and/or body mass index correction. Viewable in the provided additional file and https://osf.io/jr8m2/?view_only=29906bc730f64cf58a81d67ff5c50363 ... 78

Supplementary Table 2.10: Multivariate analysis of each tier 1 ICD-10 recorded diagnoses on total cerebellar volume with additional head motion and body mass index correction..... 79

Supplementary Table 2.11: Tier 2 ICD-10 recorded diagnoses on total cerebellar volume. Viewable in the provided additional file and https://osf.io/jr8m2/?view_only=29906bc730f64cf58a81d67ff5c50363 80

Supplementary Table 2.12: Tier 2 ICD-10 recorded diagnoses on total cerebellar volume with additional head motion and body mass index correction. Viewable in the provided additional file and https://osf.io/jr8m2/?view_only=29906bc730f64cf58a81d67ff5c50363 80

Supplementary Table 3.1: The prevalence of schizophrenia-associated copy number variants (SCZ CNVs) present in our UK Biobank sub-sample 100

Supplementary Table 3.2: The effect on total brain volume of increasing polygenic schizophrenia risk scores or carrier status for schizophrenia-associated copy number variants (SCZ CNVs) 101

Supplementary Table 3.3: The effect on the 17 cerebellar lobules of increasing polygenic schizophrenia risk scores 102

Supplementary Table 3.4: The effect on the 17 cerebellar lobules of carrier status for schizophrenia-associated copy number variants (SCZ CNVs) 106

Supplementary Table 4.1: Demographic information for phase 1 (n=17,818) and phase 2 (n=15,447) sub-samples of our total UK Biobank cohort..... 138

Supplementary Table 4.2A: Conditionally independent genome-wide association results for total cerebellar volumes in phase 1 (n=17,818) sub-cohort, including replication values from phase 2 (n=15,447)..... 139

Supplementary Table 4.3: Polygenic (PGS) score between-phase prediction of total cerebellar volume..... 141

Supplementary Table 4.4A: Genetic correlation of total cerebellar volume with previously published cerebellar measures	142
Supplementary Table 4.5: Positional gene mapping of each independent COJO identified extended LD region.....	145
Supplementary Table 4.6: Functional annotation results for the most deleterious SNP (index SNP and SNPs $r^2>0.8$) within each independent genomic region.....	152
Supplementary Table 4.7: The cis-expression quantitative tract loci (cis-eQTL) overlapping with each independent genomic region which shows the greatest expression change	154
Supplementary Table 4.8: Genes identified by summary data-based Mendelian randomisation (SMR) analysis.....	156
Supplementary Table 4.9: Sign test results for independent schizophrenia-associated SNPs with total cerebellar volume.....	157
Supplementary Table 5.1: Demographic information and premorbid risk factors for treatment resistance in the schizophrenia and schizoaffective depression sub-cohort, split by treatment resistance status	188
Supplementary Table 5.2: The association between polygenic scores of total cerebellar volume and outcomes of interest in individuals with either schizophrenia or schizoaffective depression diagnosis (n=660).....	189
Supplementary Note 5.1: Total brain volume genome wide association study (GWAS)	186
Supplementary Figure 4.1: Principal component analysis (PCA) of genetic ancestry to British/Irish (GBR) similarity for A) phase 1 and B) phase 2.....	137

1 Background

In this chapter, I outline the literature for our current understanding of schizophrenia diagnosis and treatment options. I then highlight how both an improved understanding of the genetic aetiology behind schizophrenia and the neuroanatomical differences seen in those with overt diagnosis, are aiding in this regard. This is particularly apparent when combined together, in the field of genetic neuroimaging, which aims to bridge the gap between genetic variants and complex disorder phenotypes. Importantly, I highlight that while there has been a certain cerebral bias to such studies, our growing appreciation for non-motor roles played by the cerebellum, as well as accumulating evidence of its potential relevance to neurodevelopmental and psychiatric disorder symptomatology, mean that further investigations into its potential relevance to schizophrenia and its genetic aetiology are promising avenues for further research.

1.1 Schizophrenia

1.1.1 *Prevalence, symptomatology and treatments*

Schizophrenia is a debilitating and enduring psychiatric disorder, being one of the costliest mental disorders both for the individual and for society (Hjorthøj, Stürup, McGrath, & Nordentoft, 2017; Ko et al., 2018). It is diagnosed in a categorical manner, based on presence of broadly overlapping inclusion/exclusion criteria from ICD-10 (international statistical classification of diseases and related health problems - version 10) and DSM-5 (diagnostic and statistical manual of mental disorders - version 5) clinical assessments of presence of symptoms and their impact upon lifestyle. These symptoms are typically grouped according to “positive” i.e. an exaggeration of normal function (e.g. hallucinations, delusions), “negative” i.e. a reduction in function (e.g. social withdrawal, emotional blunting) and “cognitive” deficits (e.g. in working memory, executive functioning and processing speed) (McCutcheon, Reis Marques, & Howes, 2020). There is also a growing appreciation of “motor” deficits and their relation to poorer outcomes, such as neurological soft signs and gait deficits (Apthorp, Bolbecker, Bartolomeo, O’Donnell, & Hetrick, 2019; Burton et al., 2016; Cuesta et al., 2018; Filatova et al., 2017; Hirjak, Meyer-Lindenberg, Kubera, Thomann, & Wolf, 2018). Onset and diagnoses of first psychotic period are usually around young adulthood, between 25-30 yrs, with prodromal periods of dysfunction preceding the first psychotic episode, though younger childhood and adolescent onset schizophrenia also can occur.

Our understanding of the biology behind schizophrenia and its symptomologies is limited. Most current pharmacological medications only address the “positive” symptomology aspect of schizophrenia: predominately acting as blockers at the dopamine D₂ receptors. Cognitive, negative and motor symptomatology, therefore, remain largely unaddressed (Carbon & Correll, 2014; Fusar-Poli et al., 2015; Keefe et al., 2007). This reflects a major limitation of current treatment options, for instance, with low negative symptomology at presentation seemingly being the greater predictor of long-term functional and social outcomes (Marchesi et al., 2015; Rabinowitz et al., 2012; Robertson et al., 2014). This limited treatment of all schizophrenia symptomatology, in combination with the complex side-effect profiles of most antipsychotics, often leads to non-continuation of treatment and poorer outcomes for these individuals (Bowtell et al., 2018; Leucht et al., 2013). Furthermore, another fifth to a half of individuals with schizophrenia display “treatment-resistant” symptomatology which does not respond to first-line medication (Nucifora, Woznica, Lee, Cascella, & Sawa, 2019).

Progress, therefore, in better understanding the underlying pathophysiology of schizophrenia, allowing for earlier diagnosis, more biologically relevant stratification, and improved treatment targeting and development, is greatly desired.

1.1.2 Aetiology

One way in which our understanding of schizophrenia has advanced, is through increased understanding of risk factors associated with its development. Schizophrenia has a median estimated lifetime morbidity risk of 0.7% (McGrath, Saha, Chant, & Welham, 2008), however, various risk factors are associated with an increased schizophrenia incidence. For example, schizophrenia is more common in those with early life complications and childhood adversity such as low birth weight and prematurity (Matheson, Shepherd, Pinchbeck, Laurens, & Carr, 2013; Pugliese et al., 2019; Simoila et al., 2018), winter/spring season of birth (Davies, Welham, Chant, Torrey, & McGrath, 2003), being male (Thorup et al., 2014), recent migratory and minority status (Dykxhoorn et al., 2019), lower socioeconomic status (Y. Luo et al., 2019) and cannabis use (Marconi, Di Forti, Lewis, Murray, & Vassos, 2016). Since randomised control trials would be highly unethical, for many of these factors, separating causal from correlative factors is still an ongoing challenge. Of note, recent developments through the deployment of tools such as Mendelian Randomisation hold promise for inferring causality, though have their own limitations (Emdin, Khera, & Kathiresan, 2017).

The strongest predictor of schizophrenia is a family history of the disorder, with first-degree relative, twin and adoptee studies showing increasing incidences of a diagnosis in family members as genomic relatedness increases (Henriksen, Nordgaard, & Jansson, 2017). By analysing these different relative types, these studies also allow for separation of genetic from non-genetic factors such as those caused by shared environment. The estimated proportion of variance in schizophrenia liability estimated to be attributable to inherited genetic variation, termed the “heritability” (h^2), is around 80% (P. F. Sullivan, Kendler, & Neale, 2003), being one of the highest of all psychiatric disorders (Geschwind & Flint, 2015).

The inheritance pattern of schizophrenia, however, is complex, and reflects how schizophrenia is a polygenic disorder, with many different associated genomic regions, frequencies and types of genetic variation; each carrying a small individual risk increase for the development of schizophrenia (Henriksen et al., 2017) (Figure 1.1). For modelling purposes, heritability for schizophrenia is thus described on a continuous, normally distributed schizophrenia liability model; constituting the theoretical summated independent small effects of multiple genetic and nongenetic factors, and with those above the liability threshold having the disorder (Sang Hong Lee, Goddard, Wray, & Visscher, 2012; Visscher, Hill, & Wray, 2008). Identification and improved understanding of these underlying genetic risk factors, therefore, has been a major focus of the last few decades of research into schizophrenia.

1.1.3 Common genetic variants

One type of genetic variation associated with increased schizophrenia risk is those identified through Genome-wide association studies (GWASs). GWASs are biologically agnostic studies, which run multiple independent univariate regression analyses, each testing for the variance explained in an outcome trait by differences in allele frequencies for each tagged common single nucleotide polymorphisms (SNP) in large cohorts of unrelated individuals. These “common” SNPs are typically defined as those with a minor allele frequency $>1\%$ in the population being studied. As the analysis is conducted in unrelated individuals, this allows for effect sizes estimates for each SNP to be free from shared environmental confounding. Imputation of untagged SNPs by comparing with a reference genome, further expands the SNP effects which can be tested. Due to the high number of tests conducted (often in the millions of SNPs), typically, statistically “significant” associations are defined as $p < 5 \times 10^{-8}$ (termed “genome-wide significant”), so as to minimise false-positive results. The output of GWAS studies are summary statistics, containing information on the SNP studied, its effect size estimates (typically log odds

ratios (OR) for a binary trait like schizophrenia) and p-values for the strength of association between each SNP and schizophrenia liability.

Since many associations below the genome-wide significant benchmark, however, will eventually achieve this threshold with increasing sample sizes and still carry useful information, several genetic tools which utilise these results typically include all SNPs and weight analyses by their association strength. Indeed, the majority of SNP-based heritability (h^2_{SNP}) (i.e. variation in the phenotype attributable to variation in SNPs) for complex (polygenic) traits is accounted for by SNPs below the genome-wide significant threshold (J. Yang et al., 2010). For schizophrenia liability, while each genome-wide significant SNP only carries a small individual risk association with schizophrenia (typically OR < 1.1), its SNP-based heritability is estimated to be around 20-30% (Loh et al., 2015; Ripke, Walters, O'Donovan, & Consortium, 2020).

An important factor of genetic analyses is that DNA variants nearer to each other on the genome show highly correlated frequencies of allele distributions across a population, termed “linkage disequilibrium” (LD). This is due to the variants being inherited together through historical evolutionary forces, including mutate and recombination rates, finite population size and natural selection (Visscher et al., 2017). This is important for several reasons. Firstly, it means that the reported SNPs are not independent and are in LD. When summarising results of a GWAS study, therefore, researchers take this LD structure into account and report the number of “independent” genome-wide significant signals using a predefined LD value. Usually, the start and end SNPs within each defined genomic region (the LD defined block of that genome-wide significant signal), and the lead/index SNP within that block (typically that with the strongest association strength with the trait) are provided. The latest published GWAS of schizophrenia identified 145 independent genome-wide significant signals associated with schizophrenia liability (Pardiñas et al., 2018).

Secondly, this means that the index SNP presented are not necessarily the actual causal (risk conferring) SNPs within that genomic region. Advances in follow-up fine-mapping, using statistical approaches to further refine the genomic associations in that region (Spain & Barrett, 2015), and combination with functional annotations of consequences of the SNPs within each independent genomic region (as discussed in a later section) (Broekema, Bakker, & Jonkers, 2020), have helped identify SNPs and genes which are more likely causally related with schizophrenia and their possible pathophysiological role.

1.1.4 Rare genetic variants

In addition to these common variants, rare (<1% population) single nucleotide variants and copy number variants (CNVs) of larger (>500kb) duplications, deletions, inversions or translocation of whole sections of the genome also account for a significant proportion for schizophrenia heritability (Singh et al., 2017). Many of these variants carry much higher penetrance (i.e. higher association effect sizes) for schizophrenia and other related neurodevelopmental disorders (as discussed later in *Pleiotropy*). This reflects a key aspect of genetic variants associated with most complex disorders: that those with higher penetrance for a disorder are often rarer in the population, due to negative selection reducing their prevalence over time (O'Connor et al., 2019). While CNVs are a natural form of genetic variation (Stankiewicz & Lupski, 2010), their presence in 15 genomic loci so far have been statistically associated with increased schizophrenia liability (Odds-ratio: 2-60) and collectively are found in around 2.5% of patients (Rees et al., 2014). With increasing numbers of individuals genotyped, including the continual development and reduction in cost of (whole) genome sequencing and analyses in non-European cohorts, many more rare variants are likely to be identified which are associated with increased schizophrenia risk.

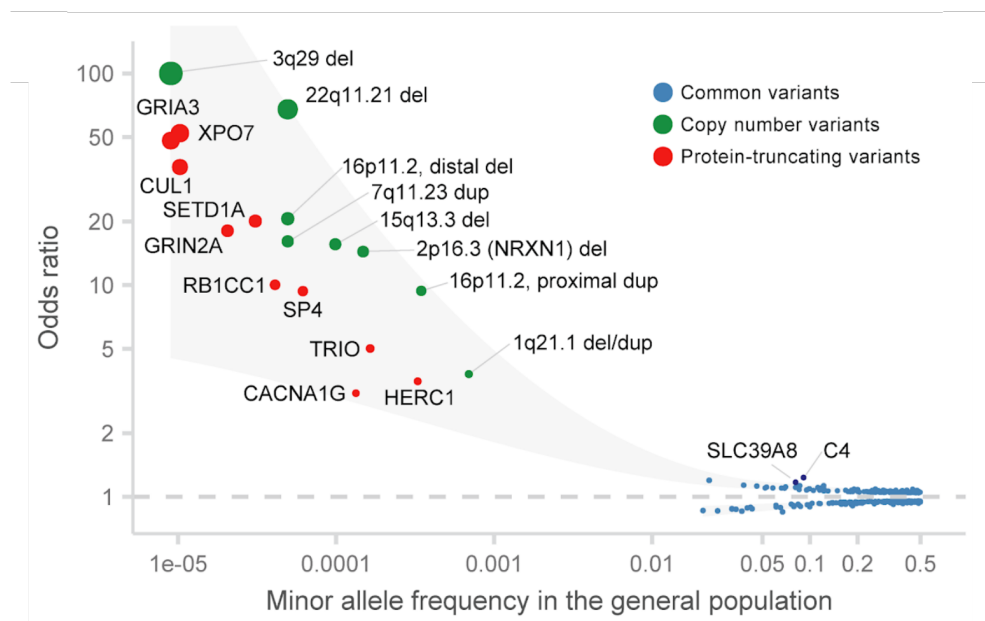


Figure 1.1: Genetic variants associated with increased schizophrenia liability across allele frequencies and strength of association. Dot size indicates strength of association. Shaded area indicates loess-smoothed upper and lower bounds of point estimates. From (Singh, Neale, Daly, & Consortium, 2020)

1.1.5 Functional annotation and gene mapping

Following identification of genetic variants associated with schizophrenia, variants can then be annotated with functional information and mapped to nearby genes, improving our understanding of the developmental and molecular pathways affected by schizophrenia's genetic risk. While a minority of disease and trait related genetic associations identified through GWASs lie with protein-coding sections of the genome, the majority lie within non-coding sections - predominately being in regulatory elements – and therefore indirectly impact upon altered gene expression (Maurano et al., 2012). While positional mapping can help identify nearby gene transcripts to each SNP, the majority of GWAS identified SNPs appear to have their impact on genes which are not those nearest to the SNP (Zhu et al., 2016). Instead, GWAS results are combined with information on nearby genomic regions (quantitative trait loci; eQTL), where genetic variation is known to impact expression of local (cis-eQTL) or further away – often on differing chromosomes - gene transcripts (trans-eQTL) (Broekema et al., 2020). By analysing expression differences in different tissues, it is possible to identify which particular tissues could be impacted by the genetic variants identified in the GWAS signal. Equally, other methods allow for the partitioning of the trait heritability into functional, tissue or cell-specific categories, so as to allow assessments of enrichment of overall GWAS signal (Finucane et al., 2018).

For schizophrenia, such functional annotation of associated common genetic variants and mapping to gene expression data have shown enrichment of various sets of genes; particularly being those involved in glutamatergic, calcium signalling, synaptic functioning, immunological pathways and, more recently, dopaminergic signalling (including the *DRD2* gene encoding the dopamine D₂ receptor: the target of most current antipsychotic); and with expression predominately altered in early brain development (Genovese et al., 2016; Howrigan et al., 2020; Jaffe et al., 2018; O'dushlaine et al., 2015; Pardiñas et al., 2018; Rees et al., 2020; Smeland, Frei, Dale, & Andreassen, 2020). Since CNVs often span multiple genes, functional annotation is more difficult, however, generally these CNVs also show enrichment for synaptic signalling, and glutamatergic and GABAergic neurotransmission (G. Kirov et al., 2012; Pocklington et al., 2015). It is interesting that despite the clear importance of aberrant dopaminergic signalling to psychosis – being the major focus of antipsychotic medication -, molecular networks identified via genetic evidence thus far have mostly pointed toward more upstream systems, such as glutamatergic and gamma-aminobutyric acid (GABA) signalling pathways, which then appear to sensitise the dopaminergic system to later disruptive stress events (Howes, McCutcheon, Owen, & Murray, 2017).

The summation and interaction of genetic and early environmental factors, therefore, appear to lead to perturbed neurodevelopment and network establishment (Cattane, Richetto, & Cattaneo, 2018; Guloksuz et al., 2019; McCutcheon et al., 2020; Myllyaho et al., 2019; Wong et al., 2020). For example, individuals with early life complications show a much greater genetic liability to schizophrenia than those without; with the interaction of these greatly increasing their predictive power for schizophrenia diagnosis; and with the genes contributing to this interaction shown to be upregulated in placental tissue and associated with altered neurodevelopment (Ursini et al., 2018). The developmental risk factor model for schizophrenia suggests that due to these early neurodevelopmental effects, the brain is less plastic and more at risk to subsequent later-childhood/adolescent environmental exposures such as isolation, social fragmentation and cannabis use, as well as later genetic effects on synaptic pruning in adolescence; with these then impacting upon developmental trajectories, disrupting neural networks and leading to psychosis onset (Murray, Bhavsar, Tripoli, & Howes, 2017).

1.1.6 Pleiotropy

Advances of our understanding of the genetic architecture behind schizophrenia has also greatly impacted upon our appreciation of its relationship with other psychiatric (e.g. bipolar disorder, major depressive disorder) and neurodevelopmental disorders (e.g. autism spectrum disorder (ASD), intellectual disability). Rather than there being distinct separations between disorders and between disorder groupings (i.e. psychiatric vs neurodevelopmental), there exists a high overlap of symptomatology and presentation between disorders. For examples, this has led to recent developments to capture these into a single shared latent “psychopathology/p-factor” (Caspi et al., 2014), analogous to the latent “g-factor” of participants’ general cognitive ability on tasks (Deary, 2001). There is, therefore, growing appreciation for the overlap of symptoms between disorders, as well as between disorder “symptoms” and normal-range behavioural measures in unaffected individuals (Cuthbert & Insel, 2013; M. J. Owen, 2014).

Such overlap is reflected at the genetic level. Family studies have shown that having a close family member with a non-schizophrenia psychiatric/neurodevelopmental disorder increases your risk for schizophrenia, as does having a close-family member with schizophrenia increase your risk for other non-schizophrenia psychiatric/neurodevelopmental disorders (Song et al., 2015). In regard to genetic variants themselves, this overlap, termed “pleiotropy”, has been well documented for common (Anttila et al., 2018; Frei et al., 2019; P. H. Lee et al., 2019; O’dushlaine et al., 2015; Selzam, Coleman, Caspi, Moffitt, & Plomin, 2018; Wu et al., 2020) and rare genetic variants (George Kirov et al., 2014; Rees et al., 2014; Singh et al., 2016, 2017), as

well as at the gene and molecular expression levels (Gandal et al., 2018). The overlap of disorder symptomatology with normal-range behavioural traits have equally been replicated at a genetic level (Barkhuizen, Pain, Dudbridge, & Ronald, 2020; Roelfs et al., 2020). In addition to genetic risk overlap, many environmental risk factors for schizophrenia are also shared across disorders, such as early life stressors of low birth weight or childhood maltreatment (Abel et al., 2010; Schmitt, Malchow, Hasan, & Falkai, 2014).

In general, therefore, it appears that psychiatric disorders are not distinct but instead exist on a neurodevelopmental continuum alongside other such psychiatric and neurodevelopmental conditions. This continuum is characterised by a gradient of decreasing neurodevelopmental impairment - indexed by factors such as age at onset, severity of cognitive symptoms and persistence of functional impairment-, ranging from early life neurodevelopmental disorders such as intellectual disability and autism spectrum disorder, to later adult disorder such as schizophrenia and bipolar disorder (Fatemi & Folsom, 2009; Murray et al., 2017; M. J. Owen, O'Donovan, Thapar, & Craddock, 2011; Selemon & Zecevic, 2015).

1.1.7 Neurological pathophysiology

In tandem with the growing appreciation of neurodevelopmental impairment and genetic enrichment in schizophrenia, there has been an expanding understanding of the structural, molecular and functional brain differences in adolescent and adult individuals with overt schizophrenia diagnoses.

Post-mortem studies in schizophrenia reveal reductions in neuronal number and size; dendritic number and complexity; and synapse number (Bakhshi & Chance, 2015; Glausier & Lewis, 2013; Roeske, Konradi, Heckers, & Lewis, 2020). Genetic effects on these neuronal processes can occur both directly as well as via interaction with genetic and environmental immune-related risk (Allswede & Cannon, 2018; Anttila et al., 2018; Benros et al., 2016; Sekar et al., 2016; Sellgren et al., 2019). These differences in cellular morphology and cellular connectivity (axons, dendrites and synapses) have been shown to lead to reductions in cortical volume in those with schizophrenia, as well as enlargement of lateral ventricles (Bakhshi & Chance, 2015). While post-mortem studies can greatly aid in analysing cellular and molecular differences in those with schizophrenia compared to those without, the small sample sizes, time and nature of collection (separation of medication effects and variance in preservation effects), and lack of participant clinical and demographic information, mean that they can only provide limited inferences into

neuroanatomical differences which relate to the underlying schizophrenia pathophysiology itself.

In addition, therefore, the expansion in use of non-ionising Magnetic resonance imaging (MRI) has greatly advanced our understanding of altered neuroanatomy and functionality in schizophrenia. MRI allows for much deeper phenotyping, more feasible repeat scanning, and the possibility of analysing much larger sample sizes of both affected and unaffected individuals for comparison. Furthermore, while earlier MRI studies were often hampered by small sample sizes, recent literature meta-analyses and large collaborations such as ENIGMA (Enhancing Neuro Imaging Genetics through meta-analysis) and COCORO (Cognitive Genetics Collaborative Research Organization) working groups, have allowed for much larger, well-powered studies with standardised analytical approaches, so as to more robustly ascertain schizophrenia-related brain differences (Koshiyama, Miura, et al., 2020; Thompson et al., 2020). These have been particularly useful for structural brain imaging, being easier to standardise across sites.

Structural MRI results have generally replicated the ventricular volume enlargement and cortical atrophy noted in post-mortem studies (Kuo & Pogue-Geile, 2019; Shenton, Whitford, & Kubicki, 2010). Cortical volume is a product of both surface area and thickness. Reductions in both have been reported in those with schizophrenia, particularly in frontal and temporal regions (Spalthoff, Gaser, & Nenadić, 2018; Theo G.M. van Erp et al., 2018). In addition to cortical structures, several independent meta-analyses have shown volume reductions in subcortical structures of hippocampal, amygdala, thalamus and nucleus accumbens, as well as enlargements of pallidum and putamen volumes (Okada et al., 2016; T. G.M. Van Erp et al., 2016). In addition to mean volume measure differences, those with schizophrenia also show differences in more latent features, such as in increased heterogeneity of intracranial, ventricular and hippocampal volumes reported (Alnæs et al., 2019; Kuo & Pogue-Geile, 2019), and in an accelerated brain-age measure (a machine learning assessment trained on a large neuroimaging reference of “healthy” participants) (Hajek et al., 2019; Koutsouleris et al., 2014). Agreeing with the discussed genetic analyses and with electrophysiological studies (Koshiyama et al., 2018), regional molecular MRI studies have also noted cortical glutamatergic and GABAergic disruption (Sydnor & Roalf, 2020), which also appears to be linked with altered striatal dopaminergic signalling (Jauhar et al., 2018). In addition to regional differences, widespread reductions in measures of structural connectivity (Holleran et al., 2020; Kelly et al., 2018; Koshiyama, Fukunaga, et al., 2020; Van Den Heuvel et al., 2019) and functional

connectivity (Adhikari et al., 2019; Dong, Wang, Chang, Luo, & Yao, 2018) between regions are also seen; particularly in associative cortical regions.

There are, therefore, numerous reports of structural, functional and molecular brain alterations in those with a schizophrenia diagnosis compared to those without. In addition to noting these differences and improving our understanding of schizophrenia biology, studies have also been focused on ascertaining if such differences associate with particular features of schizophrenia presentation, so as to improve diagnosis and treatment. While an extensive review of the extent of these findings is beyond the scope of this chapter overview (though are discussed in regard to the cerebellum in a later section), we highlight recent publications of associations with symptomologies (Holleran et al., 2020; Walton et al., 2018), subtyping of schizophrenia diagnosis (Chand et al., 2020; Takahashi et al., 2017), separation of schizophrenia from other psychiatric disorders (C. C. Huang et al., 2020; Koshiyama, Fukunaga, et al., 2020), and relation to treatment response (Barry et al., 2019; Kochunov et al., 2019; Molent, Olivo, Wolf, Balestrieri, & Sambataro, 2019).

1.1.8 Limitations of traditional case-control studies

A limitation of such case-control samples, however, is in the difficulty of ascertaining which of the neuroanatomical and functional differences seen are due to schizophrenia pathophysiology itself, as opposed to those which might reflect associated features. For instance, comorbidities with other neurological and psychiatric disorders are common in schizophrenia (Buckley, Miller, Lehrer, & Castle, 2009), as are commodities with other physical disorders such as cardiac, diabetes and metabolic disorders, and related health effects such as elevated weight (Annamalai, Kosir, & Tek, 2017; Scott et al., 2016; Vancampfort et al., 2013). These factors can have their own negative effect on recorded brain volume (Dekkers, Jansen, & Lamb, 2019), though are little considered in psychiatric neuroimaging studies. The use of antipsychotic medications themselves is often associated with elevated weight gain and metabolic complications, which is one way in which many of these comorbidities can arise, though is not the sole causative pathway (Annamalai et al., 2017).

In addition to having true pathophysiological negative effects on brain volume, these comorbidities can also change the participants' position or behaviour within the scanner, inducing imaging artefacts of reduced volume when no real difference might be present (Beyer et al., 2020). One such behavioural difference is of increased head motion in those with psychiatric diagnoses, having the potential to be confounding many of the structural (an

addition to functional) results seen; being described as psychiatry's "dirty little secret" (Makowski, Lepage, & Evans, 2019). Studying brain differences in those with first episode, drug-naïve diagnoses can help address some of these issues, such as separating out those factors caused by chronicity of disorder or by medication effects. However, the effects of comorbidities and features such as elevated head motion are likely to remain, and more research is required in better understanding their effect on the brain, and in identifying whether the presence of reported neuroanatomical differences in those with schizophrenia continue, when taking these factors into account.

1.2 Genetic neuroimaging

In addition to investigating the above in clinical samples, in the following section, I outline how the advancement of neuroimaging genetics approaches can help to bridge the gap between genetic risk factors identified for schizophrenia and neuroanatomical differences identified in case-control studies. These can help to not only control for reverse causative factors which might confound results, such as arising through medication treatment itself, however, also improving our understanding of biologically plausible pathways which might mediate genetic risk.

1.2.1 Family-based studies

Family studies have shown that unaffected close family members of those with schizophrenia diagnoses also show brain alterations similar to those with overt diagnosis, though smaller in effect size. This includes, for example, reductions in brain grey and white matter volumes, as well as increased intracranial volume (de Zwarte, Brouwer, Agartz, et al., 2019; Greenstein et al., 2011). These studies, therefore, suggest that reverse causation alone through factors such as antipsychotic medication use, are not the sole cause of neuroanatomical differences. Furthermore, they begin to suggest an inherent relationship between genetic risk for schizophrenia, and neuroanatomical differences. However, such studies can still be confounded by any residual shared environment between family members, ascertainment bias and, if comparing across different generations, by differences in age and life experiences (Rasetti & Weinberger, 2011).

Importantly, studies in twins - which allow for better separation of associations driven by shared genetic from environmental signals - have shown structural brain measures also appear highly

heritable, with estimates between 50 to 90% heritability for regional volumetric measures; being generally higher for global measures (Blokland, De Zubicaray, McMahon, & Wright, 2012). These results indicate that, similar to schizophrenia, variation in neuroanatomy can be largely accounted for by variation in genetic differences. While there appears some evidence for brain structure differences to show significant co-heritability with schizophrenia in twin-based studies (i.e. for differences to be due to shared genetic rather than environmental factors), such as for reduced cerebral white matter and increased ventricular volume (Van Haren et al., 2012), the limited power means that results remain inconsistent as to the extent these can be attributed to shared genotype (de Zwarte, Brouwer, Agartz, et al., 2019).

1.2.2 Copy number variants

In addition to family-based studies, therefore, another approach has been in analysing brain differences in those carriers of known schizophrenia-associated copy number variants (CNVs) compared to non-carriers. For example, one of the CNVs with highest penetrance for schizophrenia is a deletion in the 22q11.2 chromosomal region (Schneider et al., 2014). Carriers of this CNV show numerous brain abnormalities similar to those seen in those with schizophrenia, including decreased total grey and white matter brain volume (Rogdaki et al., 2020). As discussed previously, however, these CNVs are rare and, therefore, sample sizes for such studies are often small. Furthermore - and related to these CNV's high penetrance for schizophrenia (and other psychiatric and neurodevelopmental disorders) - these studies often actively recruit participants through clinical referral, meaning ascertainment bias is a potential problem, as well the confounding factors discussed in relation to clinical imaging studies (e.g. medication status), which can equally apply here and complicate interpretation of any brain differences.

The advent of large, volunteer cohorts, such as the UK Biobank, are offering a concordant approach to analyse the effect of these CNVs on neuroanatomy. Of a total cohort of around 500,000 UK based adult individuals who have provided extensive phenotyping information, including demographic, clinical, genetic and medical health record access, a 100,000 participant sub-cohort will eventually undergo neuroimaging scanning (Collins, 2012; Littlejohns et al., 2020). Such a resource provides an exceptional opportunity for studying the relationship between genetics, neuroanatomy and functionality, and disease states. Analysis of the relationship between schizophrenia-associated CNV status and brain differences in this cohort, therefore, can provide useful additional information for any such relationship identified, since these individuals were not recruited via clinical referral. Recent publications have shown that,

on average, carriers of any schizophrenia-associated CNVs who do not themselves have a psychiatric diagnosis, show reduced subcortical volumes, cortical surface and increased cortical thickness compared to non-carriers (Xavier Caseras et al., 2021; Warland, Kendall, Rees, Kirov, & Caseras, 2020). Rare copy number variants, associated with schizophrenia, therefore, do appear to affect cortical and subcortical structures in a manner similar to that seen in individuals with overt schizophrenia diagnoses.

1.2.3 Polygenic schizophrenia risk score

In addition to assessing the association between rare genetic variants and neuroanatomy, one can also ascertain if similar differences are seen in those with elevated common genetic risk for schizophrenia. Polygenic schizophrenia scores represent an individual's genetic burden for common genetic variants associated with schizophrenia; being the summated presence in an individual of common alleles previously identified in a schizophrenia GWAS as associated with schizophrenia liability, weighted by each allele's association strength. Such an approach has been used to test for how well GWAS identified genetic variants predict schizophrenia liability in independent cohorts of unrelated individuals, where results cannot then be due to shared environment (Ripke et al., 2013; Vassos et al., 2017). In cohorts of individuals with both neuroimaging and genetic data, they can be used to ascertain how much genetic variants for schizophrenia account for variance in a brain imaging measure of interest. They have been shown to associate with reduced cortical gyrification and thickness, and some evidence of reduced total brain, white matter and globus pallidus volume in individuals who do not themselves have a psychiatric diagnosis (B. Liu et al., 2017; Neilson et al., 2019; van der Merwe et al., 2019). While promising, study effects have been small and inconsistent, therefore, so far there appears no strong evidence for an association with any of the brain volume measured thus far (van der Merwe et al., 2019). Furthermore, while polygenic scores can help identify associations between genetic risk for schizophrenia and neuroanatomical differences, they are limited in not being able to ascertain where in the genome might be driving this association. In tandem with their use, therefore, better understanding of the genetic architecture behind neuroanatomy itself is key.

1.2.4 GWAS of brain-based measures

Traditionally, it has been exceptionally hard to collect large enough samples with both neuroimaging and genetic information to further probe the heritability of brain-based measures attributable to variation in common genetic variants. The advent of projects like the UK Biobank

as well as large collaborative projects such as ENIGMA - which have also analysed genetic associations with neuroimaging traits, in addition to the case-control studies already mentioned (Thompson et al., 2020) -, however, have finally allowed this to change. Recent GWAS studies on cerebral cortex and subcortical regions have reported heritability estimates range from 26 to 86%, therefore, a substantial proportion of brain measure heritability is accounted for by variation in common genetic variants (Grasby et al., 2020; Satizabal et al., 2019). Follow-up analyses of these GWAS summary statistics are also helping to improve our understanding of molecular and neuronal pathways behind these associations, such as identifying enrichment in various neuronal, myelinating and synaptic processes (Grasby et al., 2020; Satizabal et al., 2019).

Such summary statistics can also be used to ascertain pleiotropy between schizophrenia liability and neuronal processes, at the level of individual variants, loci, genes and pathways. While such investigations are relatively sparse thus far (due to the very recent availability of power for brain-based GWASs), examples including probing the association between the non-synonymous rs13107325 variant within *SLC39A8* gene transcript and both schizophrenia liability and putamen volume (Q. Luo et al., 2019). Furthermore, different methods utilising both summary statistics as well as individual-level genotype data for unrelated individuals (van Rheenen, Peyrot, Schork, Lee, & Wray, 2019), allow estimations of the genetic correlation between schizophrenia and neuroimaging-based traits across the whole genome. Thus far, results for subcortical and cortical structures show limited consistent direction of effect for a relationship with schizophrenia (Grasby et al., 2020; Satizabal et al., 2019); though whether this is the case for other regional brain areas and related traits is still to be further explored.

1.2.5 Relevance of neuroimaging genetic results

Neuroimaging phenotypes, therefore, are believed to be a useful and stable intermediate traits, where the small individual effects of genetic risk alleles associated with a psychiatric disorder like schizophrenia, coalesce on underlying neuronal processes, and lead to detectable and quantifiable differences. Investigations of the common genetic variants behind MRI brain measures, highlights the advantage of brain-based measures' reduced polygenicity and increased discoverability compared to psychiatric traits themselves (Matoba, Love, & Stein, 2020). Thus, these intermediate phenotypes, or endophenotypes have the potential to greatly aid in unravelling schizophrenia pathophysiology, allowing linking of genetic variations associated with the complex behavioural trait of schizophrenia with underlying biological mechanisms (Gottesman & Gould, 2003; Le & Stein, 2019). These have the potential to improve schizophrenia diagnosis by creating more biologically relevant subtypes and decreasing

heterogeneity of schizophrenia (and of neuroanatomical differences seen), as well as in the creation/refinement of treatments and animal models for testing. While results thus far have been mixed, substantial increases in sample sizes of both schizophrenia GWAS studies and neuroimaging genetic cohorts; careful consideration of possible comorbidities and imaging artefacts (as discussed previously); and, importantly, addressing omissions in the regions analysed thus far (see below), have the potential to greatly improve the knowledge these methods can provide of schizophrenia pathophysiology.

A major limitation to almost all of the aforementioned brain imaging studies in those with overt psychiatric disorders, as well as genetic neuroimaging studies, has been their focus, almost exclusively, upon cerebral cortical and subcortical structures. The cerebellum – a structure which contains the majority (approximately 80%) of neurones in the human brain (Herculano-Houzel, 2010) - has been largely omitted from all such studies. This is not unique to studies of psychiatric disorders and a general cerebral bias exists in cognitive studies (Parvizi, 2009). This viewpoint, however, has been changing over the preceding decades, and there is now a growing interest in the cerebellum and its contributions to normal and abnormal neuronal functionality. In the section below, I provide an overview of cerebellar neuroanatomy, the cellular functionality of the cerebellum and some of these behavioural roles to which it is believed to contribute. In a subsequent section, I highlight the evidence for cerebellar differences in those with schizophrenia, and its relevance to schizophrenia symptomatology and presentation.

1.3 The cerebellum

1.3.1 Structure

The cerebellum is a particularly unique brain region, being located in the posterior fossa and separated from cortical and subcortical structures by cerebrospinal fluid; with only three white matter tracts (the superior, middle and inferior cerebellar peduncles) providing connections to the rest of the brain. It contains three tissue types: an outer cerebellar “grey-matter” cortex, cerebellar white matter outputting to the aforementioned peduncles, and three sets of deep cerebellar nuclei located within the white matter. Viewed externally, the outer cerebellar cortex is vertically separable into a central vermis and the two hemispheres either side. Meanwhile, horizontal fissures can be used to separate the cerebellum into cerebellar lobes, such as the anterior, superior and inferior posterior and flocculonodular lobes, or with use of further fissures dividing the cerebellum into 10 individual lobules (in mammals) (Figure 1.2). Recent

advancements in the development of cerebellar-specific MRI segmentation tools, such as SUIT (Diedrichsen, 2006) or CERES (Romero et al., 2017), have aided in the mapping and production of probabilistic atlases of these cerebellar lobules (Diedrichsen, Balsters, Flavell, Cussans, & Ramnani, 2009). These atlases can then be deployed with or without the cerebellar-specific registration tools; though doing so does significantly improves the registration of images and anatomical alignment to the atlas (Diedrichsen, 2006).

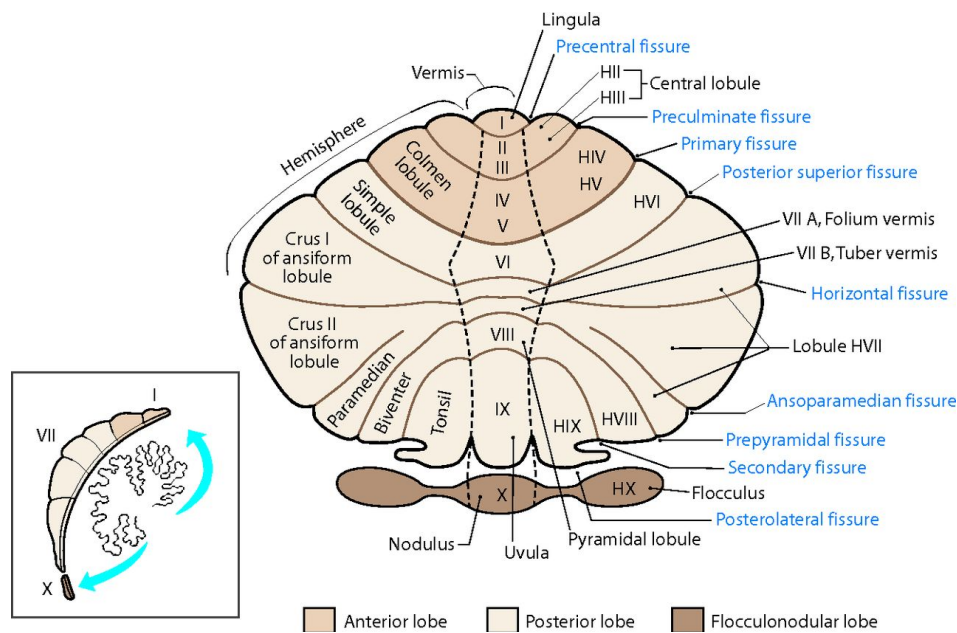


Figure 1.2: Cerebellar lobule and fissure anatomy. Insert: overlay of flattened representation of a sagittal cerebellar slice. From (Klein, Ulmer, Quinet, Mathews, & Mark, 2016)

1.3.2 Modular functionality

The cytoarchitecture, connectivity and processing roles of the cerebellum are distinct within the brain. They have been best described in regard to sensorimotor functionality and conceptualised in the “Marr-Albus-Ito” model (Cabarau et al., 2020; D’Angelo, 2018; Ito, 2008). An efference copy of motor commands from the cerebral cortex is sent to the cerebellar cortex, where the cerebellum then produces (and refines) internal forward models of motor output, allowing prediction of sensory consequences of the motor action. These prediction signals can then be compared to the actual motor feedback, with corrective signals sent from the cerebellum to the brainstem and/or cerebral cortex when deviations/errors are identified (Figure 1.3). This leads to efficient prediction, coordination and adaptation of movement; as well as allowing long-term adaptation and learning at the levels of the cerebellum, brainstem and

cerebral cortex (D'Angelo, 2018). Purkinje cells, located in the middle, molecular layer of the cerebellum, receive both input signals from the cerebral cortex (via mossy fibres and granule cell parallel fibres) and error-based signals from the inferior olive (via climbing fibres), and so allowing for the comparison and adaption of signal (Eccles, Llinás, & Sasaki, 1966). These Purkinje cells reflect the sole output of the cerebellar cortex, which project inhibitory signals back to deep cerebellar nuclei. This is a simplified viewpoint, however, with afferent fibres also projecting to deep cerebellar nuclei and other interneurons; adaption and modulation of signal occurring at various other levels of the cerebellum (D'Angelo, 2018; J. Kim & Augustine, 2020); and other forms of learning such as reward-based learning occurring at the cerebellum in addition to the error-based learning discussed (Hull, 2020).

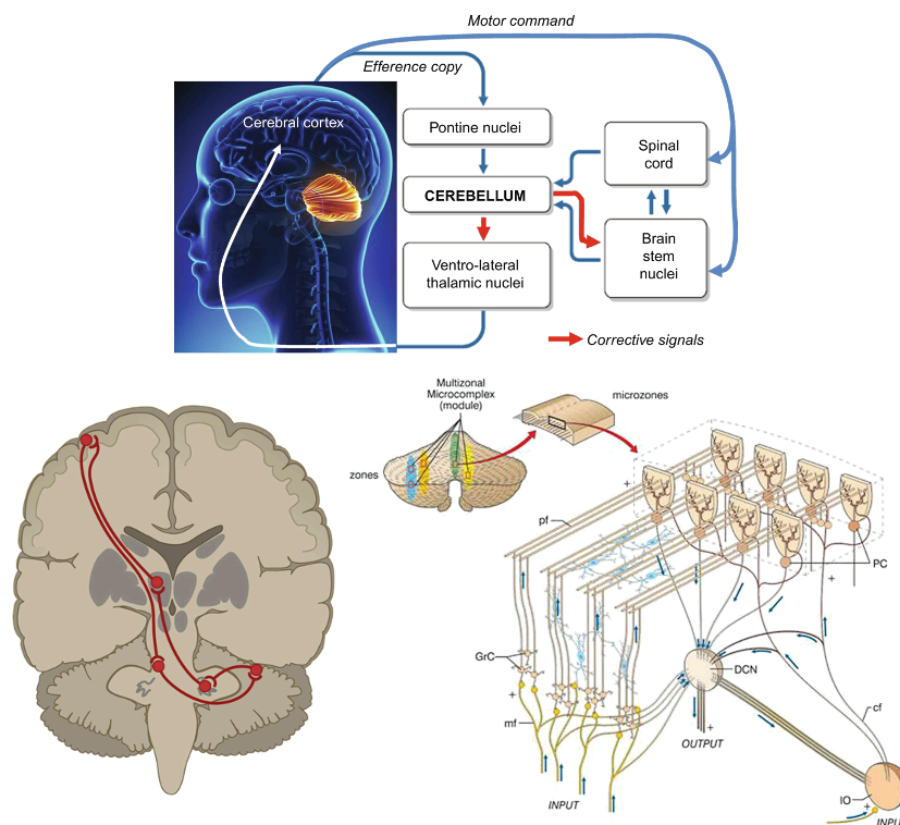


Figure 1.3: Top) The internal forward model of the cerebellum. Displaying the primary afferent and efferent loops between the cerebellum and cerebral cortex. Following the projection of an efference copy of motor commands to the cerebellum, and cerebellar comparison with sensory feedback from spinal cord and brainstem, corrective signals are sent back from the cerebellum to the brainstem (directly adapting movement) and to the cortex (adapting motor plans). From (D'Angelo, 2018)

Bottom Left) Cerebrocerebellar loops. A different visualisation of the neuronal circuitry loops that exist between the cerebellum and cerebral cortex. Motor commands from cerebral cortex projections travelling across the pontine nuclei, cerebellar cortex, deep cerebellar nuclei, thalamic nuclei and back to the cerebral cortex. Models includes the decussation of pathways in the midbrain, subsequent to leaving cerebellum via superior cerebellar peduncles. From (Buckner, 2013).

Bottom Right) Physiology of cerebellar microcircuit processing. Individual modules of interconnected inferior olive (IO), deep cerebellar nuclei (DCN), Purkinje cells (PC) and granule cell (GRc). Inputs of mossy fibres carrying the cortical signal (such as efference copy of motor command); and climbing fibres (cf) projected from the inferior olive carrying sensory feedback. Interneurons are displayed in pale blue. From (D'Angelo, 2018)

Cerebellar cytoarchitecture and functionality can be defined generally in terms of modular units, each comprised of relatively closed, independent loops, with projections to and from the same inferior olive, Purkinje cell and deep cerebellar nuclei regions (Apps et al., 2018; Fujita, Kodama, & du Lac, 2020). The architecture of modules across the cerebellum is largely homogenous, though there is growing appreciation for relative differences in molecular and cellular make up which could modify function (Beckinghausen & Sillitoe, 2019; Cerminara, Lang, Sillitoe, & Apps, 2015; Witter & De Zeeuw, 2015; Zhou et al., 2014). While broadly similar cytoarchitecture, each module shows distinct patterns of connectivity with other cortical/subcortical regions (discussed below). It appears, therefore, that these modules are conducting a generally similar function across the cerebellum, though ones which differ in their operation depending on the connectivity of that cerebellar sub-region with the rest of the brain: conceptualised as the universal cerebellar transform (UCT) (D'Angelo & Casali, 2013; Schmahmann, 2000).

In regards to connectivity, the cerebellum can be approximately divided into vestibulocerebellar (flocculonodular lobe) involved in vestibular processing, spinocerebellar (vermis and paravermis, constituting most of the anterior lobe) involved in sensorimotor processing and cerebrocerebellar (most of the lateral cerebellar hemispheres) involved in other cortical functioning (D'Angelo, 2018). Cerebello-cortical loops via afferent cortico-pontine-cerebellar and efferent cerebello-thalamo-cortical tracts have been identified with most cortical regions (Henschke & Pagan, 2020; Strick, Dum, & Fiez, 2009). Despite the difficulty of mapping long-range connections, these tracts have also been replicated in diffusion MRI (Q. Ji et al., 2019; Sokolov, Erb, Grodd, & Pavlova, 2014) and that the majority of fibres – an estimated 80% -

connect with associative cortical regions, predominantly being prefrontal and temporal (Palesi et al., 2017). Recent resting-state functional MRI studies have also highlighted the extensive connectivity with non-motor regions, particularly for the posterolateral cerebellum with frontoparietal regions (Buckner, Krienen, Castellanos, Diaz, & Thomas Yeo, 2011; Guell, Schmahmann, Gabrieli, & Ghosh, 2018; Marek et al., 2018; Riedel et al., 2015).

1.3.3 *Non-motor roles*

These results of a more universal cerebellar functionality and extensive associative cortical connectivity have seen a growing interest in the cerebellum's roles in non-motor capabilities and behavioural traits. Task-based functional MRI (fMRI) studies have indicated cerebellar activations in various cognitive roles, for instance in language (Fiez, 2016; Guell, Gabrieli, & Schmahmann, 2018; Moberget & Ivry, 2016), working-memory (Guell, Gabrieli, et al., 2018), spatial memory (Zeidler, Hoffmann, & Krook-Magnuson, 2020) and abstract reasoning (Joshua H. Balsters, Whelan, Robertson, & Ramnani, 2013). A recent fMRI study of a multi-domain battery of tasks showed cerebellar regions associated with higher cognitive performance based tasks to be in the majority, as compared to the historical perspective of a predominate role in motor coordination (King, Hernandez-Castillo, Poldrack, Ivry, & Diedrichsen, 2019) (Figure 1.4).

Indeed, ape and human evolutionary studies have shown cerebellar structure as being one of the most expanded regions in humans (Barton & Venditti, 2014; Hublin, Neubauer, & Gunz, 2015; Kochiyama et al., 2018; Neubauer, Hublin, & Gunz, 2018; Smaers & Vanier, 2019), particularly in these posterolateral regions connected with non-motor regions (J. H. Balsters et al., 2010). Regulatory effects of genetic variants differing between modern and archaic humans are found particularly enriched within the cerebellum (McCoy, Wakefield, & Akey, 2017), and enrichment of genetic variants associated with cognitive ability also show strong enrichment in the cerebellum (Lam et al., 2017). Cerebellar structure itself is associated with cognitive performance, with cerebellar grey-matter volume associated with general and specific cognitive ability in older patient cohorts (Hogan et al., 2011) and in younger cohorts (Moore, D'Mello, McGrath, & Stoodley, 2017). Finally, in patients with cerebellar lesions, there is growing understanding of the myriad cognitive deficits that this leads to, which have been formalised into the terminology of cerebellar cognitive affective syndrome (CCAS) (Argyropoulos et al., 2020; Parrell, Agnew, Nagarajan, Houde, & Ivry, 2017; Schmahmann, 2019; Schmahmann & Sherman, 1998; Tavano et al., 2007).

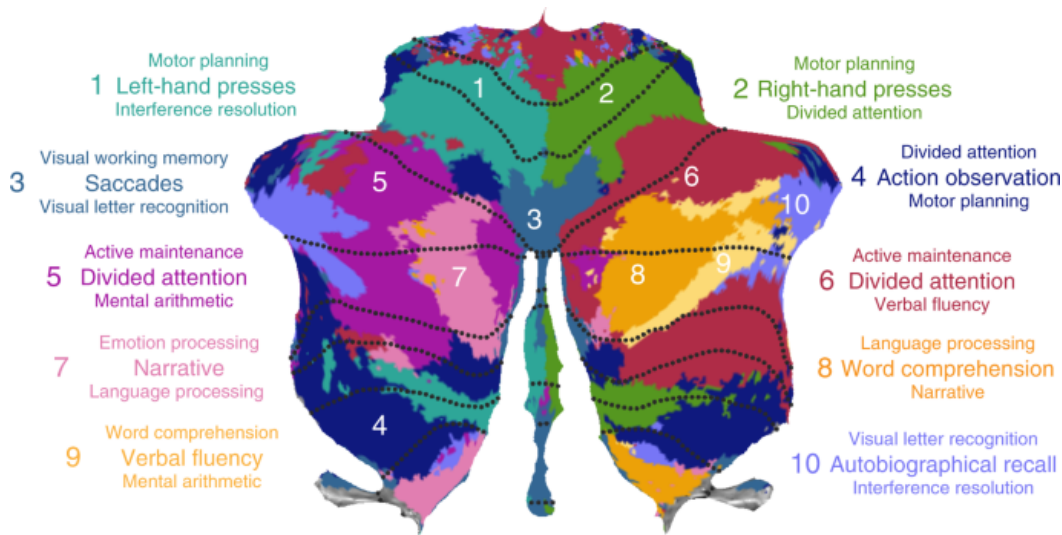


Figure 1.4: Cerebellar functional boundaries following application of a multi-domain task battery in the same subjects. Participants (n=24) performed 26 diverse tasks (comprising 47 unique conditions) in a task-based functional MRI scan, whose results were combined to provide the probabilistic atlas of cognitive domain parcellations. From (King et al., 2019)

In addition to roles in cognitive processing, the cerebellum also appears important in various aspects of emotional/affective processing. For example, the cerebellum’s connections with the periaqueductal grey, amygdala and thalamic ventral tegmental area (VTA), and moderating effect on dopaminergic network neurotransmission have been shown to be involved in fear conditioning and anxiety related disorders (Bostan & Strick, 2018; Carta, Chen, Schott, Dorizan, & Khodakhah, 2019; Frontera et al., 2020; Locke et al., 2020, 2018; Moreno-Rius, 2018; Moulton, Elman, Becerra, Goldstein, & Borsook, 2014). Those with cerebellar lesions show dysregulation of emotional/affective processes - being part of the CCAS syndrome – and include impaired emotional control/responses and social skills (Argyropoulos et al., 2020; Schmahmann, Weilburg, & Sherman, 2007). Indeed the cerebellum has been shown to be a key substrate in social cognition, with those with cerebellar damage showing an inability to appropriately identify and respond to the emotional state of others (Brady et al., 2020; Hoche, Guell, Sherman, Vangel, & Schmahmann, 2016; Schmahmann, 2019). Dysfunction of the cerebellum, therefore, appeared to not only lead to uncoordinated movement but also uncoordinated thought, emotional appraisal and response.

As previously mentioned, these traits are characteristic of psychiatric disorders, and indeed those with cerebellar pathologies also show an elevation in psychosis and autism-like symptomatology (Kronemer et al., 2020; Schmahmann et al., 2007). In the below section, I highlight how, in tandem with the growing appreciation of the cerebellar’s roles in non-motor

functionality and cerebellar pathology's association with related cognitive and psychiatric symptomatology in patients, has been the growing appreciation of cerebellar disruption in those with schizophrenia.

1.4 Cerebellum and schizophrenia

Though reports of cerebellar alterations date back to some of the earliest neuroimaging investigations in schizophrenia (Coffman, Mefferd, Golden, Bloch, & Graber, 1981; Escelsior & Murri, 2019), it is the work of Nancy Andreasen and colleagues that particularly synthesised the idea of how cerebellar disruption could be vital for schizophrenia. Andreasen proposed that the diversity of schizophrenia symptomatology could be characterised by an inability to coordinate, prioritise and express information, termed as “cognitive dysmetria”, and that dysfunction of connectivity between cerebellum and cortex appears the important biological substrate for this (N. C. Andreasen, Paradiso, & O’Leary, 1998; Nancy C. Andreasen et al., 1999). Similar overlapping theories highlight how the cerebellum’s roles in facilitating motor and non-motor prediction might underlie schizophrenia symptomatology (Moberget & Ivry, 2019).

1.4.1 Cerebellar relevance to schizophrenia symptomatology

Since the work by Andreasen et al., numerous functional MRI studies have found that measures of schizophrenia symptomatology in individuals with overt diagnosis are associated with dysfunction of cerebellar activity and its connectivity with cerebral cortex. Confirming the aforementioned associations in unaffected “healthy” individuals, cerebellar dysfunction in those with schizophrenia has been shown to be associated with cognitive deficits (P. Chen, Ye, Jin, Zhu, & Wang, 2019; Gao et al., 2020; J. L. Ji et al., 2019; Matsuoka et al., 2019) including in processing speed (P. Chen et al., 2019), working memory (Bernard & Mittal, 2015) and social cognition (Brady et al., 2020); negative symptomatology (Bernard & Mittal, 2015; Brady et al., 2019); and positive symptomatology such as verbal hallucinations (X. Chen et al., 2019; Ferri et al., 2018; Pinheiro, Schwartz, & Kotz, 2020). While a meta-analysis confirmed cognitive and negative symptomatology cerebellar associations (Bernard & Mittal, 2015), since many of the studies utilise different approaches and most analyse a specific symptomatology, an updated meta-analysis and/or systematic analysis in a single patient cohort would help clarify the extent to which cerebellar structural and functional differences associate with schizophrenia symptomatology.

While most studies are correlative in nature, the use of cerebellar transcranial stimulation in two studies showed that the recovery of cerebellar activity was also associated with improvements in negative and positive symptomatology (Brady et al., 2019; X. Chen et al., 2019), providing evidence against purely correlative associations as well as highlighting the potential benefit of cerebellar stimulation for schizophrenia treatment (Escelsior et al., 2019; Escelsior & Murri, 2019). The use of optogenetics on cerebellar neuronal activity to successfully recover cognitive ability in animal models of schizophrenia also holds promise as an avenue to confirm causality (Prestori, Montagna, D'angelo, & Mapelli, 2020).

Equally important as the growing appreciation of possible cerebellar contributions to positive, negative and cognitive symptomatology in schizophrenia, has been the already discussed growing appreciation of sensorimotor dysfunction in schizophrenia, these often being in roles where cerebellar functionality is more established (Hirjak et al., 2018). For example, those with schizophrenia show an elevation in neurological soft signs, being subtle sensorimotor coordination and sequencing deficits, and with the cerebellum seen as a key substrate for these features (Caldani et al., 2017; Hirjak et al., 2015; Kong, Herold, Cheung, Chan, & Schröder, 2019; Varambally, Venkatasubramanian, Thirthalli, Janakiramaiah, & Gangadhar, 2006). The cerebellum's roles in oculomotor behaviour, such as smooth pursuit and eye-blink conditioning, have also been linked with the same deficits seen in those with schizophrenia (Caldani et al., 2017; Coesmans et al., 2014; Kent, Bolbecker, O'Donnell, & Hetrick, 2015).

The expansion of our knowledge of the cerebellum's contribution to various motor and non-motor roles, therefore, looks to be of relevance for schizophrenia symptomatology. In addition to reports of associations between cerebellar neuroanatomy and function within cohorts of those with overt diagnoses, there has been an increasing number of reports of mean cerebellar structural and functional differences when comparing those with and without schizophrenia diagnoses.

1.4.2 Cerebellar alterations in case-control studies

Functional MRI studies have shown general reductions in cerebellar activity in those with schizophrenia, including in first-episode, drug-naïve participants (Bernard & Mittal, 2015; Ding et al., 2019; Gao et al., 2020). Equally, they have mirrored the results from Andreasen's PET studies, reporting reduced cerebello-thalamo-cortical functional connectivity; including specifically between cerebello-thalamic (Anticevic et al., 2015; Dong et al., 2018; Ferri et al., 2018; Gong et al., 2019; J. L. Ji et al., 2019; Woodward & Heckers, 2016) and cerebello-cortical

associative regions (Hua et al., 2019; Shinn, Baker, Lewandowski, Öngür, & Cohen, 2015; Xi et al., 2020; Zhuang et al., 2019). Similar results have been found for white matter connectivity, with reports of reduced cerebello-thalamic (Deng et al., 2019) and cerebellar peduncle (H. Liu, Fan, Xu, & Wang, 2011; Mamah, Ji, Rutlin, & Shimony, 2019) integrity, though increases of the latter have also been noted (Filippi et al., 2014). Interestingly, increased functional connectivity between cerebellum and motor cortical regions (Guo et al., 2015; J. L. Ji et al., 2019; Shinn et al., 2015; Walther et al., 2017) and some aspects of default mode networks (Shinn et al., 2015; Houliang Wang et al., 2016) have also been found. The effects on connectivity differences, therefore, appear to differ across the cerebellum. One difficulty in assessing these results, however, has been in the small sample sizes and heterogeneity of methodological approaches taken for such studies. The choice of regions, the treatment state of patients (Houliang Wang et al., 2016) and analysis pipelines applied, vary across studies, and can cause considerable heterogeneity of results and reported effect sizes (Ramsay, 2019).

In addition to these connectivity differences, underlying alterations to cerebellar structure have also been identified in schizophrenia. Firstly, post-mortem studies have revealed reductions in Purkinje cell number in those with schizophrenia compared to controls (Maloku et al., 2010), as well as molecular differences in calcium-binding proteins (parvalbumin and calmodulin) (Vidal-Domènech et al., 2020), immune related dysfunction (MacDowell et al., 2017), and glutamatergic and GABAergic transmission related expression (Bullock, Cardon, Bustillo, Roberts, & Perrone-Bizzozero, 2008; Fatemi & Folsom, 2015; Schmitt et al., 2010; Yeganeh-Doost, Gruber, Falkai, & Schmitt, 2011). Macroscopic differences of reduced gyrification have also been reported in post-mortem schizophrenia studies (Schmitt et al., 2011).

When reported, large-scale structural MRI investigations often note reductions in cerebellar grey-matter volume in individuals with schizophrenia compared to control subjects (He et al., 2019; Laidi et al., 2019; Moberget et al., 2018; Quinn et al., 2018; Spalthoff et al., 2018; Wolfers et al., 2018). While some studies have reported no such reductions (Guo et al., 2018), a recent meta-analysis of voxel-based morphometry (VBM) showed generally decreased cerebellar lobule IIV-V and VII grey matter volume in those with schizophrenia compared to normative controls (Ding et al., 2019).

The largest systematic study to date of cerebellar structural differences in schizophrenia was by Moberget et al. (2018), assessing volumetric differences in 983 cases and 1349 age and sex matched controls (Moberget et al., 2018). Compared to previous meta-analyses, all samples in this mega-analysis were processed using the same identical pipeline to minimise methodology

heterogeneity and included cerebellar-specific registration tools and cerebellar-specific quality control. They found small-to-moderate reductions across most of the cerebellum (Cohen's $d=0.35$), particularly for regions of the cerebellum previously associated with associative cortical regions. Notably, they found that cerebellar differences were some of the most pronounced, compared to all other subcortical and cortical features analysed, apart from hippocampal reductions and pallidal increases. Those with schizophrenia, therefore, appear to show abnormal cerebellar-cortical functional connectivity, which differs across the cerebellum depending on their cortical connectivity, but with more global volumetric reductions across the whole of the cerebellum.

Unfortunately, being a retrospective mega-analysis of different cohorts, the amount of clinical and demographic information was limited in Moberget et al.'s study (Moberget et al., 2018) as well as in all previous meta-analyses. Exploring the effect of these related comorbidities and other potential confounding factors on the cerebellum, and how these might relate to schizophrenia diagnosis, therefore, would help us better understand the aetiology of such reported cerebellar differences in clinical cases.

1.4.3 The neurodevelopmental origin of cerebellar differences

Importantly, Moberget et al. also found that the cerebellar reductions were present in the youngest of cases and generally stable over time (Moberget et al., 2018). These results, therefore, provide evidence of cerebellar differences being present before disease onset and not simply reflecting secondary deterioration of volume due to its chronicity and/or due to medication-related effects. Though, again limited in the data they could collect, Moberget et al. did show that there was no relationship between cerebellar structural differences and medication status. These results mirror others' findings of cerebellar reductions in first-episode, drug naive individuals (Ding et al., 2019) and in clinically at-risk individuals displaying symptomology associated with pro-dromal stages (Dean et al., 2014); indicating cerebellar differences to not be due to reverse causation but instead be present before primary symptom onset. Additionally, schizophrenia patients with earlier onset show more marked cerebellar reductions compared to those with later onset, indicating the cerebellar differences to be particularly associated with early brain development (C. Zhang et al., 2017).

Furthermore, in addition to these results within schizophrenia diagnosis, cerebellar alterations across other psychiatric and developmental disorders also emphasise how the cerebellum might be a key biological substrate of interest when considering neurodevelopmental differences in

schizophrenia. Compared to many of the other regional brain differences in schizophrenia, cerebellar alterations are also noted in many neurodevelopmental disorders including autism spectrum disorders (ASD) – with perinatal cerebellar injury being the leading risk factor aside from twin-sibling diagnosis-, attention deficit hyperactivity disorder (ADHD), Down’s syndrome and intellectual disability (Sathyanesan et al., 2019; Stoodley, 2016). Indeed the shared latent p-factor across psychiatric/neurodevelopmental disorders shows a cerebellar substrate (Romer et al., 2018), with the suggested implication being that disrupted cerebellar capacity in the creation of internal forward models, leads to a general inability to adapt early on in brain development, which then leads to a specific disorder via disruptions in other circuits (Hariri, 2019; Sathyanesan et al., 2019). Many of the early life environmental stressors associated with increased schizophrenia and other psychiatric/neurodevelopmental disorder risk, such as hypoxia and prematurity, have also been shown to particularly be associated with perturbed cerebellar growth and functionality (Moussa-Tooks et al., 2020; Sathyanesan, Kundu, Abbah, & Gallo, 2018; Tran et al., 2017; Volpe, 2009).

The cerebellum’s particular preponderance to neurodevelopmental perturbations is likely due to the related factors of its incredibly high neuronal number (Herculano-Houzel, 2010) and prolonged development: being one of the first brain structures to begin cellular differentiation and one of the last to mature (with the majority of granule cells generated throughout the first post-natal year) (Kiessling et al., 2014; Knickmeyer et al., 2008; Koning et al., 2017; Powell, Barton, & Street, 2019; Sathyanesan et al., 2019; Xu et al., 2020). These early perturbations affecting cerebellar processing have also been shown to lead to more global cognitive and social impairments compared to perturbations at adulthood (Badura et al., 2018).

1.5 Conclusion

In conclusion, in addition to the behavioural differences noted in those with schizophrenia, various structural and functional brain alterations have also been noted. Research thus far, however, has been predominantly limited to cerebral cortex and subcortical brain regions, with little investigation of cerebellar alterations. When systematically analysed, the cerebellum has been shown reduced in size at least as large as those reported from analysis of cerebral regions. Furthermore, cerebellar differences appear to occur early on in patients’ lives and be present before primary psychosis onset. Many of the early environmental risk factors associated with schizophrenia also show particularly large, negative cerebellar effects. The cerebellum’s

particularly sensitivity to early perturbations, in part due to its protracted development and high neuronal number, makes it particularly of interest given the growing appreciation for neurodevelopmental differences in schizophrenia. Equally, there is mounting evidence of the non-motor roles played by the cerebellum and which look to be of relevance to schizophrenia symptomatology; as well as the growing appreciation of the presence and importance of cerebellar-dependent motor symptomatology in schizophrenia; many of which provide more easily collectable and quantifiable measures to collect for research. This, in combination with the possibility of using cerebellar stimulation, opens up new avenues for subtyping, patient monitoring and treatment options in schizophrenia; in addition to advancing our understanding of schizophrenia pathophysiology.

A limitation of the case-control studies indicating regional brain differences in schizophrenia, however, is that a myriad of factors related to diagnosis (such as medications, related health and lifestyle differences, and participant behaviour in the scanner) can also affect recorded brain measures and might be confounding results. While not specific to the cerebellum, the cerebellum might be particularly sensitive to these differences due to, for instance, with its lower position in the brain (being further from set magnetic isocentre) and the use of non-cerebellar specific registration tools, meaning the cerebellum might be particularly prone to induced imaging artefacts. Further work, therefore, exploring if cerebellar differences are still present in those with overt diagnoses when considering these factors is of paramount importance.

One way to partly circumvent this problem is to analyse cerebellar alterations in those at elevated genetic risk for schizophrenia who themselves don't have the diagnosis. If cerebellar differences are still recorded in such individuals, this would indicate that these cerebellar differences are not solely reflecting confounding factors related to diagnosis but are likely present premorbid, as well as helping to bridge the gap between genetic risk for schizophrenia and the complex nature of its presentation. While, as discussed, there are many reasons to be particularly interested in addressing the current omission of the cerebellum from such analyses; the particular enrichment of GWAS schizophrenia signal in the cerebellum further highlights how such a genetic approach holds such benefit in analysing the cerebellum in schizophrenia (Cai et al., 2018).

To aid in this, identifying the genetic variants which associate with cerebellar volume is a key step, and would not only greatly enhance our understanding of pathways involved in affecting

cerebellar structure, but also allow for the analysis of pleiotropy with schizophrenia and other psychiatric traits both across the whole genome and at individual genomic regions.

Furthermore, to date, no study has utilised the availability of genetic variants associated with neuroanatomical measures, to investigate their relevance for traits within and/or across disorders, other than simply associating with case-control status. For example, whether genetic variants associated with structural brain measures also associate with neurodevelopmentally linked traits within schizophrenia and, therefore, might help in providing more biologically useful subtypes for treatment stratification.

1.6 Thesis aims

The aims of this thesis, as addressed in each upcoming experimental chapter, are four-fold:

1. Using richly phenotyped datasets, to investigate the contribution of clinical and sub-clinical comorbidity and confounding factors to the association between schizophrenia status and cerebellar volume
2. To investigate the association between common and rare allele risk for schizophrenia and cerebellar volume in a sample of unaffected adult participants
3. To identify common genetic variants associated with cerebellar volume, so as to explore the potential genetic overlap between these variants and those identified for schizophrenia
4. To ascertain if the identified common genetic variants for cerebellar volume associate with neurodevelopmentally associated features within schizophrenia diagnosis, namely a higher risk for treatment-resistant psychosis

2 Comorbidities and covarying factors to consider for both clinical and non-clinical studies of the UK Biobank

2.1 Abstract

The cerebellum is an area of growing interest to cognitive studies and clinical studies in various neuropsychiatric, neurodevelopmental and neurodegenerative disorders. These clinical studies, however, are often performed in individual specific clinical conditions, with little consideration of the effect of comorbidities and/or other covarying factors which might alter this relationship. As an alternative approach, the recent development of large volunteer population cohorts with richly phenotyped data linked to medical records, such as UK Biobank, can allow for a data-driven assessment of which medical conditions and related sub-clinical factors are associated with cerebellar structure. These investigations would aid future clinical and psychological research studies in identifying important factors to consider when analysing brain-related differences. In this study of 19,369 UK Biobank participants, we found that individuals with a recorded diagnosis of 5 of the 19 broad medical condition groupings assessed, had reductions in their total cerebellar volume (mm^3) which survived correction for the number of analyses performed. This included reductions in those with psychiatric disorders, being the focus of this study (presence of disorder: $B[95\%CI]=-1470[-2034,-907]\text{mm}^3$, $p=3.1\times 10^{-7}$). When correcting for the effect of comorbidities, these effects remain significant in 4/19 conditions, including in those with psychiatric diagnoses. We find, however, that both body mass index (BMI) and head motion have significant and independent effects on relative total cerebellar volume (1 standard deviation (SD) increase in each: $B[95\%CI]=-665[-815,-515]\text{mm}^3$, $p=3.7\times 10^{-18}$ & $B[95\%CI]=-1377[-1530,-1225]\text{mm}^3$, $p=1.0\times 10^{-69}$, respectively). Correcting for these, we find less severe, but still present, cerebellar reductions in those with psychiatric conditions ($B[95\%CI]=-815[-1367,-263]\text{mm}^3$, $p=0.0038$). In conclusion, we report that a recorded diagnosis of a psychiatric condition is associated with reduced cerebellar volume, however, we identify several comorbidities and potential confounding variables worth consideration for future cerebellar imaging analyses.

2.2 Background

Cerebellar structural and functional differences have now been reported in numerous MRI studies of different psychiatric disorders (Phillips, Hewedi, Eissa, & Moustafa, 2015; Stoodley, 2016). Indeed, cerebellar structure has also been linked with the general psychopathology(p)-factor: a latent variable reflecting the high symptomology and aetiological overlap between psychiatric disorders as well as the high rate of psychiatric comorbidities (Caspi et al., 2014; Hariri, 2019; Romer et al., 2018; Smoller et al., 2019). Psychiatric conditions, however, also show an elevated number of comorbidities with other psychiatric conditions (Clark, Cuthbert, Lewis-Fernández, Narrow, & Reed, 2017; Newman, Moffitt, Caspi, & Silva, 1998) as well as with other physical conditions such as an increased incidence of stroke, diabetes, heart disease or hypertension (Scott et al., 2016; Vancampfort et al., 2013). Several of these physical conditions have also been associated with reductions in cerebellar volume, for instance in those with cardiovascular (De Cocker et al., 2015), metabolic (Kotkowski et al., 2019) or diabetic (Hoogendam et al., 2012) disorders. While, therefore, previous studies have highlighted cerebellar differences in individuals with specific psychiatric conditions, the overall effect across psychiatric disorder and/or confounding effects by non-psychiatric medical conditions have not been properly considered.

In addition to overt diagnoses of comorbidities, other subclinical effects are likely to also confound our understanding of the link between cerebellar reductions and psychiatric conditions. Notably, those with psychiatric diagnoses are known to move more when within the MRI scanner, reducing the signal-to-noise ratio (SNR) and the accuracy of registration techniques for brain images (Makowski et al., 2019). This effect is likely exacerbated in the cerebellum due to its lower position in the brain and being further away from commonly set magnet isocentres, therefore, decreasing its SNR; as well as with commonly deployed registration techniques being often tailored for cerebral over cerebellar structures. While head motion is partially corrected for in some MRI techniques, such as functional MRI (fMRI), the effect on estimated cerebellar volume has yet to be investigated.

Individuals with psychiatric disorders also are commonly heavier than the population average, reflected by increased body mass index (BMI) measure (Vancampfort et al., 2013). Rather than this being due to a single cause, it likely reflects a mixture of genetic and environmental risk factors (Bahrami et al., 2020; Q. Luo et al., 2020), possible unhealthier lifestyles and/or medication side-effects (Bak, Fransen, Janssen, Van Os, & Drukker, 2014). Importantly, regional volumes showing negative correlations with increased weight overlap with regions reported as

particularly affected in those with psychopathologies (Minichino et al., 2017). The effect of increased weight on recorded regional brain volumes is likely partially explained by increases in head motion, with a high positive correlation reported between head motion and BMI (Beyer et al., 2020; Ekhtiari, Kuplicki, Yeh, & Paulus, 2019; Hodgson et al., 2017). While others have noted the negative effects of elevated weight on recorded cerebellar brain volume (Beyer et al., 2019), this has yet to be performed in a larger sample and with consideration of head motion differences.

In conclusion, while there has been a growing interest in the role of the cerebellum in psychiatric research, with several studies reporting reductions in specific clinical cohorts, a question remains as to whether these effects might be driven by comorbid physical disorders and/or confounded by any body weight and head motion differences. While such a large study with the required data has not been previously possible, the UK Biobank cohort (Collins, 2012; Miller et al., 2016) offers a rare opportunity to analyse homogeneously collected imaging data from a large, volunteer population of older individuals (n=21,407), who have all provided richly phenotyped data and permitted linking of this data with their medical records. The aims of this study, therefore, were three-fold. Firstly, we wished to analyse the effect of different medical conditions on cerebellar volume in a data-driven approach, with the effects of schizophrenia and related psychiatric disorders being the primary interest of this thesis. Secondly, we wished to assess if these effects remained when accounting for shared variance explained by other disorders (i.e. comorbidities). Finally, we explored the effect of differences in BMI and head motion on these relationships. Based on previous literature, we hypothesised that the cerebellum would be reduced in those with psychiatric disorders, however, we expected these effects to be partially explained by comorbidities and confounders like BMI and head motion

2.3 Methods

2.3.1 Imaging cohort characteristics

The UK Biobank is a general population, volunteer-based cohort including 500,000 participants aged between 40-69yrs old at recruitment (Collins, 2012; Sudlow et al., 2015). Baseline data collection occurred between 2006 and 2010 at 22 research assessment centres across the UK. This included providing blood, urine and saliva samples; consent for access to medical records; and extensive lifestyle, demographic, behaviour and biophysical information. It is also regularly augmented with additional assessments, where participants either update self-assessments or

attend assessment-centres (such as for neuroimaging). Ethics for UK-Biobank was granted by the North West Multi-Centre Ethics Committee, with our study being approved by the UK-Biobank Access Committee (*Project #17044*).

At the time of this study, MRI measures of the brain were available for 21,407 participants (with an eventual plan to scan 100,000 participants). A full description of the imaging acquisition, quality control and imaging-derived phenotype (IDP) generation by UK Biobank can be found elsewhere (Alfaro-Almagro et al., 2018) (https://biobank.ctsu.ox.ac.uk/crystal/crystal/docs/brain_mri.pdf). Briefly, our study utilised the IDPs generated for the gradient distortion corrected T1-weighted structural scan data (3D Magnetization Prepared Rapid Acquisition Gradient Echo with 1mm³ isotropic resolution) obtained at two UK sites, using identical protocols with the same scanner design (3-Tesla Siemens Skyra scanner; 32 channel head coil). UK Biobank processed this data to create cerebellar volume IDPs using FMRIB (Functional Magnetic Resonance Imaging of the Brain) Software Library (FSL) FAST (FMRIB's Automated Segmentation Tool) registration of cerebellar lobule atlas (Diedrichsen et al., 2009). Of the cerebellar lobule IDPs ([25893-2.0:25920-2.0](#)) we excluded Crus I vermis due to its small size and likely low signal-to-noise ratio, following previous research (Pezoulas, Zervakis, Michelogiannis, & Klados, 2017). Using R (v3.6.0) (<https://www.R-project.org/>), we grouped all the remaining cerebellar lobules into a single total cerebellar grey matter volume (mm³) measure (henceforth referred to as "cerebellar volume"). We chose this approach since our primary focus was of differing clinical effects on the cerebellum, rather than of differing effects across the cerebellum. Equally, since no cerebellar-specific registration technique was used for the production of UK Biobank cerebellar IDPs, this could lead to reduced ability to discern lobule boundaries and so poorer face validity for individual lobules (Diedrichsen et al., 2009).

2.3.2 *Medical conditions*

UK Biobank participants have provided consent for access to their medical health records. We used the tenth revision of the International Statistical Classification of Diseases and Related Health Problems (ICD-10) hospital inpatient (i.e. occupying of a bed) admission coding of primary (primary reason for admission) and secondary (all other codings) diagnoses data (collected from 1997 onwards). More information on the obtaining and curating of this data is provided by UK Biobank (<https://biobank.ctsu.ox.ac.uk/crystal/exinfo.cgi?src=UnderstandingUKB>). Of note, this data is independent of other sources of health-data (e.g. outpatient records, cancer records, self-reports), therefore, it only captures recorded diagnoses for hospital inpatient admissions

and should not be taken to represent general UK population disease rates. Under the ICD-10 revision, medical diagnoses are divided into 22 (“tier-1”) chapters ([41270](#)), which can themselves be further subdivided into 263 “tier-2” groupings. We transformed each medical condition into a binary status variable (1 = presence, 0 = absence) since UK Biobank had full coverage of medical records.

2.3.3 Statistical analysis

From the original 21,407 individuals, we removed individuals with missing values for total cerebellar volume or any of the variables used as covariates in our analysis (see below). We also removed those with outlier values ($>5 \times$ median absolute deviation from the mean) for total cerebellar volume, total brain grey and white matter volume (mm^3), mean resting-state functional MRI head motion/displacement averaged across space and time ([25741-2.0](#)) (mm) and Body Mass Index (BMI) ([21001-2.0](#)) (kg/m^2). Finally, we removed 1 male participant due to their having pregnancy-related medical conditions, indicating possible medical record misclassification or an updated self-reported sex by the participant. This left 19,369 individuals in our sample.

The number of occurrences of all tier 1 and tier 2 medical condition can be found in Supplementary Table 2.1A & 2.1B and are provided with each analysis table. To obtain nominal significance ($p < 0.05$) with 80% power to detect Cohen’s $d = 0.2$ - which appears appropriate considering previous psychiatric studies (Navarri et al., 2020) - we would require around 200 individuals with the medical condition (calculated using R “pwr” package <https://cran.r-project.org/web/packages/pwr/>). We took forward, therefore, 19 tier-1 medical conditions and 68 tier-2 medical conditions for further analysis which passed this threshold of >200 occurrences. While the number of individuals with a tier-2 schizophrenia-related diagnosis did not pass our threshold for inclusion (with only 19 incidences in our sample), since schizophrenia is a focus of this thesis, we performed an additional separate analysis to explore any schizophrenia-related cerebellar volume differences, though we note the inherent limitations of extensive interpretation of such results, given the aforementioned low case numbers (see 2.5 *Discussion*).

While the focus of this thesis is on schizophrenia and other psychiatric disorders’ effects on the cerebellum, we analysed and report the effect of all medical diagnoses on the cerebellum so as to highlight any possible comorbidity effects which might be worth considering in future psychiatric studies, as well as which might be of interest to researchers analysing non-

psychiatric, disease-related neuroanatomical effects. We present, therefore, psychiatric-relevant effects in the attached thesis Supplementary Tables (presented at the end of each chapter), while the full Supplementary Tables – including other medical conditions – are provided in an additional file and also made available at the Open Science Framework (OSF) document https://osf.io/jr8m2/?view_only=29906bc730f64cf58a81d67ff5c50363. All corrections for multiple comparisons (discussed below) are corrected across the full dataset, including all conditions.

Initially, in a univariate linear regression model, we assessed the effect on cerebellar volume of common demographic and imaging variables which, while not of direct interest to our research question, might mask or exaggerate any effects seen. These included variables of individuals' age when attending centre ([21003-2.0](#)) (yrs; age² reflecting 1st and 2nd degree orthogonal polynomials), sex ([31](#); acquired from central registry at time of recruitment, but which can be updated by participant), their interaction (age² × sex), imaging centre attended ([54-2.0](#)), attendance date at the imaging centre ([53-2.0](#)), X-, Y- and Z-head position in the scanner ([25756](#), [25757](#), [25758](#)) and the starting table-Z position in the scanner ([25759](#)). We used this list of covariates as a “default” covariate list which was added to all models throughout. The residuals of total cerebellar volume correcting for test covariates showed a normal distribution. For each covariate, the unique variance explained by the predictor ($\Delta R^2 = R^2$ of model with the predictor – R^2 of model without the predictor), unstandardised regression (B)-coefficients and 95% confidence intervals (95% CIs) reflecting the change in cerebellar volume (mm³) with one unit increase in each independent variable, and p-values are provided.

For our primary analyses we used independent univariate linear regression models to assess relative cerebellar volume differences (mm³) in those with each tier-1 ICD-10 medical condition compared to those without, while correcting for our aforementioned covariates. For pregnancy-related conditions, which were assessed only in females, we removed sex and age-sex interaction covariates.

We provided both raw p-values and p-values adjusted to control the False Discovery Rate (FDR) to control the type 1 error rate (i.e. proportion of incorrect rejections of the null hypothesis of all rejections) for the 19 tier-1 medical conditions assessed (FDR = 0.05). The latter was created using base R “*p.adjust*” function (<https://rdrr.io/r/stats/p.adjust.html>) and deploying the Benjamini-Hochberg method (Benjamini & Hochberg, 1995): creating *q* (critical) values (referred in this thesis as *p_{FDR}* for clarity) for each p-value by first ranking p-values in ascending order, then calculating:

$$p_{FDR} = (p\text{-value rank} / \text{total } p\text{-value count}) \times FDR$$

To guide interpretation, results with $p_{FDR} < 0.05$ were deemed as “significant”, though raw p-values, and related regression effect sizes and 95% confidence intervals are provided for all. For supplementary analyses, we repeated the above analysis without correction for total brain volume so as to provide uncorrected cerebellar effects, and also performed an additional analysis testing for significant interaction effects between sex and medical conditions for their effect on relative cerebellar volume ($p_{FDR} < 0.05$ across 19 conditions).

To assess the extent of comorbidities of tier-1 hospital in-patient diagnoses, we first performed a two-tailed Fisher’s exact test on each possible tier-1 pairing, under the null hypothesis that the presence of each pair of medical conditions were independent of each other with an odds-ratio (OR) of 1.0. We again controlled the FDR across the number of tests conducted ($19 \times 18 = 171$ unique pairings, $p_{FDR} < 0.05$). Next, we added all tier-1 ICD-10 codes into the same linear regression model, in addition to our list of default covariates, to see which remained in explaining a significant proportion of variance of cerebellar volume ($p_{FDR} < 0.05$ for the 19 medical conditions). For ease of interpretation, in this study we refer to our regression models as “univariate” when each predictor variable of interest (i.e. each tier 1 ICD-10 diagnosis in this instance) is tested independently, while we use “multivariate” to refer to models where all predictors of interest (i.e. all tier 1 conditions) are tested simultaneously in the same model. For both, we make clear when models also include correction for other covariates (e.g. age, sex).

We next wished to assess differences in effects seen when considering participant BMI and head motion differences in the scanner. We natural log transformed both variables since each showed distinct positive skews. We z-scored (scaled and mean-centred) BMI and head motion variables, with values now reflecting their differences in standard deviations (SD) from the mean, to allow comparisons between them. We first assessed differences in BMI and head motion in those with and without a recorded diagnosis of each tier-1 medical condition using univariate regression models with no covariates. Since the outcome variables are z-scored, each “ β -coefficients” represents the difference in each BMI and head motion measure (measured in SDs) in those with each diagnosis compared to those without.

We next assessed the effect of increasing values of each variable (head motion or BMI) on relative cerebellar volume in separate univariate regression models, which also included our default covariates. The unstandardised B-coefficient results provided represent differences in cerebellar volume (mm^3) with a single SD difference in either BMI or head motion (since we

reserve the “ β -coefficient” symbolism in this thesis for when the outcome variable is z-scored and is measured in SDs). We additionally repeated this when including both BMI and head motion in the same “multivariate” regression model, providing B-coefficients for each predictor when the other predictor (and other covariates) are controlled for. We then repeated our main analyses, of the effect of each tier-1 medical conditions on relative cerebellar volume, but with the addition of BMI and/or head motion covariates to each model along with the list of default covariates, so as to assess whether the effect of each medical condition on cerebellar volume remained. Plots of the B-coefficients and theoretical distributions of the 95% confidence intervals (i.e. under the assumption of normal distributions rather than from bootstrapping methods), to aid in visualisation of adding BMI and head motion covariates to each model, were created using the R “*jtools*” package (https://github.com/jacob-long/jtools/blob/master/R/plot_coefs.R)

Finally, we repeated our main univariate analyses but, instead, using the larger number of the 68 tier-2 medical groupings which constitute the broader tier-1 conditions. We performed this with and without our additional BMI and head motion correction, in addition to the default covariate list. For each of these tier-2 analyses, we removed those individuals from the “control”/comparison group who had a tier-2 medical condition within the same tier-1 grouping as that being assessed. For example, if assessing differences in those with psychopathology following psychoactive substance abuse (Block F10-F19 ICD-10 coding), we removed all individuals with other psychopathologies from the comparison group (i.e. all other Block F ICD-10 codings). We again controlled our FDR rate for the 68 tests conducted.

2.4 Results

There were 19,369 individuals with data available for total cerebellar volume and other covariates used (Age: mean \pm SD = 62.5 \pm 7.5yrs; Female: n(%) = 10,215(52.7%)) (Table 2.1). The effect on cerebellar volume of our list of covariates of total brain volume, age², sex, age² \times sex, imaging centre, date attended and head position in the scanner are presented in Supplementary Table 2.2 (whole model R² = 0.47; Adjusted R² for number of predictors = 0.46). Of note, the interaction between the first polynomial of age (linear effects) and sex was significant, indicating that the negative effect of age on cerebellar volume was greater in males than females (B[95% confidence intervals] = -1.20 \times 10⁵[-1.52 \times 10⁵, -8.73 \times 10⁴]mm³, p=3.79 \times 10⁻¹³)

Table 2.1: Demographic information for the UK Biobank cohort included in this study

	Total (n=19369)
Total cerebellar grey-matter volume (mm³)	
Mean (SD)	90044 (11136)
Median [Min, Max]	90319 [45312, 142148]
Total brain grey and white matter volume (mm³)	
Mean (SD)	1166323 (111179)
Median [Min, Max]	1162070 [828168, 1633670]
Sex	
Female	10215 (52.7%)
Male	9154 (47.3%)
Age at imaging centre (yrs)	
Mean (SD)	62.5 (7.46)
Median [Min, Max]	63.0 [44.0, 80.0]
Centres Attended	
ID: 11025	16654 (86.0%)
ID: 11027	2715 (14.0%)
Body Mass Index (BMI) (kg/m²)	
Mean (SD)	26.6 (4.36)
Median [Min, Max]	26.0 [13.4, 53.4]
Resting state fMRI head motion (mm)	
Mean (SD)	0.121 (0.0570)
Median [Min, Max]	0.107 [0.0290, 0.669]

2.4.1 Tier-1 ICD-10 Clinical variables

The number of participants with each of the 19 tier-1 ICD-10 medical conditions are presented in Table 2.2. This included 841 individuals with diagnoses of mental and behavioural problems (i.e. psychiatric disorders), including 359 individuals with diagnoses of mood (affective), 321 with psychoactive substance abuse related, 218 with neurotic and stress, 21 with behavioural, 19 with schizophrenia and related, 16 adult personality, 12 organic, 5 unspecified, 2 of psychological development and 1 with childhood-onset psychopathology. Of note, the number of individuals with a tier 1 psychiatric recorded diagnosis is smaller than the sum of presence of individual tier-2 conditions as 14.0% of individuals with a psychiatric diagnosis had at least two or more separate tier-2 recorded diagnoses.

We found 5/19 tier-1 ICD-10 medical conditions were associated with reduced relative cerebellar volume and survived correction for the number of comparisons ($p_{\text{FDR}} < 0.05$) (Table 2.2; Figure 2.1). This included reductions in those with psychiatric ($n=841$, $\Delta R^2=0.0007$, $B[95\%CI]=-1470[-2034,-907]\text{mm}^3$, $p=3.1 \times 10^{-7}$) as well as neurological, endocrine-metabolic, circulatory, and other abnormal clinical signs/symptoms not captured by other categories. We repeated this analysis without correction for total brain volume, showing similar results but with larger effect sizes (for example for psychiatric disorders: $\Delta R^2=0.001$, $B[95\%CI]=-1923[-2569,-1276]\text{mm}^3$, $p=5.7 \times 10^{-9}$) (Supplementary Table 2.3). The sex distributions of each medical condition are provided in Supplementary Table 2.4, with several showing significant differences in distribution across sexes, however, we found no significant difference for psychiatric conditions in our sample (46.0% Male, $OR=0.95$, $p=0.48$). We found no significant interaction between medical conditions and participant sex for their effects on relative cerebellar volume, including for psychiatric disorders ($B[95\%CI]=326[-803,1456]\text{mm}^3$, $p=0.57$) (Supplementary Table 2.5).

Table 2.2: The effect of each 19 tier 1 ICD-10 recorded hospital diagnosis on total cerebellar volume

Tier-1 ICD-10 Chapter codes	Freq.	$\Delta R^2\ddagger$	B-coefficient (mm ³)†	95% confidence intervals (mm ³)†		p	p _{FDR} *
I Infections	900	2.74×10 ⁻⁵	-277.26	-822.65	268.13	0.32	0.51
II Neoplasms	3215	1.07×10 ⁻⁵	98.80	-212.38	409.98	0.53	0.64
III Blood	749	3.19×10 ⁻⁵	-326.89	-923.66	269.88	0.28	0.49
IV Endocrine	2081	1.94×10 ⁻³	-1604.92	-1979.32	-1230.52	4.68×10 ⁻¹⁷	8.90×10⁻¹⁶
V Psychiatric	841	7.23×10 ⁻⁴	-1470.40	-2033.67	-907.13	3.14×10 ⁻⁷	1.99×10⁻⁶
VI Neurological	1200	5.28×10 ⁻⁴	-1063.40	-1540.19	-586.60	1.24×10 ⁻⁵	5.89×10⁻⁵
VII Eye	1362	1.39×10 ⁻⁴	-519.48	-973.81	-65.14	0.03	0.07
VIII Ear	288	6.84×10 ⁻⁶	240.89	-708.49	1190.27	0.62	0.69
IX Circulatory	4189	1.11×10 ⁻³	-918.45	-1202.79	-634.11	2.48×10 ⁻¹⁰	2.36×10⁻⁹
X Respiratory	1986	1.42×10 ⁻⁴	-438.44	-817.20	-59.68	0.02	0.07
XI Digestive	6123	1.21×10 ⁻⁴	-265.44	-513.97	-16.91	0.04	0.08
XII Skin	1578	5.52×10 ⁻⁶	-95.81	-515.92	324.30	0.66	0.69
XIII Musculoskeletal	2701	7.28×10 ⁻⁵	-275.31	-607.77	57.15	0.11	0.20
XIV Genitourinary	4185	1.48×10 ⁻⁵	-106.76	-392.37	178.85	0.46	0.63
XV Pregnancy-related	845	2.17×10 ⁻⁵	-191.22	-803.19	420.75	0.54	0.64
XVIII Other	5540	2.22×10 ⁻⁴	-368.81	-623.86	-113.76	0.005	0.02
XIX Injury or Poisoning	1489	2.45×10 ⁻⁵	-207.04	-638.09	224.01	0.35	0.51

XX External	925	8.40×10 ⁻⁷	-47.91	-586.59	490.77	0.86	0.86
XXI Health Status	6606	1.24×10 ⁻⁴	-264.60	-509.48	-19.73	0.03	0.08

Notes: Total cerebellar volume was regressed on each tier-1 medical condition independently, with covariates of age, sex, imaging centre attended, date attended, head and table position in scanner and overall total brain volume differences. †: Unstandardised regression (B)-coefficients and 95% confidence intervals are provided from these models. ‡: The unique variance in cerebellar volume attributable to each tier-1 medication condition (ΔR^2) is calculated by subtracting from the R^2 of the model with just the covariates from the R^2 of the model with the medical condition predictor and covariates. * p_{FDR} : values represent controlling of p-values for the number of conditions tested (FDR = 0.05), with bold signifying $p_{FDR} < 0.05$.

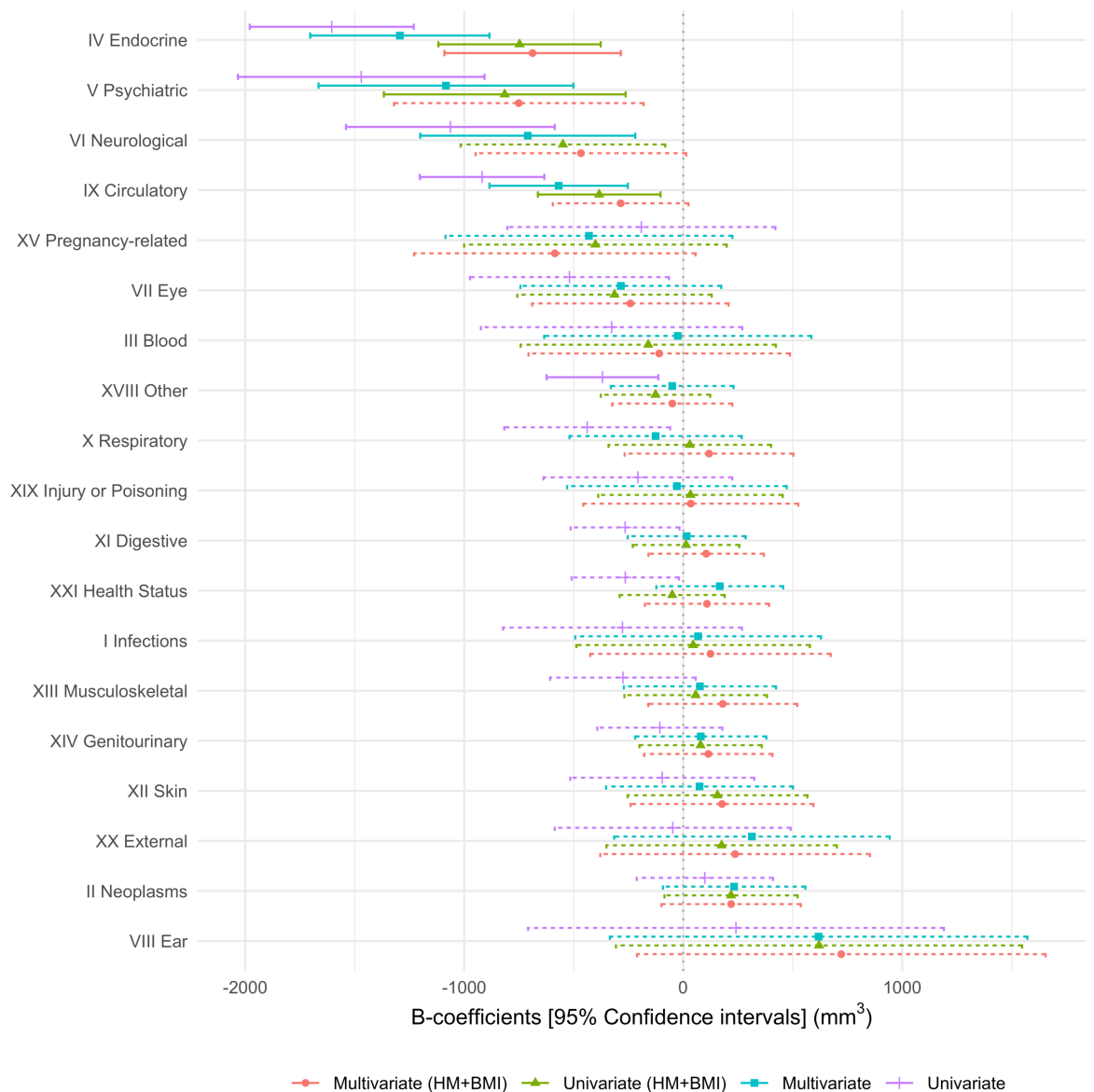


Figure 2.1: The effect of each tier-1 ICD-10 recorded hospital diagnosis on total cerebellar volume. Results are from univariate regression modelling of total cerebellar volume, regressed on each of the 19 tier-1 ICD medical conditions (with n>200 occurrences), with covariates of age, sex, imaging centre, date attended, head position in the scanner and total brain volume (Univariate). In addition, results when all medical condition predictors are included in a single multivariate model with all covariates mentioned (Multivariate); univariate analysis with additional head motion and BMI correction (Univariate HM+BMI); and multivariate analysis with additional head motion and BMI correction (Multivariate HM+BMI) are provided.

Unstandardised regression “B”-coefficients and 95% confidence intervals represent **differences** in cerebellar volume (mm³) in those with each recorded diagnosis, compared to

those without. Solid line signifies $p_{FDR} < 0.05$ (adjusting for the 19 tests performed within each type of analysis)

2.4.2 Multivariate analysis

Since several medical conditions had shown a negative relationship with relative cerebellar volume, we wished to assess and correct for the presence of possible comorbidity effects. Firstly, using Fisher’s exact test, we found comorbidities across tier-1 conditions to be relatively common in our cohort (Supplementary Table 2.6). For example, in those without compared to those with a recorded psychiatric conditions, we found a significantly ($p_{FDR} < 0.05$) elevated number of comorbidities for all other conditions aside from pregnancy-related conditions, including those with diagnoses related to injury or poisoning/toxicity effects (present in 7.0% of individuals without (w/o) psychiatric diagnoses & 23.8% of individuals with psychiatric diagnoses, $OR=4.2$, $p=6.0 \times 10^{-50}$), neurological conditions (5.7% w/o & 17.6% with: $OR=3.5$, $p=5.3 \times 10^{-32}$) and endocrine-metabolic disorders (9.9% w/o & 29.7% with: $OR=3.9$, $p=2.1 \times 10^{-54}$) (Figure 2.2).

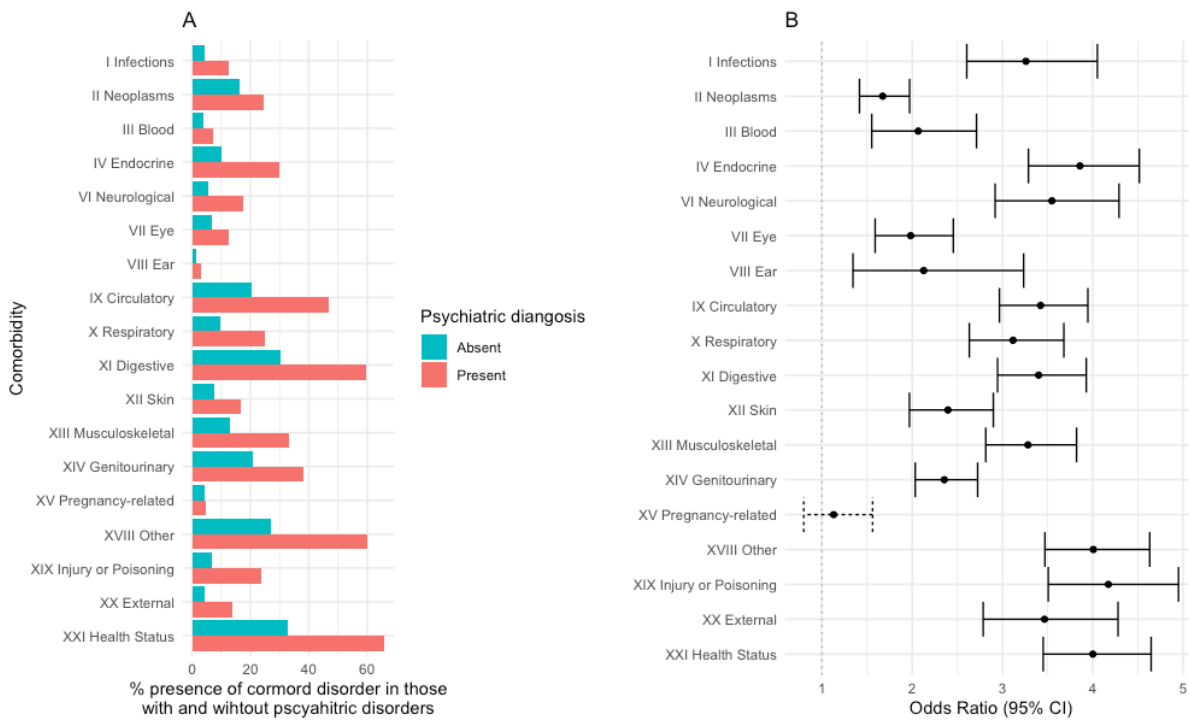


Figure 2.2: Identifying comorbidities for psychiatric disorders. A) For each of the 18 ICD-10 diagnosis other than psychiatric disorders, the presence (%) of the disorder in those with and without a psychiatric diagnosis. B) The odds ratio and 95% confidence intervals (95% CI) for the

presence of comorbidity in those with and without a psychiatric diagnosis. Solid line signifies $p_{FDR} < 0.05$

We repeated our main analysis but added all tier-1 medical conditions to the same single multivariate linear regression model (Figure 2.1; Supplementary Table 2.7). We found four medical conditions remained as having independent negative effects on relative cerebellar volume ($p_{FDR} < 0.05$), being those individuals with psychiatric ($\Delta R^2 = 3.7 \times 10^{-4}$, $B[95\%CI] = -1083[-1665, -501] \text{mm}^3$, $p = 2.6 \times 10^{-4}$), neurological ($\Delta R^2 = 2.2 \times 10^{-4}$, $B[95\%CI] = -710[-1201, -219] \text{mm}^3$, $p = 0.005$), endocrine-metabolic ($\Delta R^2 = 1.1 \times 10^{-4}$, $B[95\%CI] = -1294[-1703, -885] \text{mm}^3$, $p = 6.0 \times 10^{-10}$) and circulatory ($\Delta R^2 = 3.4 \times 10^{-4}$, $B[95\%CI] = -569[-885, -253] \text{mm}^3$, $p = 4.2 \times 10^{-4}$) system disorder diagnoses. Accounting for commodities, therefore, appears to reduce the effect sizes seen of having a recorded diagnosis for a psychiatric condition on relative cerebellar volume by approximately 0.5cm^3 .

2.4.3 BMI and head motion covariates

Next, we assessed how much psychiatric and other medical conditions were associated with increases in BMI and head motion. To compare across predictors, both were z-scored (scaled and mean-centred) with effect sizes reflecting standard deviation (SD) differences in each variable. Most medical conditions showed relative increases in BMI and head motion, including those with psychiatric conditions ($\beta[95\%CI] = 0.28[0.21, 0.35]$, $p = 4.6 \times 10^{-15}$ & $\beta[95\%CI] = 0.40[0.33, 0.47]$, $p = 2.1 \times 10^{-29}$, respectively) (Supplementary Table 2.8). Both variables were highly correlated with each other indicating that larger participants moved more in the scanner (correlation(r)[95%CI] = $0.63[0.62, 0.64]$, $p < 2.2 \times 10^{-16}$). Despite the high correlation between them, both BMI and head motion still explained a significant proportion of independent variance in cerebellar volume, with both having significant negative effects when added to the same model, in addition to the standard list of covariates already mentioned ($\Delta R^2 = 2.0 \times 10^{-3}$, $B[95\%CI] = -665[-815, -515] \text{mm}^3$, $p = 3.7 \times 10^{-18}$ & $\Delta R^2 = 8.3 \times 10^{-3}$, $B[95\%CI] = -1377[-1530, -1225] \text{mm}^3$, $p = 1.0 \times 10^{-69}$, respectively) (Figure 2.3). Variance inflation factors (VIF) also remained low (VIF = 1.8 for both), indicating only small multicollinearity despite their high correlation. Importantly, the effects for BMI in this multivariate model remained, even when further excluding 3557 individuals with current BMI in the obese range (BMI > 30) ($\Delta R^2 = 1.1 \times 10^{-3}$, $B[95\%CI] = -618[-825, -411] \text{mm}^3$, $p = 4.7 \times 10^{-9}$). Similar negative effects were also seen when

replacing BMI by waist-hip ratio ($\Delta R^2=1.0 \times 10^{-3}$, $B[95\%CI]=-585[-759,-411]mm^3$, $p=4.56 \times 10^{-11}$), suggesting results to not be specific to the BMI anthropomorphic measures.

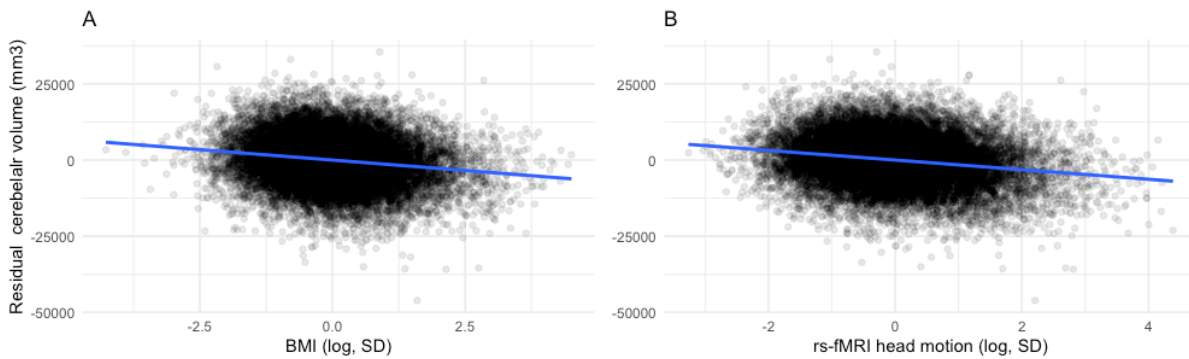


Figure 2.3: The effect of participant A) body mass index (BMI) and B) mean resting-state functional MRI (rs-fMRI) head motion on total cerebellar volume. Y-axis represents residual total cerebellar volume values following univariate regression model of total cerebellar volume regressed on covariates of age, sex, imaging centre, date attended, head position in the scanner and total brain volume (Univariate). Each predictor is scaled, mean-centred and natural log transformed, providing differences in log standard deviations (SD). Solid line signifies linear effect

We repeated our main analysis of differences in relative cerebellar volume in those with each tier-1 ICD-10 recorded diagnosis, additionally correcting for head motion and/or BMI covariates, which generally showed slight reductions in recorded effect sizes (Supplementary Table 2.9; Figure 2.4). Four medical conditions were associated with reduced cerebellar volume ($p_{FDR}<0.05$) when correcting for head motion, being the same four that remained significant in the multivariate analysis i.e. psychiatric, neurological, endocrine-metabolic and circulatory system disorders. Three of these also remained when controlling for BMI differences, while endocrine-metabolic differences did not. For example, for psychiatric conditions, the size of the reductions found when not correcting for head motion or BMI ($B=-1470mm^3$, $p=3.4 \times 10^{-7}$) were reduced when adding head motion or BMI covariates ($B[95\%CI]=-818[-1371,-265]mm^3$, $p=0.0038$ & $B[95\%CI]=-1119[-1675,-564]mm^3$, $p=7.8 \times 10^{-5}$, respectively). When correcting for both covariates, we found only psychiatric ($B[95\%CI]=-815[-1367,-263]mm^3$, $p=0.0038$), endocrine-metabolic ($B[95\%CI]=-747[-1118,-377]mm^3$, $p=7.8 \times 10^{-5}$) and circulatory ($B[95\%CI]=-384[-664,-$

104]mm³, p=0.0073) recorded diagnoses were associated with significant relative reductions in cerebellar volume following correction for multiple comparisons ($p_{FDR}<0.05$) (Supplementary Table 2.9; Figure 2.1 & Figure 2.4). For psychiatric disorders, while effect sizes appear similar when adding head motion as a covariate compared to when adding both head motion and BMI (as seen in Figure 2.4 comparing Model 3 & 4), an ANOVA (analysis of variance) F-test revealed that the model including both, significantly accounted for more variance than the more parsimonious one ($F = 75.6$, $p < 1.0 \times 10^{-100}$).

When adding both BMI and head motion covariates to the multivariate analyses, which included all tier-1 medical conditions in a single model, only the relative cerebellar volume reductions in those with endocrine-metabolic disorders remained at $p_{FDR}<0.05$ ($B[95\%CI]=-689[-1091,-285]mm^3$, $p=8.2 \times 10^{-4}$), while those with psychiatric conditions were slightly above our FDR criterion ($B[95\%CI]=-751[-1321,-181]mm^3$, $p=9.9 \times 10^{-3}$, $p_{FDR}=0.09$) (Supplementary Table 2.10; Figure 2.1).

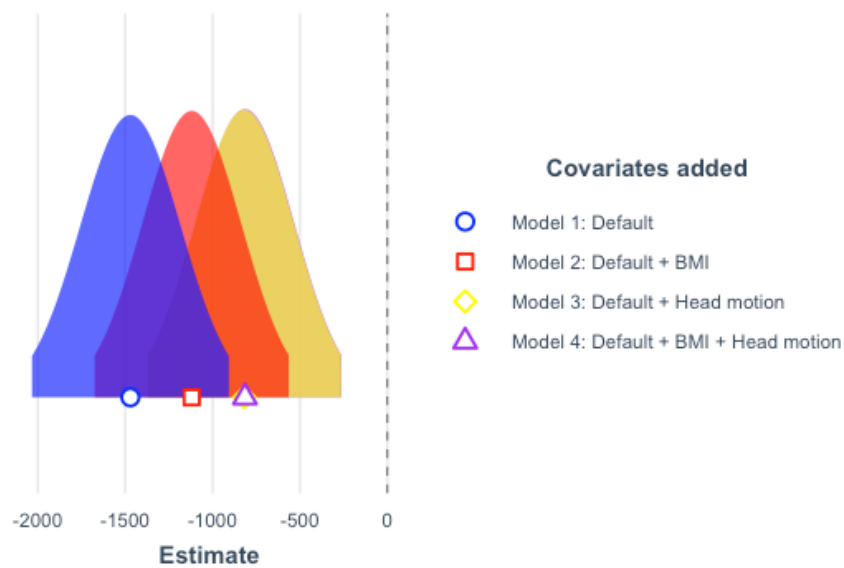


Figure 2.4: The effect of Psychiatric tier-1 ICD-10 recorded hospital diagnosis on total cerebellar volume without and with body mass index (BMI), resting-state fMRI mean head motion and both covariates. Plots are of the estimated B-coefficients (mm³) from each model described in the main text, with 95% confidence interval theoretical distributions (Table 2.2 & Supplementary Table 2.9). Each model represents a linear regression model of the effect of having a recorded hospital psychiatric diagnosis on total cerebellar volume, correcting for covariates of age, sex, imaging centre, date attended, head position in the scanner and total

brain volume in the model. Model 1 (blue): is this default model. Model 2 (red): model 1 plus including the BMI covariate. Model 2 (yellow): model 1 plus including the head motion covariate. Model 4 (purple): model 1 plus including both the BMI and head motion covariates (of note, this overlaps with Model 3).

2.4.4 Tier 2 ICD-10 medical records

Finally, we wished to further explore which medical conditions within each broader tier-1 medical groupings might drive any associations seen. To do this, we analysed cerebellar differences in those individuals with a recorded diagnosis for each of the 68 tier-2 ICD code with >200 occurrences in our sample. With our standard list of covariates, 14/68 tier-2 medical conditions showed significant reductions in relative cerebellar volume (Supplementary Table 2.11 **Error! Reference source not found.**). Of those with psychiatric tier-2 diagnoses passing this threshold, compared to those without any psychiatric diagnosis ($n_{\text{controls}}=18,528$), reductions were seen in those with psychiatric symptoms brought on by psychoactive substance abuse ($n=321$, $B[95\%CI]=-2163[-3062,-1264]\text{mm}^3$, $p=2.5\times 10^{-6}$) and in individuals with mood disorders ($n=359$, $B[95\%CI]=-1259[-2109,-410]\text{mm}^3$, $p=3.7\times 10^{-3}$), while no differences were seen in individuals with neurotic, stress and somatoform psychiatric diagnoses ($n=218$, $B[95\%CI]=-226[-1310,-858]\text{mm}^3$, $p=0.79$). With correction for BMI and head motion, only 4/68 associations remained at $p_{\text{FDR}}<0.05$ (Supplementary Table 2.12), including relative cerebellar volume reductions in those individuals with psychopathology related to psychoactive substance abuse ($B[95\%CI]=-1371[-2253,-489]\text{mm}^3$, $p=2.3\times 10^{-3}$), while those with mood disorders ($B[95\%CI]=-590[-1422,243]\text{mm}^3$, $p=0.17$) or neurotic/stress-related ($B[95\%CI]=237[-823,1297]\text{mm}^3$, $p=0.66$) disorders did not remain significant. The other three tier-2 disorders which remained significant, included diabetes mellitus ($B[95\%CI]=-2116[-2874,-1358]$, $p=4.4\times 10^{-8}$), obesity ($B[95\%CI]=-1670[-2746,-594]\text{mm}^3$, $p=2.4\times 10^{-3}$) and hypertensive diseases ($B[95\%CI]=-582[-954,-210]\text{mm}^3$, $p=2.2\times 10^{-3}$).

While the number of individuals with schizophrenia-related hospital recorded diagnoses did not pass our threshold for inclusion in the above analysis - with only 19 incidences in our sample - since schizophrenia is the particular focus of this thesis, we performed an additional separate analysis to explore any schizophrenia-related cerebellar volume differences. Those with schizophrenia diagnoses showed reductions in total cerebellar volume ($B[95\%CI]=-4480[-8132,-828]\text{mm}^3$, $p=0.016$) which broadly remained when additionally correcting for head motion and

BMI differences ($B[95\%CI]=-3770[-7342,-199]mm^3$, $p=0.039$). While we provide p-values for completeness and both pass our nominal significance threshold ($p<0.05$), these results should not be interpreted in a similar manner to the other tier-2 conditions, given their small sample sizes (see *2.5 Discussion*).

2.5 Discussion

Within this volunteer general population cohort of 19,369 UK Biobank participants, we find individuals with psychiatric disorders show reductions in relative total cerebellar volume, beyond any difference in total brain volume. We note high comorbidity with various other disorders, which were also associated with reductions of the cerebellum, notably neurological, endocrine-metabolic and cardiovascular disorders. Elevated BMI and head motion are seen in several of these medical conditions and are also associated with reduced cerebellar volume. When taking into consideration these comorbidities, or BMI and head motion confounding, the negative effects on relative cerebellar volume seen in individuals with psychiatric disorders remain, though the size of the effects are reduced. This work emphasises that psychiatric conditions are associated with reductions in cerebellar volume above any total brain volume difference, however, it also emphasises the need to consider the relationship between the diagnosis and participants' physical health status, anthropometry and head movement in the scanner when conducting clinical studies.

We found individuals with psychiatric conditions were associated with reductions in cerebellar volume. While the definition is broad, this does concur with previous studies' findings of cerebellar structural associations with latent factors of psychopathology across disorders, as well as psychopathology in unaffected samples (Hariri, 2019; Moberget et al., 2019; Romer et al., 2018), in addition to the cerebellar alterations reported in specific psychiatric disorders such as schizophrenia (Ding et al., 2019; He et al., 2019; Moberget et al., 2018), bipolar disorder (Baldaçara et al., 2011; D. Kim et al., 2013), major depression (Depping, Schmitgen, Kubera, & Wolf, 2018) and stress/trauma-related (Moreno-Rius, 2019a; Rabellino, Densmore, Théberge, McKinnon, & Lanius, 2018).

In our cohort, the numbers of each specific disorder within the main tier-1 grouping (i.e. "tier-2" conditions) varied, with many being of insufficient size for independent statistical analysis. While the number of individuals with recorded schizophrenia diagnosis were small ($n = 19$) and did not pass our threshold, since this is a particular focus of this thesis, we performed a separate

analysis that showed nominally significant ($p < 0.05$) relative cerebellar reductions of an average of 4cm^3 compared to a cohort-average total cerebellar volume of 90cm^3 . Of note, however, these are only included for completeness, as the results were unlikely to survive our false discovery rate (FDR) correction for the number of comparisons made of all tier-2 conditions, and with the small number of cases making for unstable effect sizes: increasing the chances of false-positives, exaggerated effect sizes and/or flipped effect sizes estimates (Button et al., 2013).

Of the three psychiatric tier-2 conditions with sufficient number, however, we found two which showed an association with reduced cerebellar volume. This included in individuals with mood/affective disorders and, to a greater extent, in disorders related to psychoactive substance abuse, showing between $1.2\text{-}2.2\text{cm}^3$ reductions in cerebellar volume, while there was no evidence of cerebellar volume alterations in neuroticism-related disorders. These results agree with previous reports of reduced cerebellar volume in those with mood/affective disorders (Adamaszek et al., 2017). Equally, the findings of a negative association with psychoactive substance adds to the growing evidence of the cerebellum being a key area in addiction pathways (Moulton et al., 2014) and reward processing (Carta et al., 2019), and with both alcohol (E. V. Sullivan et al., 2020) and opioid abuse (Moreno-Rius, 2019c; Wollman et al., 2017) having been previously associated with reduced cerebellar volume, while cannabis abuse is associated with cerebellar volume increases in adolescent cohorts but with reductions in individuals with recorded psychosis (Moreno-Rius, 2019b). Considering the strong association between substance abuse and schizophrenia, future clinical studies should ascertain the presence of schizophrenia-related cerebellar differences in those with no history of substance abuse, an analysis we were underpowered to investigate (Khokhar, Dwiell, Henricks, Doucette, & Green, 2018). Furthermore, these results indicate that the recorded cerebellar-related differences in those with psychiatric diagnoses are not just specific to schizophrenia, but instead agree with previous studies finding cerebellar reductions to be present across several psychiatric and neurodevelopmental disorders (Moberget et al., 2019; Romer et al., 2018). To avoid extensive repetition within this thesis, further exploration of this, including combining with similar results from other chapters, are found in *Chapter 6 General Discussion* of this thesis.

Importantly, however, these results of a negative cerebellar association with a psychiatric disorder diagnosis are without consideration of the presence of other non-psychiatric disorder diagnoses in both the “cases” and “control” sub-samples. This is likely very important considering, for example, that when analysing the relationship between diagnoses of non-psychiatric conditions and cerebellar volume, we also found average volume reductions in those

with neurological, endocrine-metabolic, circulatory, and other abnormal clinical signs/symptoms not captured by other categories. An unequal distribution of these disorders between the psychiatric “cases” and “controls”, therefore, could impact upon the results presented here. Indeed, we found those with recorded psychiatric disorders in our sample had elevated numbers of most other recorded hospital diagnoses, including neurological, endocrine-metabolic and infection ICD-10 hospital record codes, results concurring with previous reports of the high presence of comorbidities in those with psychiatric disorders (Scott et al., 2016; Vancampfort et al., 2013). For example, we found reductions in the cerebellum to be largest in those with endocrine-metabolic related disorders, particularly those with obesity and diabetic medical conditions, showing around 3.5-4.0cm³ reductions in cerebellar volume compared to those without; and with endocrine/metabolic disorders in our sample present almost 3 times higher in those with a psychiatric diagnosis compared to those without. While these comorbid conditions have been considered in previous studies of cerebellar ataxias (Manto & Hampe, 2018), their potential confounding effect is rarely considered when investigating other clinical conditions, such as psychiatric disorders. Equally, we did not remove individuals from the “control” group with any other secondary diagnosis, since – being a relatively older adult sample where having at least one diagnosis record was common (72.6%) – we felt such a restricted group of “ultra-healthy” participants would not provide a “typical” control group for the population being studied.

To address the issue of comorbidities, we next added all medical conditions into a single multivariate model. We found the negative effect of having psychiatric diagnosis on cerebellar volume remained, indicating an independent effect of psychiatric conditions not captured by other recorded diagnoses, though with effect sizes diminished by approximately a third. Negative effects of neurological, endocrine-metabolic and cardiovascular disorders also remained. Beyond their use in this study for considering psychiatric comorbidities, these results will also likely be of great interest to the wider scientific community studying these disorders.

We have confirmed cerebellar reductions in those with psychiatric conditions and, furthermore, have shown that these persist even when considering other overt medical comorbidities. We wished, however, to further establish whether these differences remained when considering other possible sub-clinical confounds. In particular, we focused on the effects of increased head motion and BMI, both of which are known to be elevated in those with psychopathology (Makowski et al., 2019; Vancampfort et al., 2013), a finding we confirm in our sample. We found both to have negative effects on the cerebellum in our total cohort, in accordance with previous

literature reports of BMI effects (Beyer et al., 2019) and introducing the novel findings of the large negative effect of elevated head motion. Of note, this whole cohort will include individuals with various disorders shown to impact upon cerebellar volume (as highlighted earlier), though, for the same reasons as stated above, we felt this approach more representative of the larger population rather than analysing these associations in an “ultra-healthy” sub-sample. While highly correlated with each other (i.e. those with higher BMI moving more in the scanner), both remained significant when added to the same model and showed little evidence of multicollinearity, suggesting independent effects. When taking into consideration possible participant head motion or/and BMI differences, cerebellar reductions in those with psychiatric diagnoses remained, though were diminished in effect size, approximately to equivalent size as that seen when considering medical comorbidities. Since an effect remains, therefore, it appears the cerebellar reductions seen in those with psychiatric diagnoses are not solely driven by increased head motion or BMI. Additional correcting for medical diagnoses comorbidities, however, does reduce the effect below our criterion for FDR correction, with effect sizes being largely similar to what they were before but with more variability.

In light of the above results, therefore, in tandem with further investigations into understanding the epidemiological and pathophysiological associations between disorders (e.g. between antipsychotic medications and weight gain, as outlined in *2.2 Background*), future psychiatric (and non-psychiatric) studies might wish to aim to control for possible differences in participant head motion in the scanner, increased waist-hip ratio/BMI and/or other medical diagnoses. As it might prove impractical for clinical studies to collect all this information due to requiring additional permissions for access of medical history data or carrying out specific resting-state functional MRI scans, we suggest that, at least, prioritising participant comfort in the scanner to prospectively decrease head motion, and inclusion of supplementary analyses with correction for possible waist-hip/BMI differences, should be considered. Importantly, we show that the negative effects of increased BMI on the cerebellum appear to be present even when excluding those at levels indicative of obesity (BMI > 30), showing the effect is not just limited to those at the more extreme ends. As discussed in the introduction, however, beyond medication-induced weight effects, premorbid and aetiology associations between psychiatric disorders and metabolic differences (Bahrami et al., 2020; Malaspina et al., 2019) highlight how default retrospective statistical correction might not be the most appropriate approach due to possibly diminishing true effects, and will depend upon the research question being asked. Default correction for head motion differences is arguably less likely to be as problematic since it does not reflect a true physiological process; though notably even these measures do associate with

possibly relevant traits of interest within psychiatric diagnoses (Bijsterbosch et al., 2017; Siegel et al., 2017). For our future studies in this thesis, we include default correction for mean resting-state head motion in all further analyses in addition to our default covariates already listed.

Notably, we chose to use the resting-state fMRI estimated head motion measure over task-based fMRI estimations, being both nearer in time to the structural scans and more similar in participant behaviour (i.e. not engaged in a task). Recently, a single variable capturing the estimated effect of head motion – derived from various imaging quality control measures - on structural scan image quality has also been created in the UK Biobank data (Alfaro-Almagro et al., 2021). This showed only moderate correlation with the resting-state fMRI head motion estimate (correlation ≈ 0.2), therefore, it would, be interesting to investigate whether similar associations between cerebellar volume and this new structural measure – as reported in this thesis with the resting-state derived measure – are seen, so as to validate our approach. Furthermore, following a similar methodology as outlined in their paper, investigating how well both this new measure and the resting-state head motion measure predict manually derived expert assessments of image quality of the cerebellum would further help to explore the relationship between head motion, cerebellar MRI data quality and recorded morphometric measures.

There are several limitations of our findings which are important to consider when interpreting the results. Firstly, it is important to state that the UK Biobank is a self-referred, older adult cohort, with a low response rate (5.5%), and whose measures of demographic, socioeconomic and health characteristics differ to the general UK population (Fry et al., 2017), factors likely increased in those who attended the MRI element of the study. We also restricted our cohort to just those who completed the MRI, and who had all covariates of interest recorded and without having values deemed as outliers, which might diminish effects with those more on the extremes being omitted. The medical condition records themselves are only those recorded in hospitals and do not reflect complete medical history (Davis et al., 2019) – with mental health conditions also known to not be well captured by hospital records alone - as well as still being susceptible to mislabelling or data-loss. When discussing “comorbidities” of psychiatric disorders – being the focus of this thesis – it is important to remember that we are solely discussing the correlative relationship between two disorders, rather than indicating one as the primary cause. Furthermore, these hospital measures reflect any occurrence of diagnosis rather than current diagnosis. For all these reasons, the effects of medical conditions on cerebellar volumes in this study should not be interpreted as reflecting general UK population effects.

Related to this, for our analyses, we do not consider the age of diagnosis, length of disease, number of diagnoses or any medication effects (Yue et al., 2016), factors which themselves might associate with brain morphometry differences. Future releases of UK Biobank will not only allow for replication of these findings, but include updated healthcare data, including from primary healthcare sources and, therefore, will allow for testing of some of these suggested analyses.

Furthermore, for our primary analysis of interest of comparing cerebellar volumes between those with and without psychiatric conditions, the distributions of the residuals of cerebellar volume (following adjustment for our default covariates) were normally distributed and variances were similar (7.7×10^7 & 6.8×10^7). This, however, might not have been the case for each diagnosis grouping analysed and, therefore, in addition to our use of a standard linear regression model (equivalent to two sample Student's t-test but allowing for correction of covariates), we should have weighted the regression by each group's respective variance (equivalent to Welch's t-test), and which would be a preferred method for future analyses. For the effect of psychiatric group diagnosis on cerebellar volume, results were very similar for both our original unweighted results which we report in Table 2.2 ($B=-1470$, $p=3.14 \times 10^{-7}$) and the weighted regression results ($B=-1470$, $p=1.88 \times 10^{-6}$).

In conclusion, we have analysed cerebellar differences in a large, volunteer-based UK Biobank cohort, showing that individuals with recorded hospital incidences of psychiatric conditions are associated with reduced cerebellar volume. We highlight, however, the need to consider comorbidities and/or subclinical effects of increased weight and head motion when analysing brain volume differences for future clinical cohort studies.

2.6 Supplementary Tables

Supplementary Table 2.1: The frequency of A) tier 1 and B) tier 2 ICD-10 recorded hospital diagnoses present in our 19,369 UK Biobank sample. Viewable in the provided additional file and https://osf.io/jr8m2/?view_only=29906bc730f64cf58a81d67ff5c50363.

Supplementary Table 2.2: The effect of our default list of covariates on total cerebellar volume

Variable	B-coefficient (mm ³)	95% Confidence interval (mm ³)		p-value
poly(Age,2)1 †	-2.50E+05	-2.73E+05	-2.26E+05	2.00E-16
poly(Age2.0,2)2 †	-9.97E+04	-1.22E+05	-7.70E+04	2.00E-16
sex (Male)	-1.45E+03	-1.74E+03	-1.16E+03	2.00E-16
centre (11027)	1.26E+03	8.08E+02	1.71E+03	4.11E-08
Date Attended Imaging Centre	2.29E-02	-3.03E-01	3.49E-01	0.89
Scanner position (x)	-5.43E+01	-9.97E+01	-8.91E+00	0.02
Scanner position (y)	-1.87E+02	-2.14E+02	-1.61E+02	2.00E-16
Scanner position (z)	1.02E+00	-8.31E+00	1.03E+01	0.83
Table position (z)	1.23E+02	1.13E+02	1.32E+02	2.00E-16
Total brain volume (mm ³)	5.22E-02	5.09E-02	5.35E-02	2.00E-16
Interaction: poly(Age2.0,2)1:sexMale †	-1.20E+05	-1.52E+05	-8.73E+04	3.79E-13
Interaction: poly(Age2.0,2)2:sexMale †	-2.71E+04	-5.92E+04	5.00E+03	0.10

Results are from a single multiple linear regression analyses including all covariates for their effect on total cerebellar volume, providing unstandardised regression coefficients, 95% confidence intervals and raw p-values. †: first and second polynomials of Age (yrs)

Supplementary Table 2.3: The effect of each tier-1 ICD-10 recorded hospital diagnosis on total cerebellar volume (without total brain volume correction)

Tier 1 medical condition	N _{Cases}	$\Delta R^2 \ddagger$	B-coefficient (mm ³)	95% Confidence interval (mm ³)		p	p _{FDR} *
I Infections	900	8.46E-05	-486.89	-1113.3	139.53	0.13	0.17
II Neoplasms	3215	2.56E-04	482.78	125.58	839.99	8.08E-03	0.02
III Blood	749	2.46E-04	-907.9	-1593.08	-222.73	9.40E-03	0.02
IV Endocrine	2081	3.40E-03	-2120.82	-2550.36	-1691.27	4.21E-22	8.00E-21
V Psychiatric	841	1.24E-03	-1922.71	-2569.44	-1275.97	5.73E-09	3.63E-08
VI Neurological	1200	1.03E-03	-1485.27	-2032.68	-937.86	1.06E-07	5.03E-07
VII Eye	1362	2.41E-04	-685.2	-1207.03	-163.37	0.01	0.02
VIII Ear	288	3.31E-05	529.67	-560.79	1620.13	0.34	0.43
IX Circulatory	4189	1.36E-03	-1019.6	-1346.21	-692.99	9.61E-10	9.12E-09
X Respiratory	1986	3.57E-04	-694.63	-1129.57	-259.68	1.75E-03	5.54E-03
XI Digestive	6123	1.34E-04	-279.34	-564.82	6.14	0.06	0.08
XII Skin	1578	4.22E-07	-26.5	-509.06	456.07	0.91	0.91
XIII Musculoskeletal	2701	2.72E-04	-531.85	-913.62	-150.09	6.33E-03	0.02
XIV Genitourinary	4185	1.17E-05	-94.67	-422.74	233.39	0.57	0.64
XV Pregnancy-related	845	4.70E-06	137.09	-611.66	885.83	0.72	0.76
XVIII Other	5540	5.13E-04	-560.36	-853.22	-267.49	1.77E-04	6.73E-04
XIX Injury or Poisoning	1489	1.43E-04	-500.18	-995.2	-5.16	0.05	0.08
XX External	925	1.16E-05	-177.67	-796.41	441.07	0.57	0.64
XXI Health Status	6606	2.75E-04	-394.03	-675.26	-112.8	6.03E-03	0.02

Results are from independent univariate linear regression analyses, testing for the effect of each tier 1 diagnosis (with >200 occurrences) on total cerebellar volume, and including all covariates aside from total brain volume (age², sex, age²*sex, imaging centre attended, date attended). ‡ Unique R² explained by the tier 1 diagnosis. Calculated: R² of model with tier 1 diagnosis - R² of model without tier 1 diagnosis. *: p-value adjusted for correction for the number of tests performed (FDR=0.05)

Supplementary Table 2.4: Sex distribution of tier 1 ICD-10 recorded diagnoses. Viewable in the provided additional file and

https://osf.io/jr8m2/?view_only=29906bc730f64cf58a81d67ff5c50363

Supplementary Table 2.5: Sex interactional effects with tier 1 ICD-10 recorded diagnoses on total cerebellar volume. Viewable in the provided additional file and

https://osf.io/jr8m2/?view_only=29906bc730f64cf58a81d67ff5c50363

Supplementary Table 2.6: The presence of ICD-10 recorded hospital comorbidities (Non-Psych) of psychiatric diagnoses (Psych) in our cohort

Non-Psychiatric Medical Condition ("Non-Psych")	Frequency counts				% of Psych	% of those without	Odds ratio	95% Confidence interval		p	p _{FDR} *
	Both	Non-Psych only	Psych only	Neither	With a non-Psych condition	Psych with a non-Psych condition					
XIX Injury or Poisoning	200	1289	641	17239	23.8	7.0	4.2	3.5	4.9	6.02E-50	1.94E-49
XVIII Other	504	5036	337	13492	59.9	27.2	4.0	3.5	4.6	1.97E-83	1.25E-82
XXI Health Status	555	6051	286	12477	66.0	32.7	4.0	3.5	4.6	8.84E-83	5.40E-82
IV Endocrine	250	1831	591	16697	29.7	9.9	3.9	3.3	4.5	2.09E-54	7.01E-54
VI Neurological	148	1052	693	17476	17.6	5.7	3.5	2.9	4.3	5.33E-32	1.11E-31
XX External	115	810	726	17718	13.7	4.4	3.5	2.8	4.3	4.84E-25	8.54E-25
IX Circulatory	394	3795	447	14733	46.8	20.5	3.4	3.0	3.9	4.96E-62	1.84E-61
XI Digestive	502	5621	339	12907	59.7	30.3	3.4	2.9	3.9	1.13E-65	4.70E-65
XIII Musculoskeletal	278	2423	563	16105	33.1	13.1	3.3	2.8	3.8	2.23E-47	6.93E-47
I Infections	107	793	734	17735	12.7	4.3	3.3	2.6	4.1	8.93E-22	1.47E-21
X Respiratory	209	1777	632	16751	24.9	9.6	3.1	2.6	3.7	1.90E-35	4.57E-35
XII Skin	141	1437	700	17091	16.8	7.8	2.4	2.0	2.9	6.71E-17	9.89E-17
XIV Genitourinary	322	3863	519	14665	38.3	20.8	2.4	2.0	2.7	2.65E-29	5.15E-29
VIII Ear	25	263	816	18265	3.0	1.4	2.1	1.3	3.2	1.08E-03	1.18E-03
III Blood	62	687	779	17841	7.4	3.7	2.1	1.6	2.7	1.39E-06	1.64E-06
VII Eye	106	1256	735	17272	12.6	6.8	2.0	1.6	2.5	3.19E-09	3.90E-09
II Neoplasms	206	3009	635	15519	24.5	16.2	1.7	1.4	2.0	2.00E-09	2.48E-09
XV Pregnancy-related	41	804	800	17724	4.9	4.3	1.1	0.8	1.6	0.44	0.44

*For the full table for all tier 1 medical conditions pairings (of those diagnoses with >200 occurrences) please see additional file and OSF appendix https://osf.io/jr8m2/?view_only=29906bc730f64cf58a81d67ff5c50363. Results are from independent two-sided Fisher's exact tests. *: p-value adjusted for correction for the number of tests performed (FDR=0.05)*

Supplementary Table 2.7: Multivariate analysis of the effect of each tier 1 ICD-10 recorded diagnoses on total cerebellar volume

Tier-1 medical condition	Freq	$\Delta R^2 \ddagger$	B-coefficient (mm ³)	95% Confidence Interval (mm ³)		p	p _{FDR} *
I Infections	900	1.55E-06	68.01	-492.81	628.83	0.81	0.94
II Neoplasms	3215	5.40E-05	232.41	-92.63	557.44	0.16	0.53
III Blood	749	1.74E-07	-24.76	-634.82	585.31	0.94	0.94
IV Endocrine	2081	1.06E-03	-1294.04	-1703.48	-884.61	5.95E-10	1.13E-08
V Psychiatric	841	3.66E-04	-1083.37	-1665.35	-501.38	2.64E-04	2.51E-03
VI Neurological	1200	2.21E-04	-709.98	-1201.03	-218.94	4.60E-03	0.02
VII Eye	1362	4.08E-05	-284.85	-743.42	173.72	0.22	0.53
VIII Ear	288	4.44E-05	618.3	-335.02	1571.61	0.20	0.53
IX Circulatory	4189	3.42E-04	-568.76	-884.69	-252.83	4.19E-04	2.65E-03
X Respiratory	1986	1.08E-05	-126.01	-519.41	267.39	0.53	0.92
XI Digestive	6123	3.68E-07	15.89	-253.41	285.18	0.91	0.94
XII Skin	1578	3.23E-06	74.63	-352.21	501.47	0.73	0.93
XIII Musculoskeletal	2701	5.11E-06	76.37	-270.98	423.72	0.67	0.93
XIV Genitourinary	4185	7.60E-06	80.28	-219.06	379.62	0.60	0.93
XV Pregnancy-related	845	9.54E-05	-430.51	-1085.64	224.63	0.20	0.53
XVIII Other	5540	3.40E-06	-50.29	-330.54	229.95	0.73	0.93
XIX Injury or Poisoning	1489	3.46E-07	-28.69	-530.17	472.79	0.91	0.94
XX External	925	2.63E-05	313.68	-315.49	942.84	0.33	0.62
XXI Health Status	6606	3.51E-05	166.89	-122.69	456.47	0.26	0.55

*Results are from a single multivariate linear regression analysis testing the effect on total cerebellar volume of each tier 1 diagnosis (with >200 occurrences) simultaneously, including all default covariates (age², sex, age²*sex, total brain volume, imaging centre attended, date attended). ‡ Unique R² explained by the specific tier 1 diagnosis. Calculated: R² of model with the tier 1 diagnosis - R² of model without the tier 1 diagnosis. *: p-value adjusted for correction for the number of tests performed (FDR=0.05)*

Supplementary Table 2.8 : Body mass index (BMI) and head motion differences in those with/without tier 1 ICD-10 recorded diagnoses. Viewable in the provided additional file and https://osf.io/jr8m2/?view_only=29906bc730f64cf58a81d67ff5c50363

Supplementary Table 2.9: Tier 1 ICD-10 recorded diagnoses on total cerebellar volume with additional head motion and/or body mass index correction. Viewable in the provided additional file and https://osf.io/jr8m2/?view_only=29906bc730f64cf58a81d67ff5c50363

Supplementary Table 2.10: Multivariate analysis of each tier 1 ICD-10 recorded diagnoses on total cerebellar volume with additional head motion and body mass index correction

Tier-1 medical condition	Freq	$\Delta R^2 \ddagger$	B-coefficient (mm ³)	95% Confidence Interval (mm ³)		p	p_{FDR}^*
I Infections	900	5.20E-06	124.51	-424.4	673.43	0.66	0.76
II Neoplasms	3215	4.79E-05	218.93	-99.11	536.97	0.18	0.48
III Blood	749	3.40E-06	-109.53	-706.5	487.44	0.72	0.76
IV Endocrine	2081	2.95E-04	-687.81	-1090.61	-285.02	8.18E-04	0.02
V Psychiatric	841	1.75E-04	-750.9	-1320.98	-180.83	9.84E-03	0.09
VI Neurological	1200	9.54E-05	-467.03	-947.89	13.83	0.06	0.28
VII Eye	1362	2.93E-05	-241.5	-690.19	207.19	0.29	0.62
VIII Ear	288	6.06E-05	721.86	-210.92	1654.64	0.13	0.41
IX Circulatory	4189	8.61E-05	-285.78	-595.48	23.92	0.07	0.28
X Respiratory	1986	9.44E-06	117.75	-267.59	503.08	0.55	0.70
XI Digestive	6123	1.60E-05	104.74	-158.82	368.3	0.44	0.62
XII Skin	1578	1.82E-05	177.12	-240.57	594.81	0.41	0.62
XIII Musculoskeletal	2701	2.85E-05	180.31	-159.67	520.29	0.30	0.62
XIV Genitourinary	4185	1.55E-05	114.61	-178.29	407.52	0.44	0.62
XV Pregnancy-related	845	1.77E-04	-586.09	-1228.92	56.73	0.07	0.28
XVIII Other	5540	3.35E-06	-49.92	-324.18	224.34	0.72	0.76
XIX Injury or Poisoning	1489	5.00E-07	34.49	-456.19	525.18	0.89	0.89
XX External	925	1.50E-05	236.83	-378.79	852.45	0.45	0.62
XXI Health Status	6606	1.48E-05	108.52	-174.85	391.89	0.45	0.62

*Results are from a single multivariate linear regression analysis testing the effect on total cerebellar volume of each tier 1 diagnosis (with >200 occurrences), including all default covariates (age², sex, age²*sex, total brain volume, imaging centre attended, date attended), as well as both body mass index (BMI) and mean resting-state fMRI head displacement/motion and all other tier 1 diagnosis in the same model. ‡ Unique R² explained by the tier 1 diagnosis. Calculated: R² of model with tier 1 diagnosis - R² of model without tier 1 diagnosis. *: p-value adjusted for correction for the number of tests performed (FDR=0.05)*

Supplementary Table 2.11: Tier 2 ICD-10 recorded diagnoses on total cerebellar volume. Viewable in the provided additional file and

https://osf.io/jr8m2/?view_only=29906bc730f64cf58a81d67ff5c50363

Supplementary Table 2.12: Tier 2 ICD-10 recorded diagnoses on total cerebellar volume with additional head motion and body mass index correction. Viewable in the provided additional file

and https://osf.io/jr8m2/?view_only=29906bc730f64cf58a81d67ff5c50363

3 Assessing the association between common and rare allele risk for schizophrenia and cerebellar structure

3.1 Abstract

Recent research has shown cerebellar volume to be both highly heritable and reduced in participants with schizophrenia, relative to healthy controls, drawing attention to its potential use as a biomarker for the disorder. Whether allele risk for schizophrenia similarly associate with cerebellar volume differences, however, has yet to be established. In this study we investigated the association between both common (polygenic risk score) and rare (copy number variants/CNVs) allele risk for schizophrenia with cerebellar volume in a large sample of unaffected participants (n=15,802) from the UK Biobank cohort. We found total cerebellar volume to be negatively associated with polygenic risk score ($\beta=-0.02$, $p = 0.0009$), and for carrier status of the 1q21.1 duplication ($\beta=-0.60$, $p=0.005$), and positively associated with 1q21.1 deletion ($\beta=0.60$, $p=0.03$); all of which survive our correction threshold for the number of tests performed. Exploring individual cerebellar lobules, we showed the association with polygenic risk score to be relatively consistent across the posterior cerebellum, while differing sub-regional effects are seen depending on the CNV assessed. Our results show that cerebellar volume is associated with common and rare allele risk for schizophrenia in a sample of unaffected adults, adding further evidence in support of this brain marker as a potential endophenotype for this disorder.

3.2 Background

Several studies report cerebellar morphometric differences in individuals with various psychiatric disorders (Phillips et al., 2015), including schizophrenia (Gupta et al., 2015; Kühn, Romanowski, Schubert, & Gallinat, 2012; Laidi et al., 2015; Moberget et al., 2018). As with studies of differences in other brain regions in those with psychiatric disorders, however, the effect of confounding factors in driving this association have been little considered (Annamalai et al., 2017; Makowski et al., 2019; Yao et al., 2017). In *Chapter 2*, we showed the substantial effects that elevated clinical and sub-clinical comorbidities, as well as participant behaviour in the scanner, can have on estimated cerebellar volumes in those with psychiatric diagnoses. Given the high heritability of schizophrenia ($h^2 \approx 80\%$) (Cardno & Gottesman, 2000; Dennison, Legge, Pardiñas, & Walters, 2020; Hilker et al., 2018), we next wished to ascertain if cerebellar volume differences are related to the underlying genetic risk for schizophrenia and whether similar differences are seen in individuals at increased genetic risk for the disorder but who are “unaffected” and do not have a psychiatric diagnosis. If the cerebellum shows similar reductions in these individuals, it adds evidence that these volumetric reductions reported in clinical cases are not due solely to reverse causative factors – such as caused by psychotropic medicines– and instead might represent a premorbid biomarker for the disorder.

One way of accomplishing this is by studying the effect of carrying one of the several rare copy number variants (CNVs) which have been linked to increased schizophrenia liability as well as to other neurodevelopmental disorders (George Kirov et al., 2014; Marshall et al., 2017). Studies, mostly of 22q11.2, 16p11.2 and 15q11.2 CNVs, have shown robust brain morphological differences (Ahtam, Link, Hoff, Ellen Grant, & Im, 2019; Ching et al., 2020; Hoogman et al., 2017; A. Lin et al., 2017; Van Der Meer et al., 2020) including the former two CNVs in the cerebellum (Cárdenas-de-la-Parra et al., 2019; Haenssler et al., 2020; Maillard et al., 2015; J. P. Owen et al., 2018; Rogdaki et al., 2020). To date, however, these studies often still include individuals with overt neurological and psychiatric diagnoses, therefore not fully addressing the potential of aforementioned reverse causative effects driving the association. Recent large, volunteer genetic imaging datasets, such as UK Biobank (Collins, 2012), have allowed a different approach, revealing subcortical differences in psychiatrically “unaffected” individuals who carry a schizophrenia-associated CNV compared to non-carriers (Warland et al., 2020). This study, however, did not explore cerebellar differences. Furthermore, being from an earlier release of UK Biobank data with fewer carriers of CNVs, it was limited to grouping all CNVs together into a binary variable, including both duplications and deletions, despite possible opposing effects (Qureshi et al., 2014; Van Der Meer et al., 2020), meaning the majority of individual CNV effects are still to be explored.

In addition to these rare alleles, common allele variation captures a substantial proportion of schizophrenia heritability ($h^2_{\text{SNP}} \approx 22.5\%$) (Dennison et al., 2020; Pardiñas et al., 2018). Polygenic scores can be created in genotyped individuals, representing a summed score of presence of these common independent risk markers weighted by each marker's association with schizophrenia, as estimated from genome wide associations study (GWAS) (Wray et al., 2014). The association between an increased polygenic score for schizophrenia and brain morphometry has been less consistent, with some reports of significant brain differences (Alnæs et al., 2019; X Caseras, Tansey, Foley, & Linden, 2015; B. Liu et al., 2017; Neilson et al., 2017, 2019; Terwisscha Van Scheltinga et al., 2013; Westlye, Alnæs, van der Meer, Kaufmann, & Andreassen, 2019), while other studies report no associations (Fonville et al., 2019; Lancaster et al., 2019; Reus et al., 2017; Van der Auwera et al., 2015; Voineskos et al., 2016). One study which analysed various brain structures in UK Biobank included whole cerebellar hemisphere measures (Alnæs et al., 2019), however, the reductions seen did not reach their threshold for statistical significance. Since this publication, there have been the aforementioned increases in UK Biobank imaging data releases as well as updated GWAS summary statistics of single nucleotide polymorphisms' (SNPs) associations with schizophrenia (Pardiñas et al., 2018), the increased statistical power of which might better capture any related genetic effects on cerebellar volume. Furthermore, most genetic studies have analysed only more grouped cerebellar effects, and while negative cerebellar effects in patients are generally quite global, there also appears some indication of particular regional sensitivity in those with overt diagnosis (Moberget et al., 2018), therefore, analysis of sub-regionals effects is an important step. Finally, to our knowledge, no study has investigated the effect of both common and rare genetic variants on any brain morphometry measures. This would not only allow assessment of shared effects, but also allow for correction for any differences in CNV carriers' common genetic variant burden (Tansey et al., 2016), better elucidating their unique effect on the brain.

This study, therefore, aimed to address these questions by analysing both forms of schizophrenia genetic risk of rare CNVs and polygenic scores of common variants on both global and sub-regional cerebellar volumes in a large sample of unaffected adult participants. In this exploratory analysis, we hypothesised for cerebellar reductions to be present in those individuals with increased polygenic scores for schizophrenia and in schizophrenia associated CNV carriers compared to non-carriers, though recognising the latter might differ depending on inclusion of both duplications and deletions.

3.3 Methods

3.3.1 Participants

This cohort consisted of 21,407 UK Biobank (Collins, 2012) individuals whose raw and processed data had been released by the time of initiation of this study, and which has been described in *Chapter 2*. From these, we excluded participants with personal history of severe neuropsychiatric disorders (i.e. schizophrenia psychosis, autistic spectrum disorder, dementia or intellectual disability) or medical/neurological conditions that could affect cerebellar anatomy (i.e. alcohol or other substances dependency, Parkinson's, Alzheimer, multiple sclerosis or neurodegenerative conditions), based on self-reported diagnoses obtained from an interview with a trained nurse (UK Biobank data-field: [20002](#)) or from hospital in-patient records (data-field: [41270](#)). We additionally removed individuals based on genotyping and MRI data quality control (see below), providing a final sample of 15,802 individuals. Ethics for UK Biobank was granted by the North West Multi-Centre Ethics Committee. Data for this study was obtained through the approved project ref 17044.

3.3.2 Genetic data

A full description of UK Biobank's data collection, quality control and imputation process can be found elsewhere (<http://www.ukbiobank.ac.uk/scientists-3/genetic-data/>) (Bycroft et al., 2018). In brief, genetic data was obtained from blood samples of 488,377 individuals enrolled in UK Biobank, and assayed on two Axiom arrays to capture common and rare genetic variation (and indels) of interest. Imputation of the remaining genotypes was performed using Haplotype Reference Consortium (HRC) and UK10K haplotype resources, providing a final ~96million SNP resource per individual, harmonised to GRCh37 (hg19) genome build assembly of the human genome.

Further quality control of the autosomal genotypes from the UK Biobank imaging sample was performed locally using self-authored *Stata* functions (https://github.com/ricanney/stata_summaryqc function) (by Dr Richard Anney) leveraging *PLINK* (C. C. Chang et al., 2015) (v1.90b5.4; <https://www.cog-genomics.org/plink2/>) and the use of which has been described previously (Underwood et al., 2019). Firstly, across the whole 500k sample, markers were quality controlled based on imputation quality (INFO>0.8), minor allele frequency (MAF >0.1%) and those present in HRC reference. Within the imaging subsample itself, markers were further excluded based on low minor allele count (present in <5 individuals) so as to exclude markers with too few occurrences which can lead to unstable effect sizes, and excess individual marker missingness (>2% of all individuals), deviations from Hardy-Weinberg equilibrium ($p < 10^{-10}$) and from the expected minor allele frequency (MAF; >4 standard deviations (SD) from GBR reference MAF reported in 1000G phase 3), all of which

can indicate genotyping errors, assortative mating or residual population structure. Of the initial 7,726,488 genetic markers, 7,232,075 markers remained following these quality control steps. Quality control steps also removed those individuals with excess overall marker missingness rate (>2%), excess heterozygosity which can indicate inbreeding or sample contamination (>4 x SD from sample mean), those of non-British/Irish self-reported or based on similar genetic ancestry so as to maximise the available sample size of a similar genetic ancestry (derived from the first 3 principal components comparison 1000G GBR ancestry reference) and those with close relatives in the cohort so as to not bias SNP effect sizes and standard errors (>0.0442 i.e. 3rd degree relatives).

Using PRSice (v2) (Euesden, Lewis, & O'Reilly, 2015), dosage polygenic schizophrenia risk scores ("polygenic scores") were created for each individual following a previously published method (Ripke et al., 2014) (conducted by Dr Sophie Legge). These were created using the more recent GWAS summary statistics of schizophrenia available to date, being a meta-analysis between Psychiatric Genetics Consortium (PGC) and CLOZUK samples (40,675 cases; 64,643 controls; European genetically similar ancestry) (Pardiñas et al., 2018). Of these SNPs, indels and any markers with low genotype quality (<0.9), low MAF (<0.1%) or those within the high long-range linkage disequilibrium (LD) region of the major histocompatibility complex (chromosome 6, 25MB-35MB) were removed. Clumping was performed to retain only the most significant SNP within each LD block ($r^2 < 0.2$, window size <500kb) for the remaining SNPs. Polygenic scores were generated at 7 different thresholds of SNPs' p-value association with schizophrenia (p_T -value): $p_T < 1 \times 10^{-7}$ (including 353 SNPs), 5×10^{-6} (665 SNPs), 5×10^{-5} (1395 SNPs), 5×10^{-4} (3395 SNPs), 0.005 (9885 SNPs), 0.05 (33740 SNPs) and 0.1 (50091 SNPs). We estimated we had 80% power to detect an effect of 0.025% variance explained in total cerebellar volume by a polygenic score for schizophrenia liability (based on $p_T < 0.05$ threshold; schizophrenia $h^2_{SNP} = 20\%$; Lifestyle schizophrenia population prevalence = 1%; proportion of SNPs of null effect = 0.95; $\alpha < 0.05$) (Dudbridge, 2013).

The calling of copy number variants (CNVs) in the UK Biobank cohort has been reported previously (Kendall et al., 2017; Warland et al., 2020) (conducted by Prof George Kirov & Dr Kimberly Kendell). In brief, genotype calls were performed using *Affymetrix Power Tools* software with ~750,000 biallelic markers, with genotyping calls and summary files processed using *PennCNV-Affy* software to create canonical genotype clusters, log-R ratios and β allele frequencies (K. Wang et al., 2007). Individuals were excluded during quality control steps if they had ≥ 30 CNVs, a large waviness factor (outside of 0.03:-0.03) or low call rate (<96%), and with CNVs excluded with insufficient probe coverage (<10) or probe density coverage (<1 per 20,000 base pairs). CNVs were judged to be present if they covered more than half of the critical interval and included the key genes in the region (if known). The

schizophrenia-associated CNVs were defined based upon previous work (Kendall et al., 2017; George Kirov et al., 2014; Marshall et al., 2017; Rees et al., 2016) and are a sub-section of the 93 CNVs previously associated with neurodevelopmental disorders (Coe et al., 2014; Dittwald et al., 2013). Individuals carrying any schizophrenia-associated CNV were compared to normative controls who carried no schizophrenia-associated or any other of the 93 neurodevelopmentally-linked CNVs. This was also repeated for each specific schizophrenia-associated CNV with $n > 5$ occurrences in our sample. In addition to providing the demographic information for the full cohort, we performed a comparison of demographic information between carriers of CNVs and non-carriers using two-sided t-tests and Fisher's exact statistical tests.

3.3.3 *Imaging data*

A full description of the brain imaging protocols and data available from the UK Biobank can be found elsewhere (Miller et al., 2016). In this study, we used the imaging-derived phenotypes (IDPs) of cerebellar volume generated and provided by UK Biobank (Alfaro-Almagro et al., 2018) (data-fields: [25893:25920](#)) by registering a 28 cerebellar lobule atlas (Diedrichsen et al., 2009) to each individual's T1-weighted scan with FMRIB's (Functional Magnetic Resonance Imaging of the Brain) Software Library (FSL) tools (Jenkinson, Beckmann, Behrens, Woolrich, & Smith, 2012) including FAST (FMRIB's Automated Segmentation Tool) (Y. Zhang, Brady, & Smith, 2001). A total cerebellar volume measure was obtained by summing the volume of all cerebellar lobules with the exception of Crus I vermis, which was excluded due to its small size and, therefore, likely low signal-to-noise ratio and high variability, as has been done previously (Pezoulas et al., 2017).

3.3.4 *Statistical analysis*

Within R (v3.6.0) (<https://www.R-project.org/>), we used independent multiple linear regression analyses to assess the effect on total cerebellar volume of each genetic risk variable while controlling for potential confounding of imaging, demographic and genetic variables. The genetic risk predictor variables assessed were continuous polygenic scores at the 7 SNP inclusion thresholds (p_T -values), binary presence of each schizophrenia-associated CNV with $n > 5$ occurrences, as well as an overall binary presence of any schizophrenia-associated CNV (including those which individually had $n < 5$ occurrences). This involved adding covariates of age^2 (1st and 2nd degree polynomials. Data-field: [21003-2.0](#)), sex (data-field: [31](#)), and their interaction ($\text{age}^2 \times \text{sex}$), the first 10 genetic principal components to control for population structure, and imaging-related covariates of total brain volume (total grey + white matter; data-field: [25010](#)), imaging centre attended (data-field: [54-2.0](#)) and X-, Y- and Z-head position in the scanner (data-fields: [25756](#), [25757](#) & [25758](#)), starting table-Z position (data-

field: [25759](#)) and mean head motion obtained during the resting state functional MRI scan (log-transformed; data-field: [25741-2.0](#)). The distribution of total cerebellar volume residuals (following correction for these covariates) showed a normal distribution, both for the whole cohort, and for those with and without any schizophrenia-related CNV. Analysis on total brain volume with these same covariates (minus total brain volume) was also conducted to allow a comparison of overall brain differences. We excluded individuals from all analyses with imaging covariates or total cerebellar volume values deemed as outliers (>5x median absolute deviation from the overall median).

Both outcome brain volume variables and polygenic score predictors were converted to z-scores (scaled and mean-centred); providing standardised β -coefficients (along with 95% confidence intervals) which reflect the standard deviation (SD) difference in outcome volume with a 1xSD difference in polygenic scores or presence of CNV. The variance explained uniquely by the genetic factors in each model (ΔR^2) were calculated by subtracting R^2 obtained from models without the predictor from those with them. The Benjamini & Hochberg method (Benjamini & Hochberg, 1995) was used to control the false discovery rate (FDR) – the proportion of type 1 errors amongst all rejections of the null) - for the number of genetic predictors assessed, i.e. for 14 tests (7 polygenic score p_T -values, 6 CNVs with $n > 5$ and 1 any CNV groupings). We chose this approach for all our genetic analyses in this thesis as is most common in the literature, since controlling for the family-wise error rate using Bonferroni method would be too conservative in highlighting avenues to explore in future work due to the large number of signals being tested. P-values adjusted for the FDR (termed “ p_{FDR} ” in this thesis; alias “q-values”) were calculated using R ‘*p.adjust*’ (<https://rdrr.io/r/stats/p.adjust.html>) function ($p_{FDR} = (p\text{-value rank} / \text{total } p\text{-values}) \times \text{FDR}$), with a guide significance threshold $p_{FDR} < 0.05$ used to highlight particular results. When examining the associations across each cerebellar lobule ($n=17$), our correction for multiple testing increased accordingly (FDR correction for the 14 genetic predictors and 17 lobules = 238 tests).

3.4 Results

3.4.1 Demographic information

A total of 15,802 participants were included in the study, of whom 52.3% were female ($n=8,265$), having a mean age of 62.7 years ($SD=7.44$, range=45-80 yrs) at the time of MRI scanning. The sample had an average total cerebellar volume of 86.2 cm^3 ($SD=10.6$, range=43-136 cm^3) and total brain volume of 1170 cm^3 ($SD=111$, range=828-1630 cm^3), respectively. Of these, 110 were carriers of

schizophrenia-associated CNVs (Supplementary Table 3.1). We found 6 CNVs with >5 occurrences, being 15q11.2 deletion (n=56), 16p13.1 duplication (n=21), 1q21.1 duplication (n=11) and deletion (n=7), 16p12.1 deletion (n=7) and NRXN1 deletion (n=6). The demographic information for any CNV carriers, non-carriers and the overall population is available in Table 3.1. Carriers of CNVs showed no significant difference in age ($t=0.23$, $p=0.81$), sex (Odd's ratio/OR: 0.83, $p=0.34$) or imaging centre attended (OR=1.39, $p=0.15$) to non-carriers.

Table 3.1: Demographic information for the total 15,802 cohort, including carriers of schizophrenia-associated copy number variants (CNVs) carriers

	Total (n=15,802)	CNV carrier (n=110)	Non-carrier‡ (n=15,692)
Total cerebellar size (cm3)			
Mean (SD)	86.2 (10.6)	85.4 (10.6)	86.2 (10.6)
Median [Min, Max]	86.5 [43, 136]	85.7 [59, 108]	86.5 [43, 136]
Total brain volume (cm3)			
Mean (SD)	1170 (111)	1150 (115)	1170 (111)
Median [Min, Max]	1160 [828, 1630]	1150 [874, 1470]	1160 [828, 1630]
Sex			
F	8325 (52.7%)	63 (57.3%)	8262 (52.7%)
M	7477 (47.3%)	47 (42.7%)	7430 (47.3%)
Age (years)			
Mean (SD)	62.7 (7.44)	62.6 (6.58)	62.7 (7.44)
Median [Min, Max]	63.0 [45.0, 80.0]	63.0 [49.0, 77.0]	63.0 [45.0, 80.0]
Imaging centre attended			
1	13273 (84.0%)	87 (79.1%)	13186 (84.0%)
2	2529 (16.0%)	23 (20.9%)	2506 (16.0%)

‡: Non-carriers were defined as those not carrying any neurodevelopmentally associated CNV

3.4.2 Polygenic risk score

We found a significant ($p_{\text{FDR}} < 0.05$) negative association between total cerebellar volume and polygenic scores, an effect seen across most SNP inclusion association thresholds (p_{T} -values) (Table 3.2; Figure 3.1). The greatest amount of variance explained in total cerebellar volume uniquely attributable to a polygenic score was for the SNP inclusion threshold of $p_{\text{T}} < 5.0 \times 10^{-5}$, uniquely explaining approximately 0.04% variance in total cerebellar volume ($\Delta R^2 = 3.5 \times 10^{-4}$, β [95% confidence intervals/CI] = -0.02[-0.03, -0.01], $p = 0.0009$). While we also found evidence for significant ($p_{\text{FDR}} < 0.05$) negative associations between total brain volume and polygenic scores, this was only the case for the less stringent SNP inclusion thresholds tested (i.e. $p_{\text{T}} < 0.1$: $\Delta R^2 = 5.3 \times 10^{-4}$, $\beta = -0.02[-0.04, -0.01]$, $p = 0.0002$ and $p_{\text{T}} < 0.05$: $\Delta R^2 = 4.0 \times 10^{-4}$, β [95%CI] = -0.02[-0.03, -0.01], $p = 0.002$) (Supplementary Table 3.2; Figure 3.1).

3.4.3 CNV carrier-status

Comparing carriers of each schizophrenia-associated CNV to non-carriers we found a significant ($p_{\text{FDR}} < 0.05$) dose-effect for the 1q21.1 CNV, with carriers of the duplication and deletion showing reductions and increases in total cerebellar volume, respectively ($\Delta R^2 = 2.5 \times 10^{-4}$, $\beta = -0.60[-1.02, -0.17]$, $p = 0.005$ & $\Delta R^2 = 1.6 \times 10^{-4}$, $\beta = 0.60[0.07, 1.13]$, $p = 0.03$, respectively) (Table 3.2; Figure 3.1). This can be compared to their effect on total brain volume, where the opposite effect is seen in carriers of the deletion and duplication ($\Delta R^2 = 9.2 \times 10^{-4}$, $\beta = -1.44[-2.02, -0.86]$, $p = 1.1 \times 10^{-6}$ & $\Delta R^2 = 1.8 \times 10^{-4}$, $\beta = 0.51[0.05, 0.97]$, $p = 0.03$, respectively) though only the former survives our correction for multiple comparisons (Supplementary Table 3.2; Figure 3.1). We found no evidence for the other CNVs with $n > 5$, i.e. 15q11.2del, 16p13.11dup, 16p12.1del and NRXN1del, having any alterations of total cerebellar or total brain volume ($p < 0.05$). We also found no evidence for total cerebellar or total brain volume differences when comparing carriers of any schizophrenia-CNV compared to non-carriers ($\beta = -0.07[-0.21, 0.06]$, $p = 0.28$ & $\beta = -0.10[-0.25, 0.05]$, $p = 0.19$, respectively). We found both effects of 1q21.1 duplication and deletion CNVs on total cerebellar volume to remain significant after adding the SCZ polygenic risk score ($p_{\text{T}} < 5.0 \times 10^{-5}$: being the most predictive score) in the model, indicating that these two genetic risk factors account for independent variance components in the total cerebellar volume ($\Delta R^2 = 2.5 \times 10^{-4}$, $\beta = -0.59[-1.02, -0.17]$, $p = 0.006$ & $\Delta R^2 = 1.6 \times 10^{-4}$, $\beta = 0.60[0.07, 1.13]$, $p = 0.03$, respectively). We did not find an overall elevation in polygenic scores for schizophrenia ($p_{\text{T}} < 5.0 \times 10^{-5}$) in carriers of any schizophrenia CNV compared to those without ($\Delta R^2 = 4.8 \times 10^{-5}$, $\beta = 0.08[-0.10, 0.27]$, $p = 0.39$).

Table 3.2: The effect on total cerebellar volume of increasing polygenic schizophrenia risk score and schizophrenia-associated copy number variants (SCZ CNVs) carrier status

Genetic Risk Factor		ΔR^2^\ddagger	β^\ddagger	95% Confidence intervals [‡]		p	p_{FDR}^*
Polygenic scores	$p_T < 0.0000001$	2.67E-04	-0.016	-0.028	-0.005	4.12E-03	1.15E-02
	$p_T < 0.000005$	2.88E-04	-0.017	-0.028	-0.006	2.88E-03	1.01E-02
	$p_T < 0.00005$	3.55E-04	-0.019	-0.030	-0.008	9.46E-04	8.95E-03
	$p_T < 0.0005$	3.13E-04	-0.018	-0.029	-0.007	1.92E-03	8.95E-03
	$p_T < 0.005$	3.16E-04	-0.018	-0.029	-0.007	1.80E-03	8.95E-03
	$p_T < 0.05$	2.25E-04	-0.015	-0.027	-0.004	8.47E-03	0.02
	$p_T < 0.1$	1.94E-04	-0.014	-0.026	-0.003	1.45E-02	0.03
SCZ CNVs	Any SCZ CNV	3.83E-05	-0.075	-0.209	0.060	0.28	0.30
	15q11.2del	7.66E-05	-0.147	-0.335	0.041	0.13	0.18
	16p13.11dup	8.72E-06	0.081	-0.226	0.388	0.61	0.61
	1q21.1dup	2.48E-04	-0.596	-1.020	-0.172	5.84E-03	1.36E-02
	1q21.1del	1.60E-04	0.600	0.068	1.131	0.03	0.04
	16p12.1del	3.97E-05	0.299	-0.232	0.830	0.27	0.30
	NRXN1del	6.83E-05	-0.423	-0.997	0.151	0.15	0.19

Notes: Results are from independent univariate regression models including correction for demographic, genetic and imaging covariates in the model (including total brain volume); with predictors of polygenic schizophrenia risk scores at different SNP inclusion thresholds (p_T -values) or schizophrenia-associated CNV carrier status. ‡: Standardised β coefficients and 95% confidence intervals are provided. †: Variance of total cerebellar volume uniquely explained by the genetic predictor; *: False Discovery Rate (FDR) corrected p -values for the number of genetic predictors are provided. Bold signifies results with $p_{FDR} < 0.05$.

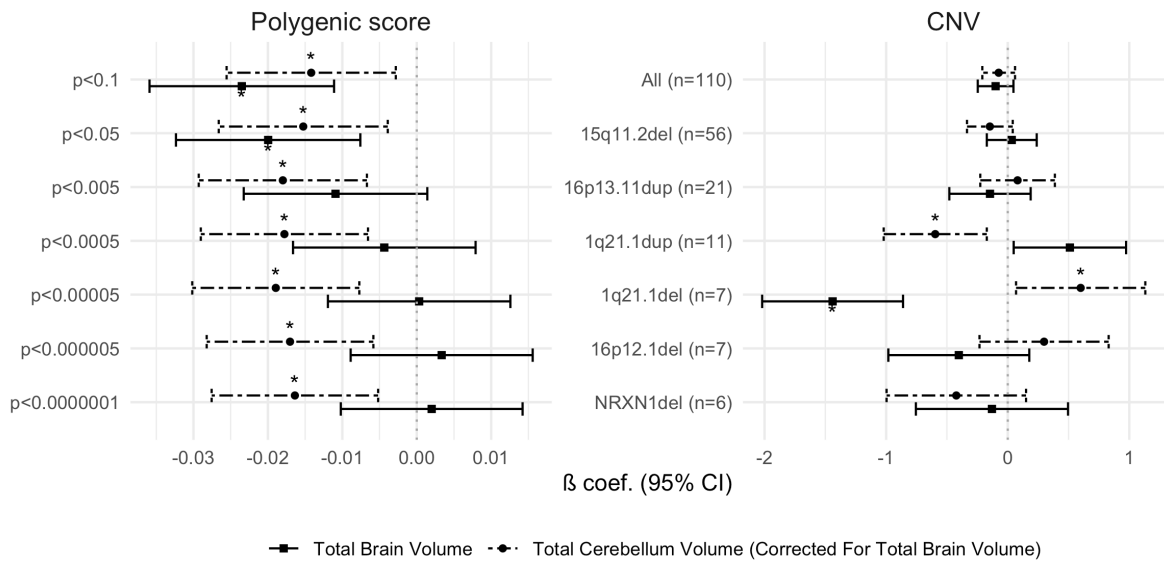


Figure 3.1: The effect on total cerebellar volume and total brain volume of increasing polygenic schizophrenia risk score at different SNP inclusion thresholds (p_T -values) and of carrier status for the different schizophrenia-associated copy number variants (CNVs). Results are from independent univariate regression models with correction for demographic, genetic and imaging covariates in the model (including the total brain volume covariate when analysing relative total cerebellar volume differences). Standardised beta-coefficients (β) & 95% confidence intervals (CI) are provided. *: signifies results with $p_{FDR} < 0.05$

3.4.4 Cerebellar lobules

Polygenic risk score

Polygenic scores across different SNP inclusion p -value thresholds (p_T) negatively predicted the volume of several cerebellar lobules, therefore, there appeared a global cerebellar effect (Figure 3.2A; Supplementary Table 3.3). In particular, lobules of Crus II, VIIb and IX hemispheres and VIIb vermal regions showed nominally significant ($p < 0.05$) associations across most p_T -values, with Crus II and VIIb vermal surviving correction for the number of tests performed across multiple SNP inclusion thresholds (Figure 3.2A).

CNV carrier-status

The 1q21.1duplication was associated with a reduction in volume across Crus II-VIIb hemispheres and vermis, IX and X vermal lobules, while the 1q21.1 deletion was associated with increased volume in VIIIa-IX hemispheres, and IX vermal regions which all survived our correction for multiple tests ($p_{FDR}<0.05$) (Figure 3.2B; Supplementary Table 3.4). While no cerebellar differences in carriers of other specific CNVs survived multiple comparison correction, we found the effects across schizophrenia-CNVs to show similar reductive patterns at Crus II lobules and positive at lobule X, with the vermis of Crus II being the only lobule to show significant reductions in cerebellar volume in carriers of any schizophrenia CNV compared to non-carriers ($\Delta R^2=6.0\times 10^{-4}$, $\beta=0.29[0.47,-0.12]$, $p=0.001$).

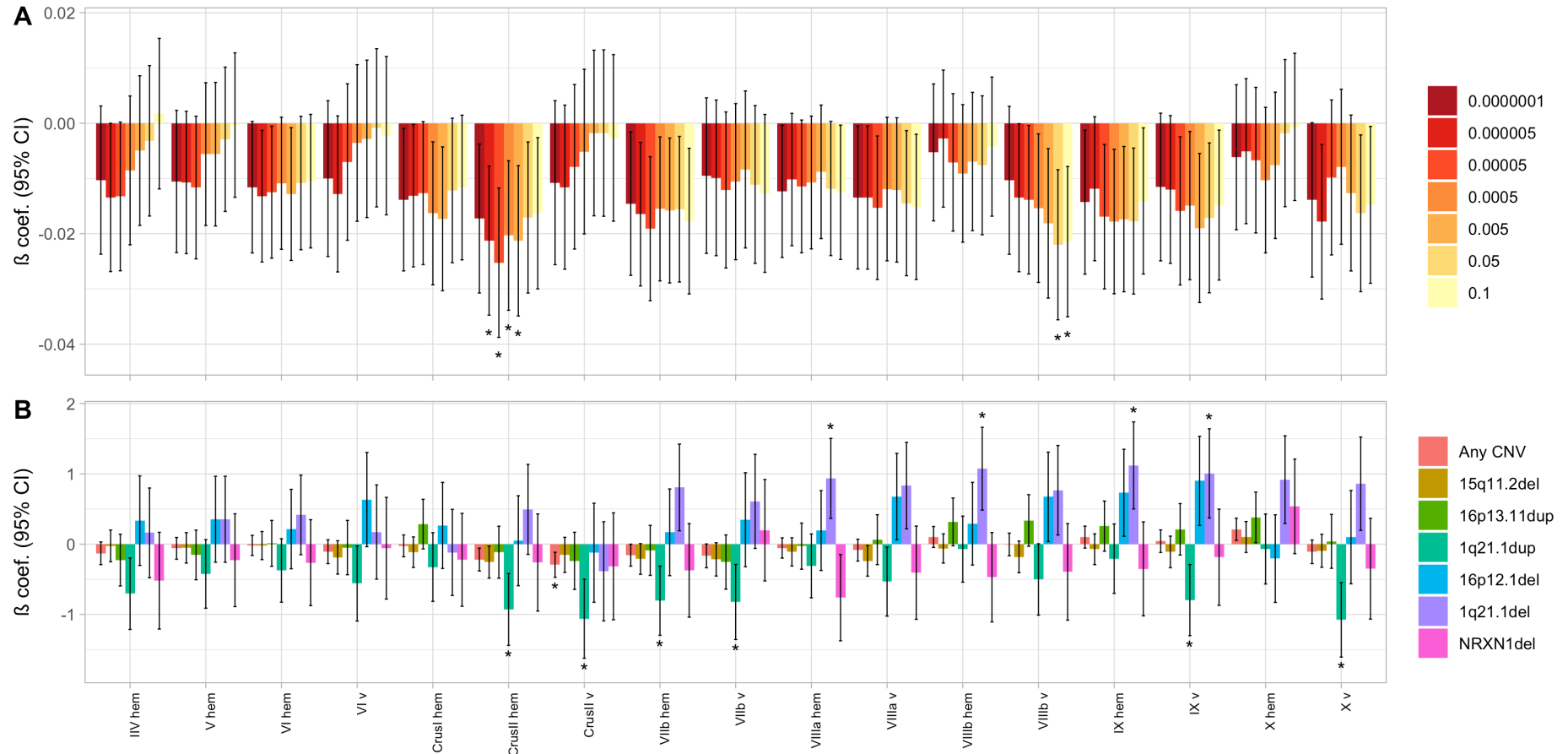


Figure 3.2: The effect on cerebellar lobules of increasing (A) polygenic schizophrenia risk score and of (B) carrier status for the different schizophrenia-associated copy number variants (SCZ-CNVs) ($n>5$) in a UK Biobank sample. Results are from independent univariate regression models, including correction for demographic, genetic and imaging covariates in the model (including total brain volume). Standardised beta coefficients (β) & 95% confidence intervals (CI) are provided. * signifies results with $p_{FDR}<0.05$

3.5 Discussion

In this study we aimed to examine the effect of both common (polygenic scores) and rare (copy number variant/CNV) risk alleles for schizophrenia on cerebellar volume in a large cohort of unaffected participants. We found polygenic scores to be negatively associated with total cerebellar volume and, while effects were relatively general across the cerebellum, we identify particular regions of greater effect. While we found evidence for some schizophrenia-associated CNVs to show global effects on the cerebellum, most showed differing effects across cerebellar sub-regions, though with particular sub-regions where effects appear to coalesce. Our findings add further evidence in support of this brain structure as a potential endophenotype for the disorder and provide relevant information on schizophrenia's neurophysiological underpinnings.

Polygenic scores were associated with reductions in cerebellar volume, over any effects on total brain volume. Previous reports of the effect of polygenic scores on brain morphometry in the literature have been inconsistent (Alnæs et al., 2019; X Caseras et al., 2015; Fonville et al., 2019; Lancaster et al., 2019; B. Liu et al., 2017; Neilson et al., 2017, 2019; Reus et al., 2017; Terwisscha Van Scheltinga et al., 2013; Van der Auwera et al., 2015; Voineskos et al., 2016; Westlye et al., 2019). Of these previous studies, only one study – using an earlier release of UK Biobank and investigating the effects of increase schizophrenia polygenic score on brain heterogeneity - also included mean hemispheric cerebellar volume difference assessments, reporting no significant effect (Alnæs et al., 2019). Our similar direction of effect (raw t-values are not reported, preventing comparisons of effect sizes) but significant findings could reflect our increased power through using updated UK Biobank and schizophrenia GWAS data releases (Pardiñas et al., 2018), and/or differences in analysis approach (e.g. our additional correction for imaging artefact related covariates in our models, or in the MRI processing tools used). One aspect of interest is that, compared to their use of a single polygenic score SNP-inclusion threshold derived from principal component analysis (Alnæs et al., 2019), we assessed effects across different thresholds. This showed cerebellar effects to be consistently reduced across all SNP inclusion thresholds (p_T -values), meaning that the negative effects on the cerebellum are still present even when limited to those fewer SNPs with greatest statistical association with schizophrenia.

Furthermore, beyond the effects on total cerebellar volume, our study also investigated sub-regional cerebellar effects. Similar to the reports in patients with schizophrenia (Moberget et al., 2018), we found a general negative effect across most lobules of the cerebellum, though

with a gradient of being less predictive in the anterior compared to the posterior lobe. Notably, Crus II lobules, in addition to other superior-posterior lobules (Crus I & VIIb), vermal VIIIb and IX lobules showed the greatest reductions and across multiple p_T -values. While functional boundaries within the cerebellum are highly individual and do not map well to anatomical lobule boundaries (King et al., 2019) (being also one of the reasons for our analysis of total cerebellar effects), these lobules are more commonly functionally associated with non-motor processes (Guell, Gabrieli, et al., 2018). They are part of the frontoparietal and default mode networks (Buckner et al., 2011), whose activity is known to be altered in individuals with schizophrenia at both cerebellar (Moberget et al., 2018; Houliang Wang et al., 2016) and cerebral cortical levels (W. Jia et al., 2019; Sharma et al., 2018; Huaning Wang et al., 2015). Furthermore, these cerebellar lobules are also major contributors to the cerebello-thalamo-cortical tract emanating from the cerebellum (Palesi et al., 2015), whose functional and structural alterations are noted in individuals with schizophrenia diagnosis and individuals at high-risk for schizophrenia (Bernard, Orr, & Mittal, 2017; H. Cao et al., 2018; Deng et al., 2019).

Unlike the consistent patterns found with polygenic scores, the anatomical effects of the different schizophrenia associated CNVs on both cerebellar and total brain morphometry were more heterogenous. This might be expected by their rarity (discussed below), as well as the inclusion of both duplications and deletions of the same genomic regions (which could have opposing effects on the brain) and the differing clinical presentation (prevalence of schizophrenia within carriers, and the proportion to others diagnoses) across CNVs (Kendall et al., 2019, 2017; George Kirov et al., 2014). We found that carriers of the 1q21.1 duplication had reduced relative total cerebellar volume and, while the number of carriers were still relatively small, our findings of the opposite effect with the deletion of this CNV gives us confidence of a dose-effect of this CNV on cerebellar structure. Interestingly, this was the reverse of this CNV's effects on total brain volume in our study or its effects on overall head size or cerebral cortical thickness, as reported elsewhere (Bernier et al., 2016; Xavier Caseras et al., 2021). The 1q21.1 CNV, therefore, looks to be of particular interest when looking for differing cerebral and cerebellar effects. Future studies should ascertain whether the pathophysiology of this difference for this CNV (and for all CNVs analysed) between cerebellar and non-cerebellar regions is driven by truly opposing effects or is driven by a negative effect in one and relative preservation in the other. Rodents studies provide some evidence for the former, where opposing directions of 1q21.1 microdeletion effect are seen for the cerebellum and total brain volumes, in accordance with our results (Reinwald et al., 2020). Additionally, clinical case-reports of this CNV have indicated the presence of Chiari malformations (extensions of the base

of the cerebellum into the spinal canal) (Bernier et al., 2016; Brunetti-Pierri et al., 2008; Busè et al., 2017) and further manual segmentation techniques in carriers of these CNVs in this UK Biobank cohort would be an exciting next avenue for study. Generally, therefore, more targeted analysis of cerebellar differences in this specific CNV, and with larger number of carriers analysed (a limitation of this study discussed below), would be a promising avenue for research.

While no other schizophrenia associated CNV in our cohort had global effects on total cerebellar or total brain volume, we were able to identify other significant sub-regional cerebellar effects, however, none reached our threshold for corrected significance for the number of tests performed. Carriers of 15q11.2 deletion were the most common schizophrenia associated CNV in this cohort, accounting for around half of all CNV incidences, and showed volumetric reductions of Crus II hemispheres, even if narrowly missing our corrected statistical threshold. The Crus II lobules, therefore, look of particular interest to pursue for future schizophrenia genetic studies, showing reductions across all polygenic score p_T -values, and in carriers of 1q21.1dup and 15q11.2del CNVs. Equally, the Crus II vermal regions were the only region to show a significant reduction when comparing carriers of any CNV to those without.

An important consideration when interpreting these results is the low variance in volume accounted for by the different genetic factors. This is a common issue across neuroimaging genetic studies in schizophrenia (Alnæs et al., 2019; X Caseras et al., 2015; Reus et al., 2017) and should not prevent the comparisons across regions of the brain, such as in highlighting the need not to ignore the cerebellum in schizophrenia studies and in identifying particular sub-regions of greatest effect. Furthermore, there are reasons to think that the explained variance of cerebellar structure can be improved. Firstly, no cerebellar-specific registration technique was used (Diedrichsen, 2006) compared, for example, to those used for previously mentioned subcortical analyses (Reus et al., 2017; Warland et al., 2020). Its use in future studies would improve signal-to-noise ratio (SNR) and, therefore, likely the variance explained in cerebellar volumes. Of note, to partially address variations in SNR, we added additional covariates to correct for any noise introduced due to participants' lower position in the scanner or increased head motion. Also, the use of gene-set polygenic scores (Pardiñas et al., 2018), including those particularly relevant to neurodevelopment (Spalthoff et al., 2019), might also greatly improve the prediction accuracy of brain morphometry as well as provide more biologically meaningful measures. Equal improvement might be made with the analysis of non-linear effects or interactions with early life environmental effects (to avoid extensive repetition, this is discussed extensively in *Chapter 6.3*).

In addition to the small amount of variance explained, there are other limitations of our study design which, while we have tried to address these, are also important to consider when interpreting the results presented here. Firstly, while the number of schizophrenia-associated CNV carriers in our cohort were some of the largest reported in biobank imaging cohort, the numbers for certain CNVs are still small. This can provide unstable estimates of association and might also account for the heterogeneity of CNV results. Additionally, while total cerebellar volume residuals following correction for our default covariates showed normal distributions and similar variances for both those with and without any schizophrenia-associated CNV (0.54 & 0.51, respectively), this might not be the case for each individual CNV, and regression weighted by variances (equivalent to Welch's t-test) would be advisable for future analyses. Furthermore, the low CNV carrier numbers meant we did not have the power to test for any CNV and polygenic score interactions, which we feel will be of interest considering the diminished polygenic scores reported in CNV carriers compared to non-CNV schizophrenia cases (an effect we did not corroborate in our smaller sample of carriers) and interaction with CNV effect size (Bergen et al., 2019). Instead, to control for any possible differences in polygenic scores in those carriers of CNVs, we re-ran our analysis including an additional covariate of the polygenic score which accounted for the most variance in total cerebellar volume. We found very similar results, indicating the CNV and polygenic score effects to be independent. With UK Biobank's plan to eventually scan 100,000 individuals, carrier numbers will increase in future releases and these interactional analyses will be more feasible.

Additionally, and of particular importance to polygenic score work, access to the raw genotypes is not currently available for the Psychiatric Genetics Consortia (PGC) samples within the latest schizophrenia GWAS, therefore, preventing the removal of potentially overlapping samples within the UK Biobank. We feel, however, that the effects of any overlap should be minimal in our study due to our exclusion of individuals with a history of psychiatric conditions, meaning potential overlap should be limited to only PGC control samples. We have already highlighted some UK Biobank limitations in *Chapter 2* and testing in different cohorts, especially prospective cohorts before onset of schizophrenia would be beneficial in establishing the effect of genetic risk on cerebellar development. While we corrected for population structure using genetic principal components, other techniques such as linkage disequilibrium score regression (LDSC) might allow better account for residual population structure (Bulik-Sullivan, Finucane, et al., 2015) and can estimate the genetic correlation between the cerebellum and schizophrenia across the genome (*Chapter 4*). This, and others mentioned, would add further weight to the importance of the cerebellum in regard to schizophrenia pathophysiology, as reported here.

In conclusion, increased common variant genetic risk of schizophrenia is associated with reduced cerebellar volume in individuals without overt neuropsychiatric diagnoses. Similarly, carriers of CNVs previously associated with increased schizophrenia liability show altered cerebellar morphology, though the effect depends on the CNV. We show that any effects of these two forms of genetic risk are independent of each other and identify particular sub-regions of the cerebellum most affected. We intend to build on this work by exploring regions of the genome showing pleiotropy for cerebellar and schizophrenia development

3.6 Supplementary Tables

Supplementary Table 3.1: The prevalence of schizophrenia-associated copy number variants (SCZ CNVs) present in our UK Biobank sub-sample

CNV	n	Prevalence (%) in the sample‡	Prevalence (%) among SCZ CNV carriers
All SCZ CNVs	110	0.70	100.00
15q11.2del	56	0.35	50.91
16p13.11dup	21	0.13	19.09
1q21.1dup	11	0.07	10.00
1q21.1del	7	0.04	6.36
16p12.1del	7	0.04	6.36
NRXN1del*	6	0.04	5.45
WBSdup**	1	0.01	0.91
16p11.2dup	1	0.01	0.91
3q29del	0	0.00	0.00
PWSdup***	0	0.00	0.00
15q13.3del	0	0.00	0.00
22q11.2del	0	0.00	0.00
16p11.2distal-del	0	0.00	0.00

Source: Schizophrenia-associated CNVs (Kendall et al., 2017; George Kirov et al., 2014; Marshall et al., 2017; Rees et al., 2016). Includes duplications (dup) and deletions (del). ‡: % of total 15,802 sample. *Neuroexin-1-alpha (2p16.3); **Williams-Beuren syndrome (7q11.23); ***Prader-Willi Syndrome (15q11-13)

Supplementary Table 3.2: The effect on total brain volume of increasing polygenic schizophrenia risk scores or carrier status for schizophrenia-associated copy number variants (SCZ CNVs)

Genetic Risk Factor		ΔR^2 †	β	95% Confidence intervals		p	p_{FDR} *
Polygenic scores $p_T <$	0.0000001	4.01E-06	0.002	-0.010	0.014	0.75	0.81
	0.000005	1.11E-05	0.003	-0.009	0.016	0.59	0.81
	0.00005	1.02E-07	0.000	-0.012	0.013	0.96	0.96
	0.0005	1.88E-05	-0.004	-0.017	0.008	0.49	0.76
	0.005	1.16E-04	-0.011	-0.023	0.001	0.08	0.23
	0.05	3.86E-04	-0.020	-0.032	-0.008	1.59E-03	7.40E-03
	0.1	5.34E-04	-0.024	-0.036	-0.011	2.03E-04	1.42E-03
SCZ CNVs	Any SCZ CNV	6.88E-05	-0.100	-0.247	0.047	0.18	0.37
	15q11.2del	3.85E-06	0.033	-0.172	0.238	0.75	0.81
	16p13.11dup	2.85E-05	-0.146	-0.481	0.188	0.39	0.69
	1q21.1dup	1.82E-04	0.511	0.049	0.973	0.03	0.11
	1q21.1del	9.23E-04	-1.440	-2.020	-0.861	1.11E-06	1.55E-05
	16p12.1del	7.21E-05	-0.402	-0.982	0.177	0.17	0.37
	NRXN1del	6.45E-06	-0.130	-0.756	0.496	0.68	0.81

Results are from independent univariate regression models including correction for demographic, genetic and imaging covariates in the model; with predictors of polygenic schizophrenia risk scores at different SNP inclusion thresholds (p_T -values) or binary presence of schizophrenia-associated CNV carrier status ($n > 5$). †: Variance of total brain volume uniquely explained by the genetic predictor. *: False Discovery Rate corrected p-values (p_{FDR}) for the number of genetic predictors tested ($FDR=0.05$) are provided

Supplementary Table 3.3: The effect on the 17 cerebellar lobules of increasing polygenic schizophrenia risk scores

Lobule volume	Genetic Risk Factor	$\Delta R^2 \ddagger$	β	95 % Confidence Interval		p	p_{FDR}^*
I-IV (hem)	pT<0.0000001	1.06E-04	-0.010	-0.024	0.003	0.13	0.25
I-IV (hem)	pT<0.000005	1.79E-04	-0.013	-0.027	0.000	0.05	0.15
I-IV (hem)	pT<0.00005	1.74E-04	-0.013	-0.027	0.000	0.05	0.16
I-IV (hem)	pT<0.0005	7.20E-05	-0.009	-0.022	0.005	0.21	0.35
I-IV (hem)	pT<0.005	2.40E-05	-0.005	-0.019	0.009	0.47	0.59
I-IV (hem)	pT<0.05	9.80E-06	-0.003	-0.017	0.010	0.65	0.74
I-IV (hem)	pT<0.1	2.94E-06	0.002	-0.012	0.015	0.80	0.86
V (hem)	pT<0.0000001	1.11E-04	-0.011	-0.023	0.002	0.11	0.23
V (hem)	pT<0.000005	1.14E-04	-0.011	-0.024	0.002	0.10	0.22
V (hem)	pT<0.00005	1.34E-04	-0.012	-0.025	0.001	0.08	0.18
V (hem)	pT<0.0005	3.09E-05	-0.006	-0.019	0.007	0.40	0.53
V (hem)	pT<0.005	3.07E-05	-0.006	-0.019	0.007	0.40	0.53
V (hem)	pT<0.05	8.15E-06	-0.003	-0.016	0.010	0.66	0.75
V (hem)	pT<0.1	1.04E-07	0.000	-0.013	0.013	0.96	0.96
VI (hem)	pT<0.0000001	1.34E-04	-0.012	-0.023	0.000	0.06	0.16
VI (hem)	pT<0.000005	1.74E-04	-0.013	-0.025	-0.001	0.03	0.13
VI (hem)	pT<0.00005	1.54E-04	-0.012	-0.024	-0.001	0.04	0.14
VI (hem)	pT<0.0005	1.17E-04	-0.011	-0.023	0.001	0.07	0.18
VI (hem)	pT<0.005	1.61E-04	-0.013	-0.025	-0.001	0.04	0.14
VI (hem)	pT<0.05	1.13E-04	-0.011	-0.023	0.001	0.08	0.18
VI (hem)	pT<0.1	1.06E-04	-0.010	-0.023	0.002	0.09	0.20
VI (vermal)	pT<0.0000001	1.00E-04	-0.010	-0.024	0.004	0.16	0.29
VI (vermal)	pT<0.000005	1.63E-04	-0.013	-0.027	0.001	0.08	0.18
VI (vermal)	pT<0.00005	4.88E-05	-0.007	-0.021	0.007	0.33	0.46
VI (vermal)	pT<0.0005	1.26E-05	-0.004	-0.018	0.011	0.62	0.72
VI (vermal)	pT<0.005	7.79E-06	-0.003	-0.017	0.011	0.70	0.78
VI (vermal)	pT<0.05	6.65E-07	-0.001	-0.015	0.013	0.91	0.93
VI (vermal)	pT<0.1	4.86E-06	-0.002	-0.017	0.012	0.76	0.83
Crus I (hem)	pT<0.0000001	1.91E-04	-0.014	-0.027	-0.001	0.04	0.13
Crus I (hem)	pT<0.000005	1.71E-04	-0.013	-0.026	0.000	0.05	0.15
Crus I (hem)	pT<0.00005	1.58E-04	-0.013	-0.026	0.000	0.06	0.16
Crus I (hem)	pT<0.0005	2.63E-04	-0.016	-0.029	-0.003	1.35E-02	0.08

Crus I (hem)	pT<0.005	2.93E-04	-0.017	-0.030	-0.004	9.19E-03	0.07
Crus I (hem)	pT<0.05	1.43E-04	-0.012	-0.025	0.001	0.07	0.18
Crus I (hem)	pT<0.1	1.31E-04	-0.012	-0.025	0.001	0.08	0.18
Crus II (hem)	pT<0.0000001	2.97E-04	-0.017	-0.031	-0.004	1.20E-02	0.08
Crus II (hem)	pT<0.000005	4.49E-04	-0.021	-0.035	-0.008	2.01E-03	0.03
Crus II (hem)	pT<0.00005	6.31E-04	-0.025	-0.039	-0.012	2.52E-04	0.02
Crus II (hem)	pT<0.0005	4.09E-04	-0.020	-0.034	-0.007	3.22E-03	0.05
Crus II (hem)	pT<0.005	4.43E-04	-0.021	-0.035	-0.008	2.16E-03	0.03
Crus II (hem)	pT<0.05	2.82E-04	-0.017	-0.031	-0.003	1.44E-02	0.09
Crus II (hem)	pT<0.1	2.57E-04	-0.016	-0.030	-0.003	0.02	0.10
Crus II (vermal)	pT<0.0000001	1.15E-04	-0.011	-0.026	0.004	0.16	0.28
Crus II (vermal)	pT<0.000005	1.33E-04	-0.012	-0.026	0.003	0.13	0.25
Crus II (vermal)	pT<0.00005	6.14E-05	-0.008	-0.023	0.007	0.30	0.43
Crus II (vermal)	pT<0.0005	2.61E-05	-0.005	-0.020	0.010	0.50	0.62
Crus II (vermal)	pT<0.005	3.05E-06	-0.002	-0.017	0.013	0.82	0.86
Crus II (vermal)	pT<0.05	3.05E-06	-0.002	-0.017	0.013	0.82	0.86
Crus II (vermal)	pT<0.1	6.80E-06	-0.003	-0.018	0.012	0.73	0.81
VIIb (hem)	pT<0.0000001	2.11E-04	-0.015	-0.028	-0.002	0.03	0.12
VIIb (hem)	pT<0.000005	2.70E-04	-0.016	-0.029	-0.003	1.30E-02	0.08
VIIb (hem)	pT<0.00005	3.61E-04	-0.019	-0.032	-0.006	4.07E-03	0.05
VIIb (hem)	pT<0.0005	2.38E-04	-0.016	-0.029	-0.002	0.02	0.10
VIIb (hem)	pT<0.005	2.44E-04	-0.016	-0.029	-0.003	0.02	0.10
VIIb (hem)	pT<0.05	2.34E-04	-0.016	-0.029	-0.002	0.02	0.10
VIIb (hem)	pT<0.1	3.03E-04	-0.018	-0.031	-0.005	8.47E-03	0.07
VIIb (vermal)	pT<0.0000001	8.96E-05	-0.009	-0.024	0.005	0.19	0.32
VIIb (vermal)	pT<0.000005	9.73E-05	-0.010	-0.024	0.004	0.17	0.30
VIIb (vermal)	pT<0.00005	1.44E-04	-0.012	-0.026	0.002	0.09	0.20
VIIb (vermal)	pT<0.0005	1.11E-04	-0.011	-0.025	0.004	0.14	0.27
VIIb (vermal)	pT<0.005	6.84E-05	-0.008	-0.023	0.006	0.25	0.39
VIIb (vermal)	pT<0.05	1.19E-04	-0.011	-0.025	0.003	0.13	0.25
VIIb (vermal)	pT<0.1	1.56E-04	-0.013	-0.027	0.002	0.08	0.18
VIIIa (hem)	pT<0.0000001	1.51E-04	-0.012	-0.024	0.000	0.04	0.14
VIIIa (hem)	pT<0.000005	1.03E-04	-0.010	-0.022	0.002	0.10	0.20
VIIIa (hem)	pT<0.00005	1.29E-04	-0.011	-0.023	0.001	0.06	0.17
VIIIa (hem)	pT<0.0005	1.14E-04	-0.011	-0.023	0.001	0.08	0.18
VIIIa (hem)	pT<0.005	7.56E-05	-0.009	-0.021	0.003	0.15	0.28
VIIIa (hem)	pT<0.05	1.35E-04	-0.012	-0.024	0.000	0.06	0.16

VIIIa (hem)	pT<0.1	1.51E-04	-0.013	-0.025	0.000	0.04	0.14
VIIIa (vermal)	pT<0.0000001	1.80E-04	-0.013	-0.026	-0.001	0.04	0.14
VIIIa (vermal)	pT<0.000005	1.80E-04	-0.013	-0.026	-0.001	0.04	0.14
VIIIa (vermal)	pT<0.00005	2.32E-04	-0.015	-0.028	-0.002	0.02	0.10
VIIIa (vermal)	pT<0.0005	1.40E-04	-0.012	-0.025	0.001	0.07	0.18
VIIIa (vermal)	pT<0.005	1.42E-04	-0.012	-0.025	0.001	0.07	0.18
VIIIa (vermal)	pT<0.05	2.03E-04	-0.014	-0.028	-0.001	0.03	0.13
VIIIa (vermal)	pT<0.1	2.21E-04	-0.015	-0.028	-0.002	0.02	0.11
VIIIb (hem)	pT<0.0000001	2.78E-05	-0.005	-0.018	0.007	0.40	0.53
VIIIb (hem)	pT<0.000005	7.71E-06	-0.003	-0.015	0.010	0.66	0.75
VIIIb (hem)	pT<0.00005	4.97E-05	-0.007	-0.020	0.005	0.26	0.40
VIIIb (hem)	pT<0.0005	8.16E-05	-0.009	-0.022	0.003	0.15	0.28
VIIIb (hem)	pT<0.005	4.69E-05	-0.007	-0.019	0.006	0.28	0.41
VIIIb (hem)	pT<0.05	5.61E-05	-0.008	-0.020	0.005	0.24	0.38
VIIIb (hem)	pT<0.1	1.73E-05	-0.004	-0.017	0.008	0.51	0.62
VIIIb (vermal)	pT<0.0000001	1.06E-04	-0.010	-0.024	0.003	0.13	0.25
VIIIb (vermal)	pT<0.000005	1.81E-04	-0.013	-0.027	0.000	0.05	0.15
VIIIb (vermal)	pT<0.00005	1.90E-04	-0.014	-0.027	0.000	0.04	0.14
VIIIb (vermal)	pT<0.0005	2.34E-04	-0.015	-0.029	-0.002	0.03	0.11
VIIIb (vermal)	pT<0.005	3.21E-04	-0.018	-0.032	-0.005	8.59E-03	0.07
VIIIb (vermal)	pT<0.05	4.68E-04	-0.022	-0.036	-0.008	1.51E-03	0.03
VIIIb (vermal)	pT<0.1	4.44E-04	-0.021	-0.035	-0.008	2.01E-03	0.03
IX (hem)	pT<0.0000001	2.04E-04	-0.014	-0.027	-0.001	0.03	0.13
IX (hem)	pT<0.000005	1.40E-04	-0.012	-0.025	0.001	0.07	0.18
IX (hem)	pT<0.00005	2.83E-04	-0.017	-0.030	-0.004	1.12E-02	0.08
IX (hem)	pT<0.0005	3.13E-04	-0.018	-0.031	-0.005	7.66E-03	0.07
IX (hem)	pT<0.005	2.95E-04	-0.017	-0.031	-0.004	9.68E-03	0.07
IX (hem)	pT<0.05	3.03E-04	-0.018	-0.031	-0.004	8.64E-03	0.07
IX (hem)	pT<0.1	1.91E-04	-0.014	-0.027	-0.001	0.04	0.14
IX (vermal)	pT<0.0000001	1.33E-04	-0.012	-0.025	0.002	0.09	0.20
IX (vermal)	pT<0.000005	1.43E-04	-0.012	-0.025	0.001	0.08	0.18
IX (vermal)	pT<0.00005	2.49E-04	-0.016	-0.029	-0.002	0.02	0.10
IX (vermal)	pT<0.0005	2.20E-04	-0.015	-0.028	-0.001	0.03	0.13
IX (vermal)	pT<0.005	3.52E-04	-0.019	-0.032	-0.005	5.86E-03	0.07
IX (vermal)	pT<0.05	2.84E-04	-0.017	-0.031	-0.004	1.33E-02	0.08
IX (vermal)	pT<0.1	2.12E-04	-0.015	-0.028	-0.001	0.03	0.13
X (hem)	pT<0.0000001	3.77E-05	-0.006	-0.019	0.007	0.36	0.49

X (hem)	pT<0.000005	2.54E-05	-0.005	-0.018	0.008	0.45	0.58
X (hem)	pT<0.00005	4.41E-05	-0.007	-0.020	0.006	0.32	0.45
X (hem)	pT<0.0005	1.05E-04	-0.010	-0.023	0.003	0.13	0.25
X (hem)	pT<0.005	5.67E-05	-0.008	-0.021	0.006	0.26	0.40
X (hem)	pT<0.05	3.10E-06	-0.002	-0.015	0.012	0.79	0.85
X (hem)	pT<0.1	4.26E-07	-0.001	-0.014	0.013	0.92	0.93
X (vernal)	pT<0.0000001	1.92E-04	-0.014	-0.028	0.000	0.05	0.15
X (vernal)	pT<0.000005	3.16E-04	-0.018	-0.032	-0.004	1.25E-02	0.08
X (vernal)	pT<0.00005	9.53E-05	-0.010	-0.024	0.004	0.17	0.30
X (vernal)	pT<0.0005	6.14E-05	-0.008	-0.022	0.006	0.27	0.41
X (vernal)	pT<0.005	1.56E-04	-0.013	-0.027	0.001	0.08	0.18
X (vernal)	pT<0.05	2.57E-04	-0.016	-0.030	-0.002	0.02	0.11
X (vernal)	pT<0.1	2.11E-04	-0.015	-0.029	-0.001	0.04	0.14

*Results are from independent univariate regression models including correction for demographic, genetic and imaging covariates (including total brain volume) in the model; with predictors of polygenic schizophrenia risk scores at different SNP inclusion thresholds (p_T -values). ‡: Variance of total brain volume uniquely explained by the genetic predictor. *: False Discovery Rate corrected p -values (p_{FDR}) for the number of genetic predictors tested ($FDR=0.05$) are provided*

Supplementary Table 3.4: The effect on the 17 cerebellar lobules of carrier status for schizophrenia-associated copy number variants (SCZ CNVs)

Lobule volume	Genetic Risk	$\Delta R^2 \ddagger$	β	95 % Confidence		p	p_{FDR}^*
	Factor			Interval			
I-IV (hem)	Any SCZ CNV	1.16E-04	-0.129	-0.291	0.032	0.12	0.24
I-IV (hem)	15q11.2del	2.13E-06	-0.025	-0.250	0.201	0.83	0.87
I-IV (hem)	16p13.11dup	6.86E-05	-0.227	-0.595	0.141	0.23	0.37
I-IV (hem)	1q21.1dup	3.46E-04	-0.704	-1.213	-0.196	6.63E-03	0.07
I-IV (hem)	1q21.1del	1.16E-05	0.161	-0.476	0.799	0.62	0.72
I-IV (hem)	16p12.1del	4.97E-05	0.334	-0.303	0.971	0.30	0.43
I-IV (hem)	NRXN1del	1.03E-04	-0.519	-1.207	0.168	0.14	0.26
V (hem)	Any SCZ CNV	2.45E-05	-0.060	-0.214	0.095	0.45	0.58
V (hem)	15q11.2del	9.76E-06	-0.053	-0.269	0.164	0.63	0.73
V (hem)	16p13.11dup	3.12E-05	-0.153	-0.506	0.200	0.40	0.53
V (hem)	1q21.1dup	1.25E-04	-0.423	-0.911	0.065	0.09	0.20
V (hem)	1q21.1del	5.57E-05	0.354	-0.257	0.966	0.26	0.40
V (hem)	16p12.1del	5.58E-05	0.354	-0.257	0.965	0.26	0.40
V (hem)	NRXN1del	1.98E-05	-0.228	-0.888	0.432	0.50	0.62
VI (hem)	Any SCZ CNV	2.11E-06	-0.017	-0.161	0.126	0.81	0.86
VI (hem)	15q11.2del	1.39E-06	-0.020	-0.220	0.180	0.85	0.88
VI (hem)	16p13.11dup	1.88E-07	0.012	-0.315	0.338	0.94	0.95
VI (hem)	1q21.1dup	9.73E-05	-0.374	-0.825	0.078	0.10	0.22
VI (hem)	1q21.1del	7.68E-05	0.416	-0.150	0.982	0.15	0.28
VI (hem)	16p12.1del	2.05E-05	0.215	-0.350	0.780	0.46	0.58
VI (hem)	NRXN1del	2.63E-05	-0.263	-0.873	0.348	0.40	0.53
VI (vermal)	Any SCZ CNV	7.93E-05	-0.107	-0.277	0.062	0.22	0.35
VI (vermal)	15q11.2del	1.25E-04	-0.188	-0.425	0.049	0.12	0.24
VI (vermal)	16p13.11dup	3.13E-06	-0.048	-0.435	0.338	0.81	0.86
VI (vermal)	1q21.1dup	2.18E-04	-0.558	-1.093	-0.024	0.04	0.14
VI (vermal)	1q21.1del	1.33E-05	0.173	-0.498	0.843	0.61	0.72
VI (vermal)	16p12.1del	1.79E-04	0.634	-0.036	1.304	0.06	0.17
VI (vermal)	NRXN1del	1.27E-06	-0.058	-0.781	0.666	0.88	0.90
Crus I (hem)	Any C SCZ NV	4.02E-06	-0.024	-0.179	0.131	0.76	0.83
Crus I (hem)	15q11.2del	4.58E-05	-0.114	-0.331	0.103	0.30	0.43
Crus I (hem)	16p13.11dup	1.09E-04	0.285	-0.068	0.639	0.11	0.23
Crus I (hem)	1q21.1dup	7.40E-05	-0.325	-0.814	0.163	0.19	0.33

Crus I (hem)	1q21.1del	6.07E-06	-0.117	-0.729	0.496	0.71	0.79
Crus I (hem)	16p12.1del	3.16E-05	0.266	-0.345	0.878	0.39	0.53
Crus I (hem)	NRXN1del	1.89E-05	-0.223	-0.883	0.438	0.51	0.62
Crus II (hem)	Any SCZ CNV	3.30E-04	-0.219	-0.381	-0.057	8.10E-03	0.07
Crus II (hem)	15q11.2del	2.31E-04	-0.256	-0.482	-0.029	0.03	0.12
Crus II (hem)	16p13.11dup	1.73E-05	-0.114	-0.483	0.256	0.55	0.66
Crus II (hem)	1q21.1dup	6.02E-04	-0.928	-1.439	-0.418	3.66E-04	0.02
Crus II (hem)	1q21.1del	1.09E-04	0.494	-0.146	1.135	0.13	0.25
Crus II (hem)	16p12.1del	1.06E-06	0.049	-0.591	0.688	0.88	0.90
Crus II (hem)	NRXN1del	2.60E-05	-0.261	-0.952	0.430	0.46	0.58
Crus II (vermal)	Any SCZ CNV	5.94E-04	-0.293	-0.472	-0.115	1.26E-03	0.03
Crus II (vermal)	15q11.2del	8.14E-05	-0.152	-0.401	0.098	0.23	0.38
Crus II (vermal)	16p13.11dup	7.52E-05	-0.237	-0.644	0.169	0.25	0.40
Crus II (vermal)	1q21.1dup	7.85E-04	-1.060	-1.622	-0.498	2.20E-04	0.02
Crus II (vermal)	1q21.1del	6.62E-05	-0.386	-1.090	0.319	0.28	0.42
Crus II (vermal)	16p12.1del	6.65E-06	-0.122	-0.826	0.582	0.73	0.81
Crus II (vermal)	NRXN1del	3.79E-05	-0.315	-1.075	0.446	0.42	0.54
VIIb (hem)	Any SCZ CNV	1.69E-04	-0.156	-0.313	0.000	0.05	0.15
VIIb (hem)	15q11.2del	1.57E-04	-0.210	-0.428	0.008	0.06	0.16
VIIb (hem)	16p13.11dup	1.03E-05	-0.088	-0.444	0.268	0.63	0.72
VIIb (hem)	1q21.1dup	4.51E-04	-0.804	-1.296	-0.311	1.37E-03	0.03
VIIb (hem)	1q21.1del	2.89E-04	0.807	0.190	1.423	1.04E-02	0.08
VIIb (hem)	16p12.1del	1.26E-05	0.168	-0.448	0.785	0.59	0.70
VIIb (hem)	NRXN1del	5.29E-05	-0.372	-1.038	0.293	0.27	0.41
VIIb (vermal)	Any SCZ CNV	1.90E-04	-0.166	-0.335	0.003	0.05	0.16
VIIb (vermal)	15q11.2del	1.67E-04	-0.217	-0.454	0.020	0.07	0.18
VIIb (vermal)	16p13.11dup	8.60E-05	-0.254	-0.640	0.132	0.20	0.33
VIIb (vermal)	1q21.1dup	4.72E-04	-0.822	-1.356	-0.289	2.51E-03	0.04
VIIb (vermal)	1q21.1del	1.64E-04	0.608	-0.061	1.277	0.07	0.18
VIIb (vermal)	16p12.1del	5.38E-05	0.348	-0.321	1.016	0.31	0.44
VIIb (vermal)	NRXN1del	1.51E-05	0.199	-0.523	0.921	0.59	0.70
VIIIa (hem)	Any SCZ CNV	2.02E-05	-0.054	-0.198	0.090	0.46	0.58
VIIIa (hem)	15q11.2del	4.27E-05	-0.110	-0.311	0.091	0.28	0.42
VIIIa (hem)	16p13.11dup	1.03E-06	-0.028	-0.356	0.300	0.87	0.89
VIIIa (hem)	1q21.1dup	6.68E-05	-0.309	-0.763	0.144	0.18	0.31
VIIIa (hem)	1q21.1del	3.89E-04	0.936	0.367	1.504	1.26E-03	0.03
VIIIa (hem)	16p12.1del	1.68E-05	0.194	-0.374	0.762	0.50	0.62

VIIIa (hem)	NRXN1del	2.21E-04	-0.761	-1.375	-0.147	0.02	0.09
VIIIa (vermal)	Any SCZ CNV	4.93E-05	-0.084	-0.240	0.071	0.29	0.42
VIIIa (vermal)	15q11.2del	2.00E-04	-0.237	-0.455	-0.020	0.03	0.13
VIIIa (vermal)	16p13.11dup	5.45E-06	0.064	-0.291	0.419	0.72	0.81
VIIIa (vermal)	1q21.1dup	1.98E-04	-0.532	-1.023	-0.042	0.03	0.13
VIIIa (vermal)	1q21.1del	3.08E-04	0.833	0.218	1.448	7.92E-03	0.07
VIIIa (vermal)	16p12.1del	2.04E-04	0.677	0.063	1.292	0.03	0.13
VIIIa (vermal)	NRXN1del	6.29E-05	-0.406	-1.069	0.258	0.23	0.37
VIIIb (hem)	Any SCZ CNV	7.23E-05	0.102	-0.047	0.251	0.18	0.31
VIIIb (hem)	15q11.2del	1.32E-05	-0.061	-0.269	0.147	0.57	0.68
VIIIb (hem)	16p13.11dup	1.34E-04	0.317	-0.023	0.657	0.07	0.18
VIIIb (hem)	1q21.1dup	3.48E-06	-0.071	-0.540	0.399	0.77	0.83
VIIIb (hem)	1q21.1del	5.13E-04	1.074	0.485	1.662	3.52E-04	0.02
VIIIb (hem)	16p12.1del	3.78E-05	0.291	-0.297	0.880	0.33	0.46
VIIIb (hem)	NRXN1del	8.45E-05	-0.470	-1.106	0.165	0.15	0.27
VIIIb (vermal)	Any SCZ CNV	9.24E-08	-0.004	-0.165	0.157	0.96	0.96
VIIIb (vermal)	15q11.2del	1.16E-04	-0.181	-0.406	0.044	0.11	0.24
VIIIb (vermal)	16p13.11dup	1.52E-04	0.337	-0.030	0.704	0.07	0.18
VIIIb (vermal)	1q21.1dup	1.76E-04	-0.502	-1.009	0.006	0.05	0.15
VIIIb (vermal)	1q21.1del	2.62E-04	0.767	0.131	1.404	0.02	0.10
VIIIb (vermal)	16p12.1del	2.02E-04	0.673	0.038	1.309	0.04	0.14
VIIIb (vermal)	NRXN1del	5.93E-05	-0.394	-1.081	0.292	0.26	0.40
IX (hem)	Any SCZ CNV	6.93E-05	0.100	-0.056	0.257	0.21	0.35
IX (hem)	15q11.2del	1.84E-05	-0.072	-0.291	0.147	0.52	0.63
IX (hem)	16p13.11dup	8.79E-05	0.257	-0.100	0.614	0.16	0.28
IX (hem)	1q21.1dup	2.98E-05	-0.206	-0.700	0.287	0.41	0.54
IX (hem)	1q21.1del	5.57E-04	1.120	0.501	1.739	3.92E-04	0.02
IX (hem)	16p12.1del	2.38E-04	0.731	0.113	1.350	2.05E-02	0.10
IX (hem)	NRXN1del	4.72E-05	-0.352	-1.020	0.316	0.30	0.43
IX (vermal)	Any SCZ CNV	1.25E-05	0.043	-0.118	0.203	0.60	0.71
IX (vermal)	15q11.2del	4.32E-05	-0.110	-0.335	0.114	0.33	0.46
IX (vermal)	16p13.11dup	5.97E-05	0.211	-0.155	0.577	0.26	0.40
IX (vermal)	1q21.1dup	4.43E-04	-0.795	-1.301	-0.290	2.05E-03	0.03
IX (vermal)	1q21.1del	4.51E-04	1.007	0.373	1.641	1.86E-03	0.03
IX (vermal)	16p12.1del	3.62E-04	0.901	0.267	1.535	5.34E-03	0.06
IX (vermal)	NRXN1del	1.32E-05	-0.186	-0.870	0.498	0.59	0.70
X (hem)	Any SCZ CNV	3.10E-04	0.212	0.054	0.369	8.45E-03	0.07

X (hem)	15q11.2del	3.69E-05	0.102	-0.118	0.322	0.36	0.49
X (hem)	16p13.11dup	1.93E-04	0.381	0.021	0.740	0.04	0.14
X (hem)	1q21.1dup	3.34E-06	-0.069	-0.566	0.428	0.79	0.85
X (hem)	1q21.1del	3.74E-04	0.918	0.294	1.541	3.91E-03	0.05
X (hem)	16p12.1del	1.87E-05	-0.205	-0.828	0.418	0.52	0.63
X (hem)	NRXN1del	1.10E-04	0.537	-0.135	1.210	0.12	0.24
X (vernal)	Any SCZ CNV	8.13E-05	-0.109	-0.277	0.059	0.21	0.34
X (vernal)	15q11.2del	3.11E-05	-0.094	-0.329	0.141	0.43	0.56
X (vernal)	16p13.11dup	2.17E-06	0.040	-0.343	0.423	0.84	0.87
X (vernal)	1q21.1dup	8.09E-04	-1.076	-1.606	-0.546	6.84E-05	0.02
X (vernal)	1q21.1del	3.29E-04	0.860	0.196	1.524	1.11E-02	0.08
X (vernal)	16p12.1del	4.45E-06	0.100	-0.564	0.764	0.77	0.83
X (vernal)	NRXN1del	4.66E-05	-0.349	-1.066	0.367	0.34	0.47

*Results are from independent univariate regression models including correction for demographic, genetic and imaging covariates (including total brain volume) in the model; with predictors of binary presence of schizophrenia-associated CNV carrier status ($n>5$). ‡: Variance of total brain volume uniquely explained by the genetic predictor. *: False Discovery Rate corrected p -values (p_{FDR}) for the number of genetic predictors tested ($FDR=0.05$) are provided*

4 Investigating the shared genetic architecture between the cerebellum, schizophrenia and other psychiatric traits

4.1 Abstract

The cerebellum has been reported to be reduced in volume in individuals with a diagnosis of schizophrenia, as well as in both unaffected close family-members and, as we report in the preceding chapter, in unaffected and unrelated individuals at elevated genetic risk for schizophrenia. This suggests a level of overlap between the genetic architecture of schizophrenia liability and the cerebellar volume, though without any indication as to the quantifiable extent or regionality of this pleiotropy. In this study, we conducted a Genome Wide Association Study (GWAS) in 33,265 UK-Biobank participants of European-similar ancestries to identify single nucleotide polymorphisms (SNPs) associated with adult total cerebellar volume. We functionally annotated and mapped these SNPs to associated genes and assessed the overlap of genetic architecture with schizophrenia. We hypothesised a negative genetic correlation between common allele variants for schizophrenia liability and cerebellar volume. Results show cerebellar volume to be moderately heritable ($h^2_{\text{SNP}}=50.6\%$). We identified 33 independent genome-wide regions associated with total cerebellar volume, including 21 unique candidate genes which look to be of particular interest for follow-up functional studies of their role in altering cerebellar volume. We found no significant evidence for a negative genetic correlation between the two traits, and with little indication that genome-wide significant SNPs for each trait were more commonly found in the opposing direction for the other trait. In conclusion, we did not find any evidence for a significantly enriched overlap of common genetic variants affecting both total cerebellar volume and schizophrenia liability in consistent directions of effect.

4.2 Introduction

In addition to those with overt schizophrenia diagnosis (Moberget et al., 2018), cerebellar volume reductions have also been reported in their non-affected first degree relatives (Bolbecker et al., 2014; de Zwarte, Brouwer, Agartz, et al., 2019; Guo et al., 2015; Van Leeuwen et al., 2018). In *Chapter 3*, we showed that an increased polygenic score of common genetic variants for schizophrenia is associated with reduced cerebellar volume in a large, unaffected non-familial participant sample of individuals from the UK Biobank (Collins, 2012) cohort. While all the above suggests a shared genetic architecture between variants important for schizophrenia liability and for cerebellar volume, further work is required to better understand the genomic location and extent of pleiotropy between these traits.

To achieve this, the genetic variants important for cerebellar morphology need to be established. Twin studies have estimated cerebellar volume to have moderate-to-high heritability (33.6% to 86.4%) (Blokland et al., 2012) in line with other structural brain phenotypes. Recent genome-wide association studies (GWAS) for cerebral anatomical phenotypes have revealed their highly polygenic nature with a substantial contribution to heritability from variation in common alleles (e.g. thalamus SNP-based heritability $h^2_{\text{SNP}} = 47\%$, cortical surface area $h^2_{\text{SNP}} = 34\%$) (Grasby et al., 2020; Hibar et al., 2017; Satizabal et al., 2019). To our knowledge, only two previous GWAS studies have included any cerebellar volumetric measures amongst the multiple brain-wide phenotypes analysed within each study (Elliott et al., 2018; Zhao et al., 2019). Neither study, however, included a total cerebellar volume measure, despite the homogenous cerebellar gene expression reported (Hawrylycz et al., 2015). Furthermore, being brain-wide analyses, the focus of neither study was on systematically analysing the overlap with a specific disorder/trait of interest. One of these studies, however, did include whole-genome genetic correlation analyses between regional cerebellar lobes/lobules and schizophrenia (Elliott et al., 2018), finding no association (though this analysis is only assumed to have occurred since cerebellar measures would have passed their threshold for inclusion in genetic correlation analysis, but no results are provided for values of effect size, direction or strength of association, suggesting that they did not reach their statistical cut-off for reporting of said statistics). With scarce research so far into the genetic overlap between the cerebellum and schizophrenia, this remains an area of interest. Moreover, the UK Biobank sample size has quadrupled since the aforementioned study as well as an updated, larger, GWAS for schizophrenia having been released (Pardiñas et al., 2018), which both result in increased power to detect any such relationship.

The aims of this study were twofold. Firstly, we aimed to run a GWAS of total cerebellar volume to identify its common allele influences, and map these to related genes. Secondly, we wished to investigate the overlap of common allele architecture between the cerebellum and schizophrenia liability across the whole genome, for identified genome-wide significant associated SNPs and for overlap at the associated gene level. In keeping with previous findings in those with overt diagnoses (Moberget et al., 2018), we hypothesised that a negative association would exist, with variants increasing schizophrenia liability associated with reductions in total cerebellar volume.

4.3 Methods

This study used Magnetic Resonance Imaging (MRI) data from the ongoing UK-Biobank project (Collins, 2012; Littlejohns et al., 2020). Based on successive downloads of UK Biobank data, we first analysed approximately 20,000 individuals' data (the data which has been used in previous chapter analyses) and then, with a subsequent download of a further 20,000 individuals, analysed these separately as a second, independent sample (referred to as phase 1 and 2, respectively). We then compared results across phases and combined the results in a meta-analysis, which we used for all subsequent functional annotation and mapping. Ethics for UK-Biobank was granted by the North West Multi-Centre Ethics Committee, with our study being approved by the UK-Biobank Access Committee (*Project #17044*).

4.3.1 Processing genetic data

A full description of UK-Biobank's data collection, quality control and imputation process can be found elsewhere (<http://www.ukbiobank.ac.uk/scientists-3/genetic-data/>). Locally, we further harmonised and applied additional quality control to the raw genotypes from the UK-Biobank imaging as described previously (Underwood et al., 2019) (*Chapter 3*, including justification for these measures chosen) (<https://github.com/ricanney/stata> *summaryqc* function) (Dr Richard Anney). Briefly, all markers were harmonised to genome build hg19 and common nomenclature based on the Haplotype Reference Consortium r1.1. Markers across the whole 500k sample were also limited to those of high imputation quality (INFO>0.8) and based on minor allele frequency (MAF >0.1%). Within the imaging subsample itself, we further excluded markers based on individual marker missingness (>2%), low minor allele count (<5), deviations from Hardy-Weinberg equilibrium ($p < 1 \times 10^{-10}$) and the deviations from the expected Minor Allele Frequency (MAF; >4 standard deviations (SD) from British/Irish (GBR) MAF reported in 1000G

phase 3). Individuals were removed with excess overall marker missingness rate (>2%) or heterozygosity (>4 × SD from sample mean), those with genetic ancestry not similar to British/Irish genetic ancestry (defined as >4 × SD from 1000G phase 3 GBR sub-sample mean based on first 3 principal components (PCs); Supplementary Figure 4.1) and those with close relatives in the cohort (estimated kinship coefficient > 0.0442 i.e. 3rd degree relatives). Of note, for phase 2 this also included removing individuals with close relatives in phase 1 (kinship coefficient > 0.0442). Of the initial 21,390 and 26,541 individuals with genetic and MRI data for phase 1 and phase 2, 19,170 and 22,808 passed our genetic quality control, respectively. From the initial download of over 90M genetic markers, 7,003,604 and 6,935,580 markers remained for phase 1 and phase 2 following quality control, respectively.

4.3.2 Total cerebellar volume measure generation

We used R (v3.6.0) (<https://www.R-project.org/>) for the generation of our phenotype and all statistical analysis. This study utilises the image derived phenotypes (IDPs) generated from structural T1-weighted MRI scans whose generation and quality control have been described previously (Alfaro-Almagro et al., 2018). As has been described in previous chapters, we generated a summated total cerebellar grey-matter volume measure from all the 28 cerebellar lobule IDPs (Diedrichsen et al., 2009), with the exception of Crus I vermis which was excluded due to its very small size which can cause unreliable results, following previous research (Pezoulas et al., 2017). The distribution of total cerebellar volume values in each phase were normal. We removed individuals missing any of our key covariates (listed below) or with outlier total cerebellar or total brain grey- and white-matter volume (UK-Biobank data-field code: [25010](#)). Outliers were defined as values greater than five times the median absolute deviation from overall median.

To correct for possible imaging and non-brain imaging related variables which might confound our results, in a univariate multiple linear regression model we regressed total cerebellar volume on total brain volume, age (UK-Biobank data-field code: [21003-2.0](#)), age² (1st and 2nd degree orthogonal polynomials), sex ([31](#)), age²*sex, mean resting-state functional MRI head motion averaged across space and time points ([25741-2.0](#)) (log transformed; [21001-2.0](#)), imaging centre attended ([54-2.0](#)), date attended imaging centre ([53-2.0](#)), X-, Y- and Z-head position in the scanner ([25756](#), [25757](#), [25758](#)) and starting table-Z position ([25759](#)). The cerebellar residuals derived from this for each phase showed a normal distribution. We z-scored (i.e. scaled) the residuals obtained from this model, with values now representing differences in standard deviations from the mean.

4.3.3 Genome-wide association study (GWAS)

Following generation of phenotype measures as outline above, we ran two separate GWASs for phase 1 (including 17,818 participant; age mean[*min,max*] = 63[45,80]yrs, 53% female) and for phase 2 (including 15,447 participants; age mean[*min,max*] = 65[48,81]yrs, 53% female) (Supplementary Table 4.1). Note that the larger drop in phase 2 was explained by the actual availability of MRI data at time of downloading (where subjects had undergone MRI but the data had not yet been processed), rather than differences in quality control filtering between both phases. Subsequent to our initial genetic quality control, since we had then further excluded individuals without imaging data, we repeated our removal of any markers with minor allele counts < 5 within each phase, leaving 6,402,132 and 6,303,745 markers respectively. GWAS analyses were run on PLINK (v1.9) (C. C. Chang et al., 2015), inputting our cerebellar residuals and covariates of the first 10 genetic PCs to correct for potential effects of remaining population structure (A1 allele = effect allele). The model assumed linear additive genetic effects. Manhattan plots were created in to display the distribution of SNP cerebellar associations ($-\log_{10}$ p-values) across the genome. Equally, we created quantile-quantile (QQ) plots to compare SNP p-values to their empirical distributions (both $-\log_{10}$ p-values). QQ plots can indicate confounding (usually residual population structure) when the observed p-values show a consistent leftward deviation from the diagonal line even amongst the higher observed p-values. Without confounding, instead observed SNP results are expected to follow the diagonal, until a sharp increase at the lowest p-values, indicative of true associations.

4.3.4 SNP-based heritability (h^2_{SNP})

For each phase we estimated the lower-bound of narrow-sense (additive) single nucleotide polymorphism (SNP)-based heritability (h^2_{SNP}) using GCTA-GREML (Genome-wide complex trait analysis – genome-based restricted maximum likelihood) (64bit; v1.26.0) (Sang Hong Lee, Wray, Goddard, & Visscher, 2011) on the raw genotypes (using default settings unless otherwise stated). This uses the REML approach to estimate the proportion of variance of total cerebellar volume measures explained by all common variants together (rather than independent tests), derived via genetic relationship matrices (GRM) between individuals. As with the GWAS analysis, the first 10 genetic principal components were added to help correct for population structure. While SNP heritability estimates are more accurate using the raw genotypes of GCTA-GREML approach, we also provide linkage disequilibrium score (LDSC) (Bulik-Sullivan, Loh, et al., 2015) regression estimates of SNP-based heritability calculated on the summary statistics, so as to aid with comparisons to previous literature. LDSC calculates h^2_{SNP} differently, by regressing SNP's

trait association (χ^2) on their linkage disequilibrium (LD) scores (sum of LD r^2 with all other SNPs). It also provides an estimate and correction of inflation of test statistics arising through confounding bias such as residual population structure and sample overlap (intercept should be close to 1 and with a low ratio of $(\text{intercept}-1)/(\text{mean}(\chi^2)-1)$). For LDSC, we utilised the default settings and restricted SNPs to those within the high imputation quality HapMap3 reference panel (Altshuler et al., 2010), with minor allele frequency (MAF) $>1\%$, and using LD scores and weights based on the 1000G European reference cohort (Altshuler et al., 2012).

4.3.5 Identification of independent regions

Genome-wide association signals in each region were refined to identify independently associated signals (from now on termed “index SNPs”) using the COJO (multi-SNP-based conditional & joint association analysis using GWAS summary data) function in GCTA (64bit; v1.93.2beta) (J. Yang et al., 2012; J. Yang, Lee, Goddard, & Visscher, 2011). COJO applies a conditional stepwise analysis of SNPs within a locus, identifying variants (other than the index SNP) which have a conditionally independent association with cerebellar volume. Linkage disequilibrium (LD) data for this analysis was derived from genotypes of the respective UK-Biobank phases, with analysis of correlation structure limited to 10Mb blocks around genome-wide signals. All other settings were the default settings. We provide extended LD-ranges (start and end SNPs) for each COJO index SNP of those SNPs in modest LD ($r^2 > 0.2$) and with a nominal association ($p < 0.05$) with cerebellar volume.

4.3.6 Comparison of phase data

COJO identified index SNPs in each phase were assessed for replication in the other phase using with SNP result replication defined as those passing Bonferroni correction for the number of tests performed ($p < 0.05 / \text{the number of index SNPs identified in each phase}$).

Genetic correlation (r_g) analysis was performed using the Linkage disequilibrium score (LDSC) software (v1.0.1) (Bulik-Sullivan, Finucane, et al., 2015). Similar to its use in heritability estimates, LDSC regress the SNPs’ association measures (now the products of the z-scores between the two traits) on the SNPs’ LD scores. Again, all summary statistics were limited to a common subset of HapMap3 SNPs prior to analysis and MAF $>1\%$. Of note, LDSC regression is not a bounded estimator, therefore, upper bounds of genetic correlation can exceed 1.0 due to sampling variation, though – since none of our results greatly exceeded this level and standard errors were low – we capped them at 1.0 for display.

Finally, we used PLINK (v1.9) (C. C. Chang et al., 2015) to generate polygenic scores for all participants in each phase using, as a guide, a previously published approach (Choi, Mak, & O'Reilly, 2020). Polygenic scores were generated for each phase (SNP clumping $r^2 > 0.1$ across 250kb windows), filtering SNPs to just those present in both phases, and then producing 5 different scores per individual by filtering SNPs at 5 different p-value thresholds: $p_T < 0.1, 0.05, 0.01, 0.005, 0.001$. Multiple linear regression was used to ascertain the unique variance of total cerebellar volume explained by each polygenic score (ΔR^2), accounting for the same covariates as used to generate the GWAS (see above section) and calculated by subtracting the R^2 of the model without covariates from the R^2 of model with covariates. Bonferroni correction was applied for the number of tests performed ($p < 0.005 \{0.05/(5 \times 2)\}$)

4.3.7 Meta-analysis

We meta-analysed the two phases of GWAS using METAL (2011-03-25 release) (Willer, Li, & Abecasis, 2010), weighting the effect size estimates by the inverse of the corresponding standard errors. Again, we retained only the 6,193,476 markers present in both phases. Identification of independent SNPs and calculations of SNP-based heritability were performed using the same methods as outlined above. For the GCTA-GREML analysis of h^2_{SNP} we created a merged phase dataset using PLINK (*--bmerge* function), so as to obtain the raw genotypes for the whole sample.

4.3.8 Annotation of GWAS Loci

We first performed positional mapping of transcripts (ftp://ftp.ensembl.org/pub/grch37/current/gtf/homo_sapiens/Homo_sapiens.GRCh37.87.gtf.gz), assessing transcript boundary overlap with the extended LD ranges of each COJO-identified index SNP ($r^2 > 0.2, p < 0.05$). We annotated all COJO-identified index SNPs as well as high-LD proxy-SNPs ($r^2 > 0.8$) to the index SNPs with functional annotations based on data resources of SNP consequence (<http://www.ensembl.org/>), combined annotation-dependent depletion (CADD) Phred-like scores (Kircher et al., 2014), Polyphen category (Adzhubei et al., 2010) and SIFT category (Kumar, Henikoff, & Ng, 2009) (conducted by Dr Richard Anney). These index and proxy-SNPs were similarly mapped to known cis-expression quantitative trait loci (eQTL) loci using GTEx-v7 human data for cerebellum and cerebellar hemisphere labelled tissues (<https://gtexportal.org/home>), being genomic regions where SNP allelic variation is known to affect expression of a gene transcript (<1Mb distance) within these tissues.

4.3.9 Summary-data-based Mendelian randomization (SMR)

We used summary-based Mendelian randomization (SMR) (v.103) (Pavlidis et al., 2016; Zhu et al., 2016) to explore whether the effect size of a SNP on the phenotype was mediated by altering gene transcript expression, allowing prioritisation of genes which indicate a “causal” or pleiotropic relationship (conducted by Dr Richard Anney). SMR was implemented using the SMR package (<https://cnsgenomics.com/software/smr>), with the same two GTEx-v7 labelled cerebellar eQTL data used as before (<https://gtexportal.org/home>). SMR analysis was limited to genome-wide significant SNPs reported in the cerebellar volume meta-GWAS. In SMR, SNP-on-trait associations are regressed on the SNP-on-gene expression associations to estimate the gene expression-on-trait effects. Since different causal variants might lie within the region and so the associations be due to linkage between these SNPs, SMR also deploys a test for heterogeneity of SNP-gene expression effects at the locus (indicating linkage rather than pleiotropy) via the HEIDI (heterogeneity in dependent instruments) test ($p_{\text{HEIDI}} \geq 0.05$ indicates pleiotropy rather than linkage). To provide sufficient data to implement the HEIDI test, analysis was limited to transcripts with a minimum of 10 SNPs in the model. We applied an SMR wide Bonferroni correction based on the number of transcripts that pass inclusion criteria, specifically cerebellum ($p_{\text{SMR}} < 1.42 \times 10^{-6}$ {0.05/3526}) and cerebellar hemisphere ($p_{\text{SMR}} < 2.09 \times 10^{-5}$ {0.05/2389}).

4.3.10 Genetic correlation analyses with other traits

Using the LDSC approach as described above, we calculated genetic correlations between our total cerebellar volume summary statistics and those of previously published cerebellar measures, other regional brain structure measures, anthropomorphic measures and psychiatric traits. This included harmonising all downloaded summary statistics to the same hg19 genome build and common Haplotype Reference Consortium r1.1 nomenclature (https://github.com/ricanney/stata_summaryqc function) (Dr Richard Anney), as well as applying the LDSC-based pre-analyses quality control procedures already discussed (HapMap filtering, $\text{MAF} > 1\%$). Of note, we also provide the LDSC calculated SNP-based heritability estimates for each trait calculated automatically in the LDSC software by regressing each SNP's trait association (χ^2) on their LD (as described previously). To standardise our approach, these are calculated on the observed scale and use the default 1000G EUR reference, therefore, might differ to original publications if estimates are provided on the liability scale or study-specific references genomes are used.

We identified two previously published brain-wide studies which included GWASs of cerebellar measures in the literature: Elliot et al (Elliott et al., 2018) FreeSurfer (Dale, Fischl, & Sereno, 1999) segmented left & right cerebellum volume measures and FSL FAST (Y. Zhang et al., 2001) segmented 28 individual cerebellar lobule volume measures in $n = 8,428$ EUR; and Zhao et al (Zhao et al., 2019) ANT (<http://stnava.github.io/ANTs/>) segmented left and right cerebellar hemispheres and 3 vermal division cerebellar volume measures in $n = 19,629$ EUR. To limit the number of analyses, the comparison with results from Elliot et al were limited to their FreeSurfer analysis. For these cerebellar measures, we additionally assessed the number of novel COJO-identified genomic regions identified in our meta-GWAS compared to those previously identified in these published works. We deemed our COJO-identified index SNPs as novel if each index SNPs extended LD range did not include a genome-wide significant SNP identified in the previous publications, and that our index SNP was not within $r^2 > 0.1$ of their previously identified index SNPs (i.e. their lead SNP within each genomic region).

As several of our identified index SNPs were associated with anthropomorphic measures, in a post-hoc analysis we wished to ascertain that all our identified genomic associations were not simply a function of these measures. To do this, we explored the genomic correlations between our meta-GWAS results and a collection of anthropomorphic measures collected from the full UK-Biobank cohort (<http://www.nealelab.is/uk-biobank/> GWAS round 1 2017 release version limited to EUR ancestry). These included standing height (data-field: [50](#); $n = 336,474$), sitting height ([20015](#); $n = 336,172$), birth weight ([20022](#); $n = 193,063$), body mass index ([21001](#); $n = 336,107$), weight ([21002](#); $n = 336,227$) and body fat percentage ([23099](#); $n = 331,117$).

We additionally assessed genetic correlations between our cerebellar and other regional brain-based measures, using summary statistics from the ENIGMA group for mean total cortical thickness and surface area using FreeSurfer analysis ($n = 33,992$ EUR) (Grasby et al., 2020), and for the hippocampus ($n = 26,814$ EUR) (Hibar et al., 2017) and other subcortical volumes of the putamen, pallidum, thalamus, amygdala, nucleus accumbens, caudate nucleus and brainstem ($n = 37,741$ EUR) (Satizabal et al., 2019).

Finally, we assessed the genetic correlation between our cerebellar GWAS results and those of schizophrenia and various other psychiatric and neurodevelopmental disorders. For this we used the latest GWAS summary statistics for schizophrenia (40,675 cases; 64,643 controls) (Pardiñas et al., 2018), bipolar disorder (20,352 cases; 31,585 controls) (Stahl et al., 2019), major depressive disorder (59,851 cases; 113,154 controls) (Wray et al., 2018), autism spectrum disorder (ASD) (18,381 cases; 27,969 controls) (Grove et al., 2019), attention deficit hyperactivity

disorder symptom scores (ADHD) (17,666 children) (Middeldorp et al., 2016) and cannabis use disorder (2,387 cases; 48,985 controls) (Demontis et al., 2019).

Bonferroni correction was used for each set of correlations (cerebellar traits: $p < 0.0071$ {0.05/7}; anthropomorphic traits: $p < 0.0083$ {0.05/6}; brain regions: $p < 0.0050$ {0.05/10}; psychiatric traits: $p < 0.0083$ {0.05/6}).

4.3.11 SNP sign test

We also performed a SNP sign test between our cerebellar and the downloaded schizophrenia GWAS summary statistics (Pardiñas et al., 2018), as deployed previously (Franke et al., 2016). For each of our identified index SNPs present and reaching nominal significance ($p < 0.05$) within the schizophrenia GWAS, we ascertained if they showed the hypothesised opposing direction of effect using a two-sided binomial test. We performed the same approach in reverse, testing for opposing directions of the 179 independent index SNPs as defined in the schizophrenia paper in our cerebellar GWAS results (or most significant SNP in COJO defined LD region if absent in our GWAS) (obtained from their Supplementary Table 3 (Pardiñas et al., 2018) and as can be seen in our Supplementary Table 4.9).

4.4 Results

4.4.1 Generation of total cerebellar volume GWAS summary statistics

We obtained similar GCTA-GREML estimated SNP-based heritability values (h^2_{SNP}) for the two separate GWASs of each phase of data (phase 1 h^2_{SNP} [standard error(SE)] = 46.8[3.4]% and phase 2 h^2_{SNP} [SE] = 45.3[3.9]%), and found a strong between-phase genetic correlation (r_g [SE] = 1.0[0.1], $p = 2.2 \times 10^{-33}$). COJO identified 6 conditionally independent index SNPs in the phase 1 GWAS, and 6 index SNPs in the phase 2 GWAS (Figure 4.1; Supplementary Tables 4.2A & 4.2B). Five phase 1 index SNPs were nominally replicated ($p < 0.05$) in phase 2 and all phase 2 index SNPs nominally replicated in phase 1, with 4 index SNPs genome-wide significant in both phases (Supplementary Tables 4.2A & 4.2B). Polygenic scores derived from one phase significantly predicted cerebellar volume in the other phase across all SNP p-value inclusion thresholds (pT-value) (Supplementary Table 4.3). The SNP-inclusion thresholds from phase 1 and phase 2 GWASs which explained the most unique variance (ΔR^2) in phase 2 and phase 1 participants' cerebellar volumes explained 1.9% (phase 1 GWAS pT-value < 0.01 ; statistic p-value = 1.9×10^{-121}) and 1.5% (phase 2 GWAS pT-

value < 0.05 ; statistic p -value = 1.4×10^{-113}), respectively. Given this general replication between phases, we combined the summary statistics in a meta-analysis, including the total of 33,265 participants and 6,193,476 SNPs present in both phases (Figure 4.1).

The GCTA-GREML SNP-based heritability estimate in the combined sample was $h^2_{\text{SNP}}[\text{SE}] = 50.6[2.0]\%$, though we also provide the LDSC-calculated estimate to allow comparison to other literature ($h^2_{\text{SNP}}[\text{SE}] = 31.6[3.1]\%$). LDSC also confirmed that any inflation observed in quantile-quantile (QQ) plots was likely due to polygenic effects rather than residual population structure, with little inflation of χ^2 not ascribed to polygenicity (ratio = 0.09 ± 0.05 ; intercept = 1.02 ± 0.01) (Figure 4.1). In this combined sample, COJO identified a total of 33 conditionally independent genome-wide significant SNPs (index SNPs) associated with total cerebellar volume (Table 4.1).

In addition to confirming replicability across phases, we performed a number of supplementary analyses to confirm the validity of our GWAS summary results. We found high genetic correlation between our results and those of previous studies including cerebellar volumes of Elliot et al (2018) (Elliott et al., 2018) (left and right cerebellum: $r_g[95\% \text{ Confidence Intervals(CI)}] = 0.92[0.75,1.00]$ & $0.98[0.77,1.00]$, respectively) and Zhao et al (2019) (Zhao et al., 2019) (left & right hemispheres; IIV-V, VI-VII & VIII-IX vermal regions: $r_g[95\% \text{CI}] = 0.91[0.84,0.97]$ & $0.91[0.84,0.98]$; $0.44[0.28,0.60]$, $0.45[0.32,0.57]$ & $0.56[0.46,0.65]$, respectively), with all passing Bonferroni corrected significance threshold ($p < 0.0071 \{0.05/7\}$) (Supplementary Table 4.4A). Of the 33 index SNPs (and extended LD-defined genomic regions), 15 were present in these previous works (our index SNP $r^2 > 0.1$ or LD region $< 500\text{kb}$ away from their identified independent regions) while 18 were novel to the literature. We found no genetic correlations significant after Bonferroni correction ($p < 0.0083 \{0.05/6\}$) between our GWAS summary statistics and a battery of anthropomorphic measures in UK Biobank (e.g. birth weight, Birth Weight, Body Fat Percentage, Body Mass Index, Sitting Height, Standing Height and Weight) (Supplementary Table 4.4B). Two measure reached nominal significance ($p < 0.05$) for a relationship, but the overall genetic correlations were small in effect (Body Mass Index: $r_g[95\% \text{CI}] = -0.07[-0.12,-0.01]$, $p = 0.01$; Body fat percentage: $r_g[95\% \text{CI}] = -0.07[-0.12,-0.01]$, $p = 0.01$). These results, therefore, indicated our cerebellar GWAs associations were not simply a function of these measures.

Finally, we examined the genetic correlation between our meta-GWAS for cerebellar volume and the most recent GWAS for subcortical volumes (Hibar et al., 2017; Satizabal et al., 2019) and cortical thickness and surface area (Grasby et al., 2020). We found positive genetic correlations between the volumes of the cerebellum and the volume of brainstem ($r_g[95\% \text{CI}] =$

0.47[0.37,0.58] , $p = 1.0 \times 10^{-18}$), pallidum ($r_g[95\%CI] = 0.31[0.19,0.43]$, $p = 4.5 \times 10^{-7}$) and thalamus ($r_g[95\%CI] = 0.24[0.12,0.36]$, $p = 6.5 \times 10^{-5}$), as well as a negative correlation with cerebral cortical surface area that fell just short of the Bonferroni corrected significant threshold ($p < 0.005 \{0.05/10\}$) ($r_g[95\%CI] = -0.14[-0.25,-0.04]$, $p = 0.007$) (Supplementary Table 4.4C).

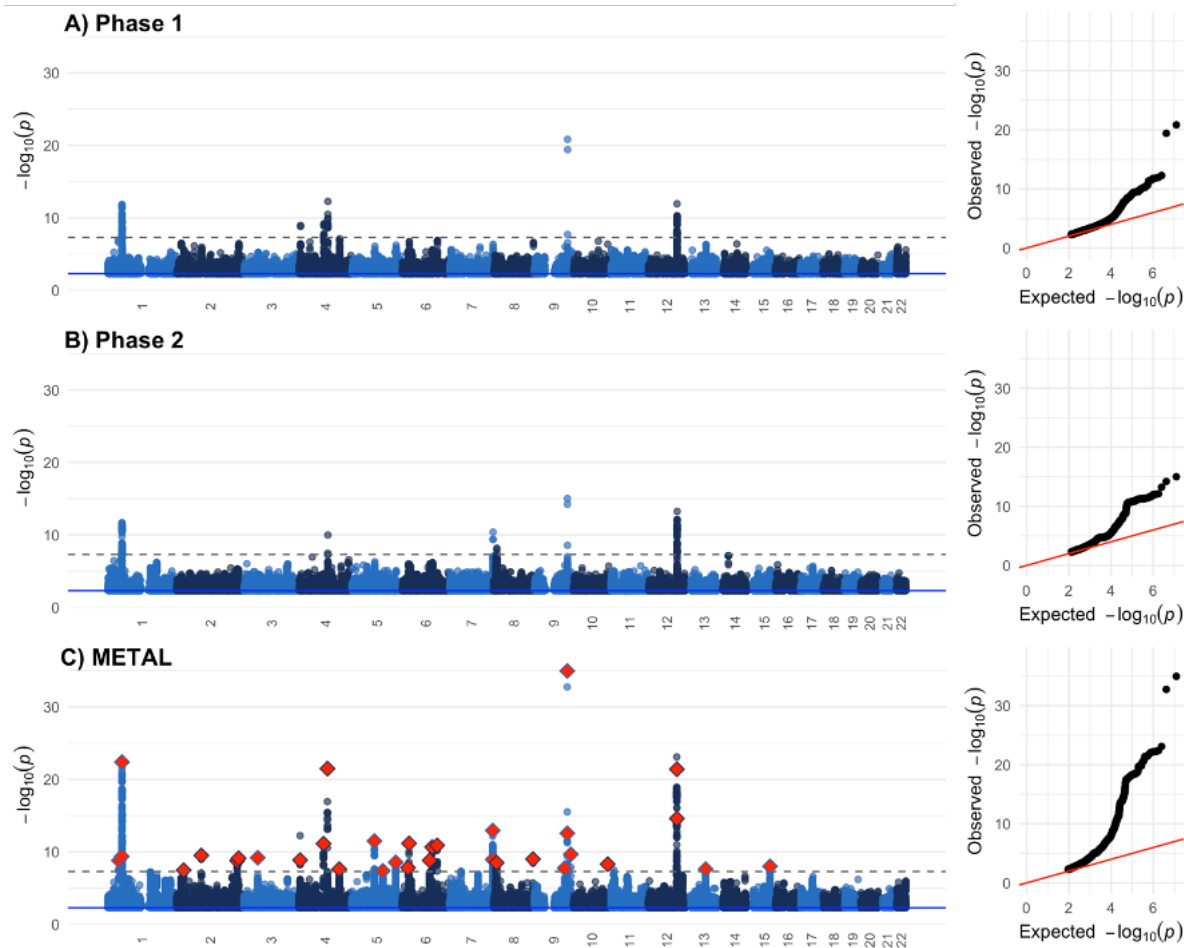


Figure 4.1: Manhattan plots of associations with total cerebellar volume for A) Phase 1 data release (n= 17,818), B) Phase 2 data release (n= 15,447), and C) Phase 1 + Phase 2 combined METAL meta-GWAS. For the METAL meta-GWAS plot, the 33 COJO identified independent index SNPs are highlighted (red diamond). In all cases, the dashed line indicates genome-wide significance at $p < 5 \times 10^{-8}$. Quantile-quantile (QQ) plots for each GWAS are provided next to the Manhattan plot. For all plots, points $p > 5 \times 10^{-3}$ (blue solid line) are removed for ease of presentation.

4.4.2 Functional consequences and associated genes of identified genome-wide significant loci

We identified a list of 732 gene transcripts within 500kb of our 33 index SNPs' extended LD ranges (Supplementary Table 4.5). To refine this list to identify genes more likely related to altering cerebellar volume, we functionally annotated the index and high-LD proxy-SNPs ($r^2 > 0.8$ to the index SNPs) within these regions to help identify likely causal variants, being those affecting protein-coding sections of the genome and mapping them to known GTEx-v7 cerebellar tissue cis-eQTLs altering gene transcript expression.

Functional annotation identified 5 index SNPs (or their proxy SNPs) which were annotated non-synonymous, i.e. leading to a changed amino acid and altered protein structure (Supplementary Tables 4.6). These included 2 variants flagged as likely having deleterious consequences (based on CADD scores), being within the *HFE* (Human homeostatic iron regulator) and *SLC39A8* (Zinc transporter ZIP8) gene transcripts. The other 3 non-synonymous variants were flagged as tolerated/benign, being within *EIF2AK3* (Eukaryotic translation initiation factor 2-alpha kinase 3), *PPP2R4* (Protein Phosphatase 2A regulatory subunit B; alias *PTPA*), and *MYCL* (L-myc-1 proto-oncogene) gene transcripts. One additional independent SNP was annotated as synonymous – i.e. coding for the same amino acid - being within the *PAPPA* (Pregnancy-associated plasma protein A) gene. This was also the index SNP with the most significant association with cerebellar volume from our results.

Six of the 33 index SNPs (and their high LD proxy SNPs) mapped to genome-wide significant cis-eQTLs for cerebellar labelled tissue (at cytobands: 3p21.31, 5q14.2, 6q16.2, 8p23.1, 8q24.3, 9q34.11), identifying a total of 14 gene transcripts: *AMT* (Aminomethyltransferase), *CCDC71* (Coiled-Coil Domain Containing 71), *NCKIPSD* (NCK Interacting Protein With SH3 Domain), *WDR6* (WD Repeat Domain 6), *GPX1* (Glutathione Peroxidase 1), *VCAN* (Versican), *PPP2R4/PTPA*, *PTK2* (Protein Tyrosine Kinase 2) and six transcripts of unknown transcripts (*RP11-247A12.2*, *RP11-247A12.7*, *RP1-199J3.5*, *RP11-481A20.10*, *RP11-481A20.11* and *AF131216.5*) (Supplementary Tables 4.7). SMR analysis further identified 6 transcripts which showed evidence supporting a causal or pleiotropic relationship (over those caused by linkage) between SNP-trait association and gene transcript cerebellar tissue expression at 3 of the eQTL identified regions: *VCAN* at 5q14.2; *RP11-247A12.2*, *RP11-247A12.7* and *PPP2R4/PTPA* at 9q34.11; and the lncRNA *FAM85B* (family with sequence similarity 85 member B) and pseudogene *FAM86B3P* (family with sequence similarity 86 member B3, pseudogene) at 8p23.1, the latter two being novel to the SMR analysis (Supplementary Table 4.8).

In total, therefore, from a list of 732 proximal genes we identified a list of 21 unique gene transcripts across 11/33 of our COJO identified genomic regions, for which either functional annotation, eQTL mapping and/or SMR analysis provided stronger evidence for follow-up analyses (Table 4.2).

Table 4.1: List of 33 conditionally independent index SNPs and corresponding LD ranges following COJO analysis of the genome-wide association results for total cerebellar volumes in UK Biobank, and their association statistics in the latest Schizophrenia GWAS

Cytoband	Extended LD range	Index SNP	Index SNP Position	A1/A2	β_{GWAS} (SE) [†]	P_{GWAS} [†]	β_{COJO} (SE) [‡]	P_{COJO} [‡]	β_{SCZ} (SE) [§]	P_{SCZ} [§]
1p34.2	40236396 - 40434968	rs12127002	40384968	G/A	0.033 (0.005)	1.26E-09	0.033 (0.005)	1.36E-09	-0.058 (0.015)	1.12E-04
1p32.3	50841117 - 52638689	rs7530673	51558856	A/C	0.054 (0.005)	6.55E-23	0.053 (0.005)	1.58E-21	-0.028 (0.018)	0.11
1p32.3	50776624 - 51682964	rs1278519	50897342	C/A	0.034 (0.005)	3.99E-10	0.032 (0.005)	8.74E-09	0.016 (0.010)	0.10
2p23.3	25479624 - 25619823	rs6546070	25531779	A/G	0.030 (0.005)	3.61E-08	0.030 (0.005)	4.08E-08	0.029 (0.010)	2.20E-03
2p11.2	88749514 - 89179064	rs7593335	88878133	A/G	0.035 (0.005)	3.55E-10	0.035 (0.005)	4.22E-10	-0.011 (0.011)	0.29
2q35	217673928 - 217980232	rs2542212	217803906	G/A	0.033 (0.005)	1.76E-09	0.033 (0.005)	2.24E-09	0.009 (0.025)	0.73
2q36.1	222949007 - 223309955	rs75779789	223057209	A/G	0.034 (0.005)	7.97E-10	0.034 (0.005)	1.03E-09	-0.007 (0.020)	0.72
3p21.31	48184492 - 50153917	rs7640903	49338465	A/G	0.034 (0.005)	7.11E-10	0.034 (0.005)	8.62E-10	-0.031 (0.010)	1.30E-03
4p16.2	4638654 - 4902425	rs10033073	4775401	A/G	0.033 (0.005)	1.26E-09	0.033 (0.005)	1.50E-09	0.005 (0.010)	0.64
4q22.1	88611354 - 89316460	rs4148155	89054667	A/G	0.038 (0.005)	8.12E-12	0.038 (0.005)	9.17E-12	0.007 (0.015)	0.65
4q24	102657791 - 103426409	rs13135092	103198082	G/A	0.053 (0.005)	3.94E-22	0.053 (0.005)	5.57E-22	0.149 (0.018)	7.87E-16
4q31.21	145330633 - 146224823	rs6812830	145613807	A/G	0.031 (0.005)	2.64E-08	0.037 (0.006)	4.89E-11	0.013 (0.010)	0.18
5q14.2	81667102 - 82008326	rs55803832	81920587	C/A	0.038 (0.005)	3.32E-12	0.038 (0.005)	4.44E-12	-0.008 (0.010)	0.44
5q22.2	111934537 - 112311278	rs3846716	112059594	G/A	0.030 (0.005)	4.00E-08	0.030 (0.005)	4.52E-08	0.013 (0.010)	0.17
5q33.3	158058006 - 158536993	rs7380908	158396062	C/A	0.033 (0.005)	3.08E-09	0.033 (0.005)	3.41E-09	-0.012 (0.012)	0.33
6p22.3	22006131 - 22184959	rs9393227	22100912	A/G	0.031 (0.005)	1.41E-08	0.031 (0.005)	1.23E-08	0.008 (0.010)	0.43
6p22.2	25264597 - 28544225	rs1800562	26093141	G/A	0.038 (0.005)	7.15E-12	0.038 (0.005)	5.94E-12	0.002 (0.020)	0.94
6q16.2	99654270 - 100334555	rs546897	100132856	G/A	0.033 (0.005)	1.58E-09	0.033 (0.005)	1.95E-09	0.008 (0.012)	0.50
6q21	108635716 - 109080753	rs1935951	108999101	A/G	0.037 (0.005)	2.22E-11	0.037 (0.005)	3.06E-11	-0.049 (0.010)	3.11E-06

6q22.32	126598460 - 127377494	rs72971190	127088303	G/A	0.037 (0.005)	1.19E-11	0.037 (0.005)	1.46E-11	-0.026 (0.011)	0.02
7q36.3	156100022 - 156273180	rs57131976	156167072	A/C	0.041 (0.005)	1.03E-13	0.046 (0.005)	2.82E-16	-0.003 (0.010)	0.77
7q36.3	156016471 - 156178006	rs11764163	156066865	A/G	0.034 (0.005)	1.00E-09	0.039 (0.005)	2.10E-12	-0.004 (0.010)	0.70
8p23.1	8042025 - 11945009	rs2572397	11176403	G/A	0.033 (0.005)	3.44E-09	0.033 (0.005)	4.05E-09	-0.024 (0.010)	0.02
8q24.3	141983550 - 142130336	rs6984592	142040038	A/G	0.034 (0.005)	1.12E-09	0.034 (0.005)	1.35E-09	0.027 (0.010)	5.10E-03
9q31.2	109365922 - 109976563	rs7027172	109571457	G/A	0.031 (0.005)	1.74E-08	0.030 (0.005)	2.78E-08	0.057 (0.035)	0.11
9q33.1	119007741 - 119200439	rs72754248	119061396	A/G	0.068 (0.005)	2.08E-35	0.072 (0.005)	3.62E-38	-0.008 (0.021)	0.68
9q33.1	119117887 - 119553742	rs17220352	119248059	A/G	0.040 (0.005)	3.08E-13	0.045 (0.005)	2.17E-16	0.007 (0.011)	0.55
9q34.11	131364336 - 132013262	rs3118634	131905854	G/A	0.035 (0.005)	2.50E-10	0.035 (0.005)	2.65E-10	-0.080 (0.017)	3.32E-06
10q26.13	123306938 - 123606457	rs4752582	123443605	G/A	0.032 (0.005)	4.78E-09	0.032 (0.005)	5.00E-09	-0.000 (0.017)	0.98
12q23.2	102349379 - 102996220	rs5742632	102856474	G/A	0.053 (0.005)	5.61E-22	0.048 (0.005)	5.95E-18	-0.007 (0.011)	0.52
12q23.2	102405447 - 103009565	rs703545	102943000	G/A	0.044 (0.005)	1.93E-15	0.038 (0.005)	1.24E-11	0.015 (0.013)	0.23
13q21.33	72807523 - 73006046	rs529059	72933970	G/A	0.031 (0.005)	2.14E-08	0.031 (0.005)	2.42E-08	0.024 (0.010)	0.02
15q25.2	82339282 - 84014925	rs62012045	82521707	A/G	0.032 (0.005)	1.02E-08	0.032 (0.005)	1.15E-08	-0.049 (0.011)	4.94E-06

[†]Standardised coefficients (β)_{GWAS} (Standard Error) & p-values from meta-GWAS total cerebellar volume; [‡] β _{COJO} (SE) & p-values for neighbouring SNPs (10Mb sliding window) following GCTA-COJO (Standard Error); [§] β _{SCZ} (SE) & p-values for the schizophrenia GWAS (Pardiñas et al., 2018)

Table 4.2: The prioritised 21 unique genes from functional annotation, positional and cis-eQTL mapping and SMR analysis

Cytoband	Variant within protein-coding region†	Variant altering gene expression	
		eQTL‡	SMR§
1p34.2	MYCL		
2p11.2	EIF2AK3		
3p21.31		AMT, CCDC71, GPX1, NCKIPSD, WDR6	
4q24	SLC39A8		
5q14.2		VCAN	VCAN
6q16.2		RP1-199J3.5	
6p22.2	HFE		
8p23.1		AF131216.5, RP11-481A20.10, RP11-481A20.11	FAM85B, FAM86B3P
8q24.3		PTK2	
9q33.1	PAPPA		
9q34.11	PPP2R4	PPP2R4, RP11-247A12.2, RP11-247A12.7	PPP2R4, RP11-247A12.2, RP11-247A12.7

† Protein-coding associated genes from Supplementary Table 4.5; ‡ cis-expression quantitative trait loci (cis-eQTL) associated genes from Supplementary Table 4.6; § Summary data-based Mendelian Randomisation (SMR) associated genes from Supplementary Table 4.8

4.4.3 Analysis of overlap in genetic architecture with schizophrenia

We found no significant evidence for a genetic correlation between our summary statistics for total cerebellar volume and those from the latest schizophrenia GWAS (Pardiñas et al., 2018) ($r_g[95\%CI] = -0.04[-0.10,0.02]$, $p = 0.18$) (Table 4.3). We equally found no significant genetic correlations with other neuropsychiatric and neurodevelopmental disorders, including bipolar disorder (Stahl et al., 2019) ($r_g[95\%CI] = -0.04[-0.12,0.04]$, $p = 0.33$), major depressive disorder ($r_g[95\%CI] = -0.02[-0.10,0.08]$, $p = 0.61$), autism spectrum disorder (Grove et al., 2019) ($r_g[95\%CI] = -0.10[-0.22,0.02]$, $p = 0.10$), attention deficit hyperactivity disorder ($r_g[95\%CI] = -0.07[-0.17,0.03]$, $p = 0.18$) or cannabis use disorder ($r_g[95\%CI] = -0.22[-0.46,0.02]$, $p = 0.07$).

We found a substantial proportion (11/33; 33%) of our identified index SNPs reached nominal significance ($p < 0.05$) for an association with schizophrenia liability. Of these, however, we found no significant evidence for our hypothesised opposing directions of effect (7/11 opposing sign direction, 63.6%, $p = 0.55$) (Table 4.1). Of the 179 identified schizophrenia significant index associations, we found 106 (59.2%) reaching nominal significance ($p < 0.05$) in our meta-GWAS cerebellar results, with also no significant evidence for an opposing direction of effect (54/106, 49.1%, $p = 0.92$) (Supplementary Table 4.9). Only one loci reached genome-wide significance for both total cerebellar volume and schizophrenia liability, containing the rs13107325 missense variant within *SLC39A8* protein-coding region, whose minor T allele (frequency 8% in EUR) is associated with decreased cerebellar volume and increased schizophrenia liability (cerebellum: $\beta[\text{Standard error/SE}] = -0.053 (0.006)$, $p = 5.57 \times 10^{-22}$; schizophrenia liability: odd's ratio[SE] 1.17[0.02], $p = 1.19 \times 10^{-16}$). We also found this the only gene to overlap with the list of fine-mapped or SMR identified genes provided (their Supplementary Tables 11 & 13) in the schizophrenia GWAS paper (Pardiñas et al., 2018).

Table 4.3: Genetic correlation of total cerebellar volume with psychiatric previously associated with cerebellar anatomy/function

	h^2_{SNP} (%)	h^2_{SNP} SE (%)	r_g	95% Confidence interval		p	$p_{\text{Bonferroni}}$
Schizophrenia Disorder	42.1	1.5	-0.04	-0.10	0.02	0.18	1.00
Bipolar Disorder	34.6	1.9	-0.04	-0.12	0.04	0.33	1.00
Attention Deficit Hyperactivity Disorder	22.7	1.7	-0.07	-0.17	0.03	0.18	1.00
Autism Spectrum Disorder	19.5	1.5	-0.10	-0.22	0.02	0.10	0.60
Cannabis use Disorder	16.1	5.8	-0.22	-0.46	0.02	0.07	0.42
Major Depressive Disorder	7.8	0.5	-0.02	-0.10	0.08	0.61	1.00

Calculated using LDSC regression analysis software. h^2_{SNP} : SNP-based heritability estimates (on the observed scale); SE: standard error; r_g : genetic correlation; p : uncorrected p -values; $p_{\text{Bonferroni}}$: p -values adjusted with Bonferroni correction for the 6 tests performed

4.5 Discussion

In this study we combined the UK-Biobank imaging and genotype data of 33,265 individuals of European ancestry to investigate common allele influences on cerebellar volume and pleiotropic effects with schizophrenia liability. We ascertained that total cerebellar volume was moderately heritable in our sample ($h^2_{\text{SNP}} = 50.6\%$) and identified 33 independent genome-wide significant (“index”) SNPs associated with this phenotype. Functional annotation, cis-eQTL mapping and follow-up summary data-based mendelian randomisation (SMR) identified a credible list of 21 unique genes which we prioritise for follow-up analyses. We did not find, however, evidence for genetic pleiotropy in a consistent direction of effect between total cerebellar volume and schizophrenia liability at either the whole genome or independent genome-wide significant SNPs.

We initially performed two independent GWASs of cerebellar volume (phase 1 and phase 2) following two consecutive brain imaging data releases from the UK-Biobank. We obtained a high replication of independent index SNPs across phases, a very strong correlation between both GWASs and a significant out-of-sample polygenic score prediction of cerebellar volume of similar effect size to previous reports of other brain regions (Grasby et al., 2020). Given this, we combined results from both phases into a meta-analysis to increase power. We compared the main results from our meta-analysis to the two previous GWASs reported in the literature thus far which have included cerebellar grey-matter measures, both using UK-Biobank samples including approximately 10,000 (Elliott et al., 2018) and 20,000 (Zhao et al., 2019) participants each. We found high genetic correlation with left and right cerebellar measures in both these studies (all $r_g > 0.90$), but only moderate, although significant, correlation with those reported specifically for vermal regions (Zhao et al., 2019) (average $r_g \approx 0.50$), likely due to their small volumes and so contributing less to our total cerebellar volume measure. Furthermore, the SNP heritability estimate we obtained is in keeping with those previously reported for other non-cerebellar grey-matter volumes (Elliott et al., 2018; Grasby et al., 2020; Hibar et al., 2017; Satizabal et al., 2019; Zhao et al., 2019). Finally, since several of the index SNPs we identified had also previously been shown associated with multiple anthropometric traits (<http://www.nealelab.is/uk-biobank/>) – in addition to other brain-based and brain-related traits – we confirmed our results were not simply a function of these anthropomorphic measures, finding no genetic correlation with various such measures. All of the above provide confidence about the reliability and validity of the results reported here.

Our meta-GWAS identified 33 index SNPs of association with total cerebellar volume. Of note, these were spread across 29 loci, with the use of COJO identifying a second conditionally independent association in 4 different loci, which would have otherwise been missed if using only the lead SNP

within each genomic locus. Of the 33 index SNPs, 18 were novel, while 15 had been identified previously (Elliott et al., 2018; Zhao et al., 2019).

Despite reports of cerebellar differences in individuals with schizophrenia diagnosis (Nancy C. Andreasen & Pierson, 2008; Moberget et al., 2018) and unaffected close family members (de Zwarte, Brouwer, Agartz, et al., 2019), and our finding of several of our COJO GWAS signals to be in LD with variants at genome-wide significance for an association with schizophrenia, we did not find any significant negative genetic correlation across the genome between cerebellar volume and schizophrenia liability as we had hypothesised. Equally, outside our primary focus on schizophrenia, we also found a similar lack of whole genome correlations with other psychiatric and neurodevelopmental conditions, again despite reports of cerebellar differences in case-control studies (Phillips et al., 2015; Stoodley, 2016). Notably, despite clinical research showing brain-wide anatomical differences, previous GWASs of other structural brain phenotypes have also generally reported a lack of genetic association with most of these psychiatric traits (Franke et al., 2016; Grasby et al., 2020; Satizabal et al., 2019; Toulopoulou et al., 2015); with the exception of small genetic correlations between brainstem and ADHD (Satizabal et al., 2019), and cortical surface area with ADHD and depression (Grasby et al., 2020). To avoid repetition, in the *General Discussion (Chapter 6)* of this thesis we examine these results of the genetic relationship between the cerebellum, schizophrenia and other psychiatric/neurodevelopmental traits, combining with the other findings reported within this thesis, including the potential for uncorrected confounding in high-risk individuals (*Chapter 2*) and our reported cerebellar differences in unrelated individuals at elevated genetic risk when controlling for some of these factors (*Chapter 3*). In specific regard to the findings reported here, however, while we find an enrichment of genome-wide significant associations with schizophrenia in our genome-wide significant cerebellar results, we find no evidence for a consistent, across-genome shared common association between cerebellar volume and schizophrenia. We discuss later how other approaches could build on this work.

Given the general lack of genetic trait associations with individual brain regions, analysis of shared networks might prove more fruitful for future research. In this regard, we found high genetic correlation between our cerebellar volume GWAS and those previously run on the volume of the brainstem, the pallidum and the thalamus, indicating similar common allele architecture. A clustering of genetic correlations of these subcortical structures has already been noted (Satizabal et al., 2019), as well as basal ganglia-thalamic pairings in twin-based imaging studies (Eyler et al., 2011), differing to the raw volumes for these regions (i.e. phenotypic correlation) where all subcortical regions are correlated with each other (Satizabal et al., 2019). Our results, therefore, add cerebellar volume to

this cluster of regions sharing common allele influences and indicate a more co-heritable network to pursue for further genetic and neuroimaging analyses. Considering the unique gene transcription profile of the cerebellar cortical tissue (Hawrylycz et al., 2015), these results suggest that the genetic correlation might be driven by the shared structural connectivity of these structures rather than shared genetic expression within the tissues themselves. Indeed, the major input and output nuclei of the cerebellum are located within the brainstem and thalamus, respectively, and interaction between the pallidum and the cerebellum is also well known, occurring at the level of cortex, at the ventrolateral thalamus and directly between the structures and with roles in motor and reward-based learning (Bostan & Strick, 2018; Hintzen, Pelzer, & Tittgemeyer, 2018; Milardi et al., 2016). These networks have been shown altered in schizophrenia individuals (Tarcijonas, Foran, Haas, Luna, & Sarpal, 2020), as well as implicated in both sensorimotor (Hirjak et al., 2017; X. Wang, Herold, Kong, & Schroeder, 2019) and salience network deficits (Peters, Dunlop, & Downar, 2016) in schizophrenia. Investigations of the relation between structural and functional connectivity of these areas and genetic liability to schizophrenia, therefore, would be an interesting next stage for this research.

Outside of our primary aim, we feel these, and other findings from this report, will be of interest to the wider neuroscientific field. For instance, we also annotated and mapped our identified genetic regions (index SNPs and SNPs in high LD) to genes which might mediate this relationship. We found 6 of our 33 genomic regions overlapped with protein-coding *PAPPA*, *EIF2AK3*, *PPP2R4/PTPA*, *MYCL*, *HFE* and *SLC39A8* gene transcripts, with the latter two including SNPs annotated as likely deleterious missense variants. We also mapped our independent genomic regions to cis-eQTLs known to alter gene transcript expression in cerebellar tissue and performed summary data-based mendelian randomisation (SMR) analysis to further add evidence of causal (or pleiotropic) relations between our identified SNPs, altered cerebellar gene expression and our cerebellar volume measures. We found, across 6 of our 33 independent regions, a total of 16 unique gene transcripts through these two eQTL analyses: *AMT*, *CCFC71*, *GPX1*, *NCKIPSD*, *WDR6*, *VCAN*, *RP1-199J3.5*, *FAM85B*, *FAM86B3*, *AF131216.5*, *RP11-481A20.10*, *RP11-481A20.11*, *PTK2*, *PPP2R4/PTPA*, *RP11-247A12.2* and *RP11-247A12.7*. Of note, SMR's requirement for multiple eQTL signals to exist (>10 required for HEIDI test) within each region means that while it can provide more evidence for an association with a gene transcript, a transcript's absence from SMR results does not mean it might not be relevant. In total, therefore, using functional annotation, eQTL mapping and SMR, we provide a list of 21 unique gene transcripts – identified across for 11/29 genomic loci - worth future follow-up study for to investigate the impact of their altered expression on cerebellar volume.

While a systematic discussion of these transcripts is beyond the scope of this thesis, we note that previous associations with brain measures, neurological and psychiatric traits, as well as known biological roles in neuronal development, offer additional evidence for many of these genes. For example, *PPP2R4* – identified by functional annotation, eQTL and SMR analyses - encodes an activator of phosphatase 2A. This has been implicated in controlling cell growth and division; being expressed in neurones and glia in the brain - including the cerebellum – and where it plays a role in regulating dendritic spine morphology (J. Wang et al., 2019), and whose dysfunction is a known cause of spinocerebellar ataxia (Srivastava, Takkar, Garg, & Faruq, 2017). The strongest SMR association was with *VCAN*, which encodes the extracellular matrix protein Versican, and which plays a number of crucial roles in maintaining the extracellular matrix, including in nervous system development (Rutten-Jacobs et al., 2018; Theocharis, 2008). Finally, the *SLC39A8* and the associated missense variant rs13107325 have been associated with a variety of traits, including schizophrenia, neurodevelopmental outcomes and brain volumes (Costas, 2018; Elliott et al., 2018; Hill et al., 2019; Q. Luo et al., 2019; Mealer et al., 2020; Pardiñas et al., 2018; Wahlberg et al., 2018). This was also the only independent region reaching genome-wide significance for both our cerebellar measure and schizophrenia liability. A previous study found rs13107325 minor T allele to associate with reduced putamen volume and decreased putamen *SLC39A8* expression, with the SNP-trait association decreased in those with schizophrenia and unaffected siblings (Q. Luo et al., 2019).

There are several considerations and limitations to our findings. While we have previously discussed the advantages and disadvantages of the UK Biobank's approach in preceding chapters, in specific regard to this GWAS analysis, we limited our analysis to a total cerebellar measure rather than lobule-specific analyses, given the highly conserved gene expression architecture of the cerebellum (Negi & Guda, 2017) in addition to the lack of cerebellar-specific registration being undertaken by UK Biobank, which would likely lead to less successful lobule registration (Diedrichsen, 2006). Of note, our inclusion of potential participant head motion and position-induced artefacts in the MRI scanner, so as to improve the face validity of our results, is not always performed across the literature and will be an important consideration for future neuroimaging genetic studies. Furthermore, the use of a single, large, homogeneously collected and processed UK-Biobank dataset helped to decrease methodological variation and improve our ability to detect genetic-phenotype associations. For example, it allowed for a relatively lower minor allele count, which helped identify several novel SNPs which would have otherwise been missed. The population, however, is predominantly European and to avoid any residual population effects driving our associations, we limited our analysis to only those of similar European (specifically British/Irish) genetic ancestry, in addition to correcting for principal components of genetic ancestry. These steps limit the interpretation of our results beyond this

population. Additionally, residual population structure can remain, however, which can still pose a problem for LDSC heritability estimates, while co-heritability estimates should be less affected (with inflation being captured by the intercept) (Yengo, Yang, & Visscher, 2018). Problems of selection and collider bias can cause specific problems such as inflated co-heritability estimates, potentially being a particular problem in UK Biobank given the relatively poor response rate (5%) (Munafò, Tilling, Taylor, Evans, & Davey Smith, 2018). Since the UK Biobank data is imputed to 1000G reference panels, large differences in linkage disequilibrium (LD) to the 1000G European LD results used for the LDSC heritability and genetic correlation analyses are unlikely to be present, however, repetition with a population-specific LD could also be conducted to improve the accuracy of results.

Another consideration of our study cohort is its inclusion of those with various recorded diagnoses which have been shown to associate with reduced cerebellar volume (see *Chapter 2*). We chose this approach in accordance with previous GWASs of brain imaging measures (Elliott et al., 2018; Zhao et al., 2019) so as to produce results of most use to the broad neuroscientific community and since the drawing of exclusion criteria around negative impacts on the cerebellum would be fairly arbitrary given the large number of diagnoses with negative associations with cerebellar volume (as highlighted in *Chapter 2*). One effect of this could be that several of the genome-significant signals identified in this study could specifically reflect those related to common disorders in our sample with relatively moderate-large effects. For example, we did identify several variants with previously reported statistical associations with endocrine/metabolic disorders and anthropomorphic measures. As discussed above, however, we found no general genetic correlation between our cerebellar summary statistics and those of various anthropomorphic-related traits, as well as highlighting previous reports of known neuronal effects of several of these variants - reflecting the pleiotropic effects of many of these variants in different tissues. While our two-step GWAS approach, as well as our comparison to previous brain measure GWASs, helps to validate these SNP-cerebellar associations within similar demographic (including diagnoses prevalence) UK Biobank samples, validation of these associations in an external sample, ideally in those without any recorded diagnoses of disorders highlighted as impacting cerebellar volume, would help to confirm these associations as not being solely driven by diagnosis-status. GWAS investigation in another ancestry group would also not only aid in making results more informative for ancestry groups outside of the commonly studied European ancestry, but also can aid in the identification of the causal variants (Asimit, Hatzikotoulas, McCarthy, Morris, & Zeggini, 2016).

Another specific consequence of not applying specific hospital record diagnosis exclusion criteria in this cohort, is in the inclusion of those with a recorded history of psychiatric condition. While

schizophrenia numbers in UK Biobank are relatively low and below UK population averages, UK Biobank does include a larger proportion of individuals with other psychiatric conditions such as mood/affective disorders and psychosis-related disorders (see *Chapter 2*). It also includes possibly overlapping “control” samples, which cannot be identified since the raw genotypes of the schizophrenia GWAS are unavailable for analysis. Such inclusion of those with psychopathologies and/or overlapping controls could, theoretically, inflate genetic correlation analyses. As discussed above, a study-specific exclusion of these individuals from the GWAS, therefore, could be beneficial to ascertain that this is not the case. Since, however, LDSC controls for such overlap (being indicated in the intercept and where we show little inflation) and since our results did not reach nominal significance, this is unlikely to change the overall interpretation of results presented here.

Due to the lack of raw genotypes available for the schizophrenia GWAS, we were unable to deploy correlation methods such as bivariate GREML (S. H. Lee, Yang, Goddard, Visscher, & Wray, 2012), which would improve the accuracy of our genetic correlation estimates between traits. Furthermore, given our finding of several of our genome-wide significant cerebellar associated variants are also significantly associated with schizophrenia - though no hypothesised general consistent opposing direction of effect was seen between the traits at these variants or across the whole genome - analysis of enrichment of cerebellar GWAS signal for psychiatric associations (and vice-versa), irrespective of a consistent direction of effect across the genome, might also be worth pursuing, as has recently been highlighted by the pleiotropic enrichment between bipolar disorder and intelligence despite no whole-genome genetic correlation (Andreassen et al., 2013; Smeland, Bahrami, et al., 2020). Equally, other genetic methods are also available for directly analysing pleiotropic effects at individual loci and separating these from shared signals due to linkage (Pickrell et al., 2016; Zhu et al., 2018). While we only used the autosomal sample of genotypes, recent work on sex-specific autosomal GWAS and GWAS of the X-chromosome indicate interesting regional brain effects, including on cerebellar white matter, and would therefore be interesting avenues for future research on the cerebellum (Smith et al., 2020). Finally, the cis-eQTL analysis we report in this study is also limited to only adult cerebellar (GTEx-v7) tissue, however, other tissue and time-specific effects could undoubtedly also contribute to eventual adult cerebellar volume, as has been shown for epigenetic effects on subcortical volumes (T. Jia et al., 2019) and, therefore, would be of interest to include, given that they are unlikely captured by the unique cerebellar expression profiles (Negi & Guda, 2017) and/or can provide increased power for detection (Qi et al., 2018).

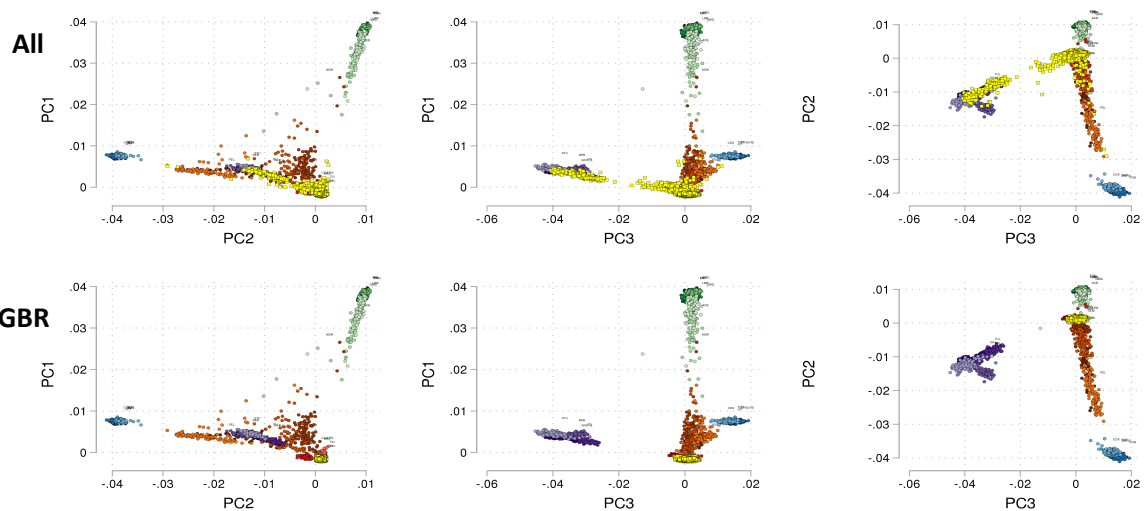
In conclusion, we provide a genome-wide association study of the common genetic variation underlying human cerebellar volume. We find, similar to previous reports of cortical and subcortical

regions, a moderate-to-high heritability, and identify 33 index SNPs associated with cerebellar volume. While further replication and follow-up functional studies are required, we highlight 21 unique candidate genes which show a possible association with altered cerebellar volume. We do not observe, however, any substantial genetic correlation between these identified variants and those of schizophrenia liability, suggesting that cerebellar differences reported in schizophrenia do not appear to be due to a shared common allele architecture. Overall, these results advance our knowledge on the genetic architecture of the cerebellum which, while not seemingly associated with schizophrenia liability, might still have important implications for sub-types and features within schizophrenia, as well as their hopeful use to the wider neuroscientific research community.

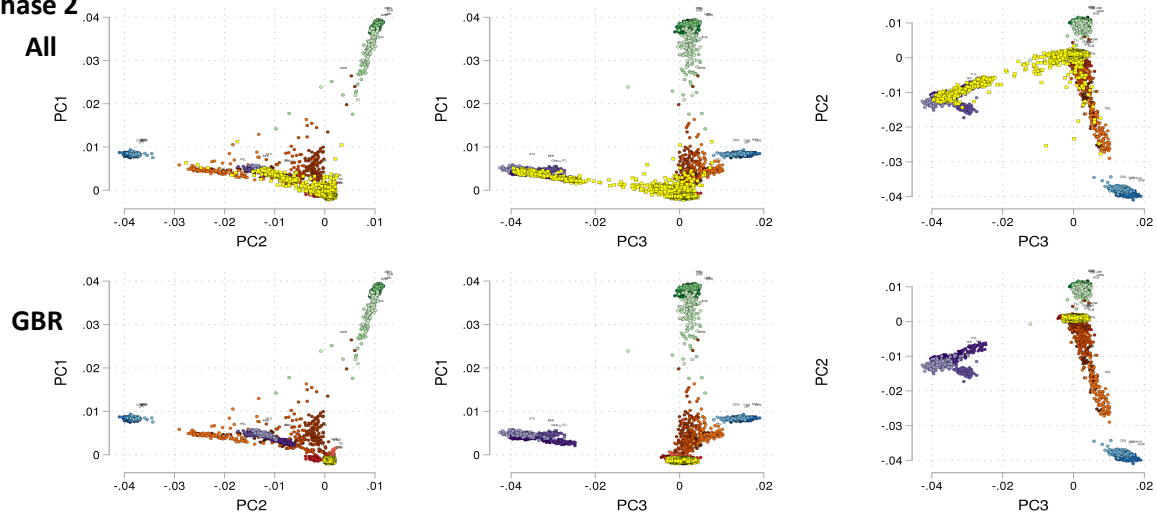
4.6 Supplementary Figures

Supplementary Figure 4.1: Principal component analysis (PCA) of genetic ancestry to British/Irish (GBR) similarity for A) phase 1 and B) phase 2. The first 3 principal components (PCs) following PCA analysis on individuals' genotypes were compared to 1000G phase 3 super-population ancestries using *bim2ancestry* function (<https://github.com/ricanney/stata>). Each plot shows the test participant ancestries (yellow squares) and the 1000G super-populations (circles, colour-coded by super-population ancestries). For "All" plots, all test participants are included, while "GBR" plots show the exclusion of those with ancestries dissimilar to British/Irish super-populations (<4 standard deviations).

A) Phase 1



B) Phase 2



4.7 Supplementary Tables

Supplementary Table 4.1: Demographic information for phase 1 (n=17,818) and phase 2 (n=15,447) sub-samples of our total UK Biobank cohort

	Phase 1 (n=17818)	Phase 2 (n=15447)
Total Cerebellar Grey-Matter Volume (mm³)		
Mean (SD)	90258 (11128)	91720 (10539)
Median [Min, Max]	90566 [45312, 142148]	91689 [46535, 141529]
Total Brain Grey & White Matter Volume (mm³)		
Mean (SD)	1168404 (111437)	1159542 (110703)
Median [Min, Max]	1163915 [828168, 1633670]	1155060 [785719, 1710590]
Sex		
Female	9380 (52.6%)	8158 (52.8%)
Male	8438 (47.4%)	7289 (47.2%)
Age (years)		
Mean (SD)	62.6 (7.44)	64.9 (7.40)
Median [Min, Max]	63.0 [45.0, 80.0]	65.0 [48.0, 81.0]
Centre's Attended (Site IDs)		
11025	14985 (84.1%)	5575 (36.1%)
11026		4216 (27.3%)
11027	2833 (15.9%)	5656 (36.6%)
Resting-State fMRI Head Motion (mm)		
Mean (SD)	0.121 (0.0589)	0.123 (0.0567)
Median [Min, Max]	0.107 [0.0290, 1.39]	0.110 [0.0305, 0.705]

Supplementary Table 4.2A: Conditionally independent genome-wide association results for total cerebellar volumes in phase 1 (n=17,818) sub-cohort, including replication values from phase 2 (n=15,447)

Cytoband	Index SNP	Chromosome: Physical Location	A1	A2	β (SE) - GWAS	p - GWAS	β (SE) - COJO‡	p - COJO‡	β (SE) - GWAS [†] Phase 2*	p - GWAS Phase 2*	$p_{\text{Bonferroni}} -$ GWAS Phase 2*
1p32.3	rs7530673	chr1:51558856	A	C	0.0530 (0.0074)	1.32E-12	0.0530 (0.0075)	1.57E-12	0.0555 (0.0080)	4.82E-12	2.89E-11
4q22.1	rs2728118	chr4:88929305	A	G	-0.0463 (0.0074)	6.24E-10	-0.0463 (0.0075)	7.15E-10	-0.0197 (0.0080)	1.43E-02	0.08604
4q24	rs13135092	chr4:103198082	G	A	0.0541 (0.0075)	5.11E-13	0.0541 (0.0075)	6.25E-13	0.0521 (0.0080)	1.03E-10	6.17E-10
9q33.1	rs72754248	chr9:119061396	A	G	0.0714 (0.0074)	1.27E-21	0.0748 (0.0075)	3.51E-23	0.0646 (0.0080)	9.55E-16	5.73E-15
12q23.2	rs2195240	chr12:102856647	G	A	0.0492 (0.0074)	4.75E-11	0.0437 (0.0076)	8.64E-09	0.0572 (0.0080)	1.09E-12	6.51E-12
12q23.2	rs703545	chr12:102943000	A	G	-0.0494 (0.0075)	5.87E-11	-0.0439 (0.0076)	9.76E-09	-0.0371 (0.0081)	4.62E-06	0.0000277

‡ From GCTA (Genome-wide complex trait) - COJO (Conditional or joint) analysis. * Beta coefficient and p-values from the alternative phase unadjusted and adjusted for Bonferroni correction = 0.05/6.

Supplementary Table 4.2B: Conditionally independent genome-wide association results for total cerebellar volumes in phase 2 (n=15,447) sub-cohort, including replication values from phase 1 (n=17,818)

Cytoband	Index SNP	Chromosome: Physical Location	A1	A2	β (SE) - GWAS	p - GWAS	β (SE) - COJO‡	p - COJO‡	β (SE) - GWAS Phase 1*	p - GWAS Phase 1*	$p_{\text{Bonferroni}}$ - GWAS Phase 1*
1p32.3	rs12091097	chr1:51659401	C	A	0.0565 (0.0080)	2.03E-12	0.0565 (0.0080)	2.37E-12	0.0470 (0.0074)	3.45E-10	2.07E-09
4q24	rs13135092	chr4:103198082	G	A	0.0521 (0.0080)	9.97E-11	0.0521 (0.0080)	1.16E-10	0.0541 (0.0075)	5.32E-13	3.19E-12
7q36.3	rs10244637	chr7:156157853	G	A	0.0531 (0.0080)	4.03E-11	0.0531 (0.0081)	6.89E-11	0.0275 (0.0075)	0.000247	0.00148
8p23.1	rs2572397	chr8:111176403	A	G	-0.0466 (0.0080)	6.67E-09	-0.0466 (0.0081)	9.24E-09	-0.0202 (0.0075)	0.00703	0.0422
9q33.1	rs72754248	chr9:119061396	A	G	0.0646 (0.0080)	8.89E-16	0.0682 (0.0081)	3.69E-17	0.0714 (0.0074)	1.44E-21	8.63E-21
12q23.2	rs5742632	chr12:102856474	G	A	0.0577 (0.0080)	6.99E-13	0.0577 (0.0081)	1.22E-12	0.0489 (0.0074)	6.65E-11	3.99E-10

‡ From GCTA (Genome-wide complex trait) - COJO (Conditional or joint) analysis. * Beta coefficient and p-values from the alternative phase unadjusted and adjusted for Bonferroni correction = 0.05/6.

Supplementary Table 4.3: Polygenic (PGS) score between-phase prediction of total cerebellar volume

GWAS	SNP inclusion p-value threshold	$\Delta R^2 \ddagger$	β	95% Confidence interval		p	$p_{\text{Bonferroni}}^*$
Phase 1 GWAS predicting Phase 2 individuals' cerebellar volume	0.001	0.017	0.13	0.11	0.14	2.9E-106	2.9E-105
	0.005	0.019	0.13	0.12	0.15	7.6E-121	7.6E-120
	0.01	0.019	0.13	0.12	0.15	1.9E-121	1.9E-120
	0.05	0.019	0.13	0.12	0.14	5.9E-118	5.9E-117
	0.1	0.019	0.13	0.12	0.15	3.0E-121	3.0E-120
Phase 2 GWAS predicting Phase 1 individuals' cerebellar volume	0.001	0.009	0.09	0.08	0.11	3.2E-67	3.2E-66
	0.005	0.011	0.11	0.09	0.12	3.1E-83	3.1E-82
	0.01	0.012	0.11	0.10	0.12	1.7E-95	1.7E-94
	0.05	0.015	0.12	0.11	0.13	1.4E-113	1.4E-112
	0.1	0.014	0.12	0.11	0.13	3.4E-112	3.4E-111

*Results are from independent univariate linear regression models of each polygenic score derived from GWAS results of the opposing phase, predicting total cerebellar volume, with correction for covariates of age, sex, total brain volume, imaging centre attended, data attended, participant head and table position in the scanner, and the first 10 genetic principal components. \ddagger Unique R^2 explained by polygenic score. Calculated: R^2 of model with polygenic score - R^2 of model without polygenic score. * p-value adjusted for Bonferroni correction = 0.05/10*

Supplementary Table 4.4A: Genetic correlation of total cerebellar volume with previously published cerebellar measures

GWAS		h^2_{SNP} (%)†	h^2_{SNP} SE (%)†	rg ‡	95% Confidence interval‡		p	$p_{\text{Bonferroni}}$ *
Elliott et al 2018 ¹	Total cerebellum (R)	25.2	6.4	0.98	0.77	1.20	1.23E-18	8.60E-18
	Total cerebellum (L)	31.9	6.3	0.92	0.75	1.08	8.86E-28	6.20E-27
Zhao et al 2019 ²	Cerebellar hemisphere (R)	35.7	4.1	0.91	0.84	0.98	1.86E-149	1.30E-148
	Cerebellar hemisphere (L)	36.2	4.0	0.91	0.84	0.97	6.55E-145	4.58E-144
	Cerebellar vermis IV-V	31.9	4.1	0.44	0.28	0.60	8.75E-08	6.12E-07
	Cerebellar vermis VI-VII	24.4	3.7	0.45	0.32	0.57	5.29E-12	3.71E-11
	Cerebellar vermis VIII-X	36.7	4.7	0.56	0.46	0.65	2.86E-29	2.00E-28

† LDSC calculated SNP-based heritability and standard error (SE) and ‡ LDSC calculated genetic correlation (rg) and 95% confidence intervals. * p -value adjusted for Bonferroni correction = 0.05/7

Sources 1: (Elliott et al., 2018)

2: (Zhao et al., 2019)

Supplementary Table 4.4B: Genetic correlation of total cerebellar volume with anthropomorphic measures of interest

GWASs ¹	h^2_{SNP} (%)†	h^2_{SNP} SE (%)†	rg ‡	95% Confidence intervals‡		p	$p_{\text{Bonferroni}}$ *
Standing Height	46.5	2.3	0.04	-0.01	0.09	0.11	0.68
Sitting Height	33.2	1.8	0.05	0.00	0.11	0.07	0.40
Birth Weight	10.9	0.6	-0.03	-0.10	0.04	0.46	1.00
Body Mass Index	24.8	0.8	-0.07	-0.12	-0.01	0.01	0.08
Weight	26.6	1.0	-0.04	-0.09	0.01	0.15	0.88
Body Fat %	21.8	0.7	-0.07	-0.12	-0.01	0.01	0.09

† LDSC calculated SNP-based heritability and standard error (SE). ‡ LDSC calculated genetic correlation (rg) and 95% confidence intervals. * p-value adjusted for Bonferroni correction = 0.05/7

Sources: 1: All GWASs from <http://www.nealelab.is/uk-biobank/>

Supplementary Table 4.4C: Genetic correlation of total cerebellar volume with other brain-based measures

GWASs	h^2_{SNP} (%)†	h^2_{SNP} SE (%)†	rg ‡	95% Confidence interval‡		p	$p_{\text{Bonferroni}}$ *
Brainstem 1	31.7	3.4	0.47	0.37	0.58	1.02E-18	1.02E-17
Caudate 1	28.6	2.6	-0.07	-0.18	0.04	0.20	1.00
Putamen 1	28.6	2.8	0.01	-0.10	0.11	0.88	1.00
Accumbens 1	20.2	2.3	-0.07	-0.20	0.06	0.29	1.00
Pallidum 1	16.9	2.3	0.31	0.19	0.43	0.00000045	0.0000045
Thalamus 1	16.0	2.1	0.24	0.12	0.36	0.0000645	0.000645
Amygdala 1	8.4	1.9	-0.18	-0.37	0.01	0.07	0.67
Hippocampus 2	13.0	2.7	-0.14	-0.29	0.02	0.08	0.84
Cortical surface area 3	35.3	3.2	-0.14	-0.25	-0.04	0.007	0.07
Cortical thickness 3	26.5	2.2	-0.01	-0.11	0.10	0.91	1.00

† LDSC calculated SNP-based heritability and standard error (SE). ‡ LDSC calculated genetic correlation (rg) and 95% confidence intervals. * p-value adjusted for Bonferroni correction = 0.05/10

Sources:

1: (Satizabal et al., 2019)

2: (Hibar et al., 2017)

3: (Grasby et al., 2020)

Supplementary Table 4.5: Positional gene mapping of each independent COJO identified extended LD region

Locus	Cytoband	Index SNP	Antisense	lincRNA (long intergenic non-coding RNA)	miRNA (microRNA)	Protein - coding	Pseudogene
1	1p34.2	rs12127002	RP1-118J21.25 RP1-118J21.5			BMP8B MFSD2A MYCL OXCT2 TRIT1	RP1-118J21.24 RP3-342P20.2
2	1p32.3	rs7530673	RP11-191G24.1 RP11-253A20.1 RP11-275F13.1 RP11-296A18.6 RP11-91A18.4 RP4-657D16.3 RP4-657D16.6 RP5-850O15.3 TXNDC12-AS1	RP11-296A18.3 RP5-850O15.4	AL162430.1 AL162430.2 AL589663.1 MIR4421 MIR761	BTF3L4 C1orf185 CDKN2C DMRTA2 EPS15 FAF1 KTI12 NRD1 OSBPL9 RAB3B RNF11 TTC39A TXNDC12 ZFYVE9	CALR4P CFL1P2 FCF1P6 GAPDHP51 HMGB1P45 MRPS6P2 PHBP12 RP11-275F13.3 RP11-296A18.5 RP11-91A18.1 RP4-800M22.1 RP4-800M22.2 SLC25A6P3 TSEN15P2
2	1p32.3	rs1278519	RP5-850O15.3	RP11-296A18.3 RP5-850O15.4	AL162430.1 AL162430.2 MIR4421	C1orf185 CDKN2C DMRTA2 FAF1	CFL1P2 FCF1P6 HMGB1P45 MRPS6P2 PHBP12 RP11-183G22.1
3	2p23.3	rs6546070		AC012074.2	MIR1301	DNMT3A DTNB	AC012074.1
4	2p11.2	rs7593335	AC062029.1 AC104134.2		AC012671.1 AC096579.1 MIR4436A	EIF2AK3 RPIA TEX37	ANKRD36BP2

			AC007557.2				
5	2q35	rs2542212	AC007557.4	AC007557.3 RP11-		AC007557.1 TNP1	
			AC007563.1	574O16.1			
			AC007563.5				
6	2q36.1	rs75779789		RP11-384O8.1		CCDC140 PAX3 SGPP2	AC010980.2
						AMIGO3 AMT APEH ARIH2	
						ARIH2OS ATRIP BSN C3orf62	
						C3orf84 CAMKV CAMP	
						CCDC36 CCDC51 CCDC71	
						CDC25A CDHR4 CELSR3	
			BSN-AS1 CTD-			COL7A1 CTD-2330K9.3 DAG1	
			2330K9.2 NICN1-		AC104448.1	DALRD3 FAM212A FBXW12	
			AS1 PRKAR2A-AS1		AC139451.1	GMPPB GPX1 IMPDH2 IP6K1	ACTBP13 COX6CP14 FCF1P2
			RP11-148G20.1	BSN-AS2 RP11-572O6.1	MIR191 MIR2115	IP6K2 KLHDC8B LAMB2	MRPS18AP1 NDUFB1P1 RP11-
7	3p21.31	rs7640903	RP11-24C3.2	RP13-131K19.7	MIR425 MIR4271	MON1A MST1 MST1R	3B7.7 RP11-694I15.7 RP13-
			RP11-493K19.3		MIR4443	NCKIPSD NDUFAF3 NICN1	1056D16.2 SNRPFP4
			RP13-131K19.1		MIR4793	NME6 P4HTM PFKFB4 PLXNB1	
			RP13-131K19.2		MIR5193 MIR711	PRKAR2A QARS QRICH1 RBM5	
			RP13-131K19.6			RBM6 RHOA RNF123 RP11-	
						3B7.1 SHISA5 SLC25A20	
						SLC26A6 SPINK8 TCTA TMA7	
						TMEM89 TRAIPTREX1 UBA7	
						UCN2 UQCRC1 USP19 USP4	
						WDR6 ZNF589	

8	4p16.2	rs10033073	STX18-AS1	RP11-326I19.3		MSX1	LDHAP1
9	4q22.1	rs4148155	RP11-742B18.1	RP11-10L7.1		ABCG2 HERC6 IBSP MEPE PKD2 PPM1K SPP1	CHCHD2P7 HSP90AB3P RP11- 147K6.1 RP11-147K6.2
10	4q24	rs13135092	AF213884.2 RP11- 498M5.2	RP11-499E18.1		BANK1 NFKB1 SLC39A8	AF213884.1 MTND5P5
11	4q31.21	rs6812830	HHIP-AS1	RP11-361D14.2 RP13- 539F13.3		ABCE1 ANAPC10 HHIP OTUD4	HSPD1P5 KRT18P51 RP13- 539F13.2 RPS23P4
12	5q14.2	rs55803832		CTD-2015A6.1 CTD- 2015A6.2		ATP6AP1L	
13	5q22.2	rs3846716	CTC-487M23.5 CTC-487M23.7	RP11-159K7.2	AC008536.1	APC CTC-487M23.8 CTC- 554D6.1 REEP5 SRP19 ZRSR1	CBX3P3 XBP1P1
14	5q33.3	rs7380908	CTD-2363C16.1 CTD-2363C16.2	RP11-175K6.1		EBF1	
15	6p22.3	rs9393227		CASC14 CASC15			
16	6p22.2	rs1800562	RP1-313I6.12 U91328.21 ZSCAN16-AS1	CTA-14H9.5 HCG11 LINC00240 RP1- 153G14.4 RP1- 265C24.8 RP1-86C11.7 RP11-239L20.6 RP11- 457M11.5 U91328.19 U91328.20 U91328.22	AL021917.1 AL160037.1 MIR3143 TRNAI2 TRNAI6	ABT1 BTN1A1 BTN2A1 BTN2A2 BTN3A1 BTN3A2 BTN3A3 GPX5 GPX6 HFE HIST1H1A HIST1H1B HIST1H1C HIST1H1D HIST1H1E HIST1H1T HIST1H2AA HIST1H2AB HIST1H2AC HIST1H2AD HIST1H2AE HIST1H2AG HIST1H2AH HIST1H2AI HIST1H2AJ HIST1H2AK	AL022393.7 BTN2A3P COX11P1 GUSBP2 HIST1H1PS1 HIST1H1PS2 HIST1H2APS1 HIST1H2APS2 HIST1H2APS3 HIST1H2APS4 HIST1H2BPS1 HIST1H2BPS2 HIST1H3PS1 HIST1H4PS1 HNRNPA1P1 IQCB2P LARP1P1 MCFD2P1 OR1F12 OR2B7P OR2B8P OR2E1P OR2W2P OR2W4P

HIST1H2AL HIST1H2AM	OR2W6P PRELID1P2 RP1-
HIST1H2BA HIST1H2BB	15D7.1 RP1-265C24.5 RP1-
HIST1H2BC HIST1H2BD	34B20.4 RP1-97D16.1 RP11-
HIST1H2BE HIST1H2BF	209A2.1 RP11-239L20.3 RP11-
HIST1H2BG HIST1H2BH	457M11.6 RP3-522P13.2 RP5-
HIST1H2BI HIST1H2BJ	874C20.3 RP5-874C20.6
HIST1H2BK HIST1H2BL	RPLP2P1 RSL24D1P1 TOB2P1
HIST1H2BM HIST1H2BN	U91328.2 VN1R10P VN1R11P
HIST1H2BO HIST1H3A	VN1R12P VN1R13P VN1R14P
HIST1H3B HIST1H3C	XXbac-BPG34I8.3 XXbac-
HIST1H3D HIST1H3E HIST1H3F	BPGBPG24O18.1 XXbac-
HIST1H3G HIST1H3H HIST1H3I	BPGBPG34I8.1 ZNF192P1
HIST1H3J HIST1H4A HIST1H4B	ZNF192P2 ZNF204P
HIST1H4C HIST1H4D HIST1H4E	ZSCAN12P1
HIST1H4F HIST1H4G	
HIST1H4H HIST1H4I HIST1H4J	
HIST1H4K HIST1H4L HMG4	
LRRC16A NKAPL OR2B2 OR2B6	
PGBD1 POM121L2 PRSS16	
SCAND3 SCGN SLC17A1	
SLC17A2 SLC17A3 SLC17A4	
TRIM38 ZKSCAN3 ZKSCAN4	
ZKSCAN8 ZNF165 ZNF184	
ZNF322 ZNF391 ZSCAN12	

			ZSCAN16 ZSCAN23 ZSCAN31				
			ZSCAN9				
17	6q16.2	rs546897	RP1-199J3.7 RP11-98I9.4 TSTD3		CCNC COQ3 FAXC PNISR PRDM13 USP45	RP1-199J3.5	
18	6q21	rs1935951		LINC00222	FOXO3 LACE1	RP1-128O3.6 RP11-697G4.4 RP11-72I2.1 RP3-466I7.1 SUMO2P8	
19	6q22.32	rs72971190			MIR588	CENPW	PRELID1P1 RPS4XP9 VIMP1
20	7q36.3	rs57131976		AC073133.1 AC073133.2			
20	7q36.3	rs11764163				RP11-362B23.1	
21	8p23.1	rs2572397	AF131216.5 AF131216.6 CTD- 2135J3.3 FAM85B PRSS51 RP11- 10A14.3 RP11- 148O21.2 RP11- 148O21.3 RP11- 148O21.4 RP11- 177H2.2 RP11- 1E4.1 RP11- 375N15.2	AF131215.6 AF131215.8 CTA- 398F10.1 CTA- 398F10.2 CTD- 3023L14.1 CTD- 3023L14.2 CTD- 3023L14.3 LINC00208 LINC00529 LINC00599 RP11-10A14.5 RP11- 10A14.6 RP11-10A14.7 RP11-115J16.1 RP11- 115J16.2 RP11-	AC023385.1 AC087269.2 MIR4286 MIR4660 MIR597 MIR598	AF131215.5 BLK C8orf12 C8orf49 C8orf74 CLDN23 CTSB DEFB130 DEFB134 DEFB135 DEFB136 ERI1 FAM167A FDFT1 GATA4 LRLE1 MFHAS1 MSRA MTMR9 NEIL2 PINX1 PPP1R3B PRSS55 RP11- 10A14.4 RP11-297N6.4 RP11- 481A20.11 RP1L1 SGK223 SLC35G5 SOX7 TNKS XKR6	AC087269.1 AF131215.1 ALG1L13P CTC-493P15.2 ENPP7P1 FAM86B3P OR7E158P OR7E160P OR7E161P RP11-1081K18.1 RP11-10A14.8 RP11-1236K1.11 RP11-212F11.1 RP11-375N15.1 RP11-481A20.10 RP11- 481A20.4 RP11-481A20.8 RP11-589N15.1 RP11-62H7.2 RP11-62H7.3 RPL19P13 SUB1P1 TDH

				115J16.3 RP11- 148O21.6 RP11- 211C9.1 RP11-981G7.2 RP11-981G7.3 RP11- 981G7.6			
22	8q24.3	rs6984592		RP11-128L5.1		DENND3 PTK2	
23	9q31.2	rs7027172	RP11-508N12.2	RP11-196I18.4 RP11- 308N19.1 RP11- 308N19.3 RP11- 308N19.4		RP11-508N12.4 ZNF462	RP11-196I18.2 RP11-196I18.3 RP11-308N19.5 RP11-417L14.1 RP11-508N12.3
24	9q33.1	rs72754248	PAPPA-AS2 RP11- 45A16.4		AL137024.1	ASTN2 PAPPA PAPPA-AS1	
24	9q33.1	rs17220352	RP11-264C15.2 RP11-67K19.3		AL137024.1	ASTN2 PAPPA PAPPA-AS1 TRIM32	
25	9q34.11	rs3118634	HMGA1P4 RP11- 247A12.1 RP11- 247A12.2 RP11- 247A12.8 RP11- 545E17.3	RP11-167N5.5 RP11- 247A12.7	AL158151.1 AL158151.2	C9orf114 CCBL1 CRAT DOLK DOLPP1 ENDOG FAM73B IER5L LRRC8A NUP188 PHYHD1 PKN3 PPP2R4 RP11- 101E3.5 SET SH3GLB2 SPTAN1 TBC1D13 WDR34 ZDHHC12 ZER1	VTI1BP4
26	10q26.13	rs4752582	RP11-78A18.2	RP11-62L18.3		ATE1 FGFR2	RPS15AP5
27	12q23.2	rs5742632	RP11-554E23.4	RP11-554E23.2		CCDC53 DRAM1 IGF1 NUP37 PARPBP PMCH	RP11-18O15.1 RP11-21OL7.1 RP11-554E23.3

27	12q23.2	rs703545	RP11-554E23.4			CCDC53 DRAM1 IGF1 NUP37 PARPBP PMCH	RP11-18O15.1 RP11-210L7.1
28	13q21.33	rs529059					AC022558.1 ADAMTS7P1
			RP11-382A20.2			AP3B2 BNC1 BTBD1 C15orf40	ADAMTS7P2 CSPG4P10
			RP11-382A20.4			CPEB1 EFTUD1 FAM103A1	CSPG4P8 CSPG4P9 DNM1P38
			RP11-382A20.5		AC010724.1	FAM154B FSD2 GOLGA6L10	DNM1P42 GOLGA6L17P
			RP11-382A20.6		AC105339.2	GOLGA6L18 GOLGA6L19	GOLGA6L21P RP11-152F13.3
29	15q25.2	rs62012045	RP11-382A20.7	AC105339.1	AC126339.1	GOLGA6L20 GOLGA6L9	RP11-152F13.7 RP11-382A20.1
			RP11-752G15.3		AC135995.1	HDGFRP3 HOMER2 RP11-	RP11-752G15.4 RP11-
			RP11-752G15.6		MIR4515	152F13.10 RP11-379H8.1	752G15.9 RP13-608F4.5 RP13-
			RP11-752G15.8			RP11-597K23.2 RPS17 RPS17L	608F4.6 RP13-996F3.3 RPL9P8
						TM6SF1 WHAMM	UBE2Q2P2 UBE2Q2P3
							UBE2Q2P6

Notes: Overlapping gene transcripts within 500kb of the extended LD region for each COJO-identified index SNP

Supplementary Table 4.6: Functional annotation results for the most deleterious SNP (index SNP and SNPs $r^2 > 0.8$) within each independent genomic region

Locus	Cytoband	Index SNP	Highest CADD SNP	R ² between SNP and CADD	CADD Score	PolyPhen	SIFT	Consequence
1	1p34.2	rs12127002	rs3134614	0.88	4.1	benign	tolerated	Non-synonymous (MYCL)
2	1p32.3	rs7530673	rs17106445	1.00	7.7			
2	1p32.3	rs1278519	rs2784124	0.84	10.9			Non-coding change (HMGB1P45)
3	2p23.3	rs6546070	rs12104791	1.00	1.5			
4	2p11.2	rs7593335	rs867529	0.97	18.3	benign	tolerated	Non-synonymous (EIF2AK3)
5	2q35	rs2542212	rs78038594	1.00	0.1			
6	2q36.1	rs75779789	rs75239294	1.00	4.1			
7	3p21.31	rs7640903	rs6795772	1.00	5.2			
8	4p16.2	rs10033073	rs6446685	0.98	12.7			
9	4q22.1	rs4148155	rs45499402	1.00	0.1			
10	4q24	rs13135092	rs13107325	0.95	34.0	Possibly damaging	deleterious	Non-synonymous (SLC39A8)
11	4q31.21	rs6812830	rs34958276	0.89	6.2			
12	5q14.2	rs55803832	rs2385949	0.92	4.6			
13	5q22.2	rs3846716	rs396321	0.87	7.8			Non-coding change (CBX3P3)
14	5q33.3	rs7380908	rs72813911	0.89	14.8			

15	6p22.3	rs9393227	rs4711000	0.98	18.7			
16	6p22.2	rs1800562	rs1800562	1.00	25.7	Probably damaging	deleterious	Non-synonymous (HFE)
17	6q16.2	rs546897	rs12210442	0.90	8.7			
18	6q21	rs1935951	rs2153960	0.95	7.6			
19	6q22.32	rs72971190	rs4895816	1.00	11.7			
20	7q36.3	rs57131976	rs13224457	0.83	6.7			
20	7q36.3	rs11764163	rs11764163	1.00	7.7			
21	8p23.1	rs2572397	rs2572397	NA	2.8			
22	8q24.3	rs6984592	rs1868276	0.94	3.7			
23	9q31.2	rs7027172	rs62568588	1.00	14.5			
24	9q33.1	rs72754248	rs35565319	1.00	14.4			Synonymous (PAPPA)
24	9q33.1	rs17220352	rs12684144	0.95	15.7			
25	9q34.11	rs3118634	rs2480452	1.00	23.9	benign	tolerated	Non-synonymous (PTPA)
26	10q26.13	rs4752582	rs4752582	1.00	12.0			
27	12q23.2	rs5742632	rs5742629	0.81	5.4			
27	12q23.2	rs703545	rs10778177	0.93	4.4			
28	13q21.33	rs529059	rs490599	0.81	2.9			
29	15q25.2	rs62012045	rs62012044	1.00	5.8			

Notes: All SNPs (index and proxy high LD SNPs) within each independent genomic region viewable in additional file and https://osf.io/jr8m2/?view_only=29906bc730f64cf58a81d67ff5c50363)

Supplementary Table 4.7: The cis-expression quantitative tract loci (cis-eQTL) overlapping with each independent genomic region which shows the greatest expression change

Locus	Cytoband	Index SNP	Greatest eQTL (SNP-ALLELE; Beta(SE) p)	R ² between SNP and eQTL	Gene Symbol	Tissue
7	3p21.31	rs7640903	rs3774800-G; 0.437(0.064) p = 5.0e-10	0.83	AMT	Cerebellar Hemisphere
7	3p21.31	rs7640903	rs3774800-G; 0.579(0.054) p = 3.0e-19	0.83	AMT	Cerebellum
7	3p21.31	rs7640903	rs3774800-G; -0.564(0.065) p = 7.3e-14	0.83	CCDC71	Cerebellar Hemisphere
7	3p21.31	rs7640903	rs3774800-G; -0.458(0.060) p = 6.3e-12	0.83	CCDC71	Cerebellum
7	3p21.31	rs7640903	rs3774800-G; -0.314(0.053) p = 2.9e-08	0.83	GPX1	Cerebellum
7	3p21.31	rs7640903	rs3774800-G; 0.450(0.061) p = 4.2e-11	0.83	NCKIPSD	Cerebellar Hemisphere
7	3p21.31	rs7640903	rs3774800-G; 0.311(0.051) p = 1.4e-08	0.83	NCKIPSD	Cerebellum
7	3p21.31	rs7640903	rs3774800-G; -0.325(0.050) p = 2.4e-09	0.83	WDR6	Cerebellar Hemisphere
7	3p21.31	rs7640903	rs3774800-G; -0.392(0.046) p = 7.1e-14	0.83	WDR6	Cerebellum
12	5q14.2	rs55803832	rs55803832-A; 0.468(0.059) p = 1.5e-12	NA	VCAN	Cerebellum
17	6q16.2	rs546897	rs548653-A; 0.884(0.148) p = 3.2e-08	1.00	RP1-199J3.5	Cerebellar Hemisphere
21	8p23.1	rs2572397	rs2572398-A; 0.380(0.057) p = 1.0e-09	1.00	AF131216.5	Cerebellum
21	8p23.1	rs2572397	rs2251473-C; 0.661(0.102) p = 2.9e-09	0.98	RP11-481A20.10	Cerebellar Hemisphere
21	8p23.1	rs2572397	rs10481454-C; -0.591(0.087) p = 5.4e-10	0.89	RP11-481A20.10	Cerebellum
21	8p23.1	rs2572397	rs10481454-C; -0.732(0.098) p = 3.2e-11	0.89	RP11-481A20.11	Cerebellar Hemisphere
21	8p23.1	rs2572397	rs2251473-C; 0.659(0.110) p = 2.1e-08	0.98	RP11-481A20.11	Cerebellum
22	8q24.3	rs6984592	rs35807050-A; -0.333(0.056) p = 2.6e-08	0.94	PTK2	Cerebellum
25	9q34.11	rs3118634	rs3118634-G; -0.647(0.068) p = 4.0e-16	NA	PPP2R4	Cerebellum
25	9q34.11	rs3118634	rs2480452-C; 0.914(0.144) p = 3.9e-09	1.00	RP11-247A12.2	Cerebellum
25	9q34.11	rs3118634	rs2480452-C; 1.448(0.122) p = 5.9e-21	1.00	RP11-247A12.7	Cerebellar Hemisphere

25	9q34.11	rs3118634	rs2480452-C; 1.460(0.126) p = 3.7e-21	1.00	RP11-247A12.7	Cerebellum
----	---------	-----------	---------------------------------------	------	---------------	------------

Notes: All cis-eQTLs which overlap with each independent genomic region viewable in additional file and https://osf.io/jr8m2/?view_only=29906bc730f64cf58a81d67ff5c50363

Supplementary Table 4.8: Genes identified by summary data-based Mendelian randomisation (SMR) analysis

Locus	Cytoband	Tissue	Probe ID	Gene Symbol	Top SMR Marker	Top SMR Marker Position	p(eQTL) [†]	p(GWAS) [‡]	p(SMR) [§]	p(HEIDI) [¥]	N _{SNPs}	HEIDI [¥]
12	5q14.2	Cerebellum	ENSG00000038427.11	VCAN	rs55803832	81920587	1.48E-12	3.09E-12	6.93E-07	0.57	10	
21	8p23.1	Cerebellum	ENSG00000253893.2	FAM85B	rs2980439	8094870	3.58E-21	1.01E-06	1.40E-05	0.43	20	
21	8p23.1	Cerebellar Hemisphere	ENSG00000173295.3	FAM86B3P	rs1878561	8092405	2.85E-19	1.77E-06	2.44E-05	0.39	20	
21	8p23.1	Cerebellum	ENSG00000173295.3	FAM86B3P	rs1878561	8092405	2.37E-25	1.77E-06	1.39E-05	0.12	20	
25	9q34.11	Cerebellum	ENSG00000119383.15	PPP2R4	rs3118634	131905854	3.99E-16	2.14E-10	5.87E-07	0.27	14	
25	9q34.11	Cerebellum	ENSG00000204055.4	RP11-247A12.2	rs3118634	131905854	6.18E-09	2.14E-10	1.87E-05	0.47	13	
25	9q34.11	Cerebellar Hemisphere	ENSG00000268707.1	RP11-247A12.7	rs3124505	131887856	1.94E-20	1.31E-08	1.31E-06	0.17	19	
25	9q34.11	Cerebellum	ENSG00000268707.1	RP11-247A12.7	rs3118634	131905854	1.16E-20	2.14E-10	1.65E-07	0.23	19	

[†] p-values from the expression quantitative trait locus (eQTL) association within cerebellar tissue (cerebellum or cerebellar hemisphere). [‡] p-values from the total cerebellar volume meta-genome-wide association study (GWAS). [§] p-values from the SMR mediation analysis. [¥] p-values from the HEIDI (heterogeneity in dependent instruments) test with p>0.05 indicating pleiotropic (over linkage) associations. The number of single nucleotide polymorphisms (SNPs) within each HEIDI test (N_{SNPs}>10) are provided.

Supplementary Table 4.9: Sign test results for independent schizophrenia-associated SNPs with total cerebellar volume

CHR	Schizophrenia GWAS reported lead SNP†						Schizophrenia GWAS lead SNP present in cerebellar GWAS‡				Cerebellar GWAS §		Same direction of effect¶
	Start	End	rsID	A1	Odds ratio (SCZ)	P (SCZ)	rsID (LD)	A1 (LD)	Beta (SCZ.LD)	P (SCZ.LD)	Beta (tCB)	P (tCB)	
1	2368232	2402499	rs4648845	C	0.926	6.74E-12	rs34732885	G	0.015	3.89E-01	-0.019	7.65E-04	0
1	8352642	8838528	rs34269918	G	0.941	3.27E-09	rs141582190	G	0.060	4.86E-04	0.019	7.49E-04	1
1	30411185	30516776	rs6694545	A	1.080	6.20E-12					-0.005	0.35	0
1	43793214	44480093	rs2970610	T	1.070	1.39E-11	rs4141739	A	-0.034	5.79E-04	-0.020	2.42E-04	1
1	66205718	66552709	rs12129719	G	0.947	3.35E-08					0.003	0.56	0
1	73264393	74115945	rs12129573	C	0.926	8.94E-15					-0.006	0.29	1
1	95746349	95944432	rs6680011	A	0.929	2.83E-08					-0.001	0.92	1
1	97731961	97885249	rs11165867	C	0.933	3.87E-08	rs115359427	C	-0.039	1.95E-01	0.017	1.87E-03	0
1	98036832	98651527	rs2660304	G	0.897	2.18E-18	rs79230710	A	-0.034	3.08E-01	-0.015	7.63E-03	1
1	149998923	151115887	rs140505938	C	1.087	6.50E-10	rs41264469	G	-0.067	2.99E-06	-0.015	7.63E-03	1
1	173479023	175000887	rs6701877	G	1.076	2.37E-08	rs142410559	A	0.002	9.63E-01	-0.017	2.70E-03	0
1	177170720	177428790	rs4650963	T	1.056	1.16E-08	rs115668034	A	0.035	8.70E-02	0.016	2.91E-03	1
1	190585303	190719743	rs55770408	T	0.941	3.02E-08	rs6675124	C	0.078	2.11E-04	-0.014	8.75E-03	0
1	190757036	191408693	rs28374258	T	0.929	6.35E-10	rs79033056	A	-0.072	5.07E-02	-0.016	4.90E-03	1
1	200250436	200421466	rs6678676	T	0.937	3.22E-08	rs184060765	A	-0.024	6.53E-01	-0.013	0.02	1
1	239166610	239298749	rs72769124	C	0.897	4.73E-10					-0.009	0.12	1
1	243203672	243627135	rs10803138	A	0.935	2.03E-09					0.007	0.22	0

1	243614180	244025999	rs14403	C	1.077	1.71E-10	rs1417121	C	-0.064	5.02E-09	0.018	9.45E-04	0
2	22499207	22822159	rs12712510	T	1.059	8.18E-09	rs116457567	C	0.080	1.20E-03	0.014	9.65E-03	1
2	57895438	58502679	rs75575209	A	0.905	4.60E-09	rs72808453	G	0.010	5.43E-01	-0.017	2.57E-03	0
2	57941185	58500141	rs7596038	C	1.070	2.37E-12	rs72808453	G	0.010	5.43E-01	-0.017	2.57E-03	0
2	57950104	58450569	rs77011057	A	1.116	4.48E-08					-0.001	0.85	0
2	73129974	73168593	rs2077586	A	1.063	2.96E-08	rs149913304	G	0.014	6.82E-01	-0.007	0.24	0
2	73511262	74101954	rs56145559	C	0.931	1.01E-09	rs138634444	A	0.045	1.08E-01	-0.013	0.02	0
2	145120947	145214607	rs12991836	A	0.941	6.46E-10					-0.006	0.31	1
2	146363633	146441828	rs56807175	T	0.916	1.36E-11	rs72857410	T	0.083	2.09E-10	0.016	4.50E-03	1
2	185405580	186057716	rs10196799	A	1.058	4.51E-09					-0.003	0.65	0
2	198144002	198954774	rs6434928	G	1.076	3.62E-13					-0.001	0.87	0
2	199776050	200305460	rs1451488	A	0.935	4.75E-12					-0.002	0.66	1
2	199921578	200332499	rs34719143	T	1.093	7.71E-09	rs115307848	A	0.110	3.40E-03	-0.012	0.03	0
2	200387210	200632032	rs76432012	T	1.150	2.75E-08	rs116738213	A	0.117	2.44E-04	-0.015	7.76E-03	0
2	200536068	201309547	rs2949006	T	1.105	3.69E-17	rs6710393	G	0.067	2.89E-08	-0.028	2.53E-07	0
2	200768453	200768453	rs200626410	T	0.929	2.95E-09	NA	NA	NA	NA	NA	NA	NA
2	201113452	201333001	rs1347692	C	1.062	4.11E-10	rs55985986	C	0.091	1.12E-12	-0.019	5.52E-04	0
2	225308978	225469611	rs11685299	C	1.062	3.86E-09	rs62187045	A	0.046	1.36E-01	0.019	7.94E-04	1
2	233550961	233814878	rs4144797	T	1.085	4.33E-16	rs151287640	G	0.016	6.40E-01	-0.015	6.79E-03	0
3	2428745	2582549	rs35346733	C	1.075	2.42E-12	rs140058085	A	-0.078	2.44E-02	-0.014	8.74E-03	1
3	10793110	10872262	rs6800435	C	0.921	2.00E-08					0.001	0.89	0
3	16747942	17119238	rs9881798	T	1.054	2.81E-08	NA	NA	NA	NA	NA	NA	NA
3	17219137	17888256	rs11409090	A	0.942	2.11E-09	rs114483162	G	0.067	8.37E-02	0.012	0.03	1

3	36834099	36964583	rs75968099	C	0.936	9.41E-11	rs62245258	A	-0.021	3.36E-01	-0.016	4.53E-03	1
3	52217088	53281183	rs1080500	G	1.075	2.71E-12					0.002	0.69	1
3	53273192	53539241	rs312477	G	1.067	1.38E-08					-0.001	0.80	0
3	60277174	60303504	rs1353545	G	0.943	5.67E-09					-0.004	0.49	1
3	63715318	64005452	rs704373	A	1.067	1.39E-10					-0.004	0.53	0
3	71481192	71679664	rs7632921	G	1.058	9.52E-09	rs146493624	A	0.035	4.90E-01	-0.014	9.26E-03	0
3	135669219	136752653	rs7432375	G	0.923	4.07E-12					-0.002	0.76	1
3	161146130	161520740	rs489939	G	1.059	1.24E-08					0.000	0.95	0
3	180524764	181245320	rs34796896	G	1.087	3.19E-12					0.010	0.06	1
3	180860434	181256285	rs55672338	T	0.943	1.52E-09	rs2338739	G	-0.004	7.38E-01	0.015	7.14E-03	0
4	23334811	23443552	rs215411	T	0.944	1.40E-08					0.011	0.04	0
4	102547366	103388441	rs13107325	C	0.852	1.19E-16	rs13135092	G	0.149	7.87E-16	0.053	3.23E-22	1
4	143629150	143924146	rs13121251	T	1.059	4.06E-08	rs4690710	A	-0.038	1.09E-02	0.015	6.16E-03	0
4	170198392	170647421	rs10520163	A	0.948	2.81E-08	rs139971598	G	-0.030	1.49E-01	-0.017	1.84E-03	1
4	176717618	176756594	rs12498839	G	0.880	9.67E-11					0.011	0.05	0
4	176795426	176973267	rs62334820	C	0.922	9.60E-12	rs117353042	A	0.060	7.40E-03	-0.014	1.36E-02	0
5	44642670	46405055	rs16902086	A	0.936	5.55E-11					-0.003	0.54	1
5	49441779	49884022	rs77853293	C	1.056	1.77E-08	rs150661049	A	-0.078	7.70E-03	0.013	0.02	0
5	59911693	60847272	rs7701440	T	0.930	3.72E-14	rs35948426	A	0.027	6.10E-03	0.023	2.53E-05	1
5	86909526	88224419	rs254782	A	0.882	4.40E-08					-0.004	0.46	1
5	87407727	88871993	rs16867576	A	1.106	1.65E-11					0.006	0.28	1
5	137450345	137948140	rs13169274	T	0.942	7.06E-10	rs35859846	C	0.021	3.07E-02	-0.016	4.14E-03	0
5	151437972	152654479	rs79212538	G	0.868	5.55E-10	rs114314973	A	-0.048	3.37E-01	0.015	6.81E-03	0

5	151887779	152360494	rs111294930	A	1.086	9.04E-12				-0.009	0.10	0	
5	152505453	152785000	rs2910032	C	1.065	3.72E-11	rs137916909	G	-0.123	3.30E-03	0.013	1.43E-02	0
5	152744817	152899532	rs12522290	C	1.083	1.34E-09				-0.006	0.25	0	
6	24988105	33842877	rs3130820	T	1.281	2.12E-44	rs1800562	A	-0.002	9.37E-01	-0.038	6.75E-12	1
6	73058954	73172294	rs1339227	C	1.065	3.76E-10	rs17795818	G	-0.004	9.07E-01	0.012	0.03	0
6	83789798	84092546	rs4470825	G	1.057	8.94E-09	rs180941361	C	-0.021	7.27E-01	-0.013	0.02	1
6	83967454	84414411	rs217287	C	1.072	9.53E-13	rs12194342	G	-0.001	9.67E-01	-0.021	1.68E-04	1
6	93044855	93177270	rs634940	G	0.939	1.30E-08	rs2555753	T	0.017	7.46E-02	-0.014	1.18E-02	0
6	114612973	114775668	rs760608	G	1.063	1.90E-08				0.009	0.11	1	
6	128301981	128334236	rs35736453	T	0.941	2.95E-08	rs13200150	G	-0.052	5.01E-07	0.014	1.48E-02	0
6	143629340	143714330	rs72342102	T	1.067	7.93E-09	rs140533274	G	0.004	9.31E-01	-0.014	1.20E-02	0
7	1851205	2343621	rs10650434	A	0.918	1.10E-18	rs11547270	G	0.020	8.05E-02	0.016	4.82E-03	1
7	24557497	24844736	rs146678232	CA	0.932	1.63E-08	rs116997662	G	0.025	4.60E-01	-0.011	0.04	0
7	85575489	87275389	rs147922658	T	0.850	7.71E-10	rs117220979	A	-0.037	4.85E-01	-0.016	3.15E-03	1
7	85924492	86580674	rs12704290	G	1.121	3.57E-14				-0.001	0.82	0	
7	104471787	105064593	rs7789569	T	1.067	7.00E-11	rs2470934	G	0.022	2.68E-01	-0.011	0.05	0
7	109946567	110245369	rs211829	T	1.061	2.29E-09	rs56190346	A	0.039	5.61E-05	0.015	7.15E-03	1
7	110737149	111236477	rs12705761	G	1.068	5.11E-11	rs10282461	C	0.002	9.07E-01	0.012	0.03	1
7	131533769	131619847	rs7801375	A	0.926	6.27E-09				0.010	0.08	0	
7	131619693	131627573	rs4523180	T	1.107	3.83E-08	rs4731831	A	0.011	2.96E-01	0.006	0.25	1
7	137010589	137093743	rs3735025	T	1.067	7.02E-11	rs2278101	A	0.030	1.39E-02	0.014	1.35E-02	1
8	4177231	4210746	rs139425113	G	0.936	8.48E-09	rs78569612	G	-0.008	7.06E-01	0.018	8.57E-04	0
8	8092025	10283602	rs11993663	C	0.946	3.40E-08				0.023	3.47E-05	0	

8	18388177	18458140	rs2410572	G	1.056	1.07E-08	rs17517750	C	0.026	9.05E-02	-0.010	0.07	0
8	26119170	26279173	rs1042992	C	0.929	3.67E-09	rs117651549	A	0.005	9.04E-01	0.018	1.56E-03	1
8	27186652	27330813	rs2565065	A	1.066	1.74E-09	rs77303640	A	0.067	2.69E-02	-0.014	1.22E-02	0
8	27319905	27470778	rs11783093	C	1.098	7.64E-12	rs7812347	A	-0.059	1.98E-07	-0.015	5.60E-03	1
8	33604120	34674539	rs55669358	T	0.909	1.37E-08	rs150879427	A	-0.055	2.04E-01	-0.017	2.01E-03	1
8	38014429	38316849	rs10156310	A	1.076	5.56E-10					-0.005	0.34	0
8	60475926	61117903	rs1473594	T	1.066	3.33E-11	rs142000453	A	0.015	7.19E-01	0.021	1.25E-04	1
8	89188046	89761163	rs7010876	T	1.064	6.51E-09					-0.006	0.27	0
8	111460027	112015011	rs36043959	G	1.070	4.07E-12	rs34990074	A	0.071	1.77E-01	0.016	3.65E-03	1
8	143267749	143410423	rs58033671	A	1.087	8.65E-18	rs150032561	G	-0.043	2.44E-01	-0.015	7.11E-03	1
8	143267760	143413334	rs67439964	T	1.075	1.16E-09	rs150032561	G	-0.043	2.44E-01	-0.015	7.11E-03	1
8	143293307	143404118	rs4976967	G	1.067	9.07E-09	rs150032561	G	-0.043	2.44E-01	-0.015	7.11E-03	1
9	84498152	85129970	rs1319017	G	0.936	7.82E-11					0.007	0.21	0
9	100991430	101079033	rs10985817	T	0.923	1.02E-09	rs12553553	A	-0.012	5.21E-01	-0.013	0.02	1
10	18538669	18574980	rs7099380	G	1.091	1.47E-08	NA	NA	NA	NA	NA	NA	NA
10	18601928	18968668	rs7893279	T	1.118	4.80E-13	rs76772953	G	0.060	1.72E-02	0.013	0.02	1
10	104229588	105274900	rs12416331	T	1.157	7.09E-18					-0.009	0.10	0
10	104613089	105218254	rs7476192	T	1.075	3.77E-12	rs148828123	A	-0.077	1.32E-01	0.019	7.48E-04	0
11	24264778	24533962	rs1899543	A	0.944	1.23E-09					0.006	0.25	0
11	30183742	30437981	rs1765142	C	0.944	1.13E-08	rs117947435	A	-0.024	4.59E-01	0.016	4.47E-03	0
11	46227161	47371598	rs7951870	T	0.911	2.99E-13	rs11039122	A	-0.042	1.76E-05	0.022	8.25E-05	0
11	57369008	57735431	rs7129727	G	0.939	1.47E-09	rs2511988	A	-0.005	6.22E-01	0.025	6.60E-06	0
11	65378028	65577846	rs58950470	G	0.944	2.07E-08	rs11227275	A	0.037	1.45E-04	-0.014	1.01E-02	0

11	113299829	113448762	rs2514218	G	0.917	2.42E-12	rs11608109	G	0.037	1.75E-04	-0.015	8.61E-03	0
11	113431960	113451229	rs4936277	A	1.058	1.52E-08	rs78141154	A	0.075	2.83E-05	-0.009	0.12	0
11	124583878	124653926	rs12293670	A	1.084	1.70E-15	rs626260	A	0.042	9.57E-02	0.012	0.03	1
11	130706918	130894699	rs35774874	T	1.071	1.97E-11	rs111758968	C	-0.015	6.07E-01	0.014	1.10E-02	0
11	132387460	132417766	rs5795787	G	1.056	2.69E-08	rs143520433	A	0.028	3.26E-01	0.008	0.16	1
11	132506523	132581442	rs2917569	T	1.063	3.11E-10	rs73593157	G	0.005	8.28E-01	-0.010	0.07	0
11	133792743	133853694	rs4936215	A	1.096	5.32E-14	rs144335194	A	-0.023	5.56E-01	0.017	2.29E-03	0
11	134282729	134297345	rs893949	C	1.055	2.98E-08	rs733856	A	0.051	1.50E-07	0.015	5.93E-03	1
12	2285731	2440464	rs2007044	A	0.915	5.63E-20					0.000	0.97	0
12	2456062	2523772	rs12823424	A	1.066	2.28E-09					0.001	0.88	1
12	23214508	23642695	rs1120004	T	1.064	1.42E-08	rs118158307	A	0.083	5.60E-02	0.018	1.11E-03	1
12	39414371	39964006	rs10783624	C	1.062	5.44E-09					-0.007	0.23	0
12	57331741	57519694	rs324015	T	0.931	1.42E-10	rs191785641	A	0.105	4.90E-03	0.016	3.12E-03	1
12	57569478	57836098	rs61937595	C	1.133	3.28E-11	rs181971945	C	-0.014	7.37E-01	0.014	1.09E-02	0
12	92243186	92395053	rs4240748	C	0.946	2.15E-08					0.001	0.92	0
12	103347511	103390444	rs36104021	CA	1.072	7.31E-09	rs61941101	A	-0.008	7.97E-01	0.021	1.22E-04	0
12	110265586	111275317	rs4766428	C	0.927	2.68E-14	rs71442737	G	0.047	4.68E-02	-0.011	0.04	0
12	123310521	123927262	rs2851447	G	1.091	5.55E-16					0.021	1.02E-04	1
13	79855297	80192906	rs9545047	A	1.058	1.15E-08					-0.007	0.20	0
14	29275791	29594625	rs10148671	T	0.939	5.46E-10	rs7142185	G	0.030	3.20E-03	0.019	4.82E-04	1
14	29999987	30300361	rs1191551	T	1.076	4.12E-10	rs45528442	G	0.098	2.60E-02	0.017	2.02E-03	1
14	30105291	30190833	rs199687649	C	1.095	7.31E-09	rs45528442	G	0.098	2.60E-02	0.017	2.02E-03	1
14	33257891	33309495	rs34179565	CA	0.946	8.88E-09	rs149481611	A	0.020	6.28E-01	0.016	4.97E-03	1

14	59585932	60088992	rs150437760	A	1.129	4.58E-08	rs117420433	G	0.014	6.19E-01	-0.017	1.72E-03	0
14	72382471	72467631	rs2332700	C	1.073	1.52E-10					-0.007	0.19	0
14	99657227	99735480	rs35604463	G	1.058	1.66E-08	rs11624408	G	-0.056	1.91E-08	0.020	4.33E-04	0
14	103793539	104511206	rs80020004	C	0.918	1.85E-08	rs77275237	A	0.019	4.25E-01	-0.019	4.77E-04	0
14	103849715	104537680	rs10083370	G	1.078	3.44E-14					-0.007	0.18	0
15	40550149	40599296	rs56282503	T	0.940	2.30E-08	rs7183540	A	-0.047	9.84E-05	0.008	0.16	0
15	47524423	47751837	rs281299	C	0.946	2.19E-08	rs8040612	G	0.036	2.60E-04	-0.014	1.18E-02	0
15	61813790	61909712	rs12898315	G	0.945	2.51E-09					0.008	0.15	0
15	70573650	70603159	rs12148337	G	0.921	1.16E-08	rs11072156	A	0.017	1.58E-01	0.016	3.51E-03	1
15	78711803	79021464	rs3743078	C	0.925	3.11E-12					-0.005	0.35	1
15	82426170	83575025	rs783540	A	0.943	8.45E-10	rs62012045	A	-0.049	4.94E-06	0.032	9.79E-09	0
15	84608488	85392298	rs12908161	A	1.069	9.41E-10					-0.007	0.23	0
15	91402803	91437388	rs17514846	A	0.934	2.55E-12	rs78192020	C	-0.007	6.59E-01	-0.011	0.05	1
16	7744180	7761736	rs12447542	G	0.918	1.44E-08	rs74011845	G	0.038	3.98E-02	-0.009	0.09	0
16	9875513	9970227	rs7191183	T	0.942	6.31E-09	rs190561736	A	-0.045	3.02E-01	-0.009	0.09	1
16	13673040	13763411	rs7499750	A	1.073	4.24E-10					0.007	0.18	1
16	24235580	24249959	rs198160	G	1.058	4.88E-08	rs198157	A	-0.026	1.77E-02	-0.012	0.04	1
16	29923510	30177807	rs11646127	G	1.073	5.52E-13					0.017	1.78E-03	1
16	58538662	58734713	rs42945	A	0.939	2.25E-10	rs137889509	G	-0.025	3.56E-01	-0.012	0.03	1
16	63547390	63776400	rs17465671	C	1.059	4.14E-09	rs12708853	C	0.049	3.55E-07	-0.016	2.81E-03	0
16	67841129	68419298	rs1975802	A	0.933	3.56E-08					-0.002	0.66	1
16	71003590	71575281	rs2161711	A	1.072	4.22E-08					0.010	0.08	1
17	2017029	2220814	rs7216638	T	1.067	4.59E-10	rs12943566	A	-0.060	3.35E-09	0.024	1.65E-05	0

17	17649172	18035019	rs4925114	A	1.058	2.64E-08	rs76089176	G	-0.021	2.77E-01	-0.015	8.24E-03	1
17	18917237	19322062	rs66885728	G	0.947	1.47E-08	rs79626005	A	0.011	5.77E-01	-0.011	0.05	0
17	78456708	78704618	rs7225476	G	0.949	4.86E-08	NA	NA	NA	NA	-0.004	0.52	1
18	52704850	53601811	rs79926379	A	0.845	1.61E-11					-0.004	0.46	1
18	52716306	52827668	rs5825114	G	0.930	5.03E-14	rs117913816	A	-0.101	1.20E-03	0.019	5.44E-04	0
18	53022896	53630222	rs144158419	C	1.142	5.03E-13	rs112621325	G	-0.054	2.77E-01	0.016	4.33E-03	0
18	53183396	53477819	rs28758902	C	0.934	4.75E-13	rs12965620	C	-0.072	3.40E-02	0.014	1.35E-02	0
18	53230650	53230650	rs66791238	T	1.072	6.41E-09	NA	NA	NA	NA	NA	NA	NA
18	53768975	53804156	rs1789595	A	1.068	2.23E-09	rs182395441	G	0.102	5.53E-02	-0.008	0.16	0
18	77563334	77580712	rs56775891	C	0.936	2.03E-09	rs75047634	A	-0.010	8.18E-01	0.007	0.19	0
19	11849736	11943697	rs72986630	C	0.869	8.09E-10	rs6511751	G	-0.012	2.08E-01	-0.013	0.02	1
19	19331847	19800987	rs2905432	G	1.071	6.62E-12					0.000	0.93	0
19	30981639	31052274	rs2053079	A	0.932	1.82E-10					0.011	0.04	0
19	50067508	50182697	rs7508148	T	1.080	4.06E-11	rs118087022	A	-0.016	4.48E-01	-0.011	0.04	1
20	20814132	20843441	rs6035706	A	0.942	7.24E-09	rs2092944	G	-0.009	5.97E-01	-0.009	0.11	1
20	37277618	37512698	rs6065094	A	0.918	7.91E-17					0.003	0.56	0
22	39838892	39856356	rs9611177	C	1.060	3.84E-08	rs139684264	A	-0.049	2.30E-01	-0.010	0.07	1
22	39866938	40058186	rs5757730	A	0.931	1.76E-12					-0.002	0.67	1
22	40043812	40091818	rs4820386	C	0.941	4.07E-10	rs732381	T	0.073	1.11E-11	-0.011	0.05	0
22	41027819	42386534	rs9607782	T	0.922	5.54E-13					0.002	0.71	0
22	41733262	42690311	rs1023497	C	1.085	2.04E-11					0.016	4.46E-03	1
22	42225018	42689370	rs6002655	C	0.928	2.15E-14	rs2228314	C	-0.038	6.31E-04	-0.019	4.67E-04	1
X	5859733	6029533	rs12009217	A	0.937	1.78E-10	NA	NA	NA	NA	NA	NA	NA

X	68377126	68377205	rs62606711	A	1.075	1.26E-12	NA						
---	----------	----------	------------	---	-------	----------	----	----	----	----	----	----	----

† Results from the schizophrenia GWAS (Pardiñas et al., 2018) Supplementary Table 3, where odd's ratio (OR) and p-values are provided. ‡ When the original rsID is not present in our total cerebellar volume meta-GWAS, the SNP within its LD (linkage disequilibrium) range (i.e. start to end column) with the lowest p-value which is in our meta-GWAS is identified and used instead. Blank cells indicate where the original schizophrenia SNP was identified in our meta-GWAS (and hence no LD SNP lookup was performed), while NA indicates that no SNP within the LD range could be found in our meta-GWAS. § Our total cerebellar volume meta-GWAS association statistics for either the schizophrenia GWAS's original SNP or LD SNP (see above). ¶ Ascertaining if the Beta value for total cerebellar volume meta-GWAS and either schizophrenia OR or Beta value is in same direction (1 = yes)

5 The effect of increased common genetic burden for total brain and cerebellar volume on treatment-resistance in schizophrenia

5.1 Abstract

Around one third of individuals with schizophrenia experience symptoms that are resistant to standard treatments, resulting in poorer patient outcomes. Our understanding of the underlying neurobiology behind such treatment-resistance psychosis (TRP) is limited. Reductions in brain volume, earlier age of schizophrenia onset and poorer premorbid cognitive ability in TRP, compared to non-TRP individuals, indicate altered neurodevelopment to be an important feature in TRP's development. There is growing appreciation of cerebellar reductions in schizophrenia, a region whose structural and functional performance appears particularly sensitive to perturbed neurodevelopment. Recent studies have indicated cortical and cerebellar structures to have moderate to high heritability and have identified multiple common genetic variants associated with their volumes. In this proof-of-concept study we investigated whether individuals with TRP showed a reduced genetic burden for these brain volume-associated common variants, by way of lower polygenic scores, compared to individuals with psychiatric diagnoses who respond to first-line treatment. We did not find evidence for polygenic scores for total brain volume or for relative cerebellar volume to predict TRP status (SNP inclusion p-value threshold (p_T) < 0.01: $\Delta R^2 = 2.7 \times 10^{-4}$, $\beta[95\%CI] = -0.03[-0.17,0.12]$, $p = 0.71$ & $\Delta R^2 = 5.1 \times 10^{-4}$, $\beta[95\%CI] = -0.04[-0.19,0.11]$, $p = 0.60$, respectively). In conclusion, we did not find any evidence to support the idea that common genetic variants important for treatment resistance status are shared with those for adult brain volume.

5.2 Background

Around a third of individuals with schizophrenia have a symptomatology presentation that are considered treatment resistant, showing minimal symptomatic response to standard antipsychotic treatments (Gillespie, Samanaite, Mill, Egerton, & MacCabe, 2017). Clozapine, an atypical antipsychotic which interacts with several receptors (dopamine D₁, D₂, 5-HT_{2A}, α_1 -adrenoceptors and muscarinic receptors), is the only licensed medication for treatment-resistant psychosis (TRP) and can be effective in up to two-thirds of these patients, however, is not used as a first-line treatment due to its own complex side-effect profile (De Fazio et al., 2015). Symptomatic and functional outcomes for individuals with TRP are often poor compared to those who respond to first-line medications (non-TRP), in part due to the delay in prescription of clozapine (Iasevoli et al., 2016; Shah et al., 2018). Research into the identification of individuals who are likely to develop treatment-resistance as well as into improving our understanding of its underlying neurobiology, therefore, are of paramount importance in improving outcomes for individuals with schizophrenia.

One key question is whether TRP status reflects a more severe form of schizophrenia risk or might reflect a more homogenous subgroup with a shared latent risk factor (Gillespie et al., 2017; Nucifora et al., 2019). As with schizophrenia, family studies indicate at least a partial genetic aetiology to TRP (Legge et al., 2020; Nucifora et al., 2019), with incidence increasing in closer family members. One of the largest studies to date found increased genetic risk for schizophrenia, in the form of both common and rare variants associated with schizophrenia diagnosis, did not significantly predict TRP status in individuals with schizophrenia for the moderate-to-large effects it was powered to detect, indicating that liability to schizophrenia and to treatment resistance within schizophrenia appear to be at least partially independent (Legge et al., 2020). Instead, the authors found TRP status risk factors to include earlier age of onset, poorer premorbid cognitive and social ability (Legge et al., 2020). The authors suggest, therefore, that rather than reflecting a more severe form of general liability to schizophrenia, TRP status risk might be particularly associated with a more severe impaired neurodevelopmental origin within schizophrenia, which is characterised by such features (Kochunov et al., 2019; Legge et al., 2020; M. J. Owen et al., 2011).

These results mirror the few studies directly analysing neuroanatomical differences in individuals with TRP compared to non-TRP individuals, which indicate that TRP individuals do indeed show more pronounced cortical and subcortical grey matter volume reductions and white matter vulnerability, than those seen in non-TRP individuals with schizophrenia (Barry et

al., 2019; De Assunção-Leme et al., 2020; Kochunov et al., 2019; Vita et al., 2019). Importantly, structural and functional brain differences have also been found to be predictive of treatment response in prospective study designs of first episode individuals with schizophrenia (B. Cao et al., 2020; E. A. Nelson et al., 2020). Altered neuroanatomy and functionality in TRP individuals, therefore, appear to be present at onset of schizophrenia and do not simply reflect effects of other medications or longer periods of ineffectual treatment.

Regional brain structures show moderate-to-high heritability, indicating a substantial proportion of variance in volume of these regions can be accounted for by genetic variation between individuals (Jansen, Mous, White, Posthuma, & Polderman, 2015). Similarly, recent work has shown a substantial proportion of this heritability in general population samples can be accounted for by variation in common genetic variants, and that polygenic scores (PGSs) - a linear sum of presence of these variants weighted by their association with each volume measure- can predict the same regional brain volumes in independent samples, including brain structure in younger cohorts (Grasby et al., 2020; Satizabal et al., 2019; Zhao et al., 2019). Given, therefore, the familial risk factors for TRP status, premorbid volumetric differences and heritability of brain volume measures, of interest is whether genetic variants associated with structural brain measures might themselves predict TRP status.

In this study we assessed if individuals with treatment-resistant symptomatology carry, on average, lower genetic predisposition (i.e. lower polygenic scores) associated with brain volume compared to non-resistant individuals with schizophrenia: reflecting the generally reduced brain volumes seen in clinical cases. Importantly, such an approach would capture both if the traits were directly related in a vertical manner (e.g. that volume-related variants cause increased TRP liability due to their known effect on brain volume) and/or if they were related through independent processes (e.g. that the variants' effects on brain volume and increased TRP liability are not causal and are independent, though could share some underlying neurobiological processes. For instance, how common variants for cortical and subcortical MRI structural measures are enriched for various neuronal, synaptogenic and myelination processes (Grasby et al., 2020; Satizabal et al., 2019)).

In addition to analysing variants important for total brain volume, we specifically focused our analysis on variants important for relative cerebellar grey-matter volume given: the growing interest in the relevance of the cerebellum to psychiatric disorders (Moberget & Ivry, 2019; Phillips et al., 2015) including reduced volume both in individuals with overt schizophrenia diagnosis (Moberget et al., 2018) (*Chapter 2*) and unaffected individuals at greater genetic risk

(de Zwarte, Brouwer, Agartz, et al., 2019) (*Chapter 3*); evidence of moderate common variant heritability (*Chapter 4*); and its potential use as a specific biomarker for neurodevelopmental outcomes (Keunen et al., 2016; Matsufuji, Sano, Tsuru, & Takashima, 2017; Stoodley, 2016). Finally, we investigated if these genetic scores were associated with the premorbid factors which were previously reported as increasing risk of treatment resistance (Legge et al., 2020), including poorer premorbid IQ and social adjustment, and an earlier age at onset of schizophrenia, and, if so, whether these premorbid factors mediated the association between brain structure genetic scores and treatment resistance status.

5.3 Methods

5.3.1 CardiffCogs participants

Study individuals were from the CardiffCogs (COGnition in Schizophrenia) cohort of 1307 individuals recruited from UK centres (principally Cardiff) with diagnoses of schizophrenia or other psychiatric schizoaffective, psychotic or mood-related disorders. A description of the CardiffCogs study design has been reported previously (Legge et al., 2020; Lynham et al., 2018; Pardiñas et al., 2018). In brief, individuals (16-65yrs) were recruited from a UK community, in-patient and voluntary sector mental health services, with particular targeting of clozapine clinics to increase numbers of treatment-resistant individuals within the study sample. Consensus research (DSM-4) diagnoses were determined based on SCAN interviews (schedules for clinical assessment in neuropsychiatry (Wing et al., 1990) and clinical note information (inter-rater reliability κ : 0.63-0.85). National Health Service (NHS) ethics approval was provided (reference number: 07/WSE03/110) and written informed consent obtained from all study participants.

Individuals were defined as having treatment resistant psychosis (TRP) based on OPCRIT ratings (Operational Criteria Checklist for Psychotic Illness and Affective Illness) (McGuffin, Farmer, & Harvey, 1991) as having failed to respond to at least two antipsychotics or if they had been administered clozapine treatment, while treatment-responders (non-TRP) were defined as those who had responded to antipsychotics or in whom relapse occurred when medication was halted. Excluded from analysis were those individuals where insufficient information on antipsychotic response was available and/or two adequate trials of antipsychotics had not yet occurred, as well as individuals with neurological conditions which might impact on ability to participate in the study or current substance abuse disorders. Other measures of interest to this study were those previously identified as premorbid risk factors for treatment resistance (Legge

et al., 2020), namely premorbid IQ (national adult reading test (NART) (H. E. Nelson, 1991): predicted revised Weschler Adult Intelligence Scale full scale IQ = $130.6 - 1.24 * \text{NART error score}$), poor premorbid social adjustment (OPCRIT 10: difficulty entering or maintaining normal social relationships, persistent social isolation, withdrawal or maintenance of solitary interests prior to onset of psychotic symptoms) and age at onset of psychosis (OPCRIT 4: earliest age at which medical advice was sought for psychiatric reasons or at which symptoms began to cause subjective distress or impair functioning).

5.3.2 Genetic analysis

Of the full cohort, 988 individuals provided blood samples for extraction of genetic data. Genotyping (Illumina OmniExpress-12), basic quality control and imputation of the CardiffCOGS sample has been described previously (Legge et al., 2020; Pardiñas et al., 2018) (Dr Anontio Pardiñas). In brief, SNP imputation was performed using IMPUTE2 (Howie, Donnelly, & Marchini, 2009) with 1000 Genomes (phase 3) and UK10K reference panels (J. Huang et al., 2015). Single nucleotide polymorphisms (SNPs) were excluded with low imputation quality removed (<0.9), excess missingness ($>2\%$), low minor allele frequency ($\text{MAF} < 1\%$) or with deviations from Hardy-Weinberg equilibrium ($< 1 \times 10^{-10}$). We also excluded participants with excessive missingness ($>2\%$), extreme heterozygosity ($F > 3$ standard deviations/SD), one of each pair of related individuals (> 0.0442 i.e. third cousins) and those of non-European genetic ancestry similarity (1000G phase 3 EUR) so that linkage disequilibrium (LD) structure matched those of the cerebellar GWAS data. The latter was conducted excluding individuals outside ($>90\%$) a hyper-ellipsoid of the first 5 genetic principal components using R 'covMCD' function from 'robustbase' package (<http://robustbase.r-forge.r-project.org/>), as described previously (Conomos et al., 2016).

The base data for polygenic scores were from our GWAS meta-analysis results for total cerebellar volume derived from UK Biobank ($n = 33,265$) as outlined in *Chapter 4*. This reflected a relative total cerebellar volume measure, having corrected for genetic, demographic and imaging covariates, which included total brain (grey and white) matter volume differences. For this study, we conducted a GWAS on the same cohort for total brain volume itself, using the same procedure (omitting the total brain volume covariate correction). A full description of the total brain volume GWAS methodology and results is included in Supplementary Note 5.1. We removed ambiguous SNPs (C/G or A/T SNPs) from both UK Biobank summary statistics and CardiffCogs genotype datasets, performed strand flipping on CardiffCogs data to align with UK Biobank, and, since we had the raw genotypes of UK Biobank, merged datasets using *PLINK*

(v1.09) (C. C. Chang et al., 2015) to remove any closely related individuals across cohorts (kinship coefficient >0.0442).

From the original 988 individuals with genetic data, 877 CardiffCogs individuals passed the genetic quality control steps as outlined above (1,805,906 SNPs). Following clumping to remove highly correlated SNPs ($r^2 < 0.1$, 250kb), polygenic scores of total brain and relative total cerebellar volume summary statistics were created using *PLINK* for each individual in CardiffCogs sample who had passed genetic quality control (see *Chapter 3* for a fuller description of polygenic score generation). Five SNP inclusion thresholds were chosen to create polygenic scores: $p_T < 0.001$ (1986 SNPs), 0.05 (5865 SNPs), 0.01 (9794 SNPs), 0.05 (32834 SNPs) & 0.1 (54426 SNPs). We chose the $p_T < 0.01$ threshold for our *a priori* central score and primary analysis to report, given this was the threshold which best predicted total cerebellar volume in an out-of-sample cohort (*Chapter 4*).

5.3.3 Statistical analysis

Of the 877 individuals within CardiffCogs who passed genetic quality control, 44 individuals were excluded with non-psychotic mood disorders, and a further 7 individuals were excluded because of missing key covariate information of age at time of interview, sex and the method used for participant recruitment (via either secondary mental healthcare services, or opportunistic or third sector organisations), leaving 826 individuals for our main analysis. We used Student's t-test (age) and Fisher's exact test (sex and systematic recruitment) to identify significant differences in the distributions of these variables between individuals with and without TRP in our cohort. While our primary analysis included those with any psychopathology related to schizophrenia, since schizophrenia effects are of primary interest to this thesis, we repeated the analysis in the 660 sub-sample with only schizophrenia or schizoaffective-depression disorders (deemed highly clinically similar in presentation and time course) as a more focussed supplementary sensitivity analysis and as had been deployed previously (Legge et al., 2020).

Univariate logistic regression analyses were used to assess cerebellar polygenic scores' prediction of treatment-resistance status, accounting for covariates of age at time of interview, sex, the method used for participant recruitment and the first 10 genetic principal components to correct for residual population structure. All polygenic scores were z-scored (scaled and mean-centred), with effect sizes (β) and 95% confidence intervals (95%CI) standardised and reflecting the effect on outcome (log odds of treatment resistance status) of increasing polygenic scores by one standard deviations (SD). The unique variance of the trait explained by

each polygenic score (ΔR^2) was calculated by subtracting each model R^2 including the polygenic score along with the covariates already mentioned against the model with just the covariates. For treatment-resistance analysis, R^2 was calculated on the liability scale to account for ascertainment bias (Sang Hong Lee et al., 2012), based on a 30% lifetime prevalence in the study population (i.e. in those with psychosis-related disorders). We estimated we had 80% power to detect in our sample a polygenic cerebellar score explaining 1% of variance in treatment-resistance status ($p_T < 0.01$; $n_{SNPs} = 9794$; total cerebellar volume $h^2_{SNP} = 50.6\%$; proportion of SNPs with null effect = 0.95; whole population prevalence of TRP = 0.01 schizophrenia prevalence \times 0.30 TRP prevalence = 0.0033%; $\alpha < 0.05$) (Dudbridge, 2013). We provide both raw p-values for each association and p-values adjusted to control the false discovery rate (p_{FDR}) across the number of polygenic scores tested (2 brain measures \times 5 p_T -values), using the base R “*p.adjust*” function (<https://rdrr.io/r/stats/p.adjust.html>) and “Benjamini-Hochberg” method (Benjamini & Hochberg, 1995) to maintain a $FDR < 0.05$.

In additional analyses, we utilised the same logistic regression model as outlined above - including the same covariates - for the categorical outcome of poor premorbid social adjustment, though utilising Nagelkerke’s (Nagelkerke, 1991) pseudo- R^2 (<https://rdrr.io/cran/DescTools/man/PseudoR2.html>) since lifetime liability calculations were not possible. For continuous outcome variables of premorbid IQ and age at onset of psychosis, univariate linear regression models were used. We again controlled the FDR for the number of tests performed (2 brain measures \times 5 p_T -values \times 3 outcome traits) and reported FDR-adjusted p-values.

5.4 Results

Of our total sample of 826 individuals with psychosis-related diagnosis (43.4 mean yrs [17-74yrs], 60.9% male), 768 individuals (93.0%) had recorded treatment-resistance status, with approximately an even split of those with and without diagnosed treatment resistance ($n[\%] = 389[47.1\%]$ & $379[45.9\%]$, respectively) due to systematic recruitment from clozapine clinics (Figure 5.1; Table 5.1). Those with TRP showed no differences in the proportion of males (Odd’s ratio/OR = 1.1, $p=0.42$), were slightly younger at time of interview ($t= -2.4$, $p=0.02$) and were more likely to be systemically recruited (OR=2.0, $p=3.5 \times 10^{-5}$); covariates added in all our analyses. Confirming the results from the previously published larger but overlapping cohort (Legge et al., 2020), in our genetic sub-sample we found individuals with TRP to have a younger

average age of psychosis onset ($t=-7.5$, $p=1.6\times 10^{-13}$), lower premorbid IQ ($t=-4.0$, $p=7.1\times 10^{-5}$) and higher incidence of premorbid social impairment ($OR=1.7$, $p=4.3\times 10^{-4}$). Of the whole 826-person cohort, 660 individuals (79.9%) had schizophrenia or schizoaffective-depression diagnoses which were grouped and used for sensitivity analyses, as performed with previous literature (Legge et al., 2020) (Figure 5.1). Compared to the remaining non-schizophrenia sub-cohort which included the other remaining psychotic disorders or schizoaffective bipolar disorder, this schizophrenia sub-cohort showed no significant difference in age at recruitment ($t=0.35$, $p=0.73$), had a higher number of males ($OR=2.2$, $p=5.4\times 10^{-6}$) and were more likely to have been systemically recruited ($OR=2.0$, $p=1.2\times 10^{-4}$) (Supplementary Table 5.1). TRP was also more prevalent in the schizophrenia compared to the non-schizophrenia sub-cohort ($n[\%]$ = 346[52.4%] & 43[25.9%], respectively; $OR=2.8$, $p=8.4\times 10^{-8}$).

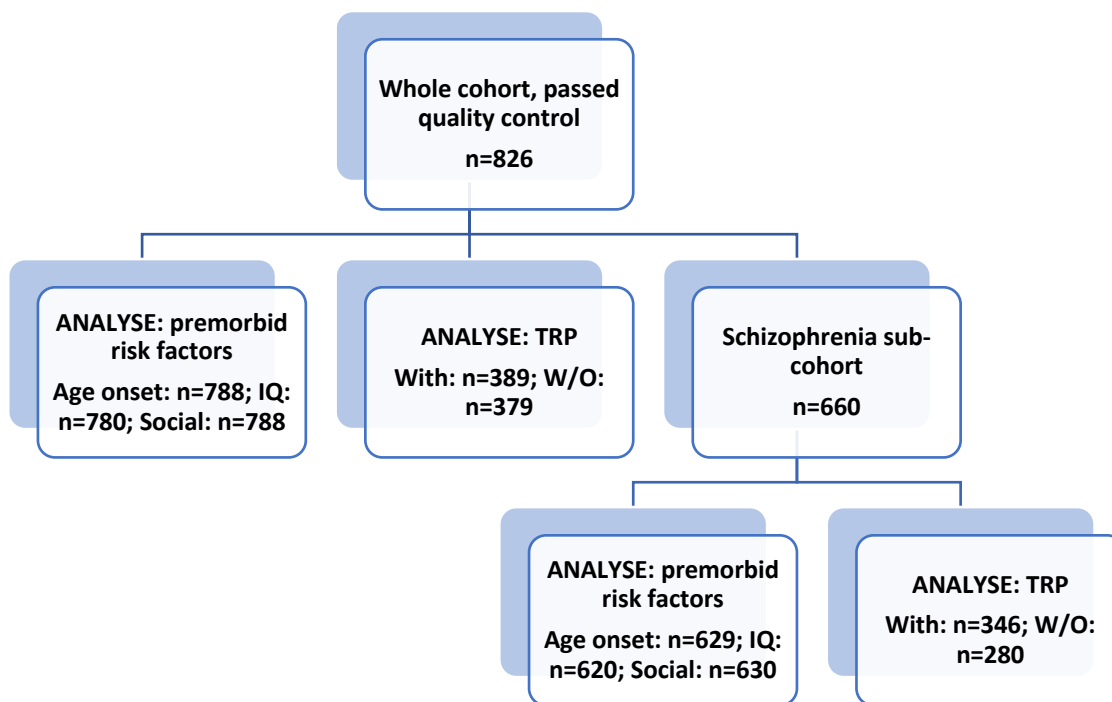


Figure 5.1: Analysis flow-chart including sample sizes for the whole cohort and the schizophrenia sub-cohort. TRP= treatment-resistance psychosis; W/O= Without.

Table 5.1: Demographic information and premorbid risk factors for treatment resistance in the whole cohort, split by treatment resistance status

	Whole cohort (n=826)	Treatment resistant (n=389)	Non-treatment resistant (n=379)	Missing (n=58)
Sex				
Female	323 (39.1%)	147 (37.8%)	155 (40.9%)	21 (36.2%)
Male	503 (60.9%)	242 (62.2%)	224 (59.1%)	37 (63.8%)
Age at interview (yrs)				
Mean (SD)	43.4 (12.0)	42.6 (11.5)	44.6 (12.3)	40.8 (12.5)
Median [Min, Max]	43.0 [17.0, 74.0]	43.0 [17.0, 74.0]	45.0 [18.0, 72.0]	41.0 [18.0, 71.0]
Recruited systematically				
Yes	590 (71.4%)	308 (79.2%)	249 (65.7%)	33 (56.9%)
No	236 (28.6%)	81 (20.8%)	130 (34.3%)	25 (43.1%)
Psychosis age at onset (yrs)				
Mean (SD)	25.5 (9.35)	23.0 (8.21)	28.1 (9.77)	25.3 (9.46)
Median [Min, Max]	24.0 [3.00, 66.1]	22.0 [3.00, 66.1]	26.0 [4.00, 62.0]	23.0 [13.0, 56.0]
Missing	38 (4.6%)	16 (4.1%)	17 (4.5%)	5 (8.6%)
Premorbid IQ				
Mean (SD)	98.6 (13.2)	96.7 (13.5)	101 (12.6)	97.8 (13.7)
Median [Min, Max]	99.6 [68.6, 129]	97.1 [68.6, 128]	101 [68.6, 129]	97.1 [68.6, 126]
Missing	46 (5.6%)	24 (6.2%)	17 (4.5%)	5 (8.6%)
Poor premorbid social adjustment				
Yes	296 (35.8%)	160 (41.1%)	112 (29.6%)	24 (41.4%)
No	492 (59.6%)	208 (53.5%)	252 (66.5%)	32 (55.2%)
Missing	38 (4.6%)	21 (5.4%)	15 (4.0%)	2 (3.4%)

5.4.1 PGS Prediction of treatment-resistance

We found no evidence for a difference in polygenic scores for total brain or total cerebellar volume in those with and without TRP at any SNP inclusion threshold (p_T -value) ($p_T < 0.01$: $\Delta R^2 = 2.7 \times 10^{-4}$, β [95%CI] = -0.03[-0.17, 0.12], $p = 0.71$ & $\Delta R^2 = 5.1 \times 10^{-4}$, β [95%CI] = -0.04[-0.19, 0.11], $p = 0.60$, respectively) (

Table **5.2**; Figure 5.2). Sensitivity analysis indicated similar non-significant results for total brain and cerebellar polygenic scores when limiting participants to just those with schizophrenia ($p_T < 0.01$: $\Delta R^2 = 2.9 \times 10^{-3}$, β [95%CI] = -0.09[-0.25,0.07], $p = 0.27$ & $\Delta R^2 = 8.0 \times 10^{-4}$, β [95%CI] = -0.05[-0.21,0.12], $p = 0.56$, respectively) (Supplementary Table **5.2**).

5.4.2 *PGS Prediction of premorbid factors*

As an additional set of analyses, we explored the effect of increased cerebellar polygenic scores on factors of premorbid IQ, poor premorbid social adjustment and age at onset of psychosis (yrs)
(

Table 5.2; Figure 5.3). While we generally found some indication for increased premorbid IQ with increased polygenic scores for total brain volume across SNP inclusion thresholds, these were only nominally significant at one p_T -value and did not survive correction for multiple comparisons ($p_T < 0.001$: $\Delta R^2 = 6.8 \times 10^{-3}$, β [95%CI] = 1.09[0.18,2.00], $p = 0.02$, $p_{FDR} = 0.56$). No significant effects were seen for relative cerebellar polygenic scores at the same threshold ($p_T < 0.001$: $\Delta R^2 = 5.7 \times 10^{-4}$, β [95%CI] = 0.61[-0.31,0.11], $p = 0.58$). We also did not find either total brain nor relative cerebellar polygenic scores to be significantly associated with premorbid social performance ($p_T < 0.01$: $\Delta R^2 = 9.0 \times 10^{-5}$, β [95%CI] = 0.02[-0.13,0.16], $p = 0.82$ & $\Delta R^2 = 1.9 \times 10^{-3}$, β [95%CI] = 0.08[-0.07,0.23], $p = 0.29$, respectively) or with age of onset of psychosis (yrs) ($p_T < 0.01$: $\Delta R^2 = 3.7 \times 10^{-4}$, β [95%CI] = 0.18[-0.40,0.76], $p = 0.54$ & $\Delta R^2 = 1.9 \times 10^{-4}$, β [95%CI] = -0.13[-0.71,0.45], $p = 0.66$, respectively). Sensitivity analysis in just those with schizophrenia showed markedly similar results to the whole cohort, with only the total brain volume polygenic score prediction of premorbid IQ reaching even nominal significance ($p_T < 0.001$: $\Delta R^2 = 8.1 \times 10^{-3}$, β [95%CI] = 1.22[0.17,2.27], $p = 0.02$, $p_{FDR} = 0.45$), and none remaining significant following correction for multiple comparisons (Supplementary Table 5.2).

Since there appeared little evidence for an association between genetic scores with treatment resistance status, we did not test for possible mediation effects via altered premorbid measures.

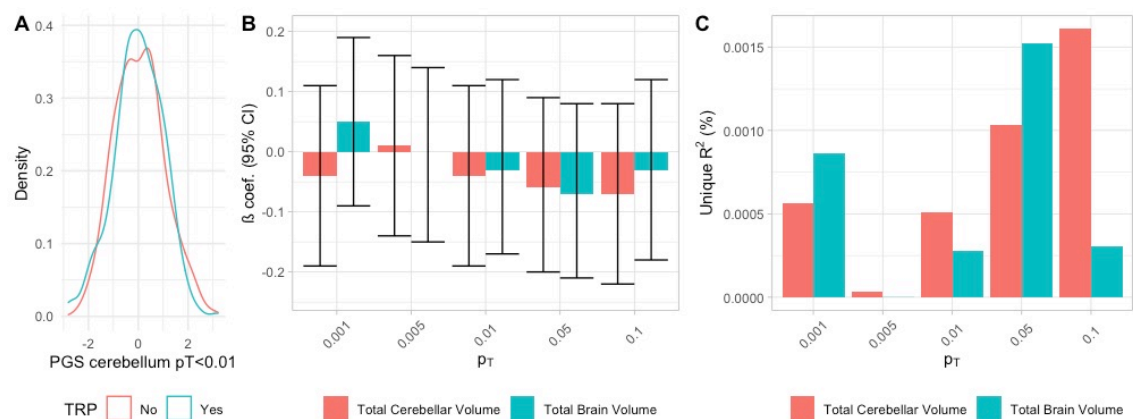


Figure 5.2: The association between polygenic scores of total cerebellar and total brain volume with treatment resistant psychosis (TRP) status in individuals with any psychosis-related diagnosis (n=868). A) An example density distribution of individuals' polygenic scores of total cerebellar volumes at SNP inclusion threshold (p_T -value) < 0.01 between those with and without treatment resistant psychosis. Polygenic scores across five SNP inclusion thresholds (p_T -values) are included for both total cerebellar volume and total brain volume. Effect size estimates of B) β coefficients and 95% confidence intervals (CI), and C) the unique variance

(ΔR^2) in outcome explained by each polygenic score (scaled and mean-centred) are provided, calculated on the liability scale.

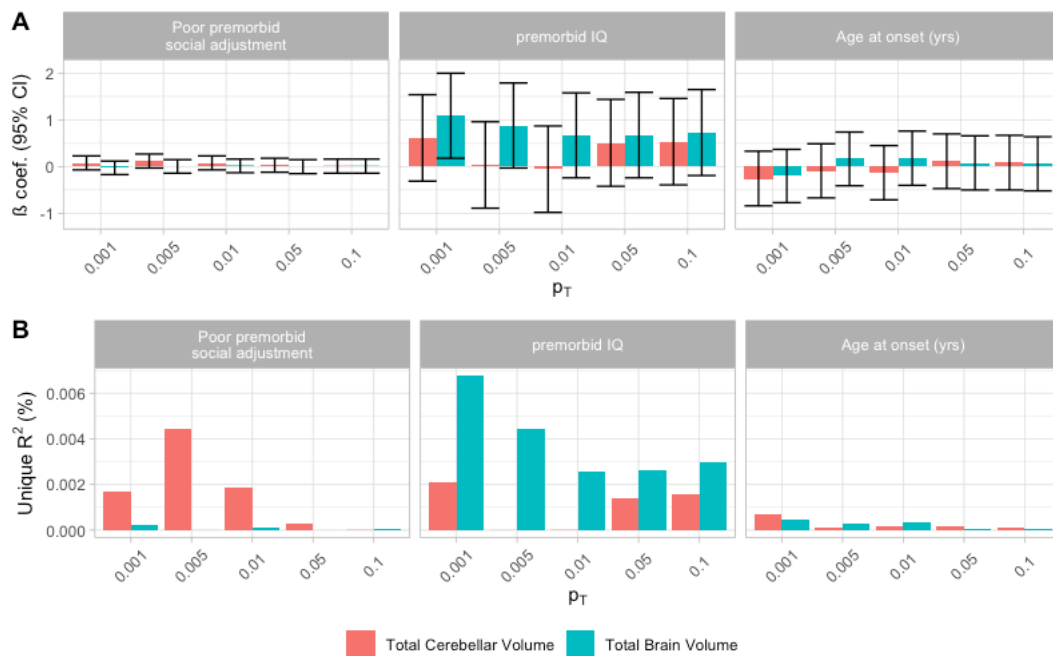


Figure 5.3: The association between polygenic scores of total cerebellar and total brain volume with outcomes of interest in individuals with any psychosis-related diagnosis ($n=868$). Polygenic scores across five SNP inclusion thresholds (p_T -values) are included. Effect size estimates of A) β coefficients and 95% confidence intervals (CI), and B) the unique variance (ΔR^2) in outcome explained by each polygenic score (scaled and mean-centred) are provided, with pseudo- R^2 used for the binary poor premorbid social adjustment trait

Table 5.2: The association between polygenic scores of total cerebellar volume and outcomes of interest in individuals with any psychosis-related diagnosis (n=868)

Outcome	Polygenic score		$\Delta R^2 \ddagger$	$\beta \S$	95% Confidence		p	p _{FDR} *
	Brain region	p _T -value †			intervals §			
Treatment resistant psychosis (TRP) status		0.001	8.64E-04	0.05	-0.09	0.19	0.50	0.88
	Total	0.005	1.54E-06	0.00	-0.15	0.14	0.98	0.98
	Brain	0.01	2.75E-04	-0.03	-0.17	0.12	0.71	0.88
	Volume	0.05	1.52E-03	-0.07	-0.21	0.08	0.37	0.88
		0.1	3.05E-04	-0.03	-0.18	0.12	0.69	0.88
	Total	0.001	5.67E-04	-0.04	-0.19	0.11	0.58	0.88
		0.005	3.05E-05	0.01	-0.14	0.16	0.90	0.98
	Cerebellar	0.01	5.06E-04	-0.04	-0.19	0.11	0.60	0.88
	Volume	0.05	1.03E-03	-0.06	-0.20	0.09	0.46	0.88
		0.1	1.61E-03	-0.07	-0.22	0.08	0.35	0.88
Premorbid IQ		0.001	6.78E-03	1.09	0.18	2.00	0.02	0.56
	Total	0.005	4.42E-03	0.88	-0.03	1.79	0.06	0.75
	Brain	0.01	2.54E-03	0.67	-0.24	1.58	0.15	0.75
	Volume	0.05	2.60E-03	0.68	-0.24	1.59	0.15	0.75
		0.1	2.98E-03	0.73	-0.19	1.65	0.12	0.75
	Total	0.001	2.10E-03	0.61	-0.31	1.54	0.19	0.82
		0.005	7.92E-06	0.04	-0.89	0.96	0.94	0.98
	Cerebellar	0.01	1.53E-05	-0.05	-0.98	0.87	0.91	0.98
	Volume	0.05	1.42E-03	0.51	-0.42	1.44	0.28	0.86
		0.1	1.58E-03	0.53	-0.39	1.46	0.26	0.86
Poor premorbid social adjustment		0.001	2.22E-04	-0.03	-0.17	0.12	0.72	0.98
	Total	0.005	4.91E-06	0.00	-0.14	0.15	0.96	0.98
	Brain	0.01	9.02E-05	0.02	-0.13	0.16	0.82	0.98
	Volume	0.05	1.03E-06	0.00	-0.15	0.15	0.98	0.98
		0.1	5.83E-05	0.01	-0.14	0.16	0.85	0.98
	Total	0.001	1.71E-03	0.08	-0.07	0.23	0.31	0.86
		0.005	4.41E-03	0.12	-0.03	0.27	0.11	0.75
	Cerebellar	0.01	1.89E-03	0.08	-0.07	0.23	0.29	0.86
	Volume	0.05	2.67E-04	0.03	-0.12	0.18	0.69	0.98
		0.1	1.50E-05	0.01	-0.14	0.16	0.93	0.98

		0.001	4.60E-04	-0.20	-0.77	0.37	0.49	0.98
	Total	0.005	3.08E-04	0.17	-0.41	0.74	0.57	0.98
	Brain	0.01	3.66E-04	0.18	-0.40	0.76	0.54	0.98
	Volume	0.05	7.19E-05	0.08	-0.50	0.66	0.79	0.98
Age at		0.1	3.60E-05	0.06	-0.52	0.64	0.85	0.98
onset (yrs)		0.001	7.21E-04	-0.26	-0.84	0.33	0.39	0.97
	Total	0.005	8.80E-05	-0.09	-0.67	0.49	0.76	0.98
	Cerebellar	0.01	1.90E-04	-0.13	-0.71	0.45	0.66	0.98
	Volume	0.05	1.46E-04	0.12	-0.47	0.70	0.70	0.98
		0.1	8.49E-05	0.09	-0.50	0.67	0.77	0.98

Results are from independent univariate linear (continuous outcome) or logistic (binary outcome) regression models of each polygenic score derived from GWAS results of total cerebellar volume; with correction for covariates of age at time of interview, sex, the method used for participant recruitment and the first 10 genetic principal components. †: Polygenic scores across five SNP inclusion thresholds (p -values). ‡: unique variance (ΔR^2) in outcome explained by the polygenic score are calculated by subtracting the R^2 of model including polygenic score and covariates against that with just covariates; with R^2 calculated on the liability scale for TRP and pseudo- R^2 for poor premorbid social adjustment. §: polygenic scores are scaled and mean-centred, representing a difference in outcome with $1 \times SD$ difference in polygenic score. *: p_{FDR} reflects p -values adjusted for the inflation of false discovery rate (FDR) due to multiple comparisons

5.5 Discussion

Identifying risk factors for treatment resistant psychosis (TRP) and improving our understanding of its underlying aetiology and pathophysiology are of paramount interest to improving outcomes for schizophrenia. While family studies indicate a genetic aetiology (Legge et al., 2020; Nucifora et al., 2019), previous work has found that this is not due to elevated genetic risk for schizophrenia (Legge et al., 2020). Instead, neurodevelopmental differences have been highlighted as potentially relevant to treatment-resistance pathophysiology and mirror findings of altered brain structure and other differences in neurodevelopmentally-linked traits in treatment-resistant individuals (Gillespie et al., 2017; Kochunov et al., 2019; Legge et al., 2020; A. S. Lin et al., 2015; Vita et al., 2019). Since brain structural measures have also been shown to be moderate-to-highly heritable (Grasby et al., 2020; Satizabal et al., 2019; Zhao et al., 2019), in this study we assessed whether individuals with TRP showed reduced genetic scores for such measures, indicating pleiotropic effects of these variants for TRP development. Counter to our

hypothesis, we found no evidence for pleiotropic effects of identified variants for brain volume and increased treatment-resistance liability. Though replication of results is required, below we outline possible implications of these findings. Furthermore, since to our knowledge this proof-of-concept study is the first to assess the relationship between genetic scores for brain imaging phenotypes and a feature within (or across) psychiatric conditions - beyond the binary presence of a psychiatric disorder diagnosis - we additionally outline why we feel such an approach holds such promise in helping to forward our understanding of neuropathophysiological processes in psychiatric disorders.

Our null results might have several implications under different assumptions. Broadly speaking, these can be grouped into whether the brain differences seen with TRP are indeed related to TRP genetic aetiology but were not detected by the specific analyses and brain measures deployed here or, alternatively, whether the genetic aetiology for TRP and for the brain differences in TRP are each independently associated with increased TRP risk. We discuss these below.

In regard to the former, there might be several ways in which the brain-related variants tested here might not best capture any neurodevelopmental differences related to TRP risk. Firstly, it might be due to our use of GWAS summary statistics of older adult brain volume phenotypes rather than younger cohorts, which might not capture any altered developmental brain growth associated with TRP. A great advantage in using adult MRI data, though, is that they are much easier to collect in large numbers, providing greater power to detect the small effects, as well as with genetic effects likely being stronger and so easier to detect in adult samples (Jha et al., 2018; Kremen et al., 2012). Additionally, genetic scores of adult brain volumes have been shown to predict the same volumes in younger adult and adolescent cohorts (Satizabal et al., 2019; Zhao et al., 2019) and, while there is some evidence that common genetic influences on infant brain measures differ in part to those for adolescent/adult brains (Xia et al., 2017), these might simply reflect limitations of power and/or reduced variability rather than underlying differences in genetic influences on brain structure. We feel, therefore, that our approach was justified and that adult genetic scores should generally capture younger brain developmental processes.

Equally, our analysis was limited to genetic scores of only two phenotypes: total brain and relative total cerebellar volume. We used these regions given the reductions in total brain volume associated with TRP and with the cerebellum, though understudied in regard to TRP, being a structure particularly sensitive to neurodevelopmental outcomes (Keunen et al., 2016; Matsufuji et al., 2017; Stoodley, 2016; Vita et al., 2019). Since genetic variants determining

individual cortical and subcortical regions appear fairly independent (Grasby et al., 2020; Satizabal et al., 2019), investigating other regional volume differences might be a promising future step, such as for frontal cortical regions which have been particularly identified as altered in TRP individuals (Nucifora et al., 2019; Vita et al., 2019). In addition, the volumetric differences seen in TRP individuals might be downstream of/better captured by associated variants for other brain measures. For example, brain volume measures are a composite of surface area and thickness; which show differing developmental pathways and underlying genetic associations (Grasby et al., 2020), and with only thickness showing reductions in treatment-resistant individuals (Barry et al., 2019; E. A. Nelson et al., 2020). Equally, functional and diffusional connectivity MRI measures might better capture any alterations to underlying neuronal circuitry with TRP. Furthermore, while our study was powered to detect an explanation of 1% of the variance in TRP status by polygenic scores, larger sample sizes in both the discovery and test datasets will allow for improved power for detection of variants associated with brain imaging phenotypes and their predictive accuracy in treatment-resistance schizophrenia, respectively. This is particularly prescient for the secondary phenotypes (such as premorbid social and IQ differences) which we were likely underpowered to detect given the presence of missing values in this sample. Finally, the use of methods such as equivalence testing and Bayesian analyses to investigate these non-significant effects would allow for separation of true null effects from those of where data was not sensitive enough to detect the effect.

In regard to the alternative assumption, our null results might indicate that genetic aetiology for TRP and neurodevelopmental differences noted in TRP are independent. This would broadly agree with a previous study which found no altered expression for several candidate neurodevelopmentally-linked genes in individuals with treatment-resistance (Moretti et al., 2018). We also found little association between genetic scores for brain structure and the premorbid factors suggested as implicating neurodevelopmental processes (Legge et al., 2020), and also hence why we did not pursue mediation analysis, though, as noted above, these sub-analyses were likely underpowered to detect a meaningful difference. While some evidence indicates TRP brain structural differences to be present from first-episode psychosis individuals (B. Cao et al., 2020; E. A. Nelson et al., 2020), the number of studies for this and general in TRP are few and small in size. Some of structural brain differences seen with TRP, therefore, could theoretically reflect processes following diagnosis, such as those related to antipsychotic medication itself and its effect on brain structure (Jørgensen et al., 2017; Veijola et al., 2014), and therefore no association would be expected with genetic TRP risk. Additionally, we (*Chapter 2*) and others (Makowski et al., 2019; Reuter et al., 2015) have highlighted the overlooked

possible confounding effects of head motion in psychiatric structural imaging and which, while to our knowledge not discussed in any treatment-resistance volumetric studies to date, might particularly be important for treatment-resistance, considering their unmedicated state. Finally, neuroanatomical differences in those with TRP might arise solely through early environmental exposure, such as through early life complications, which are known to associate with brain structural differences and particularly the cerebellum (Sathyanesan et al., 2019; Volpe, 2009) and are established risk factors for schizophrenia liability (Simoila et al., 2018). Twin studies of brain structure in individuals with TRP would greatly aid future research, allowing partial separation of genetic and environmental contributions, though obviously are exceptionally difficult to recruit.

It is clear, therefore, that more imaging studies of treatment-resistance schizophrenia, with adequate sample sizes and controlling for some of these highlighted confounding issues, are required to better understand the possible pathophysiological role played by underlying neurological differences. Such studies, however, are costly and require extensive planning to make the best use of resources and participants' time. This is where we feel such a neuroimaging genetic approach as outlined in this study could greatly aid such research design, utilising the growing number of well-powered summary statistics for brain-based measures, to analyse their predictive ability for specific features within diagnoses, such as treatment-resistance, age at onset or symptomatology severity. While in this study we focus on only two brain-based genetic scores, future studies might test for a battery of scores, such as for global (and regional) volume, thickness, surface area, diffusion or functional connectivity scores, in addition to those of other brain-related traits. Equally, with growing interest in brain features present across psychiatric disorders, such as seen with the cerebellum (Hariri, 2019), this approach also allows for expanding of the target population to include other related psychiatric disorders and, as done in this study, with a primary analysis across several psychiatric disorders but with a sensitivity analysis just in schizophrenia. While, eventually, individual GWASs of features within diagnoses might be possible - which would then allow for testing for enrichment of specific neurodevelopmentally relevant genes, differences in specific tissues etc. - these obviously require large samples of richly phenotyped data, which are extremely difficult to collect for clinical populations and for the multitude of features-of-interest to study. For instance, despite the high priority on better understanding the TRP phenotype, so far studies are still greatly limited in regard to their sample sizes and their use of proxy measures, with only candidate variants/genes having been investigated (Pisanu & Squassina, 2019). We feel, therefore, that

our approach will be particularly useful for analysing neuropathophysiological differences in TRP and other similar psychiatric features in the interim.

In addition to those already mentioned in the above, there are particular aspects of our approach, and of the CardiffCogs dataset, which should be considered when interpreting results. The general limitations of the CardiffCogs study design have been described previously along with steps taken to address them (Legge et al., 2020). These include the differences in systematic recruitment rates between TRP and non-TRP individuals, and hence our inclusion of this as a covariate in our analysis; the limited sample size meaning specific antipsychotic effects could not be assessed; and the restriction to majority white-European genetic ancestry within the cohort, limiting inference from results to other ancestry groups. In regard specifically to our study, in addition to those discussed above, the brain-based summary statistics were derived in a cohort which did not exclude individuals with neurological or psychiatric conditions, including schizophrenia. If our scores had significantly predicted TRP this might have been an issue and worth repeating a sensitivity analysis excluding these individuals. Additionally, while published genetic summary statistics were available for total brain volume (Elliott et al., 2018; Zhao et al., 2019), we generated our own summary statistics so as to use the same cohort and methodology deployed to generate our cerebellar volume summary statistics (*Chapter 4*). This also had the advantage of involving a larger sample sizes than those previously reported and included correction for possible confounding factors such as head-motion. As a sensitivity analysis for these new total brain volume summary statistics, we show our total brain volume summary statistic showed high genetic correlation with previous results (see Supplementary Note 5.1), though with higher heritability and smaller standard errors reflecting our larger sample size. Finally, our limited sample size also meant we were unable to test for any possible interaction effects which might be of interest to future studies, such as was performed with urbanicity in a recent polygenic schizophrenia risk score analysis on TRP status (Gasse et al., 2019).

In conclusion, we found no evidence for our hypothesis that common genetic variants associated with brain volume might be lower in individuals with treatment resistance compared to non-treatment resistant individuals. We highlight a little-used approach and one which is only recently possible due to the growing number of identified common genetic variants associated with brain measures, which we feel will be of great use in assessing brain related processes within and across features of psychiatric disorders

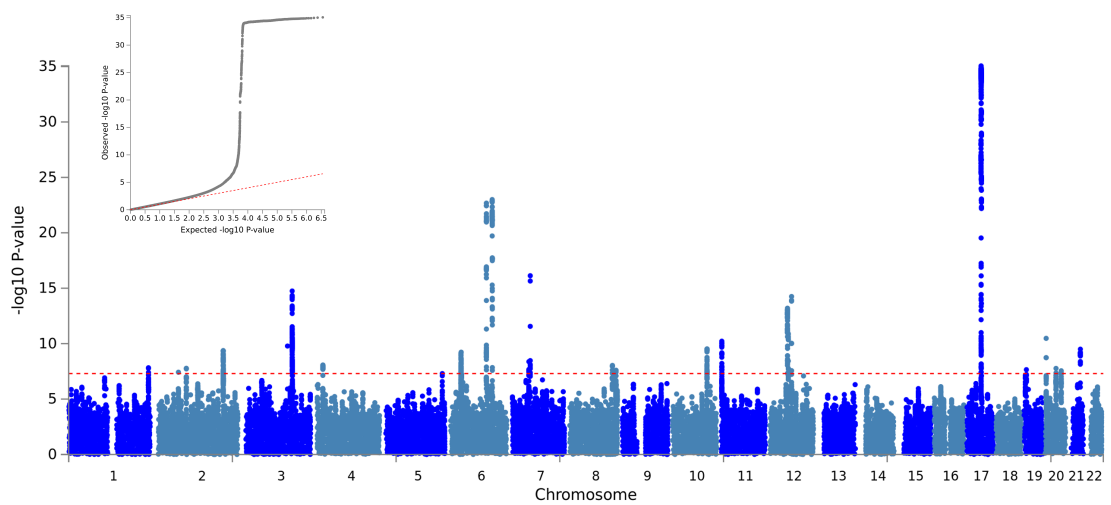
5.6 Supplementary Notes

Supplementary Note 5.1: Total brain volume genome wide association study (GWAS)

Total brain volume GWAS was conducted in the same two independent phases of UK Biobank used for total cerebellar volume GWAS (*Chapter 4*). These included 17,818 participants (age mean[*min,max*] = 63[45,80]yrs, 53% female) in phase 1 GWAS and 15,447 participants (age mean[*min,max*] = 65[48,81]yrs, 53% female) in phase 2 GWAS. The two phases were processed separately. For the generation of the total brain volume phenotype for the GWAS, since it had already been a covariate in the cerebellar GWAS, those with missing and outlier values had already been excluded. We used R(3.6.0) (<https://www.R-project.org/>) to repeat the multiple univariate linear regression analysis to obtain residuals for total brain volume ([25010](#)), regressed on the effects of age ([21003-2.0](#)), age² (1st and 2nd degree orthogonal polynomials), sex ([31](#)), their interaction (age²*sex), mean resting-state functional MRI head motion averaged across space and time points ([25741-2.0](#)) (log transformed; [21001-2.0](#)) and imaging-related covariates of imaging centre attended ([54-2.0](#)), date attended imaging centre ([53-2.0](#)), X-, Y- and Z-head position in the scanner ([25756](#), [25757](#), [25758](#)) and starting table-Z position ([25759](#)). Histogram plots showed a normal distribution of residual total cerebellar volume values. We used *PLINK* (v1.9) (C. C. Chang et al., 2015) to conduct GWAS analyses on the standardised residuals for each phase. We used METAL (2011-03-25 release) (Willer et al., 2010) to combine our two phases of GWAS to create a meta-GWAS, weighting the effect size estimates by the inverse of the corresponding standard errors. We estimated a lower-bound of narrow-sense (additive) single nucleotide polymorphism (SNP)-based heritability (h^2_{SNP}) for the combined meta-GWAS of $h^2_{\text{SNP}}[\text{Standard Error/SE}] = 35.9[3.6]\%$ using linkage disequilibrium score regression (LDSC) software (Bulik-Sullivan, Loh, et al., 2015), which also showed little inflation of the intercept (intercept[SE] = 1.03[0.01]) indicating little genomic bias. As a sensitivity analysis to our results, we aimed to compare our summary statistics to those recently published for total brain volume from other groups (Elliott et al., 2018; Zhao et al., 2019) to show similar broadly similar finding, though with greater power in our larger sample sizes. Using LDSC software to ascertain genetic correlation (Bulik-Sullivan, Finucane, et al., 2015) between our total brain volume and that of Elliott et al (N=9,707; LDSC $h^2_{\text{SNP}}[\text{SE}] = 18.0[5.5]\%$) and Zhao et al (N=19,629; $h^2_{\text{SNP}}[\text{SE}] = 36.7[3.9]\%$) results, we showed a moderate-to-high genetic correlation between traits ($r_{\text{genetic}}[\text{SE}] = 0.51[0.10]$, $p = 2.3 \times 10^{-7}$ & $r_{\text{genetic}}[\text{SE}] = 0.88[0.03]$, $p = 1.4 \times 10^{-269}$, respectively). The meta-GWAS Manhattan plot and quantile-quantile (QQ) plots from the FUMA package

(Watanabe, Taskesen, Van Bochoven, & Posthuma, 2017) are presented in Supplementary Figure 5.1.

Supplementary Figure 5.1: Manhattan and quantile-quantile (QQ) plots (insert) of for single nucleotide polymorphisms (SNPs) associations with total brain volume from a meta-GWAS in UK Biobank ($N_{\text{Total}}=33,265$). Dashed line indicates genome-wide significance at $p < 5 \times 10^{-8}$.



5.7 Supplementary Tables

Supplementary Table 5.1: Demographic information and premorbid risk factors for treatment resistance in the schizophrenia and schizoaffective depression sub-cohort, split by treatment resistance status

	Treatment resistant (n=346)	Non-treatment resistant (n=280)	Missing (n=34)
Sex			
Female	123 (35.5%)	96 (34.3%)	13 (38.2%)
Male	223 (64.5%)	184 (65.7%)	21 (61.8%)
Age at interview (yrs)			
Mean (SD)	42.6 (11.6)	44.5 (12.1)	44.1 (13.3)
Median [Min, Max]	43.0 [17.0, 74.0]	45.0 [18.0, 72.0]	43.5 [18.0, 71.0]
Recruited systematically			
Yes	279 (80.6%)	192 (68.6%)	21 (61.8%)
No	67 (19.4%)	88 (31.4%)	13 (38.2%)
Psychosis age at onset (yrs)			
Mean (SD)	22.8 (8.21)	26.8 (8.80)	26.7 (10.1)
Median [Min, Max]	21.0 [3.00, 66.1]	25.0 [6.00, 62.0]	25.0 [13.0, 56.0]
Missing	14 (4.0%)	15 (5.4%)	2 (5.9%)
Premorbid IQ			
Mean (SD)	96.4 (13.7)	99.7 (12.9)	99.4 (13.4)
Median [Min, Max]	97.1 [68.6, 128]	101 [68.6, 129]	99.0 [68.6, 123]
Missing	23 (6.6%)	13 (4.6%)	4 (11.8%)
Poor premorbid social adjustment			
Yes	147 (42.5%)	83 (29.6%)	14 (41.2%)
No	182 (52.6%)	185 (66.1%)	19 (55.9%)
Missing	17 (4.9%)	12 (4.3%)	1 (2.9%)

Supplementary Table 5.2: The association between polygenic scores of total cerebellar volume and outcomes of interest in individuals with either schizophrenia or schizoaffective depression diagnosis (n=660)

Outcome	Polygenic score		$\Delta R^2 \ddagger$	$\beta \S$	95% Confidence		p	p_{FDR}^*
	Brain region	p_T -value < †			intervals §			
Treatment resistant psychosis (TRP) status	Total Brain Volume	0.001	1.08E-04	-0.02	-0.18	0.14	0.83	0.92
		0.005	9.75E-04	-0.05	-0.21	0.11	0.52	0.73
		0.01	2.84E-03	-0.09	-0.25	0.07	0.27	0.73
		0.05	3.73E-03	-0.11	-0.27	0.06	0.21	0.73
		0.1	2.61E-03	-0.09	-0.25	0.08	0.29	0.73
	Cerebellar Volume	0.001	1.30E-03	-0.06	-0.23	0.10	0.46	0.73
		0.005	2.28E-05	-0.01	-0.17	0.16	0.92	0.92
		0.01	7.94E-04	-0.05	-0.21	0.12	0.56	0.73
		0.05	7.17E-04	-0.05	-0.21	0.12	0.58	0.73
		0.1	1.30E-03	-0.06	-0.23	0.10	0.46	0.73
Premorbid IQ	Total Brain Volume	0.001	8.14E-03	1.22	0.17	2.27	0.02	0.45
		0.005	4.22E-03	0.88	-0.17	1.92	0.10	0.45
		0.01	4.18E-03	0.87	-0.17	1.92	0.10	0.45
		0.05	4.13E-03	0.87	-0.18	1.91	0.10	0.45
		0.1	4.16E-03	0.87	-0.18	1.93	0.10	0.45
	Cerebellar Volume	0.001	3.02E-03	0.75	-0.31	1.81	0.16	0.49
		0.005	5.09E-04	0.31	-0.75	1.37	0.57	1.00
		0.01	4.06E-05	0.09	-0.98	1.15	0.87	1.00
		0.05	1.67E-03	0.56	-0.51	1.63	0.30	0.75
		0.1	1.13E-03	0.46	-0.60	1.52	0.40	0.91
Poor premorbid social adjustment	Total Brain Volume	0.001	9.85E-05	-0.02	-0.18	0.15	0.83	1.00
		0.005	7.54E-06	0.01	-0.16	0.17	0.95	1.00
		0.01	3.19E-06	0.00	-0.17	0.16	0.97	1.00
		0.05	5.05E-09	0.00	-0.17	0.17	1.00	1.00
		0.1	4.15E-05	0.01	-0.16	0.18	0.89	1.00
	Cerebellar Volume	0.001	3.27E-03	0.11	-0.06	0.27	0.21	0.57
		0.005	6.92E-03	0.16	-0.01	0.32	0.07	0.45
		0.01	4.66E-03	0.13	-0.04	0.30	0.13	0.45
		0.05	1.05E-03	0.06	-0.11	0.23	0.48	1.00
		0.1	2.84E-04	0.03	-0.14	0.20	0.71	1.00

		0.001	1.04E-05	0.03	-0.58	0.64	0.93	1.00
	Total Brain	0.005	3.20E-03	0.50	-0.11	1.12	0.11	0.45
	Volume	0.01	2.83E-03	0.47	-0.14	1.09	0.13	0.45
		0.05	2.36E-04	0.14	-0.48	0.75	0.66	1.00
Age at onset		0.1	5.15E-05	0.06	-0.55	0.68	0.84	1.00
(yrs)	Total	0.001	3.78E-04	-0.18	-0.80	0.45	0.58	1.00
		0.005	5.54E-05	-0.07	-0.69	0.56	0.83	1.00
	Cerebellar	0.01	3.05E-04	-0.16	-0.77	0.46	0.62	1.00
	Volume	0.05	5.49E-05	-0.07	-0.69	0.55	0.83	1.00
		0.1	9.29E-05	-0.09	-0.71	0.53	0.79	1.00

Results are from independent univariate linear (continuous outcome) or logistic (binary outcome) regression models of each polygenic score derived from GWAS results of total cerebellar volume; with correction for covariates of age at time of interview, sex, the method used for participant recruitment and the first 10 genetic principal components. †: Polygenic scores across five SNP inclusion thresholds (p -values). ‡: unique variance (ΔR^2) in outcome explained by the polygenic score are calculated by subtracting the R^2 of model including polygenic score and covariates against that with just covariates; with R^2 calculated on the liability scale for TRP and pseudo- R^2 for poor premorbid social adjustment. §: polygenic scores are scaled and mean-centred, representing a difference in outcome with $1 \times SD$ difference in polygenic score. *: p_{FDR} reflects p -values adjusted for the inflation of false discovery rate (FDR) due to multiple comparisons

6 General discussion

While individual experimental chapters include discussions on addressing the specific hypotheses for each analysis, their implications and their limitations, in the following section I bring together results across chapters, so as to arrive at general conclusions from this research thesis and discuss their relevance to the wider literature of investigations of cerebellar involvement in schizophrenia. Chiefly, I address the implications of results in regard to the confidence which can be placed for cerebellar volume reductions in those with schizophrenia, the aetiology behind the reductions, their pathophysiological importance, their wider relevance to psychiatric and cerebellar research and their clinical implications. Finally, I highlight current limitations and future directions to address these limitations and to build on the work presented here.

6.1 Is cerebellar volume reduced in those with schizophrenia?

Firstly, a key outcome of this thesis is in further investigating cerebellar reductions in those with schizophrenia and ascertaining whether these differences might reflect true pathophysiological reductions in volume or might instead reflect imaging artefacts, caused by differences in participants' behaviour and position in the scanner. In *Chapter 2*, I mirror previous reports of the elevated head motion of participants with psychiatric diagnoses during neuroimaging scanning (Makowski et al., 2019), and introduce to the literature findings of the substantial proportion of variance on cerebellar volume for which this can account for. Importantly, however, I show that the cerebellum is, on average, still substantially reduced in individuals with a recorded history of schizophrenia and other related psychiatric disorders, compared to those without such diagnoses, even when correcting for possible imaging artefact inducing factors such as elevated head motion or lower participant position in the scanner. Of note, I correct for these measures in all subsequent genetic imaging studies where, equally, these are routinely overlooked in the literature despite their possible substantial relationship with recorded brain volumes; for example, in our *Chapter 2* sample each variable accounts for an additional 2.7% and 9.6% variance in total cerebellar volume, respectively, even when including the other covariates of age, sex, centre and date scanned, and overall brain volume in the model. Since the initiation of this study, another group has conducted a systematic analysis of possible confounding effects on imaging variables within UK Biobank, presenting a final collection of 602 variables which could confound results (Alfaro-Almagro et al., 2021). In addition to more

conventional covariates (e.g. age, sex, head size, centre attended, date attended), this includes many non-linear, crossed-term (i.e. interactions) and far more extensive head motion variables. While these will be interesting to incorporate into any future analyses, notably, they found a “typical” simpler set of covariates – which is almost identical to that used in this study but lacking head/table position and using head size rather than total brain volume - accounted for an average of almost half of the variance across all MRI modality IDPs that was explained by the fuller set (mean R^2 : 11.1% ALL vs 4.4% SIMPLE sets of covariates). Of note, for the head and table position variables not included in this SIMPLE set, they report these to account for an average of 1% R^2 in T1-w IDPs though up to 14% for some cerebellar IDPs (though, of note, this is not accounting for other covariates included in the SIMPLE set). Since, therefore, their major confounders identified for T1w structural scans were all controlled for in the models of this thesis - being age, site, head motion estimates and table position - our results should mostly capture these effects.

The results of *Chapter 2*, therefore, expand the work of a recent systematic mega-analysis of cerebellar volumetric reductions in schizophrenia (Moberget et al., 2018) by showing that such differences are not simply due to imaging artefacts alone, and agree with previous post-mortem work showing cerebellar reductions in cell density and gyrification (Maloku et al., 2010; Schmitt et al., 2011). In addition, compared to this previous neuroimaging report in a much younger aged clinical cohort (mean age \approx 30yrs) (Moberget et al., 2018), the *Chapter 2* results show that these cerebellar reductions remain into older age (mean age \approx 60yrs), also highlighting long-term negative effects of psychiatric traits on cerebellar neuroanatomy. While the number of individuals with schizophrenia in this cohort was small, which can lead to elevated false-positive and exaggerated effect sizes (Button et al., 2013), I found similar cerebellar results across different psychiatric conditions assessed. Neuroimaging reports of cerebellar differences in schizophrenia, therefore, do not appear simply to be a function of imaging artefacts, however, given the correlation between these factors and recorded regional brain volume measures, adequate consideration and correction for these should be included in future research designs.

6.2 What is the contribution of comorbidities to the cerebellar reductions seen in psychiatric disorders?

As with many psychiatric disorders, the pathophysiology of schizophrenia is highly complex. Those with psychiatric disorders often show an elevated number of other medical comorbidities,

such as metabolic-related disorders (Annamalai et al., 2017; Scott et al., 2016; Vancampfort et al., 2013), many of which are themselves associated with reduced recorded brain volumes (Dekkers et al., 2019). Utilising the availability of linked medical records, physical trait measures and the large sample size of the UK Biobank, in *Chapter 2* I also wished to systematically investigate which non-psychiatric medical conditions and sub-clinical anthropomorphic measures are elevated in those with psychiatric conditions and might account for some of the recorded cerebellar volume seen.

I found that several clinical and sub-clinical comorbidities associated with schizophrenia diagnosis have a substantial negative correlation with cerebellar structure, most notably for those related to endocrine and metabolic dysfunction such as diabetes and obesity diagnoses, as well as elevated body mass index (BMI). While some of these effects appear mediated by imaging artefacts, such as increasing head motion, there also appear independent effects, in line with previous literature which has highlighted pathways for pathophysiological effects of these disorders on the brain, such as dyslipidaemia and systematic inflammation (Kolenič et al., 2020). These results, therefore, suggest that a significant proportion of the cerebellar reductions seen in individuals with schizophrenia could be a result of this elevation in clinical and sub-clinical comorbidities, though more formal testing of causality would be required (discussed below). Importantly, however, I show that despite this, there is a residual negative effect of psychiatric diagnosis on cerebellar volume when these are controlled for retrospectively in the statistical models, indicating that these are unlikely to be the sole cause of the recorded volume difference.

While a substantial amount of BMI/weight-related effects in patients are likely driven by medication status (Bak et al., 2014), it appears that such effects are also present in first episode and premorbid studies (Minichino et al., 2017; Pillinger et al., 2017; Tian et al., 2020), therefore, these findings will be important to consider for all psychiatric imaging studies and not just in cohorts of patients with established illness. They also highlight how the relationship between these diagnoses is complicated, and do not simply reflect a confounding effect. Both systematic analyses specifically focusing on investigating the different pathways in which elevated participant weight/body fat could negatively impact on recorded measured brain morphometry (both in those with psychiatric diagnosis and more broadly), and intervention studies analysing the effect of reduced weight on the brain, will help in better understanding the relationship between psychopathology, weight related differences and recorded regional brain structure (Bohon & Geliebter, 2019; Minichino et al., 2017; Mueller et al., 2015). This also highlights the

need for careful consideration of how best to control for such measures in future imaging studies, depending on the research question being asked (as discussed in *Chapter 2*).

6.3 Are cerebellar differences in schizophrenia related to schizophrenia's genetic aetiology?

This thesis also probed whether cerebellar volume differences in schizophrenia have, at least in part, a genetic aetiology. Common genetic variants account for a substantial proportion of the heritability of schizophrenia (Dennison et al., 2020) and, as I show in the GWAS results of *Chapter 4*, also account for a substantial proportion of the heritability of cerebellar volumes. In *Chapter 3*, I identified a negative association between a large sample of unaffected individuals' cerebellar volumes and their common genetic risk for schizophrenia. Additionally, I identified particular copy number variants (CNVs) which have previously been robustly shown to increase the risk for schizophrenia, notably in the 1q21.1 locus, associating with cerebellar volume. This effect, however, was not seen across all schizophrenia-associated CNVs tested, aside from in particular cerebellar regions (as discussed later). The pleiotropic effect of variants for schizophrenia liability on cerebellar volume adds further evidence toward cerebellar reductions seen in individuals with schizophrenia diagnoses not arising solely through reverse causation, and instead being present premorbid and reflecting an intrinsic part of schizophrenia pathophysiology. This work in unrelated individuals complements similar findings in close family members of those with psychiatric diagnosis and in those carrying more penetrant (higher odds ratio of association) CNVs for schizophrenia, such as 22q11.2 deletion, where cerebellar reductions have also been noted (de Zwarte, Brouwer, Agartz, et al., 2019; Rogdaki et al., 2020). Genetic risk for schizophrenia, therefore, appears to also be associated with reduced cerebellar volume.

In *Chapter 4*, I utilised others' approaches to assess for a shared common allele architecture between schizophrenia liability and cerebellar volume. This included analysing whether a correlation existed across the genome, for effect sizes for both traits. Counter to the clinical and above genetic findings, I did not find the hypothesised negative correlation. There are several possible reasons for this disparity between the polygenic score and genetic correlation results. Firstly, it could be that residual population structure in polygenic score analysis was driving the association and which was not present in the genetic correlation analysis due to the method's ability to better capture these effects in the intercept (Bulik-Sullivan, Loh, et al., 2015). The negligible association between genetic principal components and cerebellar volume (*Chapter 3*)

and the small inflation of the intercept in the genetic correlation analysis (*Chapter 4*), however, indicates this is unlikely to be the case.

Alternatively, as the polygenic score effect was seen even at the most stringent SNP inclusion thresholds used, these results might indicate that the association between them is driven by a more limited number of variants, a signal which could be lost in the added noise when analysing across the whole genome. Related to this, it could be that the association between traits is driven by SNPs at lower minor allele frequencies (MAF), such as the non-synonymous SNPs we identify in *Chapter 4* as important for cerebellar volume, and which were removed from the genetic correlation analysis due to its higher MAF minimum threshold (1%) but included in the more lenient polygenic score MAF threshold (0.1%). Analysing just the genome-wide significant associations for each trait to see if they showed similar directions of effect, however, showed little evidence for pleiotropy, with only the missense variants within the *SLC39A8* gene indicated as relevant to both traits. If the raw genotypes of schizophrenia traits could be obtained, other genetic correlation tools such as bivariate GCTA-GREML would allow for a more accurate assessment of genetic correlation between traits (S. H. Lee et al., 2012). Equally, other methods aside from whole genome genetic correlation might be more useful in future studies for assessing shared genetic architecture between cerebellar volume and schizophrenia, particularly since the direction of effects of variants appears mixed. For example, multi-trait conditional and conjunctive false discovery rate analysis utilises the polygenicity of the genome to condition the p-values of association of one trait on those of a related trait, allowing for an increased variant discovery as well as allowing for assessment of genetic overlap irrespective of direction of effect between two traits (Smeland, Frei, Shadrin, et al., 2020; Smeland et al., 2018). Similarly, the use of bivariate causal mixture models of polygenicity would equally help identify genetic overlap (Frei et al., 2019). Equally, the replication of the work in larger samples in UK Biobank, so as to improve power for detecting variants as well as improving accuracy of variants effect sizes – particularly for CNV analyses where several CNVs had fewer occurrences - as well as replication in other cohorts (discussed more in *6.5 Considerations and future directions*) will also be key (both of which are currently planned).

Of note, such a disparity between polygenic score and genetic correlation results is also apparent for other brain regions, where no genetic correlations have been seen so far between schizophrenia liability and brain morphometry (Franke et al., 2016; Grasby et al., 2020; Satizabal et al., 2019; van der Meer et al., 2018) while some reports – though not all - show associations with polygenic scores (Alloza et al., 2018; Alnæs et al., 2019; Bolhuis et al., 2019; Doan et al.,

2017; Fonville et al., 2019; Neilson et al., 2019). Therefore, better understanding of this association is a pressing need for all neuroimaging genetic studies and is not limited to the cerebellum and, again, highlights how the exclusion of the cerebellum from these studies does not appear justified.

Of particular interest for future studies will be combining genetic risk with neurodevelopmental information. The cerebellum shows a particular sensitivity to early neurodevelopmental perturbations (Keunen et al., 2016; Matsufuji et al., 2017) - including specific reports within the UK Biobank cohort (Gheorghe, Li, Gallacher, & Bauermeister, 2020) - as well as numerous reports of alterations in individuals with diagnosed neurodevelopmental disorders (Stoodley, 2016). Altered neurodevelopment, including early life complications and premature birth, are strong risk factors for schizophrenia (Cannon, Jones, & Murray, 2002; Kessler et al., 2010; Matheson et al., 2013; Pugliese et al., 2019) and, therefore, such factors might also be contributing to cerebellar alterations in those with schizophrenia, either independently or by moderating and/or mediating genetic risk (Guloksuz et al., 2019; Myllyaho et al., 2019; Ursini et al., 2018). Exploring for interactional effects of genetic risk for schizophrenia with early life complications in younger cohorts with richer phenotyping of these early life factors, will be an interesting future avenue. Equally, investigation of developmental cerebellar genetic expression, rather than those in adulthood, would be particularly interesting avenues to investigate if schizophrenia's genetic effects are specific to developmental differences.

Related to this, results from this thesis (*Chapter 2*) also add to the body of evidence of cerebellar structural differences being present with several other psychiatric and neurodevelopmental disorders other than schizophrenia (Lupo, Siciliano, & Leggio, 2019; Phillips et al., 2015; Stoodley, 2016). Furthermore, the schizophrenia-associated common and rare genetic variants used in *Chapter 2* are also associated with other psychiatric and neurodevelopmental traits with, respectively, moderate-to-high (r_g 0.20-0.70) genetic correlation between common variants for schizophrenia and several other psychiatric traits including bipolar, major depression, autism spectrum and anorexia nervosa disorders (P. H. Lee et al., 2019) and the schizophrenia-associated rare CNVs coming from a larger list of neurodevelopmentally linked CNVs (Rees et al., 2016). These findings, therefore, indicate that any cerebellar-associated differences are unlikely to be specific to schizophrenia alone but, instead, add evidence toward the idea of disruptions in cerebellar circuitry being one of the key network alterations associated with general liability for psychiatric disorders and general psychopathology in adolescents (Hariri, 2019; Moberget et al., 2019; Romer et al., 2018). A compelling hypothesis posited as to the

relevance of the cerebellum for psychopathology development, is in early cerebellar perturbations leading to abnormal neuronal information integration and coordination, and so poorer executive control performance (Hariri, 2019). This leads the individual to then be impaired in their regulatory ability to subsequent, environmental adverse events, which could lead to the development of later specific psychopathologies depending upon the nature of the secondary exposure.

As discussed, however, in specific regard to genetic overlap, the results from *Chapter 4* show no detectable whole-genomic correlation with some of these other psychiatric disorders in addition to the lack of genetic correlation with schizophrenia. In addition to the deployment of methods other than whole genome genetic correlation to better explore shared genetic architecture between brain and psychiatric traits (as highlighted above and in *Chapter 4*), combing these with testing of associations with common genetic variants identified as associated across multiple neurodevelopmental and psychiatric disorders (Grotzinger et al., 2019; P. H. Lee et al., 2019; Z. Yang et al., 2019) would be an interesting future step. Equally, the deployment of tools such as univariate and multivariate Mendelian randomisation (Carter et al., 2021) could help identify which psychiatric genetic risk on cerebellar effects are mediated (lying along the causal pathway) or independent (have their own separate effects) from the aforementioned early life complications and environmental neurodevelopmental traits.

6.4 What is the pathophysiological relevance of genetics for cerebellar volume?

The final experimental chapter of this thesis (*Chapter 5*) explored one of the ways in which ascertaining the genetic variants associated with cerebellar structure might be relevant for improving our understanding of schizophrenia pathophysiology. Specifically, I investigated if the identified genetic variants for cerebellar volume were related to the development of treatment-resistance psychosis in schizophrenia. This is a sub-type of schizophrenia where individuals do not respond to first-line treatments and have much poorer outcomes; and where perturbed neurodevelopment has been suggested as potentially relevant for increasing risk of its development (Gillespie et al., 2017; Legge et al., 2020). Since I found no such association between genetic variants associated with total cerebellar volume, nor for variants associated with total brain volume, the results imply that if a neurodevelopmental origin lies behind treatment-resistance psychosis, then these do not appear driven by genetic variants associated with adult brain volume (at least to an effect we deemed as meaningful). While the focus was

on cerebellar volume for this thesis, I highlight how such an approach utilising the advent of large cohorts with both genetic and neuroimaging information holds promise for future psychiatric research: where researchers can test a battery of such genetic scores for brain measures across regions and modalities to investigate their use as endophenotypes for specific features within and across diagnoses, such as age at onset, specific symptomatology, specific subtypes and/or treatment response. These then can help act as a quick and cheap first exploration, so as to better guide more targeted follow-up research work, as well as the potential to aid in improving diagnosis stratification and treatment planning.

6.5 Considerations and future directions

While specific considerations and limitations to the approaches deployed in each thesis chapter are discussed therein, below I outline those of the general approach chosen for this thesis, how these were addressed, and how future research could further advance our understanding of cerebellar differences in schizophrenia.

Firstly, throughout most analyses within this thesis, the cerebellum was treated as a whole; grouping all lobules together to analyse overall effects. I chose this approach since cerebellar reductions in those with schizophrenia were reported generally across the whole cerebellum, with no hemispheric differences though with a slight gradient of effect (Moberget et al., 2018); that the cerebellum shows high genetic homogeneity across subdivisions (Hawrylycz et al., 2015); and finally since no cerebellar-specific registration was deployed by UK Biobank for the generation of image-derived phenotypes used, which would likely impair the accuracy of estimated cerebellar lobule boundaries (Diedrichsen, 2006). Because of these and, therefore, to limit the number of tests performed on highly correlated lobules, I felt the more pragmatic approach was to present overall cerebellar effects, with sub-regionals effects presented in supplementary results.

Follow-up analysis, therefore, using cerebellar-specific segmentation tools, such as SUIT, would provide more confidence in the lobule boundaries delineated. Equally and/or in combination with this, deployment of different cerebellar atlases, including resting-state and task-based functional maps, such as used in a recent schizophrenia cohort analysis, might indicate more functionally-specific cerebellar differences (Buckner et al., 2011; King et al., 2019; Moberget et al., 2018). When analysing effects of genetic risk for schizophrenia on the cerebellum, however, I did include supplementary analyses investigating the effects across lobules, showing relatively

consistent effects of common genetic variants across the cerebellum, though with more variation across CNVs and their regions of effect, likely due to lower carrier numbers. Interestingly, schizophrenia genetic effects appeared to coalesce in regions such as Crus II. This is an area more associated with cognition (J. H. Balsters et al., 2010; Stoodley, Valera, & Schmahmann, 2012) and social functions (Van Overwalle, Ma, & Heleven, 2020), and where greater negative effects in clinical cohorts have previously been noted (Laidi et al., 2019), though, again, a recent mega-analysis analysis of lobule volume reductions suggests its reduced volume is not unique and, instead, reductions are seen across most of the cerebellum (Moberget et al., 2018). This region, therefore, might be of particular interest to focus upon in future research; though further work should first ascertain if its greater reduction simply reflects its larger volume and, therefore, perhaps less affected by poorer registration (which might have been addressed through the use of SUIT in the latter study). Critically and to our knowledge, the research design in *Chapter 3* is the first study to analyse both effects of common and rare genetic variants in the same study and the possible coalescence of effects highlights the benefit of such an approach.

Additionally, this thesis focused solely upon volumetric differences, and while analysis of the constitute components of surface area and thickness - which show relatively independent genetic aetiology (Grasby et al., 2020; Winkler et al., 2010) - are not yet available in the cerebellum, this will hopefully change in the near future (Serenio et al., 2020). These, along with metabolic differences within the cerebellum, and structural and functional connectivity between the cerebellum and the other co-heritable subcortical structures highlighted in the thesis (*Chapter 4*), would likely prove fruitful for future research. For example, the cerebellothalamocortical tracts are one of the longest standing regions of interest in schizophrenia (Nancy C. Andreasen et al., 1999; Hua et al., 2019), and results from our thesis highlighted the strong genetic correlation between the cerebellum and thalamus, and how identified genetic variants associated with schizophrenia liability had the most consistent effects on Crus II – being a major contributing site to cerebellothalamocortical projections (Palesi et al., 2015). Analysing, therefore, the effect of polygenic scores on the structural and functional connectivity between these regions seems an obvious next step and which may relate to the reported volume loss in this thesis (He et al., 2019).

Furthermore, it would be interesting to link cerebellar imaging measures with behavioural processes where the cerebellum's role is well established, such as saccadic eye movements, eye-blink conditioning and postural sway. These traits have similarly been shown altered in

schizophrenia and have been suggested as biomarkers for neurodevelopmental disorders (Apthorp et al., 2019; Coesmans et al., 2014; Kent et al., 2015; Reeb-Sutherland & Fox, 2013). They also have the advantage of being easier measures to collect - for example with eye movement measures being collectable on mobile phone devices (Z. Chang et al., 2020)- and so could allow for research (and clinical application) not limited to accessibility to large and expensive MRI infrastructure. Equally, retinal imaging shows promise for detecting differences in schizophrenia (Silverstein, Fradkin, & Demmin, 2020) and recent reports indicate that these effects might show some relation to cerebellar volumes (Mejia-Vergara, Karanjia, & Sadun, 2020).

A similar set of covariates was used for most statistical models in this thesis. This included the linear addition of total brain volume as a covariate, so as to ascertain relative cerebellar volume differences. Others, however, have suggested such approaches can fail to properly account for cerebellar-specific differences (Mankiw et al., 2017). The inclusion of both corrected and uncorrected total cerebellar volume effects and/or comparison with total brain volume differences within this thesis hopefully helps to mitigate any false inference of such differences. Equally, for most models I included correction across age and sex differences of participants, since generally no strong interactional effects with schizophrenia diagnosis were apparent for cerebellar or cerebral volumes (Moberget et al., 2018; Theo G.M. van Erp et al., 2018). However, further exploration of these effects should be deployed and also performed at a summated regional level, rather than across a single whole cerebellar measure, since regional variation of main effects are apparent (Bernard & Seidler, 2014; Mankiw et al., 2017) along with reports of regional interactional effects with schizophrenia (Womer et al., 2016). As already discussed, a logical next step for our analysis, given the interest in neurodevelopmental change, is in the investigation of genetic variants on cerebellar brain volume in younger cohorts, particularly during childhood and adolescence.

Lower socio-economic status is associated with increased schizophrenia incidence (Y. Luo et al., 2019) and there is growing appreciation for the effect of socio-economic status on brain morphometry (Cavanagh et al., 2013; Farah, 2017; Yapple & Yu, 2020). Exploration of the mediating or moderating effect of socioeconomic status on the effects discussed here should also be conducted. Related to this, familial schizophrenia effects on brain morphometry appear to be at least partly captured by shared effects of cognition, therefore, future studies could include additional analyses testing for the mediating effect of IQ on this relationship (de Zwarte, Brouwer, Tsouli, et al., 2019). As discussed in individual chapters, the UK Biobank differs to the

general UK population in age, several lifestyle and socioeconomic factors and, therefore, it is important to remember to be cautious about extrapolation of results to the wider UK population. Furthermore, to minimise capturing of general population effects, for the genetic analyses in this study I limited the sample to those with genetic ancestry defined as similar to British/Irish, the vast majority of the sample. Expanding this research into other diverse genetic ancestry groups and combining with recent developments in multi-ancestry genetic analysis tools (Atkinson et al., 2021) , will not only allow for improved applicability of results, but also allow for greatly improved discoverability of variants and identification of causal variants (Gurdasani, Barroso, Zeggini, & Sandhu, 2019).

6.6 Conclusion

The results of this thesis add evidence for cerebellar differences in schizophrenia and related psychopathologies. It advances the field by investigating the origin of these volumetric differences in clinical and non-clinical populations, highlighting how uncorrected imaging artefacts, anthropomorphic differences and comorbidities might underlie a substantial proportion of the reported effects in the literature, and that their inclusion in analyses will be of paramount importance for advancing the field of psychiatric neuroimaging. Importantly, however, we show that even with their correction, cerebellar differences remain and that genetic risk for schizophrenia, by way of common and rare genetic variants, shows some association with these differences. Further work is required, particularly for the cerebellum's association with early life complications and investigating the implications of cerebellar involvement for subtyping of diagnoses and treatment outcomes. The regular omission of the cerebellum in psychiatric studies, therefore, appears to be a severe problem, and one which I hope the results of this thesis in highlighting its reduction in individuals with clinical diagnoses and, at least in part, higher genetic burden for schizophrenia, help highlight and address.

7 References

- Abel, K. M., Wicks, S., Susser, E. S., Dalman, C., Pedersen, M. G., Mortensen, P. B., & Webb, R. T. (2010). Birth weight, schizophrenia, and adult mental disorder: Is risk confined to the smallest babies? *Archives of General Psychiatry*, *67*(9), 923–930. <https://doi.org/10.1001/archgenpsychiatry.2010.100>
- Adamaszek, M., D'Agata, F., Ferrucci, R., Habas, C., Keulen, S., Kirkby, K. C., ... Verhoeven, J. (2017). Consensus Paper: Cerebellum and Emotion. *Cerebellum (London, England)*, *16*(2), 552–576. <https://doi.org/10.1007/s12311-016-0815-8>
- Adhikari, B. M., Hong, L. E., Sampath, H., Chiappelli, J., Jahanshad, N., Thompson, P. M., ... Kochunov, P. (2019). Functional network connectivity impairments and core cognitive deficits in schizophrenia. *Human Brain Mapping*, *40*(16), 4593–4605. <https://doi.org/10.1002/hbm.24723>
- Adzhubei, I. A., Schmidt, S., Peshkin, L., Ramensky, V. E., Gerasimova, A., Bork, P., ... Sunyaev, S. R. (2010). A method and server for predicting damaging missense mutations. *Nature Methods*, *7*(4), 248–249. <https://doi.org/10.1038/nmeth0410-248>
- Ahtam, B., Link, N., Hoff, E., Ellen Grant, P., & Im, K. (2019). Altered structural brain connectivity involving the dorsal and ventral language pathways in 16p11.2 deletion syndrome. *Brain Imaging and Behavior*, *13*(2), 430–445. <https://doi.org/10.1007/s11682-018-9859-3>
- Alfaro-Almagro, F., Jenkinson, M., Bangerter, N. K., Andersson, J. L. R., Griffanti, L., Douaud, G., ... Smith, S. M. (2018). Image processing and Quality Control for the first 10,000 brain imaging datasets from UK Biobank. *NeuroImage*, *166*, 400–424. <https://doi.org/10.1016/j.neuroimage.2017.10.034>
- Alfaro-Almagro, F., McCarthy, P., Afyouni, S., Andersson, J. L. R., Bastiani, M., Miller, K. L., ... Smith, S. M. (2021). Confound modelling in UK Biobank brain imaging. *NeuroImage*, *224*, 117002. <https://doi.org/10.1016/j.neuroimage.2020.117002>
- Alloza, C., Cox, S. R., Blesa Cábez, M., Redmond, P., Whalley, H. C., Ritchie, S. J., ... Bastin, M. E. (2018). Polygenic risk score for schizophrenia and structural brain connectivity in older age: A longitudinal connectome and tractography study. *NeuroImage*, *183*, 884–896. <https://doi.org/10.1016/j.neuroimage.2018.08.075>

- Allswede, D. M., & Cannon, T. D. (2018). Prenatal inflammation and risk for schizophrenia: A role for immune proteins in neurodevelopment. *Development and Psychopathology*, *30*(3), 1157–1178. <https://doi.org/10.1017/S0954579418000317>
- Alnæs, D., Kaufmann, T., Van Der Meer, D., Córdova-Palomera, A., Rokicki, J., Moberget, T., ... Westlye, L. T. (2019). Brain Heterogeneity in Schizophrenia and Its Association with Polygenic Risk. *JAMA Psychiatry*, *76*(7), 739–748. <https://doi.org/10.1001/jamapsychiatry.2019.0257>
- Altshuler, D. M., Durbin, R. M., Abecasis, G. R., Bentley, D. R., Chakravarti, A., Clark, A. G., ... Lacroute, P. (2012). An integrated map of genetic variation from 1,092 human genomes. *Nature*, *491*(7422), 56–65. <https://doi.org/10.1038/nature11632>
- Altshuler, D. M., Gibbs, R. A., Peltonen, L., Schaffner, S. F., Yu, F., Dermitzakis, E., ... McEwen, J. E. (2010). Integrating common and rare genetic variation in diverse human populations. *Nature*, *467*(7311), 52–58. <https://doi.org/10.1038/nature09298>
- Andreasen, N. C., Paradiso, S., & O’Leary, D. S. (1998). “Cognitive Dysmetria” as an Integrative Theory of Schizophrenia: A Dysfunction in Cortical-Subcortical-Cerebellar Circuitry? *Schizophrenia Bulletin*, *24*(2), 203–218. <https://doi.org/10.1093/oxfordjournals.schbul.a033321>
- Andreasen, Nancy C., Nopoulos, P., O’Leary, D. S., Miller, D. D., Wassink, T., & Flaum, M. (1999). Defining the phenotype of schizophrenia: Cognitive dysmetria and its neural mechanisms. *Biological Psychiatry*, *46*(7), 908–920. [https://doi.org/10.1016/S0006-3223\(99\)00152-3](https://doi.org/10.1016/S0006-3223(99)00152-3)
- Andreasen, Nancy C., & Pierson, R. (2008). The Role of the Cerebellum in Schizophrenia. *Biological Psychiatry*, *64*(2), 81–88. <https://doi.org/10.1016/j.biopsych.2008.01.003>
- Annamalai, A., Kosir, U., & Tek, C. (2017). Prevalence of obesity and diabetes in patients with schizophrenia. *World Journal of Diabetes*, *8*(8), 390. <https://doi.org/10.4239/wjd.v8.i8.390>
- Anticevic, A., Haut, K., Murray, J. D., Repovs, G., Yang, G. J., Diehl, C., ... Cannon, T. D. (2015). Association of Thalamic Dysconnectivity and Conversion to Psychosis in Youth and Young Adults at Elevated Clinical Risk. *JAMA Psychiatry*, *72*(9), 882. <https://doi.org/10.1001/jamapsychiatry.2015.0566>
- Anttila, V., Bulik-Sullivan, B., Finucane, H. K., Walters, R. K., Bras, J., Duncan, L., ... Neale, B. M.

- (2018). Analysis of shared heritability in common disorders of the brain. *Science*, 360(6395), 8757. <https://doi.org/10.1126/science.aap8757>
- Apps, R., Hawkes, R., Aoki, S., Bengtsson, F., Brown, A. M., Chen, G., ... Ruigrok, T. J. H. (2018). Cerebellar Modules and Their Role as Operational Cerebellar Processing Units: A Consensus paper. *Cerebellum*, 17(5), 654–682. <https://doi.org/10.1007/s12311-018-0952-3>
- Apthorp, D., Bolbecker, A. R., Bartolomeo, L. A., O'Donnell, B. F., & Hetrick, W. P. (2019). Postural sway abnormalities in schizotypal personality disorder. *Schizophrenia Bulletin*, 45(3), 512–521. <https://doi.org/10.1093/schbul/sby141>
- Argyropoulos, G. P. D., van Dun, K., Adamaszek, M., Leggio, M., Manto, M., Masciullo, M., ... Schmahmann, J. D. (2020, February 1). The Cerebellar Cognitive Affective/Schmahmann Syndrome: a Task Force Paper. *Cerebellum*. Springer. <https://doi.org/10.1007/s12311-019-01068-8>
- Asimit, J. L., Hatzikotoulas, K., McCarthy, M., Morris, A. P., & Zeggini, E. (2016). Trans-ethnic study design approaches for fine-mapping. *European Journal of Human Genetics : EJHG*, 24(9), 1330–1336. <https://doi.org/10.1038/ejhg.2016.1>
- Atkinson, E. G., Maihofer, A. X., Kanai, M., Martin, A. R., Karczewski, K. J., Santoro, M. L., ... Neale, B. M. (2021). Tractor uses local ancestry to enable the inclusion of admixed individuals in GWAS and to boost power. *Nature Genetics*, 53(2), 195–204. <https://doi.org/10.1038/s41588-020-00766-y>
- Badura, A., Verpeut, J. L., Metzger, J. W., Pereira, T. D., Pisano, T. J., Devereett, B., ... Wang, S. S. H. (2018). Normal cognitive and social development require posterior cerebellar activity. *ELife*, 7, e36401. <https://doi.org/10.7554/eLife.36401>
- Bahrami, S., Steen, N. E., Shadrin, A., O'Connell, K., Frei, O., Bettella, F., ... Andreassen, O. A. (2020). Shared Genetic Loci between Body Mass Index and Major Psychiatric Disorders: A Genome-wide Association Study. *JAMA Psychiatry*, 77(5), 503–512. <https://doi.org/10.1001/jamapsychiatry.2019.4188>
- Bak, M., Fransen, A., Janssen, J., Van Os, J., & Drukker, M. (2014). Almost all antipsychotics result in weight gain: A meta-analysis. *PLoS ONE*, 9(4), e94112. <https://doi.org/10.1371/journal.pone.0094112>

- Bakhshi, K., & Chance, S. A. (2015). The neuropathology of schizophrenia: A selective review of past studies and emerging themes in brain structure and cytoarchitecture. *Neuroscience*, *303*, 82–102. <https://doi.org/10.1016/j.neuroscience.2015.06.028>
- Baldaçara, L., Nery-Fernandes, F., Rocha, M., Quarantini, L. C., Rocha, G. G. L., Guimarães, J. L., ... Jackowski, A. (2011). Is cerebellar volume related to bipolar disorder? *Journal of Affective Disorders*, *135*(1–3), 305–309. <https://doi.org/10.1016/j.jad.2011.06.059>
- Balsters, J. H., Cussans, E., Diedrichsen, J., Phillips, K. A., Preuss, T. M., Rilling, J. K., & Ramnani, N. (2010). Evolution of the cerebellar cortex: The selective expansion of prefrontal-projecting cerebellar lobules. *NeuroImage*, *49*(3), 2045–2052. <https://doi.org/10.1016/j.neuroimage.2009.10.045>
- Balsters, Joshua H., Whelan, C. D., Robertson, I. H., & Ramnani, N. (2013). Cerebellum and cognition: Evidence for the encoding of higher order rules. *Cerebral Cortex*, *23*(6), 1433–1443. <https://doi.org/10.1093/cercor/bhs127>
- Barkhuizen, W., Pain, O., Dudbridge, F., & Ronald, A. (2020). Genetic overlap between psychotic experiences in the community across age and with psychiatric disorders. *Translational Psychiatry*, *10*(1), 1–12. <https://doi.org/10.1038/s41398-020-0765-2>
- Barry, E. F., Vanes, L. D., Andrews, D. S., Patel, K., Horne, C. M., Mouchlianitis, E., ... Shergill, S. S. (2019). Mapping cortical surface features in treatment resistant schizophrenia with in vivo structural MRI. *Psychiatry Research*, *274*, 335–344. <https://doi.org/10.1016/j.psychres.2019.02.028>
- Barton, R. A., & Venditti, C. (2014). Rapid evolution of the cerebellum in humans and other great apes. *Current Biology*, *24*(20), 2440–2444. <https://doi.org/10.1016/j.cub.2014.08.056>
- Beckinghausen, J., & Sillitoe, R. V. (2019). Insights into cerebellar development and connectivity. *Neuroscience Letters*, *688*, 2–13. <https://doi.org/10.1016/j.neulet.2018.05.013>
- Benjamini, Y., & Hochberg, Y. (1995). Controlling the False Discovery Rate: A Practical and Powerful Approach to Multiple Testing. *Journal of the Royal Statistical Society: Series B (Methodological)*, *57*(1), 289–300. <https://doi.org/10.1111/j.2517-6161.1995.tb02031.x>
- Benros, M. E., Trabjerg, B. B., Meier, S., Mattheisen, M., Mortensen, P. B., Mors, O., ... Agerbo, E. (2016). Influence of Polygenic Risk Scores on the Association Between Infections and

- Schizophrenia. *Biological Psychiatry*, 80(8), 609–616.
<https://doi.org/10.1016/j.biopsych.2016.04.008>
- Bergen, S. E., Ploner, A., Howrigan, D., O'Donovan, M. C., Smoller, J. W., Sullivan, P. F., ... Kendler, K. S. (2019). Joint contributions of rare copy number variants and common SNPs to risk for schizophrenia. *American Journal of Psychiatry*, 176(1), 29–35.
<https://doi.org/10.1176/appi.ajp.2018.17040467>
- Bernard, J. A., & Mittal, V. A. (2015). Dysfunctional activation of the cerebellum in schizophrenia: A functional neuroimaging meta-analysis. *Clinical Psychological Science*, 3(4), 545–566.
<https://doi.org/10.1177/2167702614542463>
- Bernard, J. A., Orr, J. M., & Mittal, V. A. (2017). Cerebello-thalamo-cortical networks predict positive symptom progression in individuals at ultra-high risk for psychosis. *NeuroImage: Clinical*, 14, 622–628. <https://doi.org/10.1016/j.nicl.2017.03.001>
- Bernard, J. A., & Seidler, R. D. (2014). Moving forward: Age effects on the cerebellum underlie cognitive and motor declines. *Neuroscience and Biobehavioral Reviews*, 42, 193–207.
<https://doi.org/10.1016/j.neubiorev.2014.02.011>
- Bernier, R., Steinman, K. J., Reilly, B., Wallace, A. S., Sherr, E. H., Pojman, N., ... Chung, W. K. (2016). Clinical phenotype of the recurrent 1q21.1 copy-number variant. *Genetics in Medicine*, 18(4), 341–349. <https://doi.org/10.1038/gim.2015.78>
- Beyer, F., Masouleh, S. K., Kratzsch, J., Schroeter, M. L., Röhr, S., Riedel-Heller, S. G., ... Veronica Witte, A. (2019). A metabolic obesity profile is associated with decreased gray matter volume in cognitively healthy older adults. *Frontiers in Aging Neuroscience*, 10(JUL).
<https://doi.org/10.3389/fnagi.2019.00202>
- Beyer, F., Prehn, K., Wüsten, K. A., Villringer, A., Ordemann, J., Flöel, A., & Witte, A. V. (2020). Weight loss reduces head motion: Revisiting a major confound in neuroimaging. *Human Brain Mapping*, 41(9), 2490–2494. <https://doi.org/10.1002/hbm.24959>
- Bijsterbosch, J., Harrison, S., Duff, E., Alfaró-Almagro, F., Woolrich, M., & Smith, S. (2017). Investigations into within- and between-subject resting-state amplitude variations. *NeuroImage*, 159, 57–69. <https://doi.org/10.1016/j.neuroimage.2017.07.014>
- Blokland, G. A. M., De Zubicaray, G. I., McMahon, K. L., & Wright, M. J. (2012). Genetic and

environmental influences on neuroimaging phenotypes: A meta-analytical perspective on twin imaging studies. *Twin Research and Human Genetics*, *15*(3), 351–371. <https://doi.org/10.1017/thg.2012.11>

Bohon, C., & Geliebter, A. (2019). Change in brain volume and cortical thickness after behavioral and surgical weight loss intervention. *NeuroImage: Clinical*, *21*, 101640. <https://doi.org/10.1016/j.nicl.2018.101640>

Bolbecker, A. R., Kent, J. S., Petersen, I. T., Klaunig, M. J., Forsyth, J. K., Howell, J. M., ... Hetrick, W. P. (2014). Impaired cerebellar-dependent eyeblink conditioning in first-degree relatives of individuals with schizophrenia. *Schizophrenia Bulletin*, *40*(5), 1001–1010. <https://doi.org/10.1093/schbul/sbt112>

Bolhuis, K., Tiemeier, H., Jansen, P. R., Muetzel, R. L., Neumann, A., Hillegers, M. H. J., ... Kushner, S. A. (2019). Interaction of schizophrenia polygenic risk and cortisol level on pre-adolescent brain structure. *Psychoneuroendocrinology*, *101*, 295–303. <https://doi.org/10.1016/j.psyneuen.2018.12.231>

Bostan, A. C., & Strick, P. L. (2018, June 1). The basal ganglia and the cerebellum: Nodes in an integrated network. *Nature Reviews Neuroscience*. Nature Publishing Group. <https://doi.org/10.1038/s41583-018-0002-7>

Bowtell, M., Eaton, S., Thien, K., Bardell-Williams, M., Downey, L., Ratheesh, A., ... O'Donoghue, B. (2018). Rates and predictors of relapse following discontinuation of antipsychotic medication after a first episode of psychosis. *Schizophrenia Research*, *195*, 231–236. <https://doi.org/10.1016/j.schres.2017.10.030>

Brady, R. O., Beermann, A., Nye, M., Eack, S. M., Mesholam-Gately, R., Keshavan, M. S., & Lewandowski, K. E. (2020). Cerebellar-Cortical Connectivity Is Linked to Social Cognition Trans-Diagnostically. *Frontiers in Psychiatry*, *11*, 1159. <https://doi.org/10.3389/fpsy.2020.573002>

Brady, R. O., Gonsalvez, I., Lee, I., Öngür, D., Seidman, L. J., Schmahmann, J. D., ... Halko, M. A. (2019). Cerebellar-prefrontal network connectivity and negative symptoms in schizophrenia. *American Journal of Psychiatry*, *176*(7), 512–520. <https://doi.org/10.1176/appi.ajp.2018.18040429>

Broekema, R. V., Bakker, O. B., & Jonkers, I. H. (2020). A practical view of fine-mapping and gene

- prioritization in the post-genome-wide association era. *Open Biology*, 10(1), 190221. <https://doi.org/10.1098/rsob.190221>
- Brunetti-Pierri, N., Berg, J. S., Scaglia, F., Belmont, J., Bacino, C. A., Sahoo, T., ... Patel, A. (2008). Recurrent reciprocal 1q21.1 deletions and duplications associated with microcephaly or macrocephaly and developmental and behavioral abnormalities. *Nature Genetics*, 40(12), 1466–1471. <https://doi.org/10.1038/ng.279>
- Buckley, P. F., Miller, B. J., Lehrer, D. S., & Castle, D. J. (2009). Psychiatric comorbidities and schizophrenia. *Schizophrenia Bulletin*, 35(2), 383–402. <https://doi.org/10.1093/schbul/sbn135>
- Buckner, R. L. (2013, October). The cerebellum and cognitive function: 25 years of insight from anatomy and neuroimaging. *Neuron*. <https://doi.org/10.1016/j.neuron.2013.10.044>
- Buckner, R. L., Krienen, F. M., Castellanos, A., Diaz, J. C., & Thomas Yeo, B. T. (2011). The organization of the human cerebellum estimated by intrinsic functional connectivity. *Journal of Neurophysiology*, 106(5), 2322–2345. <https://doi.org/10.1152/jn.00339.2011>
- Bulik-Sullivan, B., Finucane, H. K., Anttila, V., Gusev, A., Day, F. R., Loh, P. R., ... Neale, B. M. (2015). An atlas of genetic correlations across human diseases and traits. *Nature Genetics*, 47(11), 1236–1241. <https://doi.org/10.1038/ng.3406>
- Bulik-Sullivan, B., Loh, P. R., Finucane, H. K., Ripke, S., Yang, J., Patterson, N., ... O'Donovan, M. C. (2015). LD score regression distinguishes confounding from polygenicity in genome-wide association studies. *Nature Genetics*, 47(3), 291–295. <https://doi.org/10.1038/ng.3211>
- Bullock, W. M., Cardon, K., Bustillo, J., Roberts, R. C., & Perrone-Bizzozero, N. I. (2008). Altered expression of genes involved in GABAergic transmission and neuromodulation of granule cell activity in the cerebellum of schizophrenia patients. *American Journal of Psychiatry*, 165(12), 1594–1603. <https://doi.org/10.1176/appi.ajp.2008.07121845>
- Burton, B. K., Hjorthøj, C., Jepsen, J. R., Thorup, A., Nordentoft, M., & Plessen, K. J. (2016). Research Review: Do motor deficits during development represent an endophenotype for schizophrenia? A meta-analysis. *Journal of Child Psychology and Psychiatry, and Allied Disciplines*, 57(4), 446–456. <https://doi.org/10.1111/jcpp.12479>
- Busè, M., Cuttaia, H. C., Palazzo, D., Mazara, M. V., Lauricella, S. A., Malacarne, M., ... Piccione,

- M. (2017). Expanding the phenotype of reciprocal 1q21.1 deletions and duplications: a case series. *Italian Journal of Pediatrics*, 43(1), 61. <https://doi.org/10.1186/s13052-017-0380-x>
- Button, K. S., Ioannidis, J. P. A., Mokrysz, C., Nosek, B. A., Flint, J., Robinson, E. S. J., & Munafò, M. R. (2013). Power failure: Why small sample size undermines the reliability of neuroscience. *Nature Reviews Neuroscience*, 14(5), 365–376. <https://doi.org/10.1038/nrn3475>
- Bycroft, C., Freeman, C., Petkova, D., Band, G., Elliott, L. T., Sharp, K., ... Marchini, J. (2018). The UK Biobank resource with deep phenotyping and genomic data. *Nature*, 562, 203–209. <https://doi.org/10.1038/s41586-018-0579-z>
- Cabaraux, P., Gandini, J., Kakei, S., Manto, M., Mitoma, H., & Tanaka, H. (2020). Dysmetria and errors in predictions: The role of internal forward model. *International Journal of Molecular Sciences*, 21(18), 6900. <https://doi.org/10.3390/ijms21186900>
- Cai, L., Huang, T., Su, J., Zhang, X., Chen, W., Zhang, F., ... Chou, K. C. (2018). Implications of Newly Identified Brain eQTL Genes and Their Interactors in Schizophrenia. *Molecular Therapy - Nucleic Acids*, 12(7), 433–442. <https://doi.org/10.1016/j.omtn.2018.05.026>
- Caldani, S., Amado, I., Bendjemaa, N., Vialatte, F., Mam-Lam-Fook, C., Gaillard, R., ... Pia Bucci, M. (2017). Oculomotricity and Neurological Soft Signs: Can we refine the endophenotype? A study in subjects belonging to the spectrum of schizophrenia. *Psychiatry Research*, 256, 490–497. <https://doi.org/10.1016/j.psychres.2017.06.013>
- Cannon, M., Jones, P. B., & Murray, R. M. (2002). Obstetric complications and schizophrenia: Historical and meta-analytic review. *American Journal of Psychiatry*, 159, 1080–1092. <https://doi.org/10.1176/appi.ajp.159.7.1080>
- Cao, B., Cho, R. Y., Chen, D., Xiu, M., Wang, L., Soares, J. C., & Zhang, X. Y. (2020). Treatment response prediction and individualized identification of first-episode drug-naïve schizophrenia using brain functional connectivity. *Molecular Psychiatry*, 25(4), 906–913. <https://doi.org/10.1038/s41380-018-0106-5>
- Cao, H., Chén, O. Y., Chung, Y., Forsyth, J. K., McEwen, S. C., Gee, D. G., ... Cannon, T. D. (2018). Cerebello-thalamo-cortical hyperconnectivity as a state-independent functional neural signature for psychosis prediction and characterization. *Nature Communications*, 9(1), 3836. <https://doi.org/10.1038/s41467-018-06350-7>

- Carbon, M., & Correll, C. U. (2014). Thinking and acting beyond the positive: The role of the cognitive and negative symptoms in schizophrenia. *CNS Spectrums*, *19*(S1), 35–53. <https://doi.org/10.1017/S1092852914000601>
- Cárdenas-de-la-Parra, A., Martin-Brevet, S., Moreau, C., Rodriguez-Herreros, B., Fonov, V. S., Maillard, A. M., ... Collins, D. L. (2019). Developmental trajectories of neuroanatomical alterations associated with the 16p11.2 Copy Number Variations. *NeuroImage*, *203*, 116155. <https://doi.org/10.1016/j.neuroimage.2019.116155>
- Cardno, A. G., & Gottesman, I. I. (2000). Twin studies of schizophrenia: From bow-and-arrow concordances to star wars Mx and functional genomics. *American Journal of Medical Genetics - Seminars in Medical Genetics*. [https://doi.org/10.1002/\(SICI\)1096-8628\(200021\)97:1<12::AID-AJMG3>3.0.CO;2-U](https://doi.org/10.1002/(SICI)1096-8628(200021)97:1<12::AID-AJMG3>3.0.CO;2-U)
- Carta, I., Chen, C. H., Schott, A. L., Dorizan, S., & Khodakhah, K. (2019). Cerebellar modulation of the reward circuitry and social behavior. *Science*, *363*(6424). <https://doi.org/10.1126/science.aav0581>
- Carter, A. R., Sanderson, E., Hammerton, G., Richmond, R. C., Davey Smith, G., Heron, J., ... Howe, L. D. (2021). Mendelian randomisation for mediation analysis: current methods and challenges for implementation. *European Journal of Epidemiology*, *36*(5), 465–478. <https://doi.org/10.1007/s10654-021-00757-1>
- Caseras, X, Tansey, K. E., Foley, S., & Linden, D. (2015). Association between genetic risk scoring for schizophrenia and bipolar disorder with regional subcortical volumes. *Translational Psychiatry*, *5*(12), e692–e692. <https://doi.org/10.1038/tp.2015.195>
- Caseras, Xavier, Kirov, G., Kendall, K. M., Rees, E., Legge, S. E., Bracher-Smith, M., ... Murphy, K. (2021). Effects of genomic copy number variants penetrant for schizophrenia on cortical thickness and surface area in healthy individuals: Analysis of the UK Biobank. *British Journal of Psychiatry*, *218*(2), 104–111. <https://doi.org/10.1192/bjp.2020.139>
- Caspi, A., Houts, R. M., Belsky, D. W., Goldman-Mellor, S. J., Harrington, H., Israel, S., ... Moffitt, T. E. (2014). The p factor: One general psychopathology factor in the structure of psychiatric disorders? *Clinical Psychological Science*, *2*(2), 119–137. <https://doi.org/10.1177/2167702613497473>
- Cattane, N., Richetto, J., & Cattaneo, A. (2018). Prenatal exposure to environmental insults and

enhanced risk of developing Schizophrenia and Autism Spectrum Disorder: focus on biological pathways and epigenetic mechanisms. *Neuroscience and Biobehavioral Reviews*. <https://doi.org/10.1016/j.neubiorev.2018.07.001>

Cavanagh, J., Krishnadas, R., Batty, G. D., Burns, H., Deans, K. A., Ford, I., ... McLean, J. (2013). Socioeconomic status and the cerebellar grey matter volume. Data from a well-characterised population sample. *Cerebellum*, *12*(6), 882–891. <https://doi.org/10.1007/s12311-013-0497-4>

Cerminara, N. L., Lang, E. J., Sillitoe, R. V., & Apps, R. (2015). Redefining the cerebellar cortex as an assembly of non-uniform Purkinje cell microcircuits. *Nature Reviews Neuroscience*, *16*(2), 79–93. <https://doi.org/10.1038/nrn3886>

Chand, G. B., Dwyer, D. B., Erus, G., Sotiras, A., Varol, E., Srinivasan, D., ... Davatzikos, C. (2020). Two distinct neuroanatomical subtypes of schizophrenia revealed using machine learning. *Brain*, *143*(3), 1027–1038. <https://doi.org/10.1093/brain/awaa025>

Chang, C. C., Chow, C. C., Tellier, L. C., Vattikuti, S., Purcell, S. M., & Lee, J. J. (2015). Second-generation PLINK: Rising to the challenge of larger and richer datasets. *GigaScience*, *4*(1), 7. <https://doi.org/10.1186/s13742-015-0047-8>

Chang, Z., Chen, Z., Stephen, C. D., Schmahmann, J. D., Wu, H. T., Sapiro, G., & Gupta, A. S. (2020). Accurate detection of cerebellar smooth pursuit eye movement abnormalities via mobile phone video and machine learning. *Scientific Reports*, *10*(1), 18641. <https://doi.org/10.1038/s41598-020-75661-x>

Chen, P., Ye, E., Jin, X., Zhu, Y., & Wang, L. (2019). Association between Thalamocortical Functional Connectivity Abnormalities and Cognitive Deficits in Schizophrenia. *Scientific Reports*, *9*(1). <https://doi.org/10.1038/s41598-019-39367-z>

Chen, X., Ji, G. J., Zhu, C., Bai, X., Wang, L., He, K., ... Wang, K. (2019). Neural Correlates of Auditory Verbal Hallucinations in Schizophrenia and the Therapeutic Response to Theta-Burst Transcranial Magnetic Stimulation. *Schizophrenia Bulletin*, *45*(2), 474–483. <https://doi.org/10.1093/schbul/sby054>

Ching, C. R. K., Gutman, B. A., Sun, D., Villalon Reina, J., Ragothaman, A., Isaev, D., ... Bearden, C. E. (2020). Mapping Subcortical Brain Alterations in 22q11.2 Deletion Syndrome: Effects of Deletion Size and Convergence With Idiopathic Neuropsychiatric Illness. *The American*

Journal of Psychiatry, 177(7), 589–600. <https://doi.org/10.1176/appi.ajp.2019.19060583>

Choi, S. W., Mak, T. S. H., & O'Reilly, P. F. (2020). Tutorial: a guide to performing polygenic risk score analyses. *Nature Protocols*, 15(9), 2759–2772. <https://doi.org/10.1038/s41596-020-0353-1>

Clark, L. A., Cuthbert, B., Lewis-Fernández, R., Narrow, W. E., & Reed, G. M. (2017). Three Approaches to Understanding and Classifying Mental Disorder: ICD-11, DSM-5, and the National Institute of Mental Health's Research Domain Criteria (RDoC). *Psychological Science in the Public Interest*, 18(2), 72–145. <https://doi.org/10.1177/1529100617727266>

Coe, B. P., Witherspoon, K., Rosenfeld, J. A., Van Bon, B. W. M., Vulto-Van Silfhout, A. T., Bosco, P., ... Eichler, E. E. (2014). Refining analyses of copy number variation identifies specific genes associated with developmental delay. *Nature Genetics*, 46(10), 1063–1071. <https://doi.org/10.1038/ng.3092>

Coemans, M., Röder, C. H., Smit, A. E., Koekkoek, S. K. E., De Zeeuw, C. I., Frens, M. A., & van der Geest, J. N. (2014). Cerebellar motor learning deficits in medicated and medication-free men with recent-onset schizophrenia. *Journal of Psychiatry and Neuroscience*, 39(1), E3-11. <https://doi.org/10.1503/jpn.120205>

Coffman, J. A., Mefferd, J., Golden, C. J., Bloch, S., & Graber, B. (1981). Cerebellar atrophy in chronic Schizophrenia. *The Lancet*, 317(8221), 666. [https://doi.org/10.1016/S0140-6736\(81\)91582-8](https://doi.org/10.1016/S0140-6736(81)91582-8)

Collins, R. (2012). What makes UK Biobank special? *The Lancet*, 379(9822), 1173–1174. [https://doi.org/10.1016/S0140-6736\(12\)60404-8](https://doi.org/10.1016/S0140-6736(12)60404-8)

Conomos, M. P., Laurie, C. A., Stilp, A. M., Gogarten, S. M., McHugh, C. P., Nelson, S. C., ... Laurie, C. C. (2016). Genetic Diversity and Association Studies in US Hispanic/Latino Populations: Applications in the Hispanic Community Health Study/Study of Latinos. *American Journal of Human Genetics*, 98(1), 165–184. <https://doi.org/10.1016/j.ajhg.2015.12.001>

Costas, J. (2018, March 1). The highly pleiotropic gene SLC39A8 as an opportunity to gain insight into the molecular pathogenesis of schizophrenia. *American Journal of Medical Genetics, Part B: Neuropsychiatric Genetics*. Blackwell Publishing Inc. <https://doi.org/10.1002/ajmg.b.32545>

- Cuesta, M. J., García de Jalón, E., Campos, M. S., Moreno-Izco, L., Lorente-Omeñaca, R., Sánchez-Torres, A. M., & Peralta, V. (2018). Motor abnormalities in first-episode psychosis patients and long-term psychosocial functioning. *Schizophrenia Research*, *200*, 97–103. <https://doi.org/10.1016/j.schres.2017.08.050>
- Cuthbert, B. N., & Insel, T. R. (2013). Toward the future of psychiatric diagnosis: The seven pillars of RDoC. *BMC Medicine*, *11*(1), 126. <https://doi.org/10.1186/1741-7015-11-126>
- D'Angelo, E. (2018). Physiology of the cerebellum. *Handbook of Clinical Neurology*, *154*, 85–108. <https://doi.org/10.1016/B978-0-444-63956-1.00006-0>
- D'Angelo, E., & Casali, S. (2013). Seeking a unified framework for cerebellar function and dysfunction: From circuit operations to cognition. *Frontiers in Neural Circuits*, *6*, 116.
- Dale, A. M., Fischl, B., & Sereno, M. I. (1999). Cortical surface-based analysis: I. Segmentation and surface reconstruction. *NeuroImage*, *9*(2), 179–194. <https://doi.org/10.1006/nimg.1998.0395>
- Davies, G., Welham, J., Chant, D., Torrey, E. F., & McGrath, J. (2003). A Systematic Review and Meta-analysis of Northern Hemisphere Season of Birth Studies in Schizophrenia. *Schizophrenia Bulletin*, *29*(3), 587–593. <https://doi.org/10.1093/oxfordjournals.schbul.a007030>
- Davis, K. A. S., Cullen, B., Adams, M., Brailean, A., Breen, G., Coleman, J. R. I., ... Hotopf, M. (2019). Indicators of mental disorders in UK Biobank—A comparison of approaches. *International Journal of Methods in Psychiatric Research*, *28*(3). <https://doi.org/10.1002/mpr.1796>
- De Assunção-Leme, I. B., Zugman, A., De Moura, L. M., Sato, J. R., Higuchi, C., Ortiz, B. B., ... Gadelha, A. (2020). Is treatment-resistant schizophrenia associated with distinct neurobiological callosal connectivity abnormalities? *CNS Spectrums*, 1–5. <https://doi.org/10.1017/S1092852920001753>
- De Cocker, L. J. L., Kloppenborg, R. P., Van Der Graaf, Y., Luijten, P. R., Hendrikse, J., & Geerlings, M. I. (2015). Cerebellar Cortical Infarct Cavities: Correlation with Risk Factors and MRI Markers of Cerebrovascular Disease. *Stroke*, *46*(11), 3154–3160. <https://doi.org/10.1161/STROKEAHA.115.010093>
- De Fazio, P., Gaetano, R., Caroleo, M., Cerminara, G., Maida, F., Bruno, A., ... Segura-García, C.

- (2015, August 6). Rare and very rare adverse effects of clozapine. *Neuropsychiatric Disease and Treatment*. Dove Medical Press Ltd. <https://doi.org/10.2147/NDT.S83989>
- de Zwarte, S. M. C., Brouwer, R. M., Agartz, I., Alda, M., Aleman, A., Alpert, K. I., ... van Haren, N. E. M. (2019). The Association Between Familial Risk and Brain Abnormalities Is Disease Specific: An ENIGMA-Relatives Study of Schizophrenia and Bipolar Disorder. *Biological Psychiatry*, *86*(7), 545–556. <https://doi.org/10.1016/j.biopsych.2019.03.985>
- de Zwarte, S. M. C., Brouwer, R. M., Tsouli, A., Cahn, W., Hillegers, M. H. J., Hulshoff Pol, H. E., ... Van Haren, N. E. M. (2019). Running in the family? Structural brain abnormalities and IQ in offspring, siblings, parents, and co-twins of patients with schizophrenia. *Schizophrenia Bulletin*, *45*(6), 1209–1217. <https://doi.org/10.1093/schbul/sby182>
- Dean, D. J., Bernard, J. A., Orr, J. M., Pelletier-Baldelli, A., Gupta, T., Carol, E. E., & Mittal, V. A. (2014). Cerebellar morphology and procedural learning impairment in neuroleptic-naive youth at ultrahigh risk of psychosis. *Clinical Psychological Science*, *2*(2), 152–164. <https://doi.org/10.1177/2167702613500039>
- Deary, I. J. (2001). Human intelligence differences: A recent history. *Trends in Cognitive Sciences*, *5*(3), 127–130. [https://doi.org/10.1016/S1364-6613\(00\)01621-1](https://doi.org/10.1016/S1364-6613(00)01621-1)
- Dekkers, I. A., Jansen, P. R., & Lamb, H. J. (2019). Obesity, brain volume, and white matter microstructure at MRI: A cross-sectional UK biobank study. *Radiology*, *291*(3), 763–771. <https://doi.org/10.1148/radiol.2019181012>
- Demontis, D., Rajagopal, V. M., Thorgeirsson, T. E., Als, T. D., Grove, J., Leppälä, K., ... Børglum, A. D. (2019). Genome-wide association study implicates *CHRNA2* in cannabis use disorder. *Nature Neuroscience*, *22*(7), 1066–1074. <https://doi.org/10.1038/s41593-019-0416-1>
- Deng, Y., Hung, K. S. Y., Lui, S. S. Y., Chui, W. W. H., Lee, J. C. W., Wang, Y., ... Cheung, E. F. C. (2019). Tractography-based classification in distinguishing patients with first-episode schizophrenia from healthy individuals. *Progress in Neuro-Psychopharmacology and Biological Psychiatry*, *88*, 66–73. <https://doi.org/10.1016/j.pnpbp.2018.06.010>
- Dennison, C. A., Legge, S. E., Pardiñas, A. F., & Walters, J. T. R. (2020). Genome-wide association studies in schizophrenia: Recent advances, challenges and future perspective. *Schizophrenia Research*, *217*, 4–12. <https://doi.org/10.1016/j.schres.2019.10.048>

- Depping, M. S., Schmitgen, M. M., Kubera, K. M., & Wolf, R. C. (2018). Cerebellar Contributions to Major Depression. *Frontiers in Psychiatry*, *9*, 634. <https://doi.org/10.3389/fpsyt.2018.00634>
- Diedrichsen, J. (2006). A spatially unbiased atlas template of the human cerebellum. *NeuroImage*, *33*(1), 127–138. <https://doi.org/10.1016/j.neuroimage.2006.05.056>
- Diedrichsen, J., Balsters, J. H., Flavell, J., Cussans, E., & Ramnani, N. (2009). A probabilistic MR atlas of the human cerebellum. *NeuroImage*, *46*(1), 39–46. <https://doi.org/10.1016/j.neuroimage.2009.01.045>
- Ding, Y., Ou, Y., Pan, P., Shan, X., Chen, J., Liu, F., ... Guo, W. (2019, January 30). Cerebellar structural and functional abnormalities in first-episode and drug-naive patients with schizophrenia: A meta-analysis. *Psychiatry Research - Neuroimaging*. Elsevier Ireland Ltd. <https://doi.org/10.1016/j.psychresns.2018.11.009>
- Dittwald, P., Gambin, T., Szafranski, P., Li, J., Amato, S., Divon, M. Y., ... Stankiewicz, P. (2013). NAHR-mediated copy-number variants in a clinical population: Mechanistic insights into both genomic disorders and Mendelizing traits. *Genome Research*, *23*(9), 1395–1409. <https://doi.org/10.1101/gr.152454.112>
- Doan, N. T., Kaufmann, T., Bettella, F., Jørgensen, K. N., Brandt, C. L., Moberget, T., ... Westlye, L. T. (2017). Distinct multivariate brain morphological patterns and their added predictive value with cognitive and polygenic risk scores in mental disorders. *NeuroImage: Clinical*, *15*, 719–731. <https://doi.org/10.1016/j.nicl.2017.06.014>
- Dong, D., Wang, Y., Chang, X., Luo, C., & Yao, D. (2018). Dysfunction of Large-Scale Brain Networks in Schizophrenia: A Meta-analysis of Resting-State Functional Connectivity. *Schizophrenia Bulletin*, *44*(1), 168–181. <https://doi.org/10.1093/schbul/sbx034>
- Dudbridge, F. (2013). Power and Predictive Accuracy of Polygenic Risk Scores. *PLoS Genetics*, *9*(3), e1003348. <https://doi.org/10.1371/journal.pgen.1003348>
- Dykxhoorn, J., Hollander, A. C., Lewis, G., Magnusson, C., Dalman, C., & Kirkbride, J. B. (2019). Risk of schizophrenia, schizoaffective, and bipolar disorders by migrant status, region of origin, and age-at-migration: a national cohort study of 1.8 million people. *Psychological Medicine*, *49*(14), 2354–2363. <https://doi.org/10.1017/S0033291718003227>

- Eccles, J. C., Llinás, R., & Sasaki, K. (1966). The excitatory synaptic action of climbing fibres on the Purkinje cells of the cerebellum. *The Journal of Physiology*, *182*, 268–296. <https://doi.org/10.1113/jphysiol.1966.sp007824>
- Ekhtiari, H., Kuplicki, R., Yeh, H. wen, & Paulus, M. P. (2019). Physical characteristics not psychological state or trait characteristics predict motion during resting state fMRI. *Scientific Reports*, *9*(1), 419. <https://doi.org/10.1038/s41598-018-36699-0>
- Elliott, L. T., Sharp, K., Alfaro-Almagro, F., Shi, S., Miller, K. L., Douaud, G., ... Smith, S. M. (2018). Genome-wide association studies of brain imaging phenotypes in UK Biobank. *Nature*, *562*(7726), 210–216. <https://doi.org/10.1038/s41586-018-0571-7>
- Emdin, C. A., Khera, A. V., & Kathiresan, S. (2017). Mendelian randomization. *JAMA - Journal of the American Medical Association*, *318*(19), 1925–1926. <https://doi.org/10.1001/jama.2017.17219>
- Escelsior, A., Belvederi Murri, M., Calcagno, P., Cervetti, A., Caruso, R., Croce, E., ... Amore, M. (2019). Effectiveness of Cerebellar Circuitry Modulation in Schizophrenia: A Systematic Review. *Journal of Nervous and Mental Disease*, *207*(11), 977–986. <https://doi.org/10.1097/NMD.0000000000001064>
- Escelsior, A., & Murri, M. B. (2019). Modulation of Cerebellar Activity in Schizophrenia: Is It the Time for Clinical Trials? *Schizophrenia Bulletin*, *45*(5), 947–949. <https://doi.org/10.1093/schbul/sbz017>
- Euesden, J., Lewis, C. M., & O'Reilly, P. F. (2015). PRSice: Polygenic Risk Score software. *Bioinformatics*, *31*(9), 1466–1468. <https://doi.org/10.1093/bioinformatics/btu848>
- Eyler, L. T., Prom-Wormley, E., Fennema-Notestine, C., Panizzon, M. S., Neale, M. C., Jernigan, T. L., ... Kremen, W. S. (2011). Genetic patterns of correlation among subcortical volumes in humans: Results from a magnetic resonance imaging twin study. *Human Brain Mapping*, *32*(4), 641–653. <https://doi.org/10.1002/hbm.21054>
- Farah, M. J. (2017). The Neuroscience of Socioeconomic Status: Correlates, Causes, and Consequences. *Neuron*, *96*(1), 56–71. <https://doi.org/10.1016/j.neuron.2017.08.034>
- Fatemi, S. H., & Folsom, T. D. (2009). The neurodevelopmental hypothesis of Schizophrenia, revisited. *Schizophrenia Bulletin*, *35*(3), 528–548. <https://doi.org/10.1093/schbul/sbn187>

- Fatemi, S. H., & Folsom, T. D. (2015). GABA receptor subunit distribution and FMRP-mGluR5 signaling abnormalities in the cerebellum of subjects with schizophrenia, mood disorders, and autism. *Schizophrenia Research*, *167*(1), 42–56. <https://doi.org/10.1016/j.schres.2014.10.010>
- Ferri, J., Ford, J. M., Roach, B. J., Turner, J. A., Van Erp, T. G., Voyvodic, J., ... Mathalon, D. H. (2018). Resting-state thalamic dysconnectivity in schizophrenia and relationships with symptoms. *Psychological Medicine*, *48*(15), 2492–2499. <https://doi.org/10.1017/S003329171800003X>
- Fiez, J. A. (2016). The cerebellum and language: Persistent themes and findings. *Brain and Language*, *161*, 1–3. <https://doi.org/10.1016/j.bandl.2016.09.004>
- Filatova, S., Koivumaa-Honkanen, H., Hirvonen, N., Freeman, A., Ivandic, I., Hurtig, T., ... Miettunen, J. (2017). Early motor developmental milestones and schizophrenia: A systematic review and meta-analysis. *Schizophrenia Research*, *188*, 13–20. <https://doi.org/10.1016/j.schres.2017.01.029>
- Filippi, M., Canu, E., Gasparotti, R., Agosta, F., Valsecchi, P., Lodoli, G., ... Sacchetti, E. (2014). Patterns of brain structural changes in first-contact, antipsychotic drug-naïve patients with schizophrenia. *American Journal of Neuroradiology*, *35*(1), 30–37. <https://doi.org/10.3174/ajnr.A3583>
- Finucane, H. K., Reshef, Y. A., Anttila, V., Slowikowski, K., Gusev, A., Byrnes, A., ... Price, A. L. (2018). Heritability enrichment of specifically expressed genes identifies disease-relevant tissues and cell types. *Nature Genetics*, *50*(4), 621–629. <https://doi.org/10.1038/s41588-018-0081-4>
- Fonville, L., Drakesmith, M., Zammit, S., Lewis, G., Jones, D. K., & David, A. S. (2019). MRI indices of cortical development in young people with psychotic experiences: Influence of genetic risk and persistence of symptoms. *Schizophrenia Bulletin*, *45*(1), 169–179. <https://doi.org/10.1093/schbul/sbx195>
- Franke, B., van Hulzen, K. J. E., Arias-Vasquez, A., Bralten, J., Hoogman, M., Klein, M., ... Ikram, M. A. (2016). Genetic influences on schizophrenia and subcortical brain volumes: Large-scale proof of concept. *Nature Neuroscience*, *19*(3), 420–431. <https://doi.org/10.1038/nn.4228>

- Frei, O., Holland, D., Smeland, O. B., Shadrin, A. A., Fan, C. C., Maeland, S., ... Dale, A. M. (2019). Bivariate causal mixture model quantifies polygenic overlap between complex traits beyond genetic correlation. *Nature Communications*, *10*(1), 1–11. <https://doi.org/10.1038/s41467-019-10310-0>
- Frontera, J. L., Baba Aissa, H., Sala, R. W., Mailhes-Hamon, C., Georgescu, I. A., Léna, C., & Popa, D. (2020). Bidirectional control of fear memories by cerebellar neurons projecting to the ventrolateral periaqueductal grey. *Nature Communications*, *11*(1), 1–17. <https://doi.org/10.1038/s41467-020-18953-0>
- Fry, A., Littlejohns, T. J., Sudlow, C., Doherty, N., Adamska, L., Sprosen, T., ... Allen, N. E. (2017). Comparison of Sociodemographic and Health-Related Characteristics of UK Biobank Participants with Those of the General Population. *American Journal of Epidemiology*, *186*(9), 1026–1034. <https://doi.org/10.1093/aje/kwx246>
- Fujita, H., Kodama, T., & du Lac, S. (2020). Modular output circuits of the fastigial nucleus for diverse motor and nonmotor functions of the cerebellar vermis. *ELife*, *9*, e58613. <https://doi.org/10.7554/elife.58613>
- Fusar-Poli, P., Papanastasiou, E., Stahl, D., Rocchetti, M., Carpenter, W., Shergill, S., & McGuire, P. (2015). Treatments of Negative Symptoms in Schizophrenia: Meta-Analysis of 168 Randomized Placebo-Controlled Trials. *Schizophrenia Bulletin*, *41*(4), 892–899. <https://doi.org/10.1093/schbul/sbu170>
- Gandal, M. J., Haney, J. R., Parikshak, N. N., Leppa, V., Ramaswami, G., Hartl, C., ... Geschwind, D. H. (2018). Shared molecular neuropathology across major psychiatric disorders parallels polygenic overlap. *Science*, *359*(6476), 693–697. <https://doi.org/10.1126/science.aad6469>
- Gao, J., Tang, X., Wang, C., Yu, M., Sha, W., Wang, X., ... Zhang, X. (2020). Aberrant cerebellar neural activity and cerebro-cerebellar functional connectivity involving executive dysfunction in schizophrenia with primary negative symptoms. *Brain Imaging and Behavior*, *14*(3), 869–880. <https://doi.org/10.1007/s11682-018-0032-9>
- Gasse, C., Wimberley, T., Wang, Y., Mors, O., Børghlum, A., Als, T. D., ... Horsdal, H. T. (2019). Schizophrenia polygenic risk scores, urbanicity and treatment-resistant schizophrenia. *Schizophrenia Research*, *212*, 79–85. <https://doi.org/10.1016/j.schres.2019.08.008>
- Genovese, G., Fromer, M., Stahl, E. A., Ruderfer, D. M., Chambert, K., Landén, M., ... McCarroll,

- S. A. (2016). Increased burden of ultra-rare protein-altering variants among 4,877 individuals with schizophrenia. *Nature Neuroscience*, *19*(11), 1433–1441. <https://doi.org/10.1038/nn.4402>
- Geschwind, D. H., & Flint, J. (2015). Genetics and genomics of psychiatric disease. *Science*, *349*(6255), 1489–1494. <https://doi.org/10.1126/science.aaa8954>
- Gheorghe, D. A., Li, C., Gallacher, J., & Bauermeister, S. (2020). Associations of perceived adverse lifetime experiences with brain structure in UK Biobank participants. *Journal of Child Psychology and Psychiatry and Allied Disciplines*. <https://doi.org/10.1111/jcpp.13298>
- Gillespie, A. L., Samanaite, R., Mill, J., Egerton, A., & MacCabe, J. H. (2017). Is treatment-resistant schizophrenia categorically distinct from treatment-responsive schizophrenia? A systematic review. *BMC Psychiatry*, *17*(1). <https://doi.org/10.1186/s12888-016-1177-y>
- Glausier, J. R., & Lewis, D. A. (2013). Dendritic spine pathology in schizophrenia. *Neuroscience*, *251*, 90–107. <https://doi.org/10.1016/j.neuroscience.2012.04.044>
- Gong, J., Luo, C., Li, X., Jiang, S., Khundrakpam, B. S., Duan, M., ... Yao, D. (2019). Evaluation of functional connectivity in subdivisions of the thalamus in schizophrenia. *British Journal of Psychiatry*, *214*(5), 288–296. <https://doi.org/10.1192/bjp.2018.299>
- Gottesman, I. I., & Gould, T. D. (2003). The endophenotype concept in psychiatry: Etymology and strategic intentions. *American Journal of Psychiatry*, *160*(4), 636–645. <https://doi.org/10.1176/appi.ajp.160.4.636>
- Grasby, K. L., Jahanshad, N., Painter, J. N., Colodro-Conde, L., Bralten, J., Hibar, D. P., ... Medland, S. E. (2020). The genetic architecture of the human cerebral cortex. *Science*, *367*(6484), eaay6690. <https://doi.org/10.1126/science.aay6690>
- Greenstein, D., Lenroot, R., Clausen, L., Chavez, A., Vaituzis, A. C., Tran, L., ... Rapoport, J. (2011). Cerebellar development in childhood onset schizophrenia and non-psychotic siblings. *Psychiatry Research - Neuroimaging*, *193*(3), 131–137. <https://doi.org/10.1016/j.psychresns.2011.02.010>
- Grotzinger, A. D., Rhemtulla, M., de Vlaming, R., Ritchie, S. J., Mallard, T. T., Hill, W. D., ... Tucker-Drob, E. M. (2019). Genomic structural equation modelling provides insights into the multivariate genetic architecture of complex traits. *Nature Human Behaviour*, *3*(5), 513–

525. <https://doi.org/10.1038/s41562-019-0566-x>

Grove, J., Ripke, S., Als, T. D., Mattheisen, M., Walters, R. K., Won, H., ... Børglum, A. D. (2019). Identification of common genetic risk variants for autism spectrum disorder. *Nature Genetics*, *51*(3), 431–444. <https://doi.org/10.1038/s41588-019-0344-8>

Guell, X., Gabrieli, J. D. E., & Schmahmann, J. D. (2018). Triple representation of language, working memory, social and emotion processing in the cerebellum: convergent evidence from task and seed-based resting-state fMRI analyses in a single large cohort. *NeuroImage*, *172*, 437–449. <https://doi.org/10.1016/j.neuroimage.2018.01.082>

Guell, X., Schmahmann, J. D., Gabrieli, J. D. E., & Ghosh, S. S. (2018). Functional gradients of the cerebellum. *ELife*, *7*. <https://doi.org/10.7554/eLife.36652>

Guloksuz, S., Pries, L. K., Delespaul, P., Kenis, G., Luykx, J. J., Lin, B. D., ... van Os, J. (2019). Examining the independent and joint effects of molecular genetic liability and environmental exposures in schizophrenia: results from the EUGEI study. *World Psychiatry*, *18*(2), 173–182. <https://doi.org/10.1002/wps.20629>

Guo, W., Liu, F., Chen, J., Wu, R., Zhang, Z., Yu, M., ... Zhao, J. (2015). Resting-state cerebellar-cerebral networks are differently affected in first-episode, drug-naive schizophrenia patients and unaffected siblings. *Scientific Reports*, *5*(1), 17275. <https://doi.org/10.1038/srep17275>

Guo, W., Zhang, F., Liu, F., Chen, J., Wu, R., Chen, D. Q., ... Zhao, J. (2018). Cerebellar abnormalities in first-episode, drug-naive schizophrenia at rest. *Psychiatry Research - Neuroimaging*, *276*, 73–79. <https://doi.org/10.1016/j.psychresns.2018.03.010>

Gupta, C. N., Calhoun, V. D., Rachakonda, S., Chen, J., Patel, V., Liu, J., ... Turner, J. A. (2015). Patterns of gray matter abnormalities in schizophrenia based on an international mega-analysis. *Schizophrenia Bulletin*, *41*(5), 1133–1142. <https://doi.org/10.1093/schbul/sbu177>

Gurdasani, D., Barroso, I., Zeggini, E., & Sandhu, M. S. (2019). Genomics of disease risk in globally diverse populations. *Nature Reviews Genetics*, *20*(9), 520–535. <https://doi.org/10.1038/s41576-019-0144-0>

Haenssler, A. E., Baylis, A., Perry, J. L., Kollara, L., Fang, X., & Kirschner, R. (2020). Impact of

Cranial Base Abnormalities on Cerebellar Volume and the Velopharynx in 22q11.2 Deletion Syndrome. *Cleft Palate-Craniofacial Journal*, 57(4), 412–419. <https://doi.org/10.1177/1055665619874175>

Hajek, T., Franke, K., Kolenic, M., Capkova, J., Matejka, M., Propper, L., ... Alda, M. (2019). Brain Age in Early Stages of Bipolar Disorders or Schizophrenia. *Schizophrenia Bulletin*, 45(1), 190–198. <https://doi.org/10.1093/schbul/sbx172>

Hariri, A. R. (2019, April 3). The Emerging Importance of the Cerebellum in Broad Risk for Psychopathology. *Neuron*. <https://doi.org/10.1016/j.neuron.2019.02.031>

Hawrylycz, M., Miller, J. A., Menon, V., Feng, D., Dolbeare, T., Guillozet-Bongaarts, A. L., ... Lein, E. (2015). Canonical genetic signatures of the adult human brain. *Nature Neuroscience*, 18(12), 1832–1844. <https://doi.org/10.1038/nn.4171>

He, H., Luo, C., Luo, Y., Duan, M., Yi, Q., Biswal, B. B., & Yao, D. (2019). Reduction in gray matter of cerebellum in schizophrenia and its influence on static and dynamic connectivity. *Human Brain Mapping*, 40(2), 517–528. <https://doi.org/10.1002/hbm.24391>

Henriksen, M. G., Nordgaard, J., & Jansson, L. B. (2017). Genetics of schizophrenia: Overview of methods, findings and limitations. *Frontiers in Human Neuroscience*, 11, 322. <https://doi.org/10.3389/fnhum.2017.00322>

Henschke, J. U., & Pakan, J. M. (2020). Disynaptic cerebrocerebellar pathways originating from multiple functionally distinct cortical areas. *eLife*, 9. <https://doi.org/10.7554/eLife.59148>

Herculano-Houzel, S. (2010). Coordinated scaling of cortical and cerebellar numbers of neurons. *Frontiers in Neuroanatomy*, 4, 12. <https://doi.org/10.3389/fnana.2010.00012>

Hibar, D. P., Adams, H. H. H., Jahanshad, N., Chauhan, G., Stein, J. L., Hofer, E., ... Ikram, M. A. (2017). Novel genetic loci associated with hippocampal volume. *Nature Communications*, 8(1), 1–12. <https://doi.org/10.1038/ncomms13624>

Hilker, R., Helenius, D., Fagerlund, B., Skytthe, A., Christensen, K., Werge, T. M., ... Glenthøj, B. (2018). Heritability of Schizophrenia and Schizophrenia Spectrum Based on the Nationwide Danish Twin Register. *Biological Psychiatry*, 83(6), 492–498. <https://doi.org/10.1016/j.biopsych.2017.08.017>

Hill, W. D., Marioni, R. E., Maghzian, O., Ritchie, S. J., Hagenaars, S. P., McIntosh, A. M., ... Deary,

- I. J. (2019). A combined analysis of genetically correlated traits identifies 187 loci and a role for neurogenesis and myelination in intelligence. *Molecular Psychiatry*, *24*(2), 169–181. <https://doi.org/10.1038/s41380-017-0001-5>
- Hintzen, A., Pelzer, E. A., & Tittgemeyer, M. (2018, March 9). Thalamic interactions of cerebellum and basal ganglia. *Brain Structure and Function*. <https://doi.org/10.1007/s00429-017-1584-y>
- Hirjak, D., Meyer-Lindenberg, A., Kubera, K. M., Thomann, P. A., & Wolf, R. C. (2018). Motor dysfunction as research domain in the period preceding manifest schizophrenia: A systematic review. *Neuroscience and Biobehavioral Reviews*, *87*, 87–105. <https://doi.org/10.1016/j.neubiorev.2018.01.011>
- Hirjak, D., Thomann, P. A., Wolf, R. C., Kubera, K. M., Goch, C., Hering, J., & Maier-Hein, K. H. (2017). White matter microstructure variations contribute to neurological soft signs in healthy adults. *Human Brain Mapping*, *38*(7), 3552–3565. <https://doi.org/10.1002/hbm.23609>
- Hirjak, D., Wolf, R. C., Kubera, K. M., Stieltjes, B., Maier-Hein, K. H., & Thomann, P. A. (2015). Neurological soft signs in recent-onset schizophrenia: Focus on the cerebellum. *Progress in Neuro-Psychopharmacology and Biological Psychiatry*, *60*, 18–25. <https://doi.org/10.1016/j.pnpbp.2015.01.011>
- Hjorthøj, C., Stürup, A. E., McGrath, J. J., & Nordentoft, M. (2017). Years of potential life lost and life expectancy in schizophrenia: a systematic review and meta-analysis. *The Lancet Psychiatry*, *4*(4), 295–301. [https://doi.org/10.1016/S2215-0366\(17\)30078-0](https://doi.org/10.1016/S2215-0366(17)30078-0)
- Hoche, F., Guell, X., Sherman, J. C., Vangel, M. G., & Schmahmann, J. D. (2016). Cerebellar Contribution to Social Cognition. *Cerebellum*, *15*(6), 732–743. <https://doi.org/10.1007/s12311-015-0746-9>
- Hodgson, K., Poldrack, R. A., Curran, J. E., Knowles, E. E., Mathias, S., Göring, H. H. H., ... Glahn, D. C. (2017). Shared Genetic Factors Influence Head Motion During MRI and Body Mass Index. *Cerebral Cortex (New York, N.Y. : 1991)*, *27*(12), 5539–5546. <https://doi.org/10.1093/cercor/bhw321>
- Hogan, M. J., Staff, R. T., Bunting, B. P., Murray, A. D., Ahearn, T. S., Deary, I. J., & Whalley, L. J. (2011). Cerebellar brain volume accounts for variance in cognitive performance in older

adults. *Cortex*, 47(4), 441–450. <https://doi.org/10.1016/j.cortex.2010.01.001>

Holleran, L., Kelly, S., Alloza, C., Agartz, I., Andreassen, O. A., Arango, C., ... Donohoe, G. (2020). The relationship between white matter microstructure and general cognitive ability in patients with schizophrenia and healthy participants in the ENIGMA consortium. *American Journal of Psychiatry*, 177(6), 537–547. <https://doi.org/10.1176/appi.ajp.2019.19030225>

Hoogendam, Y. Y., van der Geest, J. N., van der Lijn, F., van der Lugt, A., Niessen, W. J., Krestin, G. P., ... Ikram, M. A. (2012). Determinants of cerebellar and cerebral volume in the general elderly population. *Neurobiology of Aging*, 33(12), 2774–2781. <https://doi.org/10.1016/j.neurobiolaging.2012.02.012>

Hoogman, M., Bralten, J., Hibar, D. P., Mennes, M., Zwiers, M. P., Schweren, L. S. J., ... Franke, B. (2017). Subcortical brain volume differences in participants with attention deficit hyperactivity disorder in children and adults: a cross-sectional mega-analysis. *The Lancet Psychiatry*, 4(4), 310–319. [https://doi.org/10.1016/S2215-0366\(17\)30049-4](https://doi.org/10.1016/S2215-0366(17)30049-4)

Howes, O. D., McCutcheon, R., Owen, M. J., & Murray, R. M. (2017). The Role of Genes, Stress, and Dopamine in the Development of Schizophrenia. *Biological Psychiatry*, 81(1), 9–20. <https://doi.org/10.1016/j.biopsych.2016.07.014>

Howie, B. N., Donnelly, P., & Marchini, J. (2009). A flexible and accurate genotype imputation method for the next generation of genome-wide association studies. *PLoS Genetics*, 5(6). <https://doi.org/10.1371/journal.pgen.1000529>

Howrigan, D. P., Rose, S. A., Samocha, K. E., Fromer, M., Cerrato, F., Chen, W. J., ... Neale, B. M. (2020). Exome sequencing in schizophrenia-affected parent–offspring trios reveals risk conferred by protein-coding de novo mutations. *Nature Neuroscience*, 23(2), 185–193. <https://doi.org/10.1038/s41593-019-0564-3>

Hua, J., Blair, N. I. S., Paez, A., Choe, A., Barber, A. D., Brandt, A., ... Margolis, R. L. (2019). Altered functional connectivity between sub-regions in the thalamus and cortex in schizophrenia patients measured by resting state BOLD fMRI at 7T. *Schizophrenia Research*, 206, 370–377. <https://doi.org/10.1016/j.schres.2018.10.016>

Huang, C. C., Luo, Q., Palaniyappan, L., Yang, A. C., Hung, C. C., Chou, K. H., ... Robbins, T. W. (2020). Transdiagnostic and Illness-Specific Functional Dysconnectivity Across Schizophrenia, Bipolar Disorder, and Major Depressive Disorder. *Biological Psychiatry*:

Cognitive Neuroscience and Neuroimaging, 5(5), 542–553.
<https://doi.org/10.1016/j.bpsc.2020.01.010>

Huang, J., Howie, B., McCarthy, S., Memari, Y., Walter, K., Min, J. L., ... Zhang, W. (2015). Improved imputation of low-frequency and rare variants using the UK10K haplotype reference panel. *Nature Communications*, 6. <https://doi.org/10.1038/ncomms9111>

Hublin, J. J., Neubauer, S., & Gunz, P. (2015). Brain ontogeny and life history in pleistocene hominins. *Philosophical Transactions of the Royal Society B: Biological Sciences*, 370(1663), 20140062. <https://doi.org/10.1098/rstb.2014.0062>

Hull, C. (2020). Prediction signals in the cerebellum: Beyond supervised motor learning. *ELife*, 9, e54073. <https://doi.org/10.7554/eLife.54073>

Iasevoli, F., Giordano, S., Balletta, R., Latte, G., Formato, M. V., Prinziavalli, E., ... de Bartolomeis, A. (2016). Treatment resistant schizophrenia is associated with the worst community functioning among severely-ill highly-disabling psychiatric conditions and is the most relevant predictor of poorer achievements in functional milestones. *Progress in Neuro-Psychopharmacology and Biological Psychiatry*, 65, 34–48. <https://doi.org/10.1016/j.pnpbp.2015.08.010>

Ito, M. (2008). Control of mental activities by internal models in the cerebellum. *Nature Reviews Neuroscience*, 9(4), 304–313. <https://doi.org/10.1038/nrn2332>

Jaffe, A. E., Straub, R. E., Shin, J. H., Tao, R., Gao, Y., Collado-Torres, L., ... Weinberger, D. R. (2018). Developmental and genetic regulation of the human cortex transcriptome illuminate schizophrenia pathogenesis. *Nature Neuroscience*, 21, 1117–1125. <https://doi.org/10.1038/s41593-018-0197-y>

Jansen, A. G., Mous, S. E., White, T., Posthuma, D., & Polderman, T. J. C. (2015). What Twin Studies Tell Us About the Heritability of Brain Development, Morphology, and Function: A Review. *Neuropsychology Review*. Springer. <https://doi.org/10.1007/s11065-015-9278-9>

Jauhar, S., McCutcheon, R., Borgan, F., Veronese, M., Nour, M., Pepper, F., ... Howes, O. D. (2018). The relationship between cortical glutamate and striatal dopamine in first-episode psychosis: a cross-sectional multimodal PET and magnetic resonance spectroscopy imaging study. *The Lancet Psychiatry*, 5(10), 816–823. [https://doi.org/10.1016/S2215-0366\(18\)30268-2](https://doi.org/10.1016/S2215-0366(18)30268-2)

- Jenkinson, M., Beckmann, C. F., Behrens, T. E. J., Woolrich, M. W., & Smith, S. M. (2012). Review FSL. *NeuroImage*, *62*, 782–790. <https://doi.org/10.1016/j.neuroimage.2011.09.015>
- Jha, S. C., Xia, K., Schmitt, J. E., Ahn, M., Girault, J. B., Murphy, V. A., ... Gilmore, J. H. (2018). Genetic influences on neonatal cortical thickness and surface area. *Human Brain Mapping*, *39*(12), 4998–5013. <https://doi.org/10.1002/hbm.24340>
- Ji, J. L., Diehl, C., Schleifer, C., Tamminga, C. A., Keshavan, M. S., Sweeney, J. A., ... Anticevic, A. (2019). Schizophrenia Exhibits Bi-directional Brain-Wide Alterations in Cortico-Striato-Cerebellar Circuits. *Cerebral Cortex*, *29*(11), 4463–4487. <https://doi.org/10.1093/cercor/bhy306>
- Ji, Q., Edwards, A., Glass, J. O., Brinkman, T. M., Patay, Z., & Reddick, W. E. (2019). Measurement of Projections Between Dentate Nucleus and Contralateral Frontal Cortex in Human Brain Via Diffusion Tensor Tractography. *Cerebellum*, *18*, 761–769. <https://doi.org/10.1007/s12311-019-01035-3>
- Jia, T., Chu, C., Liu, Y., van Dongen, J., Papastergios, E., Armstrong, N. J., ... Desrivieres, S. (2019). Epigenome-wide meta-analysis of blood DNA methylation and its association with subcortical volumes: findings from the ENIGMA Epigenetics Working Group. *Molecular Psychiatry*, 1–12. <https://doi.org/10.1038/s41380-019-0605-z>
- Jia, W., Zhu, H., Ni, Y., Su, J., Xu, R., Jia, H., & Wan, X. (2019). Disruptions of frontoparietal control network and default mode network linking the metacognitive deficits with clinical symptoms in schizophrenia. *Human Brain Mapping*, hbm.24887. <https://doi.org/10.1002/hbm.24887>
- Jørgensen, K. N., Nesvåg, R., Nerland, S., Mørch-Johnsen, L., Westlye, L. T., Lange, E. H., ... Agartz, I. (2017). Brain volume change in first-episode psychosis: an effect of antipsychotic medication independent of BMI change. *Acta Psychiatrica Scandinavica*, *135*(2), 117–126. <https://doi.org/10.1111/acps.12677>
- Keefe, R. S. E., Bilder, R. M., Davis, S. M., Harvey, P. D., Palmer, B. W., Gold, J. M., ... Lieberman, J. A. (2007). Neurocognitive effects of antipsychotic medications in patients with chronic schizophrenia in the CATIE trial. *Archives of General Psychiatry*, *64*(6), 633–647. <https://doi.org/10.1001/archpsyc.64.6.633>
- Kelly, S., Jahanshad, N., Zalesky, A., Kochunov, P., Agartz, I., Alloza, C., ... Donohoe, G. (2018).

Widespread white matter microstructural differences in schizophrenia across 4322 individuals: Results from the ENIGMA Schizophrenia DTI Working Group. *Molecular Psychiatry*, 23(5), 1261–1269. <https://doi.org/10.1038/mp.2017.170>

Kendall, K. M., Bracher-Smith, M., Fitzpatrick, H., Lynham, A., Rees, E., Escott-Price, V., ... Kirov, G. (2019). Cognitive performance and functional outcomes of carriers of pathogenic copy number variants: Analysis of the UK Biobank. *British Journal of Psychiatry*, 214(5), 297–304. <https://doi.org/10.1192/bjp.2018.301>

Kendall, K. M., Rees, E., Escott-Price, V., Einon, M., Thomas, R., Hewitt, J., ... Kirov, G. (2017). Cognitive Performance Among Carriers of Pathogenic Copy Number Variants: Analysis of 152,000 UK Biobank Subjects. *Biological Psychiatry*, 82(2), 103–110. <https://doi.org/10.1016/j.biopsych.2016.08.014>

Kent, J. S., Bolbecker, A. R., O'Donnell, B. F., & Hetrick, W. P. (2015). Eyeblink conditioning in schizophrenia: A critical review. *Frontiers in Psychiatry*, 6, 146. <https://doi.org/10.3389/fpsy.2015.00146>

Kessler, R. C., McLaughlin, K. A., Green, J. G., Gruber, M. J., Sampson, N. A., Zaslavsky, A. M., ... Williams, D. R. (2010). Childhood adversities and adult psychopathology in the WHO world mental health surveys. *British Journal of Psychiatry*, 197(5), 378–385. <https://doi.org/10.1192/bjp.bp.110.080499>

Keunen, K., Išgum, I., Van Kooij, B. J. M., Anbeek, P., Van Haastert, I. C., Koopman-Esseboom, C., ... Benders, M. J. N. L. (2016). Brain volumes at term-equivalent age in preterm infants: Imaging biomarkers for neurodevelopmental outcome through early school age. In *Journal of Pediatrics* (Vol. 172, pp. 88–95). Mosby Inc. <https://doi.org/10.1016/j.jpeds.2015.12.023>

Khokhar, J. Y., Dwiell, L. L., Henricks, A. M., Doucette, W. T., & Green, A. I. (2018). The link between schizophrenia and substance use disorder: A unifying hypothesis. *Schizophrenia Research*, 194, 78–85. <https://doi.org/10.1016/j.schres.2017.04.016>

Kiessling, M. C., Büttner, A., Butti, C., Müller-Starck, J., Milz, S., Hof, P. R., ... Schmitz, C. (2014). Cerebellar granule cells are generated postnatally in humans. *Brain Structure and Function*, 219(4), 1271–1286. <https://doi.org/10.1007/s00429-013-0565-z>

Kim, D., Cho, H. B., Dager, S. R., Yurgelun-Todd, D. A., Yoon, S., Lee, J. H., ... Lyoo, I. K. (2013).

Posterior cerebellar vermal deficits in bipolar disorder. *Journal of Affective Disorders*, 150(2), 499–506. <https://doi.org/10.1016/j.jad.2013.04.050>

Kim, J., & Augustine, G. J. (2020). Molecular Layer Interneurons: Key Elements of Cerebellar Network Computation and Behavior. *Neuroscience*. <https://doi.org/10.1016/j.neuroscience.2020.10.008>

King, M., Hernandez-Castillo, C. R., Poldrack, R. A., Ivry, R. B., & Diedrichsen, J. (2019). Functional boundaries in the human cerebellum revealed by a multi-domain task battery. *Nature Neuroscience*, 22(8), 1371–1378. <https://doi.org/10.1038/s41593-019-0436-x>

Kircher, M., Witten, D. M., Jain, P., O’roak, B. J., Cooper, G. M., & Shendure, J. (2014). A general framework for estimating the relative pathogenicity of human genetic variants. *Nature Genetics*, 46(3), 310–315. <https://doi.org/10.1038/ng.2892>

Kirov, G., Pocklington, A. J., Holmans, P., Ivanov, D., Ikeda, M., Ruderfer, D., ... Owen, M. J. (2012). De novo CNV analysis implicates specific abnormalities of postsynaptic signalling complexes in the pathogenesis of schizophrenia. *Molecular Psychiatry*, 17(2), 142–153. <https://doi.org/10.1038/mp.2011.154>

Kirov, George, Rees, E., Walters, J. T. R., Escott-Price, V., Georgieva, L., Richards, A. L., ... Owen, M. J. (2014). The penetrance of copy number variations for schizophrenia and developmental delay. *Biological Psychiatry*, 75(5), 378–385. <https://doi.org/10.1016/j.biopsych.2013.07.022>

Klein, A. P., Ulmer, J. L., Quinet, S. A., Mathews, V., & Mark, L. P. (2016). Nonmotor functions of the cerebellum: An introduction. *American Journal of Neuroradiology*, 37(6), 1005–1009. <https://doi.org/10.3174/ajnr.A4720>

Knickmeyer, R. C., Gouttard, S., Kang, C., Evans, D., Wilber, K., Smith, J. K., ... Gilmore, J. H. (2008). A structural MRI study of human brain development from birth to 2 years. *Journal of Neuroscience*, 28(47), 12176–12182. <https://doi.org/10.1523/JNEUROSCI.3479-08.2008>

Ko, Y. S., Tsai, H. C., Chi, M. H., Su, C. C., Lee, I. H., Chen, P. S., ... Yang, Y. K. (2018). Higher mortality and years of potential life lost of suicide in patients with schizophrenia. *Psychiatry Research*, 270, 531–537. <https://doi.org/10.1016/j.psychres.2018.09.038>

Kochiyama, T., Ogihara, N., Tanabe, H. C., Kondo, O., Amano, H., Hasegawa, K., ... Akazawa, T.

- (2018). Reconstructing the Neanderthal brain using computational anatomy. *Scientific Reports*, 8(1), 6296. <https://doi.org/10.1038/s41598-018-24331-0>
- Kochunov, P., Huang, J., Chen, S., Li, Y., Tan, S., Fan, F., ... Elliot Hong, L. (2019). White matter in schizophrenia treatment resistance. *American Journal of Psychiatry*, 176(10), 829–838. <https://doi.org/10.1176/appi.ajp.2019.18101212>
- Kolenič, M., Španiel, F., Hlinka, J., Matějka, M., Knytl, P., Šebela, A., ... Hajek, T. (2020). Higher Body-Mass Index and Lower Gray Matter Volumes in First Episode of Psychosis. *Frontiers in Psychiatry*, 11, 1006. <https://doi.org/10.3389/fpsyt.2020.556759>
- Kong, L., Herold, C. J., Cheung, E. F. C., Chan, R. C. K., & Schröder, J. (2019). Neurological Soft Signs and Brain Network Abnormalities in Schizophrenia. *Schizophrenia Bulletin*. <https://doi.org/10.1093/schbul/sbz118>
- Koning, I. V., Tielemans, M. J., Hoebeek, F. E., Ecury-Goossen, G. M., Reiss, I. K. M., Steegers-Theunissen, R. P. M., & Dudink, J. (2017). Impacts on prenatal development of the human cerebellum: a systematic review. *Journal of Maternal-Fetal and Neonatal Medicine*, 30(20), 2461–2468. <https://doi.org/10.1080/14767058.2016.1253060>
- Koshiyama, D., Fukunaga, M., Okada, N., Morita, K., Nemoto, K., Usui, K., ... Hashimoto, R. (2020). White matter microstructural alterations across four major psychiatric disorders: mega-analysis study in 2937 individuals. *Molecular Psychiatry*, 25(4), 883–895. <https://doi.org/10.1038/s41380-019-0553-7>
- Koshiyama, D., Kirihara, K., Tada, M., Nagai, T., Fujioka, M., Ichikawa, E., ... Kasai, K. (2018). Electrophysiological evidence for abnormal glutamate-GABA association following psychosis onset. *Translational Psychiatry*, 8(1), 1–10. <https://doi.org/10.1038/s41398-018-0261-0>
- Koshiyama, D., Miura, K., Nemoto, K., Okada, N., Matsumoto, J., Fukunaga, M., & Hashimoto, R. (2020). Neuroimaging studies within Cognitive Genetics Collaborative Research Organization aiming to replicate and extend works of ENIGMA. *Human Brain Mapping*. <https://doi.org/10.1002/hbm.25040>
- Kotkowski, E., Price, L. R., Franklin, C., Salazar, M., Woolsey, M., DeFronzo, R. A., ... Fox, P. T. (2019). A neural signature of metabolic syndrome. *Human Brain Mapping*, 40(12), 3575–3588. <https://doi.org/10.1002/hbm.24617>

- Koutsouleris, N., Davatzikos, C., Borgwardt, S., Gaser, C., Bottlender, R., Frodl, T., ... Meisenzahl, E. (2014). Accelerated brain aging in schizophrenia and beyond: A neuroanatomical marker of psychiatric disorders. *Schizophrenia Bulletin*, *40*(5), 1140–1153. <https://doi.org/10.1093/schbul/sbt142>
- Kremen, W. S., Panizzon, M. S., Neale, M. C., Fennema-Notestine, C., Prom-Wormley, E., Eyler, L. T., ... Dale, A. M. (2012). Heritability of brain ventricle volume: Converging evidence from inconsistent results. *Neurobiology of Aging*, *33*(1), 1–8. <https://doi.org/10.1016/j.neurobiolaging.2010.02.007>
- Kronemer, S. I., Slapik, M. B., Pietrowski, J. R., Margron, M. J., Morgan, O. P., Bakker, C. C., ... Marvel, C. L. (2020). Neuropsychiatric Symptoms as a Reliable Phenomenology of Cerebellar Ataxia. *Cerebellum*, 1–10. <https://doi.org/10.1007/s12311-020-01195-7>
- Kühn, S., Romanowski, A., Schubert, F., & Gallinat, J. (2012). Reduction of cerebellar grey matter in Crus I and II in schizophrenia. *Brain Structure and Function*, *217*(2), 523–529. <https://doi.org/10.1007/s00429-011-0365-2>
- Kumar, P., Henikoff, S., & Ng, P. C. (2009). Predicting the effects of coding non-synonymous variants on protein function using the SIFT algorithm. *Nature Protocols*, *4*(7), 1073–1081. <https://doi.org/10.1038/nprot.2009.86>
- Kuo, S. S., & Pogue-Geile, M. F. (2019). Variation in fourteen brain structure volumes in schizophrenia: A comprehensive meta-analysis of 246 studies. *Neuroscience and Biobehavioral Reviews*, *98*, 85–94. <https://doi.org/10.1016/j.neubiorev.2018.12.030>
- Laidi, C., D’Albis, M. A., Wessa, M., Linke, J., Phillips, M. L., Delavest, M., ... Houenou, J. (2015). Cerebellar volume in schizophrenia and bipolar I disorder with and without psychotic features. *Acta Psychiatrica Scandinavica*, *131*(3), 223–233. <https://doi.org/10.1111/acps.12363>
- Laidi, C., Hajek, T., Spaniel, F., Kolenic, M., D’Albis, M. A., Sarrazin, S., ... Houenou, J. (2019). Cerebellar parcellation in schizophrenia and bipolar disorder. *Acta Psychiatrica Scandinavica*, *140*(5), 468–476. <https://doi.org/10.1111/acps.13087>
- Lam, M., Trampush, J. W., Yu, J., Knowles, E., Davies, G., Liewald, D. C., ... Lencz, T. (2017). Large-Scale Cognitive GWAS Meta-Analysis Reveals Tissue-Specific Neural Expression and Potential Nootropic Drug Targets. *Cell Reports*, *21*(9), 2597–2613.

<https://doi.org/10.1016/j.celrep.2017.11.028>

- Lancaster, T. M., Dimitriadis, S. L., Tansey, K. E., Perry, G., Ihssen, N., Jones, D. K., ... Linden, D. E. (2019). Structural and Functional Neuroimaging of Polygenic Risk for Schizophrenia: A Recall-by-Genotype-Based Approach. *Schizophrenia Bulletin*, *45*(2), 405–414. <https://doi.org/10.1093/schbul/sby037>
- Le, B. D., & Stein, J. L. (2019). Mapping causal pathways from genetics to neuropsychiatric disorders using genome-wide imaging genetics: Current status and future directions. *Psychiatry and Clinical Neurosciences*, *73*(7), 357–369. <https://doi.org/10.1111/pcn.12839>
- Lee, P. H., Anttila, V., Won, H., Feng, Y. C. A., Rosenthal, J., Zhu, Z., ... Smoller, J. W. (2019). Genomic Relationships, Novel Loci, and Pleiotropic Mechanisms across Eight Psychiatric Disorders. *Cell*, *179*(7), 1469–1482. <https://doi.org/10.1016/j.cell.2019.11.020>
- Lee, S. H., Yang, J., Goddard, M. E., Visscher, P. M., & Wray, N. R. (2012). Estimation of pleiotropy between complex diseases using single-nucleotide polymorphism-derived genomic relationships and restricted maximum likelihood. *Bioinformatics*, *28*(19), 2540–2542. <https://doi.org/10.1093/bioinformatics/bts474>
- Lee, Sang Hong, Goddard, M. E., Wray, N. R., & Visscher, P. M. (2012). A better coefficient of determination for genetic profile analysis. *Genetic Epidemiology*, *36*(3), 214–224. <https://doi.org/10.1002/gepi.21614>
- Lee, Sang Hong, Wray, N. R., Goddard, M. E., & Visscher, P. M. (2011). Estimating missing heritability for disease from genome-wide association studies. *American Journal of Human Genetics*, *88*(3), 294–305. <https://doi.org/10.1016/j.ajhg.2011.02.002>
- Legge, S. E., Dennison, C. A., Pardiñas, A. F., Rees, E., Lynham, A. J., Hopkins, L., ... Walters, J. T. R. (2020). Clinical indicators of treatment-resistant psychosis. *British Journal of Psychiatry*, *216*(5), 259–266. <https://doi.org/10.1192/bjp.2019.120>
- Leucht, S., Cipriani, A., Spineli, L., Mavridis, D., Örey, D., Richter, F., ... Davis, J. M. (2013). Comparative efficacy and tolerability of 15 antipsychotic drugs in schizophrenia: A multiple-treatments meta-analysis. *The Lancet*, *382*(9896), 951–962. [https://doi.org/10.1016/S0140-6736\(13\)60733-3](https://doi.org/10.1016/S0140-6736(13)60733-3)
- Lin, A., Ching, C. R. K., Vajdi, A., Sun, D., Jonas, R. K., Jalbrzikowski, M., ... Bearden, C. E. (2017).

Mapping 22q11.2 gene dosage effects on brain morphometry. *Journal of Neuroscience*, 37(26), 6183–6199. <https://doi.org/10.1523/JNEUROSCI.3759-16.2017>

Lin, A. S., Chang, S. S., Lin, S. H., Peng, Y. C., Hwu, H. G., & Chen, W. J. (2015). Minor physical anomalies and craniofacial measures in patients with treatment-resistant schizophrenia. *Psychological Medicine*, 45(9), 1839–1850. <https://doi.org/10.1017/S0033291714002931>

Littlejohns, T. J., Holliday, J., Gibson, L. M., Garratt, S., Oesingmann, N., Alfaro-Almagro, F., ... Allen, N. E. (2020, December 26). The UK Biobank imaging enhancement of 100,000 participants: rationale, data collection, management and future directions. *Nature Communications*. Nature Publishing Group. <https://doi.org/10.1038/s41467-020-15948-9>

Liu, B., Zhang, X., Cui, Y., Qin, W., Tao, Y., Li, J., ... Jiang, T. (2017). Polygenic risk for schizophrenia influences cortical gyrification in 2 independent general populations. *Schizophrenia Bulletin*, 43(3), 673–680. <https://doi.org/10.1093/schbul/sbw051>

Liu, H., Fan, G., Xu, K., & Wang, F. (2011). Changes in cerebellar functional connectivity and anatomical connectivity in schizophrenia: A combined resting-state functional MRI and diffusion tensor imaging study. *Journal of Magnetic Resonance Imaging*, 34(6), 1430–1438. <https://doi.org/10.1002/jmri.22784>

Locke, T. M., Fujita, H., Hunker, A., Johanson, S. S., Darvas, M., du Lac, S., ... Carlson, E. S. (2020). Purkinje Cell-Specific Knockout of Tyrosine Hydroxylase Impairs Cognitive Behaviors. *Frontiers in Cellular Neuroscience*, 14, 228. <https://doi.org/10.3389/fncel.2020.00228>

Locke, T. M., Soden, M. E., Miller, S. M., Hunker, A., Knakal, C., Licholai, J. A., ... Carlson, E. S. (2018). Dopamine D1 Receptor-Positive Neurons in the Lateral Nucleus of the Cerebellum Contribute to Cognitive Behavior. *Biological Psychiatry*, 84(6), 401–412. <https://doi.org/10.1016/j.biopsych.2018.01.019>

Loh, P. R., Bhatia, G., Gusev, A., Finucane, H. K., Bulik-Sullivan, B. K., Pollack, S. J., ... Price, A. L. (2015). Contrasting genetic architectures of schizophrenia and other complex diseases using fast variance-components analysis. *Nature Genetics*, 47(12), 1385–1392. <https://doi.org/10.1038/ng.3431>

Luo, Q., Chen, Q., Wang, W., Desrivieres, S., Quinlan, E. B., Jia, T., ... Feng, J. (2019). Association of a Schizophrenia-Risk Nonsynonymous Variant with Putamen Volume in Adolescents: A Voxelwise and Genome-Wide Association Study. *JAMA Psychiatry*, 76(4), 435–445.

<https://doi.org/10.1001/jamapsychiatry.2018.4126>

- Luo, Q., Zhang, L., Huang, C. C., Zheng, Y., Kanen, J. W., Zhao, Q., ... Robbins, T. W. (2020). Association between childhood trauma and risk for obesity: a putative neurocognitive developmental pathway. *BMC Medicine*, *18*(1), 1–14. <https://doi.org/10.1186/s12916-020-01743-2>
- Luo, Y., Zhang, L., He, P., Pang, L., Guo, C., & Zheng, X. (2019). Individual-level and area-level socioeconomic status (SES) and schizophrenia: Cross-sectional analyses using the evidence from 1.9 million Chinese adults. *BMJ Open*, *9*(9), e026532. <https://doi.org/10.1136/bmjopen-2018-026532>
- Lupo, M., Siciliano, L., & Leggio, M. (2019, August 1). From cerebellar alterations to mood disorders: A systematic review. *Neuroscience and Biobehavioral Reviews*. Elsevier Ltd. <https://doi.org/10.1016/j.neubiorev.2019.06.008>
- Lynham, A. J., Hubbard, L., Tansey, K. E., Hamshere, M. L., Legge, S. E., Owen, M. J., ... Walters, J. T. R. (2018). Examining cognition across the bipolar/schizophrenia diagnostic spectrum. *Journal of Psychiatry and Neuroscience*, *43*(4), 245–253. <https://doi.org/10.1503/jpn.170076>
- MacDowell, K. S., Pinacho, R., Leza, J. C., Costa, J., Ramos, B., & García-Bueno, B. (2017). Differential regulation of the TLR4 signalling pathway in post-mortem prefrontal cortex and cerebellum in chronic schizophrenia: Relationship with SP transcription factors. *Progress in Neuro-Psychopharmacology and Biological Psychiatry*, *79*(Part B), 481–492. <https://doi.org/10.1016/j.pnpbp.2017.08.005>
- Maillard, A. M., Ruef, A., Pizzagalli, F., Migliavacca, E., Hippolyte, L., Adaszewski, S., ... Jacquemont, S. (2015). The 16p11.2 locus modulates brain structures common to autism, schizophrenia and obesity. *Molecular Psychiatry*, *20*(1), 140–147. <https://doi.org/10.1038/mp.2014.145>
- Makowski, C., Lepage, M., & Evans, A. C. (2019). Head motion: The dirty little secret of neuroimaging in psychiatry. *Journal of Psychiatry and Neuroscience*. Canadian Medical Association. <https://doi.org/10.1503/jpn.180022>
- Malaspina, D., Walsh-Messinger, J., Brunner, A., Rahman, N., Corcoran, C., Kimhy, D., ... Goldman, S. B. (2019). Features of schizophrenia following premorbid eating disorders.

Psychiatry Research, 278, 275–280. <https://doi.org/10.1016/j.psychres.2019.06.035>

Maloku, E., Covelo, I. R., Hanbauer, I., Guidotti, A., Kadriu, B., Hu, Q., ... Costa, E. (2010). Lower number of cerebellar Purkinje neurons in psychosis is associated with reduced reelin expression. *Proceedings of the National Academy of Sciences of the United States of America*, 107(9), 4407–4411. <https://doi.org/10.1073/pnas.0914483107>

Mamah, D., Ji, A., Rutlin, J., & Shimony, J. S. (2019). White matter integrity in schizophrenia and bipolar disorder: Tract- and voxel-based analyses of diffusion data from the Connectom scanner. *NeuroImage: Clinical*, 21, 101649. <https://doi.org/10.1016/j.nicl.2018.101649>

Mankiw, C., Park, M. T. M., Reardon, P. K., Fish, A. M., Clasen, L. S., Greenstein, D., ... Raznahan, A. (2017). Allometric analysis detects brain size-independent effects of sex and sex chromosome complement on human cerebellar organization. *Journal of Neuroscience*, 37(21), 5221–5231. <https://doi.org/10.1523/JNEUROSCI.2158-16.2017>

Manto, M., & Hampe, C. S. (2018). Endocrine disorders and the cerebellum: from neurodevelopmental injury to late-onset ataxia. In *Handbook of Clinical Neurology* (Vol. 155, pp. 353–368). Elsevier B.V. <https://doi.org/10.1016/B978-0-444-64189-2.00023-8>

Marchesi, C., Affaticati, A., Monici, A., De Panfilis, C., Ossola, P., & Tonna, M. (2015). Severity of core symptoms in first episode schizophrenia and long-term remission. *Psychiatry Research*, 225(1–2), 129–132. <https://doi.org/10.1016/j.psychres.2014.11.005>

Marconi, A., Di Forti, M., Lewis, C. M., Murray, R. M., & Vassos, E. (2016). Meta-Analysis of the association between the level of cannabis use and risk of psychosis. *Schizophrenia Bulletin*, 42(5), 1262–1269. <https://doi.org/10.1093/schbul/sbw003>

Marek, S., Siegel, J. S., Gordon, E. M., Raut, R. V., Gratton, C., Newbold, D. J., ... Dosenbach, N. U. F. (2018). Spatial and Temporal Organization of the Individual Human Cerebellum. *Neuron*, 100(4), 977–993. <https://doi.org/https://doi.org/10.1016/j.neuron.2018.10.010>

Marshall, C. R., Howrigan, D. P., Merico, D., Thiruvahindrapuram, B., Wu, W., Greer, D. S., ... Sebat, J. (2017). Contribution of copy number variants to schizophrenia from a genome-wide study of 41,321 subjects. *Nature Genetics*, 49(1), 27–35. <https://doi.org/10.1038/ng.3725>

Matheson, S. L., Shepherd, A. M., Pinchbeck, R. M., Laurens, K. R., & Carr, V. J. (2013). Childhood

adversity in schizophrenia: A systematic meta-analysis. *Psychological Medicine*, 43(2), 225–238. <https://doi.org/10.1017/S0033291712000785>

Matoba, N., Love, M., & Stein, J. (2020). Evaluating brain structure traits as endophenotypes using polygenicity and discoverability. *Human Brain Mapping*. <https://doi.org/10.1101/2020.07.17.208843>

Matsufuji, M., Sano, N., Tsuru, H., & Takashima, S. (2017). Neuroimaging and neuropathological characteristics of cerebellar injury in extremely low birth weight infants. *Brain and Development*, 39(9), 735–742. <https://doi.org/10.1016/j.braindev.2017.04.011>

Matsuoka, K., Morimoto, T., Matsuda, Y., Yasuno, F., Taoka, T., Miyasaka, T., ... Kishimoto, T. (2019). Computer-assisted cognitive remediation therapy for patients with schizophrenia induces microstructural changes in cerebellar regions involved in cognitive functions. *Psychiatry Research - Neuroimaging*, 292, 41–46. <https://doi.org/10.1016/j.pscychresns.2019.09.001>

Maurano, M. T., Humbert, R., Rynes, E., Thurman, R. E., Haugen, E., Wang, H., ... Stamatoyannopoulos, J. A. (2012). Systematic localization of common disease-associated variation in regulatory DNA. *Science*, 337(6099), 1190–1195. <https://doi.org/10.1126/science.1222794>

McCoy, R. C., Wakefield, J., & Akey, J. M. (2017). Impacts of Neanderthal-Introgressed Sequences on the Landscape of Human Gene Expression. *Cell*, 168(5), 916–927. <https://doi.org/10.1016/j.cell.2017.01.038>

McCutcheon, R. A., Reis Marques, T., & Howes, O. D. (2020). Schizophrenia - An Overview. *JAMA Psychiatry*, 77(2), 201–210. <https://doi.org/10.1001/jamapsychiatry.2019.3360>

McGrath, J., Saha, S., Chant, D., & Welham, J. (2008). Schizophrenia: A concise overview of incidence, prevalence, and mortality. *Epidemiologic Reviews*, 30(1), 67–76. <https://doi.org/10.1093/epirev/mxn001>

McGuffin, P., Farmer, A., & Harvey, I. (1991). A polydiagnostic application of operational criteria in studies of psychotic illness: Development and reliability of the OPCRIT system. *Archives of General Psychiatry*, 48, 764–770. <https://doi.org/10.1001/archpsyc.1991.01810320088015>

- Mealer, R. G., Jenkins, B. G., Chen, C. Y., Daly, M. J., Ge, T., Lehoux, S., ... Smoller, J. W. (2020). The schizophrenia risk locus in SLC39A8 alters brain metal transport and plasma glycosylation. *Scientific Reports*, *10*(1), 1–15. <https://doi.org/10.1038/s41598-020-70108-9>
- Mejia-Vergara, A., Karanjia, R., & Sadun, A. A. (2020). OCT parameters of the optic nerve head and the retina as surrogate markers of brain volume in a normal population, a pilot study. *Journal of the Neurological Sciences*, *420*, 117213. <https://doi.org/10.1016/j.jns.2020.117213>
- Middeldorp, C. M., Hammerschlag, A. R., Ouwens, K. G., Groen-Blokhuis, M. M., St. Pourcain, B., Greven, C. U., ... Boomsma, D. I. (2016). A Genome-Wide Association Meta-Analysis of Attention-Deficit/Hyperactivity Disorder Symptoms in Population-Based Pediatric Cohorts. *Journal of the American Academy of Child and Adolescent Psychiatry*, *55*(10), 896-905.e6. <https://doi.org/10.1016/j.jaac.2016.05.025>
- Milardi, D., Arrigo, A., Anastasi, G., Cacciola, A., Marino, S., Mormina, E., ... Quartarone, A. (2016). Extensive direct subcortical cerebellum-basal ganglia connections in human brain as revealed by constrained spherical deconvolution tractography. *Frontiers in Neuroanatomy*, *10*(MAR), 29. <https://doi.org/10.3389/fnana.2016.00029>
- Miller, K. L., Alfaro-Almagro, F., Bangerter, N. K., Thomas, D. L., Yacoub, E., Xu, J., ... Smith, S. M. (2016). Multimodal population brain imaging in the UK Biobank prospective epidemiological study. *Nature Neuroscience*, *19*(11), 1523–1536. <https://doi.org/10.1038/nn.4393>
- Minichino, A., Ando, A., Francesconi, M., Salatino, A., Delle Chiaie, R., & Cadenhead, K. (2017, July 3). Investigating the link between drug-naïve first episode psychoses (FEPs), weight gain abnormalities and brain structural damages: Relevance and implications for therapy. *Progress in Neuro-Psychopharmacology and Biological Psychiatry*. Elsevier Inc. <https://doi.org/10.1016/j.pnpbp.2017.03.020>
- Moberget, T., Alnæs, D., Kaufmann, T., Doan, N. T., Córdova-Palomera, A., Norbom, L. B., ... Westlye, L. T. (2019). Cerebellar Gray Matter Volume Is Associated With Cognitive Function and Psychopathology in Adolescence. *Biological Psychiatry*, *86*(1), 65–75. <https://doi.org/10.1016/j.biopsych.2019.01.019>

- Moberget, T., Doan, N. T., Alnæs, D., Kaufmann, T., Córdova-Palomera, A., Lagerberg, T. V., ... Westlye, L. T. (2018). Cerebellar volume and cerebellocerebral structural covariance in schizophrenia: A multisite mega-analysis of 983 patients and 1349 healthy controls. *Molecular Psychiatry*, 23(6), 1512–1520. <https://doi.org/10.1038/mp.2017.106>
- Moberget, T., & Ivry, R. B. (2016). Cerebellar contributions to motor control and language comprehension: Searching for common computational principles. *Annals of the New York Academy of Sciences*, 1369(1), 154. <https://doi.org/10.1111/nyas.13094>
- Moberget, T., & Ivry, R. B. (2019, September 1). Prediction, Psychosis, and the Cerebellum. *Biological Psychiatry: Cognitive Neuroscience and Neuroimaging*. Elsevier Inc. <https://doi.org/10.1016/j.bpsc.2019.06.001>
- Molent, C., Olivo, D., Wolf, R. C., Balestrieri, M., & Sambataro, F. (2019, September 1). Functional neuroimaging in treatment resistant schizophrenia: A systematic review. *Neuroscience and Biobehavioral Reviews*. Elsevier Ltd. <https://doi.org/10.1016/j.neubiorev.2019.07.001>
- Moore, D. M., D’Mello, A. M., McGrath, L. M., & Stoodley, C. J. (2017). The developmental relationship between specific cognitive domains and grey matter in the cerebellum. *Developmental Cognitive Neuroscience*, 24, 1–11. <https://doi.org/10.1016/j.dcn.2016.12.001>
- Moreno-Rius, J. (2018). The cerebellum in fear and anxiety-related disorders. *Progress in Neuro-Psychopharmacology and Biological Psychiatry*, 85, 23–32. <https://doi.org/10.1016/j.pnpbp.2018.04.002>
- Moreno-Rius, J. (2019a). The cerebellum under stress. *Frontiers in Neuroendocrinology*, 54, 100774. <https://doi.org/10.1016/j.yfrne.2019.100774>
- Moreno-Rius, J. (2019b, June 15). The Cerebellum, THC, and Cannabis Addiction: Findings from Animal and Human Studies. *Cerebellum*. Springer New York LLC. <https://doi.org/10.1007/s12311-018-0993-7>
- Moreno-Rius, J. (2019c, December 1). Opioid addiction and the cerebellum. *Neuroscience and Biobehavioral Reviews*. Elsevier Ltd. <https://doi.org/10.1016/j.neubiorev.2019.09.015>
- Moretti, P. N., Ota, V. K., Gouvea, E. S., Pedrini, M., Santoro, M. L., Talarico, F., ... Belangero, S. (2018). Accessing Gene Expression in Treatment-Resistant Schizophrenia. *Molecular*

Neurobiology, 55(8), 7000–7008. <https://doi.org/10.1007/s12035-018-0876-4>

Moulton, E. A., Elman, I., Becerra, L. R., Goldstein, R. Z., & Borsook, D. (2014). The cerebellum and addiction: Insights gained from neuroimaging research. *Addiction Biology*, 19(3), 317–331. <https://doi.org/10.1111/adb.12101>

Moussa-Tooks, A. B., Larson, E. R., Gimeno, A. F., Leishman, E., Bartolomeo, L. A., Bradshaw, H. B., ... Hetrick, W. P. (2020). Long-Term Aberrations To Cerebellar Endocannabinoids Induced By Early-Life Stress. *Scientific Reports*, 10(1), 7236. <https://doi.org/10.1038/s41598-020-64075-4>

Mueller, K., Moller, H. E., Horstmann, A., Busse, F., Lepsien, J., Bluher, M., ... Pleger, B. (2015). Physical exercise in overweight to obese individuals induces metabolic-and neurotrophic-related structural brain plasticity. *Frontiers in Human Neuroscience*, 9, 372. <https://doi.org/10.3389/fnhum.2015.00372>

Munafò, M. R., Tilling, K., Taylor, A. E., Evans, D. M., & Davey Smith, G. (2018). Collider scope: when selection bias can substantially influence observed associations. *International Journal of Epidemiology*, 47(1), 226–235. <https://doi.org/10.1093/ije/dyx206>

Murray, R. M., Bhavsar, V., Tripoli, G., & Howes, O. (2017). 30 Years on: How the Neurodevelopmental Hypothesis of Schizophrenia Morphed into the Developmental Risk Factor Model of Psychosis. *Schizophrenia Bulletin*, 43(6), 1190–1196. <https://doi.org/10.1093/schbul/sbx121>

Myllyaho, T., Siira, V., Wahlberg, K. E., Hakko, H., Läksy, K., Roisko, R., ... Räsänen, S. (2019). Interaction of genetic vulnerability to schizophrenia and family functioning in adopted-away offspring of mothers with schizophrenia. *Psychiatry Research*, 278, 205–212. <https://doi.org/10.1016/j.psychres.2019.06.017>

Nagelkerke, N. J. D. (1991). A Note on a General Definition of the Coefficient of Determination. *Biometrika*, 78(3), 691–692. <https://doi.org/10.2307/2337038>

Navarri, X., Afzali, M. H., Lavoie, J., Sinha, R., Stein, D. J., Momenan, R., ... Conrod, P. J. (2020). How do substance use disorders compare to other psychiatric conditions on structural brain abnormalities? A cross-disorder meta-analytic comparison using the ENIGMA consortium findings. *Human Brain Mapping*. <https://doi.org/10.1002/hbm.25114>

- Negi, S. K., & Guda, C. (2017). Global gene expression profiling of healthy human brain and its application in studying neurological disorders. *Scientific Reports*, *7*(1), 1–12. <https://doi.org/10.1038/s41598-017-00952-9>
- Neilson, E., Bois, C., Gibson, J., Duff, B., Watson, A., Roberts, N., ... Lawrie, S. M. (2017). Effects of environmental risks and polygenic loading for schizophrenia on cortical thickness. *Schizophrenia Research*, *184*, 128–136. <https://doi.org/10.1016/j.schres.2016.12.011>
- Neilson, E., Shen, X., Cox, S. R., Clarke, T. K., Wigmore, E. M., Gibson, J., ... Lawrie, S. M. (2019). Impact of Polygenic Risk for Schizophrenia on Cortical Structure in UK Biobank. *Biological Psychiatry*, *86*(7), 536–544. <https://doi.org/10.1016/j.biopsych.2019.04.013>
- Nelson, E. A., Kraguljac, N. V., White, D. M., Jindal, R. D., Shin, A. L., & Lahti, A. C. (2020). A Prospective Longitudinal Investigation of Cortical Thickness and Gyrification in Schizophrenia. *Canadian Journal of Psychiatry*, *65*(6), 381–391. <https://doi.org/10.1177/0706743720904598>
- Nelson, H. E. (1991). The National Adult Reading Test (NART): Test Manual. Windsor, UK: NFER-Nelson.
- Neubauer, S., Hublin, J. J., & Gunz, P. (2018). The evolution of modern human brain shape. *Science Advances*, *4*(1), eaao5961. <https://doi.org/10.1126/sciadv.aao5961>
- Newman, D. L., Moffitt, T. E., Caspi, A., & Silva, P. A. (1998). Comorbid mental disorders: Implications for treatment and sample selection. *Journal of Abnormal Psychology*, *107*(2), 305. <https://doi.org/10.1037/0021-843X.107.2.305>
- Nucifora, F. C., Woznica, E., Lee, B. J., Cascella, N., & Sawa, A. (2019). Treatment resistant schizophrenia: Clinical, biological, and therapeutic perspectives. *Neurobiology of Disease*, *131*, 104257. <https://doi.org/10.1016/j.nbd.2018.08.016>
- O'Connor, L. J., Schoech, A. P., Hormozdiari, F., Gazal, S., Patterson, N., & Price, A. L. (2019). Extreme Polygenicity of Complex Traits Is Explained by Negative Selection. *American Journal of Human Genetics*, *105*(3), 456–476. <https://doi.org/10.1016/j.ajhg.2019.07.003>
- O'dushlaine, C., Rossin, L., Lee, P. H., Duncan, L., Parikshak, N. N., Newhouse, S., ... Breen, G. (2015). Psychiatric genome-wide association study analyses implicate neuronal, immune and histone pathways. *Nature Neuroscience*, *18*(2), 199–209.

<https://doi.org/10.1038/nn.3922>

Okada, N., Fukunaga, M., Yamashita, F., Koshiyama, D., Yamamori, H., Ohi, K., ... Hashimoto, R. (2016). Abnormal asymmetries in subcortical brain volume in schizophrenia. *Molecular Psychiatry*, 21(10), 1460–1466. <https://doi.org/10.1038/mp.2015.209>

Owen, J. P., Bukshpun, P., Pojman, N., Thieu, T., Chen, Q., Lee, J., ... Sherr, E. H. (2018). Brain MR imaging findings and associated outcomes in carriers of the reciprocal copy number variation at 16p11.2. *Radiology*, 286(1), 217–226. <https://doi.org/10.1148/radiol.2017162934>

Owen, M. J. (2014). New approaches to psychiatric diagnostic classification. *Neuron*, 84(3), 564–571. <https://doi.org/10.1016/j.neuron.2014.10.028>

Owen, M. J., O'Donovan, M. C., Thapar, A., & Craddock, N. (2011). Neurodevelopmental hypothesis of schizophrenia. *British Journal of Psychiatry*, 198(3), 173–175. <https://doi.org/10.1192/bjp.bp.110.084384>

Palesi, F., De Rinaldis, A., Castellazzi, G., Calamante, F., Muhlert, N., Chard, D., ... Wheeler-Kingshott, C. A. M. G. (2017). Contralateral cortico-ponto-cerebellar pathways reconstruction in humans in vivo: Implications for reciprocal cerebro-cerebellar structural connectivity in motor and non-motor areas. *Scientific Reports*, 7(1), 1–13. <https://doi.org/10.1038/s41598-017-13079-8>

Palesi, F., Tournier, J. D., Calamante, F., Muhlert, N., Castellazzi, G., Chard, D., ... Wheeler-Kingshott, C. A. M. (2015). Contralateral cerebello-thalamo-cortical pathways with prominent involvement of associative areas in humans in vivo. *Brain Structure and Function*, 220(6), 3369–3384. <https://doi.org/10.1007/s00429-014-0861-2>

Pardiñas, A. F., Holmans, P., Pocklington, A. J., Escott-Price, V., Ripke, S., Carrera, N., ... Walters, J. T. R. (2018). Common schizophrenia alleles are enriched in mutation-intolerant genes and in regions under strong background selection. *Nature Genetics*, 50(3), 381–389. <https://doi.org/10.1038/s41588-018-0059-2>

Parrell, B., Agnew, Z., Nagarajan, S., Houde, J., & Ivry, R. B. (2017). Impaired feedforward control and enhanced feedback control of speech in patients with cerebellar degeneration. *Journal of Neuroscience*, 37(38), 9249–9258. <https://doi.org/10.1523/JNEUROSCI.3363-16.2017>

- Parvizi, J. (2009). Corticocentric myopia: old bias in new cognitive sciences. *Trends in Cognitive Sciences*, 13(8), 354–359. <https://doi.org/10.1016/j.tics.2009.04.008>
- Pavlidis, J. M. W., Zhu, Z., Gratten, J., McRae, A. F., Wray, N. R., & Yang, J. (2016). Predicting gene targets from integrative analyses of summary data from GWAS and eQTL studies for 28 human complex traits. *Genome Medicine*, 8(1), 84. <https://doi.org/10.1186/s13073-016-0338-4>
- Peters, S. K., Dunlop, K., & Downar, J. (2016). Cortico-striatal-thalamic loop circuits of the salience network: A central pathway in psychiatric disease and treatment. *Frontiers in Systems Neuroscience*, 10(104). <https://doi.org/10.3389/fnsys.2016.00104>
- Pezoulas, V. C., Zervakis, M., Michelogiannis, S., & Klados, M. A. (2017). Resting-state functional connectivity and network analysis of cerebellum with respect to crystallized IQ and gender. *Frontiers in Human Neuroscience*, 11, 189. <https://doi.org/10.3389/fnhum.2017.00189>
- Phillips, J. R., Hewedi, D. H., Eissa, A. M., & Moustafa, A. A. (2015). The Cerebellum and Psychiatric Disorders. *Frontiers in Public Health*, 3. <https://doi.org/10.3389/fpubh.2015.00066>
- Pickrell, J. K., Berisa, T., Liu, J. Z., Séguérel, L., Tung, J. Y., & Hinds, D. A. (2016). Detection and interpretation of shared genetic influences on 42 human traits. *Nature Genetics*, 48(7), 709–717. <https://doi.org/10.1038/ng.3570>
- Pillinger, T., Beck, K., Gobjila, C., Donocik, J. G., Jauhar, S., & Howes, O. D. (2017). Impaired glucose homeostasis in first-episode schizophrenia: A systematic review and meta-analysis. *JAMA Psychiatry*, 74(3), 261–269. <https://doi.org/10.1001/jamapsychiatry.2016.3803>
- Pinheiro, A. P., Schwartze, M., & Kotz, S. A. (2020). Cerebellar circuitry and auditory verbal hallucinations: An integrative synthesis and perspective. *Neuroscience and Biobehavioral Reviews*, 118, 485–503. <https://doi.org/10.1016/j.neubiorev.2020.08.004>
- Pisanu, C., & Squassina, A. (2019). Treatment-resistant schizophrenia: Insights from genetic studies and machine learning approaches. *Frontiers in Pharmacology*, 10, 617. <https://doi.org/10.3389/fphar.2019.00617>
- Pocklington, A. J., Rees, E., Walters, J. T. R., Han, J., Kavanagh, D. H., Chambert, K. D., ... Owen,

- M. J. (2015). Novel Findings from CNVs Implicate Inhibitory and Excitatory Signaling Complexes in Schizophrenia. *Neuron*, 86(5), 1203–1214. <https://doi.org/10.1016/j.neuron.2015.04.022>
- Powell, L. E., Barton, R. A., & Street, S. E. (2019). Maternal investment, life histories and the evolution of brain structure in primates. *Proceedings of the Royal Society B: Biological Sciences*, 286(1911), 20191608. <https://doi.org/10.1098/rspb.2019.1608>
- Prestori, F., Montagna, I., D'angelo, E., & Mapelli, L. (2020). The optogenetic revolution in cerebellar investigations. *International Journal of Molecular Sciences*, 21(7), 2494. <https://doi.org/10.3390/ijms21072494>
- Pugliese, V., Bruni, A., Carbone, E. A., Calabrò, G., Cerminara, G., Sampogna, G., ... De Fazio, P. (2019). Maternal stress, prenatal medical illnesses and obstetric complications: Risk factors for schizophrenia spectrum disorder, bipolar disorder and major depressive disorder. *Psychiatry Research*, 271, 23–30. <https://doi.org/10.1016/j.psychres.2018.11.023>
- Qi, T., Wu, Y., Zeng, J., Zhang, F., Xue, A., Jiang, L., ... Yang, J. (2018). Identifying gene targets for brain-related traits using transcriptomic and methylomic data from blood. *Nature Communications*, 9(1), 2282. <https://doi.org/10.1038/s41467-018-04558-1>
- Quinn, M., McHugo, M., Armstrong, K., Woodward, N., Blackford, J., & Heckers, S. (2018). Impact of substance use disorder on gray matter volume in schizophrenia. *Psychiatry Research - Neuroimaging*, 280, 9–14. <https://doi.org/10.1016/j.pscychresns.2018.08.002>
- Qureshi, A. Y., Mueller, S., Snyder, A. Z., Mukherjee, P., Berman, J. I., Roberts, T. P. L., ... Buckner, R. L. (2014). Opposing brain differences in 16p11.2 deletion and duplication carriers. *Journal of Neuroscience*, 34(34), 11199–11211. <https://doi.org/10.1523/JNEUROSCI.1366-14.2014>
- Rabellino, D., Densmore, M., Théberge, J., McKinnon, M. C., & Lanius, R. A. (2018). The cerebellum after trauma: Resting-state functional connectivity of the cerebellum in posttraumatic stress disorder and its dissociative subtype. *Human Brain Mapping*, 39(8), 3354–3374. <https://doi.org/10.1002/hbm.24081>
- Rabinowitz, J., Levine, S. Z., Garibaldi, G., Bugarski-Kirola, D., Berardo, C. G., & Kapur, S. (2012). Negative symptoms have greater impact on functioning than positive symptoms in schizophrenia: Analysis of CATIE data. *Schizophrenia Research*, 137(1–3), 147–150.

<https://doi.org/10.1016/j.schres.2012.01.015>

- Ramsay, I. S. (2019). An Activation Likelihood Estimate Meta-analysis of Thalamocortical Dysconnectivity in Psychosis. *Biological Psychiatry: Cognitive Neuroscience and Neuroimaging*, 4(10), 859–869. <https://doi.org/10.1016/j.bpsc.2019.04.007>
- Rasetti, R., & Weinberger, D. R. (2011). Intermediate phenotypes in psychiatric disorders. *Current Opinion in Genetics and Development*, 21(3), 340–348. <https://doi.org/10.1016/j.gde.2011.02.003>
- Reeb-Sutherland, B. C., & Fox, N. A. (2013). Eyeblink Conditioning: A Non-invasive Biomarker for Neurodevelopmental Disorders. *Journal of Autism and Developmental Disorders*, 45(2), 376–394. <https://doi.org/10.1007/s10803-013-1905-9>
- Rees, E., Han, J., Morgan, J., Carrera, N., Escott-Price, V., Pocklington, A. J., ... Owen, M. J. (2020). De novo mutations identified by exome sequencing implicate rare missense variants in SLC6A1 in schizophrenia. *Nature Neuroscience*, 23(2), 179–184. <https://doi.org/10.1038/s41593-019-0565-2>
- Rees, E., Kendall, K., Pardiñas, A. F., Legge, S. E., Pocklington, A., Escott-Price, V., ... Kirov, G. (2016). Analysis of intellectual disability copy number variants for association with schizophrenia. *JAMA Psychiatry*, 73(9), 963–969. <https://doi.org/10.1001/jamapsychiatry.2016.1831>
- Rees, E., Walters, J. T. R., Georgieva, L., Isles, A. R., Chambert, K. D., Richards, A. L., ... Kirov, G. (2014). Analysis of copy number variations at 15 schizophrenia-associated loci. *British Journal of Psychiatry*, 204(2), 108–114. <https://doi.org/10.1192/bjp.bp.113.131052>
- Reinwald, J. R., Sartorius, A., Weber-Fahr, W., Sack, M., Becker, R., Didriksen, M., ... Gass, N. (2020). Separable neural mechanisms for the pleiotropic association of copy number variants with neuropsychiatric traits. *Translational Psychiatry*, 10(1), 1–13. <https://doi.org/10.1038/s41398-020-0771-4>
- Reus, L. M., Shen, X., Gibson, J., Wigmore, E., Ligthart, L., Adams, M. J., ... McIntosh, A. M. (2017). Association of polygenic risk for major psychiatric illness with subcortical volumes and white matter integrity in UK Biobank. *Scientific Reports*, 7, 42140. <https://doi.org/10.1038/srep42140>

- Reuter, M., Tisdall, M. D., Qureshi, A., Buckner, R. L., van der Kouwe, A. J. W., & Fischl, B. (2015). Head motion during MRI acquisition reduces gray matter volume and thickness estimates. *NeuroImage*, *107*, 107–115. <https://doi.org/10.1016/j.neuroimage.2014.12.006>
- Riedel, M. C., Ray, K. L., Dick, A. S., Sutherland, M. T., Hernandez, Z., Fox, P. M., ... Laird, A. R. (2015). Meta-analytic connectivity and behavioral parcellation of the human cerebellum. *NeuroImage*, *117*, 327–342. <https://doi.org/10.1016/j.neuroimage.2015.05.008>
- Ripke, S., Neale, B. M., Corvin, A., Walters, J. T. R., Farh, K. H., Holmans, P. A., ... O'Donovan, M. C. (2014). Biological insights from 108 schizophrenia-associated genetic loci. *Nature*, *511*(7510), 421–427. <https://doi.org/10.1038/nature13595>
- Ripke, S., O'Dushlaine, C., Chambert, K., Moran, J. L., Kähler, A. K., Akterin, S., ... Sullivan, P. F. (2013). Genome-wide association analysis identifies 13 new risk loci for schizophrenia. *Nature Genetics*, *45*, 1150–1159. <https://doi.org/10.1038/ng.2742>
- Ripke, S., Walters, J. T., O'Donovan, M. C., & Consortium, S. W. G. of the P. G. (2020). Mapping genomic loci prioritises genes and implicates synaptic biology in schizophrenia. *MedRxiv*.
- Robertson, B. R., Prestia, D., Twamley, E. W., Patterson, T. L., Bowie, C. R., & Harvey, P. D. (2014). Social competence versus negative symptoms as predictors of real world social functioning in schizophrenia. *Schizophrenia Research*, *160*, 136–141. <https://doi.org/10.1016/j.schres.2014.10.037>
- Roelfs, D., Alnaes, D., Frei, O., van der Meer, D., Andreassen, O. A., Westlye, L. T., & Kaufmann, T. (2020). Phenotypically independent mental health symptom profiles are genetically related. *MedRxiv*. <https://doi.org/10.1101/2020.03.30.20045591>
- Roeske, M. J., Konradi, C., Heckers, S., & Lewis, A. S. (2020). Hippocampal volume and hippocampal neuron density, number and size in schizophrenia: a systematic review and meta-analysis of postmortem studies. *Molecular Psychiatry*, 1–12. <https://doi.org/10.1038/s41380-020-0853-y>
- Rogdaki, M., Gudbrandsen, M., McCutcheon, R. A., Blackmore, C. E., Brugger, S., Ecker, C., ... Howes, O. (2020). Magnitude and heterogeneity of brain structural abnormalities in 22q11.2 deletion syndrome: a meta-analysis. *Molecular Psychiatry*, *25*(8), 1704–1717. <https://doi.org/10.1038/s41380-019-0638-3>

- Romer, A. L., Knodt, A. R., Houts, R., Brigidi, B. D., Moffitt, T. E., Caspi, A., & Hariri, A. R. (2018). Structural alterations within cerebellar circuitry are associated with general liability for common mental disorders. *Molecular Psychiatry*, *23*(4), 1084–1090. <https://doi.org/10.1038/mp.2017.57>
- Romero, J. E., Coupé, P., Giraud, R., Ta, V. T., Fonov, V., Park, M. T. M., ... Manjón, J. V. (2017). CERES: A new cerebellum lobule segmentation method. *NeuroImage*, *147*, 916–924. <https://doi.org/10.1016/j.neuroimage.2016.11.003>
- Rutten-Jacobs, L. C. A., Tozer, D. J., Duering, M., Malik, R., Dichgans, M., Markus, H. S., & Traylor, M. (2018). Genetic study of white matter integrity in UK Biobank (N=8448) and the overlap with stroke, depression, and dementia. *Stroke*, *49*(6), 1340–1347. <https://doi.org/10.1161/STROKEAHA.118.020811>
- Sathyanesan, A., Kundu, S., Abbah, J., & Gallo, V. (2018). Neonatal brain injury causes cerebellar learning deficits and Purkinje cell dysfunction. *Nature Communications*, *9*(1). <https://doi.org/10.1038/s41467-018-05656-w>
- Sathyanesan, A., Zhou, J., Scafidi, J., Heck, D. H., Sillitoe, R. V., & Gallo, V. (2019). Emerging connections between cerebellar development, behaviour and complex brain disorders. *Nature Reviews Neuroscience*, *20*(5), 298–313. <https://doi.org/10.1038/s41583-019-0152-2>
- Satizabal, C. L., Adams, H. H. H., Hibar, D. P., White, C. C., Knol, M. J., Stein, J. L., ... Ikram, M. A. (2019). Genetic architecture of subcortical brain structures in 38,851 individuals. *Nature Genetics*, *51*(11), 1624–1636. <https://doi.org/10.1038/s41588-019-0511-y>
- Schmahmann, J. D. (2000). The role of the cerebellum in affect and psychosis. *Journal of Neurolinguistics*, *13*(2–3), 189–214. [https://doi.org/10.1016/S0911-6044\(00\)00011-7](https://doi.org/10.1016/S0911-6044(00)00011-7)
- Schmahmann, J. D. (2019, January 1). The cerebellum and cognition. *Neuroscience Letters*. <https://doi.org/10.1016/j.neulet.2018.07.005>
- Schmahmann, J. D., & Sherman, J. C. (1998). The cerebellar cognitive affective syndrome. *Brain*, *121*, 561–579. <https://doi.org/10.1093/brain/121.4.561>
- Schmahmann, J. D., Weilburg, J. B., & Sherman, J. C. (2007). The neuropsychiatry of the cerebellum - Insights from the clinic. *Cerebellum*, *6*(3), 254–267.

<https://doi.org/10.1080/14734220701490995>

Schmitt, A., Koschel, J., Zink, M., Bauer, M., Sommer, C., Frank, J., ... Henn, F. A. (2010). Gene expression of NMDA receptor subunits in the cerebellum of elderly patients with schizophrenia. *European Archives of Psychiatry and Clinical Neuroscience*, *260*(2), 101–111. <https://doi.org/10.1007/s00406-009-0017-1>

Schmitt, A., Malchow, B., Hasan, A., & Falkai, P. (2014). The impact of environmental factors in severe psychiatric disorders. *Frontiers in Neuroscience*, *8*, 19. <https://doi.org/10.3389/fnins.2014.00019>

Schmitt, A., Schulenberg, W., Bernstein, H. G., Steiner, J., Schneider-Axmann, T., Yeganeh-Doost, P., ... Falkai, P. (2011). Reduction of gyrification index in the cerebellar vermis in schizophrenia: A post-mortem study. *World Journal of Biological Psychiatry*, *12*, 99–103. <https://doi.org/10.3109/15622975.2010.512090>

Schneider, M., Debbané, M., Bassett, A. S., Chow, E. W. C., Fung, W. L. A., Van Den Bree, M. B. M., ... Eliez, S. (2014). Psychiatric disorders from childhood to adulthood in 22q11.2 deletion syndrome: Results from the international consortium on brain and behavior in 22q11.2 deletion syndrome. *American Journal of Psychiatry*, *171*(6), 627–639. <https://doi.org/10.1176/appi.ajp.2013.13070864>

Scott, K. M., Lim, C., Al-Hamzawi, A., Alonso, J., Bruffaerts, R., Caldas-De-Almeida, J. M., ... Kessler, R. C. (2016). Association of mental disorders with subsequent chronic physical conditions: World mental health surveys from 17 countries. *JAMA Psychiatry*, *73*(2), 150–158. <https://doi.org/10.1001/jamapsychiatry.2015.2688>

Sekar, A., Bialas, A. R., De Rivera, H., Davis, A., Hammond, T. R., Kamitaki, N., ... McCarroll, S. A. (2016). Schizophrenia risk from complex variation of complement component 4. *Nature*, *530*(7589), 177–183. <https://doi.org/10.1038/nature16549>

Selemon, L. D., & Zecevic, N. (2015). Schizophrenia: A tale of two critical periods for prefrontal cortical development. *Translational Psychiatry*, *5*(8), e623. <https://doi.org/10.1038/tp.2015.115>

Sellgren, C. M., Gracias, J., Watmuff, B., Biag, J. D., Thanos, J. M., Whittredge, P. B., ... Perlis, R. H. (2019). Increased synapse elimination by microglia in schizophrenia patient-derived models of synaptic pruning. *Nature Neuroscience*, *22*(3), 374–385.

<https://doi.org/10.1038/s41593-018-0334-7>

Selzam, S., Coleman, J. R. I., Caspi, A., Moffitt, T. E., & Plomin, R. (2018). A polygenic p factor for major psychiatric disorders. *Translational Psychiatry*, 8(1), 205. <https://doi.org/10.1038/s41398-018-0217-4>

Sereno, M. I., Diedrichsen, J. rn, Tachrount, M., Testa-Silva, G., D Arceuil, H., & De Zeeuw, C. (2020). The human cerebellum has almost 80% of the surface area of the neocortex. *Proceedings of the National Academy of Sciences of the United States of America*, 117(32), 19538–19543. <https://doi.org/10.1073/pnas.2002896117>

Shah, P., Iwata, Y., Plitman, E., Brown, E. E., Caravaggio, F., Kim, J., ... Graff-Guerrero, A. (2018, October 1). The impact of delay in clozapine initiation on treatment outcomes in patients with treatment-resistant schizophrenia: A systematic review. *Psychiatry Research*. Elsevier Ireland Ltd. <https://doi.org/10.1016/j.psychres.2018.06.070>

Sharma, A., Kumar, A., Singh, S., Bhatia, T., Beniwal, R. P., Khushu, S., ... Deshpande, S. N. (2018). Altered resting state functional connectivity in early course schizophrenia. *Psychiatry Research - Neuroimaging*, 271, 17–23. <https://doi.org/10.1016/j.pscychresns.2017.11.013>

Shenton, M. E., Whitford, T. J., & Kubicki, M. (2010). Structural neuroimaging in schizophrenia: from methods to insights to treatments. *Dialogues in Clinical Neuroscience*, 12(3), 317–332. Retrieved from <http://www.ncbi.nlm.nih.gov/pubmed/20954428>

Shinn, A. K., Baker, J. T., Lewandowski, K. E., Öngür, D., & Cohen, B. M. (2015). Aberrant cerebellar connectivity in motor and association networks in schizophrenia. *Frontiers in Human Neuroscience*, 9, 134. <https://doi.org/10.3389/fnhum.2015.00134>

Siegel, J. S., Mitra, A., Laumann, T. O., Seitzman, B. A., Raichle, M., Corbetta, M., & Snyder, A. Z. (2017). Data quality influences observed links between functional connectivity and behavior. *Cerebral Cortex*, 27(9), 4492–4502. <https://doi.org/10.1093/cercor/bhw253>

Silverstein, S. M., Fradkin, S. I., & Demmin, D. L. (2020). Schizophrenia and the retina: Towards a 2020 perspective. *Schizophrenia Research*, 219, 84–94. <https://doi.org/10.1016/j.schres.2019.09.016>

Simoila, L., Isometsä, E., Gissler, M., Suvisaari, J., Halmesmäki, E., & Lindberg, N. (2018). Obstetric and perinatal health outcomes related to schizophrenia: A national register-based follow-

up study among Finnish women born between 1965 and 1980 and their offspring. *European Psychiatry*, 52, 68–75. <https://doi.org/10.1016/j.eurpsy.2018.04.001>

Singh, T., Kurki, M. I., Curtis, D., Purcell, S. M., Crooks, L., McRae, J., ... Barrett, J. C. (2016). Rare loss-of-function variants in SETD1A are associated with schizophrenia and developmental disorders. *Nature Neuroscience*, 19(4), 571–577. <https://doi.org/10.1038/nn.4267>

Singh, T., Neale, B. M., Daly, M. J., & Consortium, S. E. M.-A. (SCHEMA). (2020). Exome sequencing identifies rare coding variants in 10 genes which confer substantial risk for schizophrenia. *MedRxiv*.

Singh, T., Walters, J. T. R., Johnstone, M., Curtis, D., Suvisaari, J., Torniainen, M., ... Barrett, J. C. (2017). The contribution of rare variants to risk of schizophrenia in individuals with and without intellectual disability. *Nature Genetics*, 49(8), 1167–1173. <https://doi.org/10.1038/ng.3903>

Smaers, J. B., & Vanier, D. R. (2019). Brain size expansion in primates and humans is explained by a selective modular expansion of the cortico-cerebellar system. *Cortex*, 118, 292–305. <https://doi.org/10.1016/j.cortex.2019.04.023>

Smeland, O. B., Frei, O., Dale, A. M., & Andreassen, O. A. (2020). The polygenic architecture of schizophrenia — rethinking pathogenesis and nosology. *Nature Reviews Neurology*, 16, 366–379. <https://doi.org/10.1038/s41582-020-0364-0>

Smeland, O. B., Frei, O., Shadrin, A., O’Connell, K., Fan, C. C., Bahrami, S., ... Andreassen, O. A. (2020). Discovery of shared genomic loci using the conditional false discovery rate approach. *Human Genetics*, 139(1), 85–94. <https://doi.org/10.1007/s00439-019-02060-2>

Smeland, O. B., Wang, Y., Frei, O., Li, W., Hibar, D. P., Franke, B., ... Andreassen, O. A. (2018). Genetic Overlap between Schizophrenia and Volumes of Hippocampus, Putamen, and Intracranial Volume Indicates Shared Molecular Genetic Mechanisms. *Schizophrenia Bulletin*, 44(4), 854–864. <https://doi.org/10.1093/schbul/sbx148>

Smith, S. M., Douaud, G., Chen, W., Hanayik, T., Alfaro-Almagro, F., Sharp, K., & Elliott, L. T. (2020). Enhanced Brain Imaging Genetics in UK Biobank. *BioRxiv*.

Smoller, J. W., Andreassen, O. A., Edenberg, H. J., Faraone, S. V., Glatt, S. J., & Kendler, K. S. (2019). Psychiatric genetics and the structure of psychopathology. *Molecular Psychiatry*,

24(3), 409–420. <https://doi.org/10.1038/s41380-017-0010-4>

- Sokolov, A. A., Erb, M., Grodd, W., & Pavlova, M. A. (2014). Structural loop between the cerebellum and the superior temporal sulcus: Evidence from diffusion tensor imaging. *Cerebral Cortex*, 24(3), 626–632. <https://doi.org/10.1093/cercor/bhs346>
- Song, J., Bergen, S. E., Kuja-Halkola, R., Larsson, H., Landén, M., & Lichtenstein, P. (2015). Bipolar disorder and its relation to major psychiatric disorders: A family-based study in the Swedish population. *Bipolar Disorders*, 17(2), 184–193. <https://doi.org/10.1111/bdi.12242>
- Spain, S. L., & Barrett, J. C. (2015). Strategies for fine-mapping complex traits. *Human Molecular Genetics*, 24, 111–119. <https://doi.org/10.1093/hmg/ddv260>
- Spalthoff, R., Degenhardt, F., Awasthi, S., Heilmann-Heimbach, S., Besteher, B., Gaser, C., ... Nenadić, I. (2019). Effects of a neurodevelopmental genes based polygenic risk score for schizophrenia and single gene variants on brain structure in non-clinical subjects: A preliminary report. *Schizophrenia Research*, 212, 225–228. <https://doi.org/10.1016/j.schres.2019.07.061>
- Spalthoff, R., Gaser, C., & Nenadić, I. (2018). Altered gyrification in schizophrenia and its relation to other morphometric markers. *Schizophrenia Research*, 202, 195–202. <https://doi.org/10.1016/j.schres.2018.07.014>
- Srivastava, A. K., Takkar, A., Garg, A., & Faruq, M. (2017). Clinical behaviour of spinocerebellar ataxia type 12 and intermediate length abnormal CAG repeats in PPP2R2B. *Brain*, 140(1), 27–36. <https://doi.org/10.1093/brain/aww269>
- Stahl, E. A., Breen, G., Forstner, A. J., McQuillin, A., Ripke, S., Trubetskoy, V., ... Sklar, P. (2019). Genome-wide association study identifies 30 loci associated with bipolar disorder. *Nature Genetics*, 51(5), 793–803. <https://doi.org/10.1038/s41588-019-0397-8>
- Stankiewicz, P., & Lupski, J. R. (2010). Structural variation in the human genome and its role in disease. *Annual Review of Medicine*, 61, 437–455. <https://doi.org/10.1146/annurev-med-100708-204735>
- Stoodley, C. J. (2016). The Cerebellum and Neurodevelopmental Disorders. *Cerebellum*, 15(1), 34–37. <https://doi.org/10.1007/s12311-015-0715-3>
- Stoodley, C. J., Valera, E. M., & Schmahmann, J. D. (2012). Functional topography of the

cerebellum for motor and cognitive tasks: An fMRI study. *NeuroImage*, 59(2), 1560–1570.
<https://doi.org/10.1016/j.neuroimage.2011.08.065>

Strick, P. L., Dum, R. P., & Fiez, J. A. (2009). Cerebellum and nonmotor function. *Annual Review of Neuroscience*, 32, 413–434. <https://doi.org/10.1146/annurev.neuro.31.060407.125606>

Sudlow, C., Gallacher, J., Allen, N., Beral, V., Burton, P., Danesh, J., ... Collins, R. (2015). UK Biobank: An Open Access Resource for Identifying the Causes of a Wide Range of Complex Diseases of Middle and Old Age. *PLoS Medicine*, 12(3), e1001779.
<https://doi.org/10.1371/journal.pmed.1001779>

Sullivan, P. F., Kendler, K. S., & Neale, M. C. (2003). Schizophrenia as a Complex Trait: Evidence from a Meta-analysis of Twin Studies. *Archives of General Psychiatry*, 60(12), 1187–1192.
<https://doi.org/10.1001/archpsyc.60.12.1187>

Sullivan, E. V., Brumback, T., Tapert, S. F., Brown, S. A., Baker, F. C., Colrain, I. M., ... Pfefferbaum, A. (2020). Disturbed Cerebellar Growth Trajectories in Adolescents Who Initiate Alcohol Drinking. *Biological Psychiatry*, 87(7), 632–644.
<https://doi.org/10.1016/j.biopsych.2019.08.026>

Sydnor, V. J., & Roalf, D. R. (2020). A meta-analysis of ultra-high field glutamate, glutamine, GABA and glutathione 1HMRS in psychosis: Implications for studies of psychosis risk. *Schizophrenia Research*. <https://doi.org/10.1016/j.schres.2020.06.028>

Takahashi, T., Takayanagi, Y., Nishikawa, Y., Nakamura, M., Komori, Y., Furuichi, A., ... Suzuki, M. (2017). Brain neurodevelopmental markers related to the deficit subtype of schizophrenia. *Psychiatry Research - Neuroimaging*, 266, 10–18.
<https://doi.org/10.1016/j.pscychresns.2017.05.007>

Tansey, K. E., Rees, E., Linden, D. E., Ripke, S., Chambert, K. D., Moran, J. L., ... O'Donovan, M. C. (2016). Common alleles contribute to schizophrenia in CNV carriers. *Molecular Psychiatry*, 21(8), 1085–1089. <https://doi.org/10.1038/mp.2015.143>

Tarcijonas, G., Foran, W., Haas, G. L., Luna, B., & Sarpal, D. K. (2020). Intrinsic Connectivity of the Globus Pallidus: An Uncharted Marker of Functional Prognosis in People with First-Episode Schizophrenia. *Schizophrenia Bulletin*, 46(1), 184–192.
<https://doi.org/10.1093/schbul/sbz034>

- Tavano, A., Grasso, R., Gagliardi, C., Triulzi, F., Bresolin, N., Fabbro, F., & Borgatti, R. (2007). Disorders of cognitive and affective development in cerebellar malformations. *Brain*, *130*(10), 2646–2660. <https://doi.org/10.1093/brain/awm201>
- Terwisscha Van Scheltinga, A. F., Bakker, S. C., Van Haren, N. E. M., Derks, E. M., Buizer-Voskamp, J. E., Boos, H. B. M., ... Gejman, P. V. (2013). Genetic schizophrenia risk variants jointly modulate total brain and white matter volume. *Biological Psychiatry*, *73*(6), 525–531. <https://doi.org/10.1016/j.biopsych.2012.08.017>
- Theocharis, A. D. (2008). Versican in health and disease. *Connective Tissue Research*, *49*(3), 230–234. <https://doi.org/10.1080/03008200802147571>
- Thompson, P. M., Jahanshad, N., Ching, C. R. K., Salminen, L. E., Thomopoulos, S. I., Bright, J., ... Zelman, V. (2020). ENIGMA and global neuroscience: A decade of large-scale studies of the brain in health and disease across more than 40 countries. *Translational Psychiatry*, *10*(1), 1–28. <https://doi.org/10.1038/s41398-020-0705-1>
- Thorup, A., Albert, N., Bertelsen, M., Petersen, L., Jeppesen, P., Le Quack, P., ... Nordentoft, M. (2014). Gender differences in first-episode psychosis at 5-year follow-up—two different courses of disease? Results from the OPUS study at 5-year follow-up. *European Psychiatry*, *29*(1), 44–51. <https://doi.org/10.1016/j.eurpsy.2012.11.005>
- Tian, Y., Wang, D., Wei, G., Wang, J., Zhou, H., Xu, H., ... Zhang, X. Y. (2020). Prevalence of obesity and clinical and metabolic correlates in first-episode schizophrenia relative to healthy controls. *Psychopharmacology*, 1–9. <https://doi.org/10.1007/s00213-020-05727-1>
- Toulopoulou, T., Van Haren, N., Zhang, X., Sham, P. C., Cherny, S. S., Campbell, D. D., ... Kahn, R. S. (2015). Reciprocal causation models of cognitive vs volumetric cerebral intermediate phenotypes for schizophrenia in a pan-European twin cohort. *Molecular Psychiatry*, *20*, 1386–1396. <https://doi.org/10.1038/mp.2014.152>
- Tran, L., Huening, B. M., Kaiser, O., Schweiger, B., Sirin, S., Quick, H. H., ... Timmann, D. (2017). Cerebellar-dependent associative learning is impaired in very preterm born children and young adults. *Scientific Reports*, *7*(1), 1–15. <https://doi.org/10.1038/s41598-017-18316-8>
- Underwood, J. F. G., Kendall, K. M., Berrett, J., Lewis, C., Anney, R., Van Den Bree, M. B. M., & Hall, J. (2019). Autism spectrum disorder diagnosis in adults: Phenotype and genotype findings from a clinically derived cohort. *British Journal of Psychiatry*, *215*(5), 647–653.

<https://doi.org/10.1192/bjp.2019.30>

Ursini, G., Punzi, G., Chen, Q., Marengo, S., Robinson, J. F., Porcelli, A., ... Weinberger, D. R. (2018). Convergence of placenta biology and genetic risk for schizophrenia article. *Nature Medicine*, 24(6), 792–801. <https://doi.org/10.1038/s41591-018-0021-y>

Van Den Heuvel, M. P., Scholtens, L. H., De Lange, S. C., Pijenburg, R., Cahn, W., Van Haren, N. E. M., ... Rilling, J. K. (2019). Evolutionary modifications in human brain connectivity associated with schizophrenia. *Brain*, 142(12), 3991–4002. <https://doi.org/10.1093/brain/awz330>

Van der Auwera, S., Wittfeld, K., Homuth, G., Teumer, A., Hegenscheid, K., & Grabe, H. J. (2015). No Association Between Polygenic Risk for Schizophrenia and Brain Volume in the General Population. *Biological Psychiatry*, 78(11), e41–e42. <https://doi.org/10.1016/j.biopsych.2015.02.038>

van der Meer, D., Rokicki, J., Kaufmann, T., Córdova-Palomera, A., Moberget, T., Alnæs, D., ... Westlye, L. T. (2018). Brain scans from 21,297 individuals reveal the genetic architecture of hippocampal subfield volumes. *Molecular Psychiatry*. <https://doi.org/10.1038/s41380-018-0262-7>

Van Der Meer, D., Sønderby, I. E., Kaufmann, T., Walters, G. B., Abdellaoui, A., Ames, D., ... Andreassen, O. A. (2020). Association of Copy Number Variation of the 15q11.2 BP1-BP2 Region with Cortical and Subcortical Morphology and Cognition. *JAMA Psychiatry*, 77(4), 420–430. <https://doi.org/10.1001/jamapsychiatry.2019.3779>

van der Merwe, C., Passchier, R., Mufford, M., Ramesar, R., Dalvie, S., & Stein, D. J. (2019, January 1). Polygenic risk for schizophrenia and associated brain structural changes: A systematic review. *Comprehensive Psychiatry*. W.B. Saunders. <https://doi.org/10.1016/j.comppsy.2018.11.014>

Van Erp, T. G.M., Hibar, D. P., Rasmussen, J. M., Glahn, D. C., Pearlson, G. D., Andreassen, O. A., ... Turner, J. A. (2016). Subcortical brain volume abnormalities in 2028 individuals with schizophrenia and 2540 healthy controls via the ENIGMA consortium. *Molecular Psychiatry*, 21(4), 547–553. <https://doi.org/10.1038/mp.2015.63>

van Erp, Theo G.M., Walton, E., Hibar, D. P., Schmaal, L., Jiang, W., Glahn, D. C., ... Turner, J. A. (2018). Cortical Brain Abnormalities in 4474 Individuals With Schizophrenia and 5098

- Control Subjects via the Enhancing Neuro Imaging Genetics Through Meta Analysis (ENIGMA) Consortium. *Biological Psychiatry*, 84(9), 644–654. <https://doi.org/10.1016/j.biopsych.2018.04.023>
- Van Haren, N. E. M., Rijdsdijk, F., Schnack, H. G., Picchioni, M. M., Toulopoulou, T., Weisbrod, M., ... Kahn, R. S. (2012). The genetic and environmental determinants of the association between brain abnormalities and schizophrenia: The schizophrenia twins and relatives consortium. *Biological Psychiatry*, 71(10), 915–921. <https://doi.org/10.1016/j.biopsych.2012.01.010>
- Van Leeuwen, J. M. C., Vink, M., Fernández, G., Hermans, E. J., Joëls, M., Kahn, R. S., & Vinkers, C. H. (2018). At-risk individuals display altered brain activity following stress. *Neuropsychopharmacology*, 43(9), 1954–1960. <https://doi.org/10.1038/s41386-018-0026-8>
- Van Overwalle, F., Ma, Q., & Heleven, E. (2020). The posterior crus II cerebellum is specialized for social mentalizing and emotional self-experiences: a meta-analysis. *Social Cognitive and Affective Neuroscience*, 15(9), 905–928. <https://doi.org/10.1093/scan/nsaa124>
- van Rheenen, W., Peyrot, W. J., Schork, A. J., Lee, S. H., & Wray, N. R. (2019, October 1). Genetic correlations of polygenic disease traits: from theory to practice. *Nature Reviews Genetics*. Nature Publishing Group. <https://doi.org/10.1038/s41576-019-0137-z>
- Vancampfort, D., Wampers, M., Mitchell, A. J., Correll, C. U., De Herdt, A., Probst, M., & De Hert, M. (2013). A meta-analysis of cardio-metabolic abnormalities in drug naïve, first-episode and multi-episode patients with schizophrenia versus general population controls. *World Psychiatry*, 12(3), 240–250. <https://doi.org/10.1002/wps.20069>
- Varambally, S., Venkatasubramanian, G., Thirthalli, J., Janakiramaiah, N., & Gangadhar, B. N. (2006). Cerebellar and other neurological soft signs in antipsychotic-naïve schizophrenia. *Acta Psychiatrica Scandinavica*, 114(5), 352–356. <https://doi.org/10.1111/j.1600-0447.2006.00837.x>
- Vassos, E., Di Forti, M., Coleman, J., Iyegbe, C., Prata, D., Euesden, J., ... Breen, G. (2017). An Examination of Polygenic Score Risk Prediction in Individuals With First-Episode Psychosis. *Biological Psychiatry*, 81(6), 470–477. <https://doi.org/10.1016/j.biopsych.2016.06.028>
- Veijola, J., Guo, J. Y., Moilanen, J. S., Jääskeläinen, E., Miettunen, J., Kyllönen, M., ... Murray, G.

- K. (2014). Longitudinal changes in total brain volume in schizophrenia: Relation to symptom severity, cognition and antipsychotic medication. *PLoS ONE*, *9*(7), e101689. <https://doi.org/10.1371/journal.pone.0101689>
- Vidal-Domènech, F., Riquelme, G., Pinacho, R., Rodriguez-Mias, R., Vera, A., Monje, A., ... Ramos, B. (2020). Calcium-binding proteins are altered in the cerebellum in schizophrenia. *PLoS ONE*, *15*(7), e0230400. <https://doi.org/10.1371/journal.pone.0230400>
- Visscher, P. M., Hill, W. G., & Wray, N. R. (2008). Heritability in the genomics era - Concepts and misconceptions. *Nature Reviews Genetics*, *9*(4), 255–266. <https://doi.org/10.1038/nrg2322>
- Visscher, P. M., Wray, N. R., Zhang, Q., Sklar, P., McCarthy, M. I., Brown, M. A., & Yang, J. (2017). 10 Years of GWAS Discovery: Biology, Function, and Translation. *American Journal of Human Genetics*, *101*(1), 5–22. <https://doi.org/10.1016/j.ajhg.2017.06.005>
- Vita, A., Minelli, A., Barlati, S., Deste, G., Giacomuzzi, E., Valsecchi, P., ... Gennarelli, M. (2019). Treatment-resistant schizophrenia: Genetic and neuroimaging correlates. *Frontiers in Pharmacology*, *10*, 402. <https://doi.org/10.3389/fphar.2019.00402>
- Voineskos, A. N., Felsky, D., Wheeler, A. L., Rotenberg, D. J., Levesque, M., Patel, S., ... Malhotra, A. K. (2016). Limited evidence for association of genome-wide schizophrenia risk variants on cortical neuroimaging phenotypes. *Schizophrenia Bulletin*, *42*(4), 1027–1036. <https://doi.org/10.1093/schbul/sbv180>
- Volpe, J. J. (2009, September 10). Cerebellum of the premature infant: Rapidly developing, vulnerable, clinically important. *Journal of Child Neurology*. <https://doi.org/10.1177/0883073809338067>
- Wahlberg, K. E., Guazzetti, S., Pineda, D., Larsson, S. C., Fedrighi, C., Cagna, G., ... Broberg, K. (2018). Polymorphisms in Manganese Transporters SLC30A10 and SLC39A8 Are Associated With Children’s Neurodevelopment by Influencing Manganese Homeostasis. *Frontiers in Genetics*, *9*, 664. <https://doi.org/10.3389/fgene.2018.00664>
- Walther, S., Stegmayer, K., Federspiel, A., Bohlhalter, S., Wiest, R., & Viher, P. V. (2017). Aberrant hyperconnectivity in the motor system at rest is linked to motor abnormalities in schizophrenia spectrum disorders. *Schizophrenia Bulletin*, *43*(5), 982–992. <https://doi.org/10.1093/schbul/sbx091>

- Walton, E., Hibar, D. P., Van Erp, T. G. M., Potkin, S. G., Roiz-Santiañez, R., Crespo-Facorro, B., ... Ehrlich, S. (2018). Prefrontal cortical thinning links to negative symptoms in schizophrenia via the ENIGMA consortium. *Psychological Medicine*, *48*(1), 82–94. <https://doi.org/10.1017/S0033291717001283>
- Wang, Houliang, Guo, W., Liu, F., Wang, G., Lyu, H., Wu, R., ... Zhao, J. (2016). Patients with first-episode, drug-naïve schizophrenia and subjects at ultra-high risk of psychosis shared increased cerebellar-default mode network connectivity at rest. *Scientific Reports*, *6*(1), 1–8. <https://doi.org/10.1038/srep26124>
- Wang, Huaning, Zeng, L. L., Chen, Y., Yin, H., Tan, Q., & Hu, D. (2015). Evidence of a dissociation pattern in default mode subnetwork functional connectivity in schizophrenia. *Scientific Reports*, *5*(1), 1–10. <https://doi.org/10.1038/srep14655>
- Wang, J., Lou, S. Sen, Wang, T., Wu, R. J., Li, G., Zhao, M., ... Xiong, Z. Q. (2019). UBE3A-mediated PTPA ubiquitination and degradation regulate PP2A activity and dendritic spine morphology. *Proceedings of the National Academy of Sciences of the United States of America*, *116*(25), 12500–12505. <https://doi.org/10.1073/pnas.1820131116>
- Wang, K., Li, M., Hadley, D., Liu, R., Glessner, J., Grant, S. F. A., ... Bucan, M. (2007). PennCNV: An integrated hidden Markov model designed for high-resolution copy number variation detection in whole-genome SNP genotyping data. *Genome Research*, *17*(11), 1665–1674. <https://doi.org/10.1101/gr.6861907>
- Wang, X., Herold, C. J., Kong, L., & Schroeder, J. (2019). Associations between brain structural networks and neurological soft signs in healthy adults. *Psychiatry Research - Neuroimaging*, *293*, 110989. <https://doi.org/10.1016/j.psychresns.2019.110989>
- Warland, A., Kendall, K. M., Rees, E., Kirov, G., & Caseras, X. (2020). Schizophrenia-associated genomic copy number variants and subcortical brain volumes in the UK Biobank. *Molecular Psychiatry*, *25*(4), 854–862. <https://doi.org/10.1038/s41380-019-0355-y>
- Watanabe, K., Taskesen, E., Van Bochoven, A., & Posthuma, D. (2017). Functional mapping and annotation of genetic associations with FUMA. *Nature Communications*, *8*(1). <https://doi.org/10.1038/s41467-017-01261-5>
- Westlye, L. T., Alnæs, D., van der Meer, D., Kaufmann, T., & Andreassen, O. A. (2019, October 1). Population-Based Mapping of Polygenic Risk for Schizophrenia on the Human Brain:

New Opportunities to Capture the Dimensional Aspects of Severe Mental Disorders. *Biological Psychiatry*. Elsevier USA. <https://doi.org/10.1016/j.biopsych.2019.08.001>

Willer, C. J., Li, Y., & Abecasis, G. R. (2010). METAL: Fast and efficient meta-analysis of genomewide association scans. *Bioinformatics*, 26(17), 2190–2191. <https://doi.org/10.1093/bioinformatics/btq340>

Wing, J. K., Babor, T., Brugha, T., Burke, J., Cooper, J. E., Giel, R., ... Sartorius, N. (1990). Schedules for clinical assessment in neuropsychiatry. *Archives of General Psychiatry*. <https://doi.org/10.1136/bmj.c7160>

Winkler, A. M., Kochunov, P., Blangero, J., Almasy, L., Zilles, K., Fox, P. T., ... Glahn, D. C. (2010). Cortical thickness or grey matter volume? The importance of selecting the phenotype for imaging genetics studies. *NeuroImage*, 53(3), 1135–1146. <https://doi.org/10.1016/j.neuroimage.2009.12.028>

Witter, L., & De Zeeuw, C. I. (2015). Regional functionality of the cerebellum. *Current Opinion in Neurobiology*, 33, 150–155. <https://doi.org/10.1016/j.conb.2015.03.017>

Wolfers, T., Doan, N. T., Kaufmann, T., Alnæs, D., Moberget, T., Agartz, I., ... Marquand, A. F. (2018). Mapping the Heterogeneous Phenotype of Schizophrenia and Bipolar Disorder Using Normative Models. *JAMA Psychiatry*, 75(11), 1146–1155. <https://doi.org/10.1001/jamapsychiatry.2018.2467>

Wollman, S. C., Alhassoon, O. M., Hall, M. G., Stern, M. J., Connors, E. J., Kimmel, C. L., ... Radua, J. (2017, September 3). Gray matter abnormalities in opioid-dependent patients: A neuroimaging meta-analysis. *American Journal of Drug and Alcohol Abuse*. Taylor and Francis Ltd. <https://doi.org/10.1080/00952990.2016.1245312>

Womer, F. Y., Tang, Y., Harms, M. P., Bai, C., Chang, M., Jiang, X., ... Barch, D. M. (2016). Sexual dimorphism of the cerebellar vermis in schizophrenia. *Schizophrenia Research*, 176(2), 164–170. <https://doi.org/10.1016/j.schres.2016.06.028>

Wong, H. S., Wadon, M., Evans, A., Kirov, G., Modi, N., O'Donovan, M. C., & Thapar, A. (2020). Contribution of de novo and inherited rare CNVs to very preterm birth. *Journal of Medical Genetics*, 57, 552–557. <https://doi.org/10.1136/jmedgenet-2019-106619>

Woodward, N. D., & Heckers, S. (2016). Mapping Thalamocortical Functional Connectivity in

- Chronic and Early Stages of Psychotic Disorders. *Biological Psychiatry*, 79(12), 1016–1025.
<https://doi.org/10.1016/j.biopsych.2015.06.026>
- Wray, N. R., Lee, S. H., Mehta, D., Vinkhuyzen, A. A. E., Dudbridge, F., & Middeldorp, C. M. (2014, October). Research Review: Polygenic methods and their application to psychiatric traits. *Journal of Child Psychology and Psychiatry and Allied Disciplines*.
<https://doi.org/10.1111/jcpp.12295>
- Wray, N. R., Ripke, S., Mattheisen, M., Trzaskowski, M., Byrne, E. M., Abdellaoui, A., ... Sullivan, P. F. (2018). Genome-wide association analyses identify 44 risk variants and refine the genetic architecture of major depression. *Nature Genetics*, 50(5), 668–681.
<https://doi.org/10.1038/s41588-018-0090-3>
- Wu, Y., Cao, H., Baranova, A., Huang, H., Li, S., Cai, L., ... Zhang, F. (2020). Multi-trait analysis for genome-wide association study of five psychiatric disorders. *Translational Psychiatry*, 10(1), 1–11. <https://doi.org/10.1038/s41398-020-00902-6>
- Xi, C., Liu, Z. ning, Yang, J., Zhang, W., Deng, M. jie, Pan, Y. zhi, ... Pu, W. dan. (2020). Schizophrenia patients and their healthy siblings share decreased prefronto-thalamic connectivity but not increased sensorimotor-thalamic connectivity. *Schizophrenia Research*. <https://doi.org/10.1016/j.schres.2020.04.033>
- Xia, K., Zhang, J., Ahn, M., Jha, S., Crowley, J. J., Szatkiewicz, J., ... Knickmeyer, R. C. (2017). Genome-wide association analysis identifies common variants influencing infant brain volumes. *Translational Psychiatry*, 7(8), e1188. <https://doi.org/10.1038/tp.2017.159>
- Xu, F., Ge, X., Shi, Y., Zhang, Z., Tang, Y., Lin, X., ... Liu, S. (2020). Morphometric development of the human fetal cerebellum during the early second trimester. *NeuroImage*, 207, 116372.
<https://doi.org/10.1016/j.neuroimage.2019.116372>
- Yang, J., Benyamin, B., McEvoy, B. P., Gordon, S., Henders, A. K., Nyholt, D. R., ... Visscher, P. M. (2010). Common SNPs explain a large proportion of the heritability for human height. *Nature Genetics*, 42(7), 565–569. <https://doi.org/10.1038/ng.608>
- Yang, J., Ferreira, T., Morris, A. P., Medland, S. E., Madden, P. A. F., Heath, A. C., ... Visscher, P. M. (2012). Conditional and joint multiple-SNP analysis of GWAS summary statistics identifies additional variants influencing complex traits. *Nature Genetics*, 44(4), 369–375.
<https://doi.org/10.1038/ng.2213>

- Yang, J., Lee, S. H., Goddard, M. E., & Visscher, P. M. (2011). GCTA: A tool for genome-wide complex trait analysis. *American Journal of Human Genetics*, *88*(1), 76–82. <https://doi.org/10.1016/j.ajhg.2010.11.011>
- Yang, Z., Wu, H., Lee, P. H., Tsetsos, F., Davis, L. K., Yu, D., ... Paschou, P. (2019, September 16). Cross-disorder GWAS meta-analysis for Attention Deficit/Hyperactivity Disorder, Autism Spectrum Disorder, Obsessive Compulsive Disorder, and Tourette Syndrome. *BioRxiv*. bioRxiv. <https://doi.org/10.1101/770222>
- Yao, N., Winkler, A. M., Barrett, J., Book, G. A., Beetham, T., Horseman, R., ... Glahn, D. C. (2017). Inferring pathobiology from structural MRI in schizophrenia and bipolar disorder: Modeling head motion and neuroanatomical specificity. *Human Brain Mapping*, *38*(8), 3757–3770. <https://doi.org/10.1002/hbm.23612>
- Yaple, Z. A., & Yu, R. (2020). Functional and Structural Brain Correlates of Socioeconomic Status. *Cerebral Cortex*, *30*(1), 181–196. <https://doi.org/10.1093/cercor/bhz080>
- Yeganeh-Doost, P., Gruber, O., Falkai, P., & Schmitt, A. (2011). The role of the cerebellum in schizophrenia: From cognition to molecular pathways. *Clinics*, *66*(SUPPL.1), 71–77. <https://doi.org/10.1590/S1807-59322011001300009>
- Yengo, L., Yang, J., & Visscher, P. M. (2018). Expectation of the intercept from bivariate LD score regression in the presence of population stratification. *BioRxiv*, 310565. <https://doi.org/10.1101/310565>
- Yue, Y., Kong, L., Wang, J., Li, C., Tan, L., Su, H., & Xu, Y. (2016). Regional abnormality of grey matter in schizophrenia: Effect from the illness or treatment? *PLoS ONE*, *11*(1), e0147204. <https://doi.org/10.1371/journal.pone.0147204>
- Zeidler, Z., Hoffmann, K., & Krook-Magnuson, E. (2020). HippoBellum: acute cerebellar modulation alters hippocampal dynamics and function. *The Journal of Neuroscience*. <https://doi.org/10.1523/JNEUROSCI.0763-20.2020>
- Zhang, C., Wang, Q., Ni, P., Deng, W., Li, Y., Zhao, L., ... Li, T. (2017). Differential Cortical Gray Matter Deficits in Adolescent- and Adult-Onset First-Episode Treatment-Naïve Patients with Schizophrenia. *Scientific Reports*, *7*(1), 10267. <https://doi.org/10.1038/s41598-017-10688-1>

- Zhang, Y., Brady, M., & Smith, S. (2001). Segmentation of brain MR images through a hidden Markov random field model and the expectation-maximization algorithm. *IEEE Transactions on Medical Imaging*, *20*(1), 45–57. <https://doi.org/10.1109/42.906424>
- Zhao, B., Luo, T., Li, T., Li, Y., Zhang, J., Shan, Y., ... Zhu, H. (2019). Genome-wide association analysis of 19,629 individuals identifies variants influencing regional brain volumes and refines their genetic co-architecture with cognitive and mental health traits. *Nature Genetics*, *51*(11), 1637–1644. <https://doi.org/10.1038/s41588-019-0516-6>
- Zhou, H., Lin, Z., Voges, K., Ju, C., Gao, Z., Bosman, L. W. J., ... Schonewille, M. (2014). Cerebellar modules operate at different frequencies. *ELife*, *3*, e02536. <https://doi.org/10.7554/eLife.02536>
- Zhu, Z., Zhang, F., Hu, H., Bakshi, A., Robinson, M. R., Powell, J. E., ... Yang, J. (2016). Integration of summary data from GWAS and eQTL studies predicts complex trait gene targets. *Nature Genetics*, *48*(5), 481–487. <https://doi.org/10.1038/ng.3538>
- Zhu, Z., Zheng, Z., Zhang, F., Wu, Y., Trzaskowski, M., Maier, R., ... Yang, J. (2018). Causal associations between risk factors and common diseases inferred from GWAS summary data. *Nature Communications*, *9*(1), 1–12. <https://doi.org/10.1038/s41467-017-02317-2>
- Zhuang, H., Liu, R., Wu, C., Meng, Z., Wang, D., Liu, D., ... Li, Y. (2019). Multimodal classification of drug-naïve first-episode schizophrenia combining anatomical, diffusion and resting state functional resonance imaging. *Neuroscience Letters*, *705*, 87–93. <https://doi.org/10.1016/j.neulet.2019.04.039>